Holocene evolution of coastal lagoon environments in Belize, Central America: Analysis of stratigraphic patterns, mollusk shell concentrations and storm deposition

Dissertation

zur Erlangung des Doktorgrades

der Naturwissenschaften

vorgelegt beim Fachbereich Geowissenschaften

der Johann Wolfgang Goethe-Universität

in Frankfurt am Main

von

Friederike Adomat

aus Borna

Frankfurt am Main (2016)

(D30)

vom Fachbereich Geowissenschaften der

Johann Wolfgang Goethe-Universität Frankfurt am Main als Dissertation angenommen.

Dekan:	Prof. Dr. Ulrich Achatz
Gutachter:	Prof. Dr. Eberhard Gischler
	Prof. Dr. Wolfgang Oschmann
Prüfungskommission:	Prof. Dr. Eberhard Gischler
	Prof. Dr. Wolfgang Oschmann
	Prof. Dr. Peter Prinz-Grimm
	Prof. Dr. Bernd Schöne

Datum der Disputation: 12.04.2016

Table of Contents

List of Figures

List of Tables

Abbreviations

AD	*Anno Domini*
AMM	Atlantic meridional mode
AMO	Atlantic multidecadal oscillation
AMS	Accelerator mass spectrometry
BP	before present (“present” = AD 1950)
ca.	*circa*
cal	calibrated
CBi	Commerce Bight Lagoon
CP	Colson point Lagoon
e.g.	*exempli gratia*
ENSO	El Niño/Southern Oscillation
et al.	*et alii/aliae*
HURDAT	Hurricane Database
i.e.	*id est*
ITCZ	Intertropical Convergence Zone
kyrs	kilo years (1000 years)
LR-ratio	left-right-ratio (related to valve ratio)
MDR	Main development region
ML	Manatee Lagoon
MRB	Mullins River Beach
NAO	North Atlantic Oscillation
NMDS	Nonmetric Multidimensional Scaling
NOAA	National Oceanic and Atmospheric Administration
OSL	Optically Stimulated Luminescence
PAST	Palaeontological Statistics
SEM	Scanning Electron Microscope
SL	Sapodilla Lagoon
sp.	species
spp.	species (plural)
SST	sea surface temperature
TC	Tropical cyclone
XRD	X-ray diffractometry
XRF	X-ray fluorescence
yr/yrs	year/years

Acknowledgements

First of all, I would like to thank Prof. Eberhard Gischler for giving me the opportunity to work in the PhD project, to join a field trip to Belize, for the quick corrections, and for always being available for my concerns.

Further, I would like to thank Prof. Wolfgang Oschmann for being co-reviewer of my thesis and Prof. Peter Prinz-Grimm and Prof. Bernd Schöne for being part of the committee.

The project (Gi222/20) was funded by the Deutsche Forschungsgemeinschaft (DFG) and financially supported by the Alfons and Gertrud Kassel-Stiftung and the Hermann-Willkomm-Stiftung.

Special thanks to the colleagues of our working group, Lars Klostermann, Anja Isaack and David Storz.

I would like to thank the crew who supported our fieldwork in Belize, Stefan Haber, Malo Jackson, David Geban, Claire Santino and Gabi Meyer.

Many thanks to the supervisors of my diploma thesis and diploma mapping, Prof. Axel Munnecke and Prof. Roman Koch, for encouraging me to go for the PhD.

Thanks to Cornelia Anhalt, Nils Prawitz, Wolfgang Schiller, Claudia Franz, Dr. Rainer Petschick and Susanne Fondacaro for technical and laboratory work and general support.

My colleagues and friends Jessi, Iris, Miri, Claudia, Ulrike, Julia, Micha, Nils, Nico and Sijo are deeply thanked for the conversations, discussions and the lunches together. Thank you, Micha, for nice coffee breaks. I am also grateful to Sebastian, Johannes, Katrin, Chris and Chrissi.

Finally, I am deeply grateful to all my friends and my family.

Abstract

In Belize, which is well known for the Belize Barrier Reef and its offshore atolls, coastal lagoons are frequent morphological features along the coast. They represent transitional environments between siliciclastic and carbonate settings. In order to shed light into the Holocene evolution of coastal lagoon environments, five localities along the central coast of Belize were selected as coring sites. These include four coastal lagoons and one marsh area, namely Mantatee Lagoon, Mullins River Beach, Colson Point Lagoon, Commerce Bight Lagoon and Sapodilla Lagoon. A total of 26 sediment cores with core lengths ranging from 109 cm to 500 cm, were drilled using a Lanesky-vibracorer. Overall, 73 m of Holocene sediments and Pleistocene soil were recovered. Together with 58 radiocarbon dates the sediments reveal details on the sediment architecture and depositional features of the localities.

Marine inundation of the mainland and coastal lagoon formation started around 6 kyrs cal BP. As a response to sea-level rise during the Holocene transgression, facies retrograded towards the coast, as seen in marginal marine overlying brackish mollusk faunas. Evidence for late Holocene progradation of facies due to sea-level stagnation is largely lacking. The occurrence of landward thinning sand beds, hiatuses and marine fauna in lagoonal successions are indications of event (overwash) sedimentation. Sediments recovered are largely of Holocene age (<7980 cal BP), overlying Pleistocene sections. Analyses of sediment composition and texture, radiocarbon dating and mollusk shell identification were used to describe and correlate sedimentary facies. XRD analyses have identified quartz as the dominant mineral, with the Maya Mountains as main source of coastal lagoon sediments. The most common sedimentary facies include peat and peaty sediment, mud, sand, and poorly sorted sediments. Pleistocene soil forms the basement of Holocene sediments. Holocene mud represents lagoon background permanent sedimentation. Peats and peat-rich sequences were deposited in mangrove swamp environments, whereas sandy facies mainly occur in the shoreface, beach, barriers, bars, barrier spits and overwash deposits. Facies successions could be identified for each locality, but it has proven difficult to correlate the stratigraphic sequences, especially among localities. These differences among the five locations studied suggest that apart from regional influence such as sea-level rise, local environmental factors such as small-scale variation in geomorphology and resulting facies heterogeneity, connectivity of the lagoon with the sea, antecedent topography and river discharge, were responsible for coastal sedimentation and lagoon development in the Holocene of Belize.

Faunal composition and distribution patterns of mollusk assemblages from 20 shell concentrations in cores collected in coastal lagoons, a mangrove-fringed tidal inlet and the marginal marine area (shallow subtidal) show considerable variation due to environmental heterogeneity and the interplay of several environmental factors in the course of the mid-late Holocene (ca. 6000 cal BP to modern). The investigated fauna ≥2 mm comprises 2246 bivalve,

789 gastropod and 11 scaphopod specimens. Fifty-three mollusk species, belonging to 42 families, were identified. The bivalve *Anomalocardia cuneimeris* and cerithid gastropods are the dominant species and account for 78% of the total fauna. Diversity indices are low in concentrations from lagoons and relatively high in the marginal marine and tidal inlet areas. Based on cluster analysis and nonmetric multidimensional scaling (NMDS), seven lagoonal assemblages and three marginal marine/tidal inlet assemblages were defined. A separation between lagoonal and marginal marine/tidal inlet assemblages seen in ordination indicates a lagoon-onshore gradient. The statistical separation among lagoonal assemblages demonstrates environmental changes during the Holocene evolution of the coastal lagoons, which is probably related to the formation of barriers and spits. The controlling factors of species distribution patterns are difficult to figure out, probably due to the heterogeneity of the barrier-lagoon systems and the interaction of paleoecological and paleoenvironmental factors. In addition to the taxonomic analysis, a taphonomic analysis of 1827 valves of *A. cuneimeris* from coastal lagoons was carried out. There is no relationship between depth and age of shells and their taphonomic condition. Size-frequency distributions and right-left valve ratios of *A. cuneimeris* suggest that valves were not transported over long distances but were deposited parautochthonously in their original habitat. Shells from tidal inlet and marginal marine environments were also predominantly deposited in their original habitats.

Since the Belize coast was repeatedly affected by hurricanes and the paleohurricane record for this region is poor, the sediment cores have been examined in order to identify storm deposits. The paleohurricane record presented in this study spans the past 8000 years and exhibits three periods with increased evidences of hurricane strikes occurring at 6000-4900 cal yr BP, 4200-3600 cal yr BP and 2200-1500 cal yr BP. Two earlier events around 7100 and 7900 cal yr BP and more recent events around 180 cal yr BP and during modern times have been detected. Sand layers, redeposited corals and lagoon shell concentrations have been used as proxies for storm deposition. Additionally, hiatuses and reversed ages may indicate storm influence. While sand layers and corals represent overwash deposits, the lagoon shell concentrations, which mainly comprise the bivalve *Anomalocardia cuneimeris* and cerithid gastropods, have been deposited due to changes in lagoon salinity during and after storm landfalls. Comparison with other studies reveals similarities with one record from Belize, but hardly any matches with other published records. The potential for paleotempestology reconstructions of the barrier-lagoon complexes along the central Belize coast differs depending on geomorphology, and deposition of washovers in the lagoon basins is limited, probably due to the interplay of biological, geological and geomorphological processes.

Chapter 1. Introduction

1.1 Motivation and aims

Lagoons are frequent geomorphological features along the Belize coast. In general, coastal lagoons represent a buffer zone between terrestrial and marine environments. Situated at the dynamic interface between land and sea, coasts are transient landscapes shaped by the interplay between macroscale and microscale processes (Bao et al. 2007). Any change in the power of these controlling factors directly translates into morphological adjustment of the coast (Cooper 1994; Bao et al. 2007). The lagoons, barrier islands, coastal spits and peripheral wetlands provide ecotones, which support highly diversified habitats (deWit 2011). Coastal lagoons are highly productive ecosystems (Anthony et al. 2009; Kennish and Paerl 2010) and consist of a complex arrangement of interactions that fluctuate in space and time (Medina-Gómez and Herrera-Silveira 2003). The resulting spatial heterogeneity creates complex systems. They act as sediment traps (Harris and Heap 2003) and therefore contain sedimentary archives providing insights into several disciplines. Thus, the sediments can be investigated in order to shed light on their development in the past and how they will react to future changes.

So far, only few studies about the Belize coastal lagoon environments exist (High 1969; McCloskey and Keller 2009; McCloskey and Liu 2012). In contrast, the offshore Belize Barrier Reef, the three atolls Turneffe, Lighthouse and Glovers, and the shelf area, are very well studied. As a classical area for the study of modern carbonates and mixed carbonate–siliciclastic systems Belize served as study area for the investigation of facies patterns and stratigraphy (e.g., Purdy 1974; Purdy and Gischler 2003; Purdy et al. 2003), as well as the evolution of the Belize Barrier Reef and sea-level reconstructions (e.g., Gischler 1994, 2002, 2006, 2008; Gischler and Ginsburg 1996; Gischler et al. 2010).

The study area was repeatedly affected by hurricane landfalls. Since an increase in destructiveness of hurricanes was observed, the frequency of intense Atlantic hurricanes is of high interest. Up to now, the paleohurricane record for the Belize coast is poor. Some studies identified storm deposits from offshore Belize (Gischler et al. 2008, 2013; Denommee et al. 2014). Aside from geomorphic changes, hurricanes may have noticeable effects on hydrologic parameters, causing changes in environmental condition such as an increase or decrease in lagoon salinity. This, in turn, may result in changes in the faunal composition. No studies exist on mollusk fauna of Belize coastal lagoons. Studies on mollusks cover taxonomy and taphonomy of the shelf and offshore region (Hauser et al. 2007, 2008). On the mixed carbonate-siliciclastic Belize shelf, Robertson (1963) and Purdy et al. (1975) determined distribution patterns of live mollusks but the fauna from coastal lagoon environments was not included (Purdy et al. 1975).

In the light of the aforementioned issues, three main objectives were elaborated:

1. Investigation of facies distribution, facies succession, and chronology to reconstruct the Holocene evolution of coastal lagoon environments

2. Taxonomic analysis of mollusk shells from shell concentrations to figure out if changes in abundance, distribution patterns and diversity have occurred during barrier-lagoon evolution; Taphonomic analysis to investigate if taphonomic states changed in the record and to elucidate the formation of shell concentrations

3. Identification of storm deposits in order to define active and quiet periods and to evaluate the suitability of the study area for paleohurricane reconstructions

1.2 Coastal lagoons

Coastal lagoons are ephemeral dynamic systems and are common along microtidal and low-lying coasts (Bird 1994). They cover about 13% of the world's coastlines (Barnes 1980; Zenkovich 1969) and largely developed during the Holocene as a result of sea-level rise (Kjerfve 1994). Several definitions for coastal lagoons have been proposed. A widely adopted one is that by Kjerfve (1994) who defined a coastal lagoon as "a shallow coastal water body separated from the ocean by a barrier, connected at least intermittently to the ocean by one or more restricted inlets, and usually oriented shore-parallel". Kjerfve (1994) further sub-divided barrier-enclosed lagoons according to the degree of isolation by the barrier. The three geomorphic types choked, restricted and leaky are based on increasing water exchange with the ocean.

Three main theories for barrier-lagoon formation have been proposed in the 19th century: Shoreface embayment by spit progradation (Fisher 1867, 1868; Gilbert 1885, 1890), shoreface embayment by bar emergence (deBeaumont 1845) and coastal inundation by sea-level rise (McGee 1890; Hoyt 1967). Several other evolutionary models have been proposed (outlined in Cooper 1994). However, a complex interaction of processes controls the evolution of coastal lagoons (Cooper 1994). Evolutionary processes are controlled by macroscale and microscale variations. The former include sea-level changes, climate and tectonic stability. The latter include fluvial sediment supply, longshore drift, salinity, surrounding geology, coastal morphology, lagoon orientation, wave energy and tidal range.

Oertel (1985) described six major interactive sedimentary environments of barrier island systems, including mainland, backbarrier lagoon, inlet and inlet deltas, barrier island, barrier platform and shoreface (Fig. 1.1). There are differences between coastal morphologies of tide-dominated and wave-dominated coasts. Tidal currents have a strong influence on coastal lagoon morphodynamics, forming well developed incised channel systems, which are separated by relatively short barrier islands, and large ebb-tidal deltas (Oertel et al. 1992). In contrast to tide-

dominated coasts, microtidal coasts show long barrier islands, which are often backed by lagoons and are subject to overwash. Barrier islands are interrupted by only few inlets, which are backed by tidal deltas (Hayes and Kana 1976; Hayes and FitzGerald 2013).

Sediment is delivered into the lagoons by rivers, tidal currents and winds. Sources of sediments include marine (through tidal channel, by overwash) and terrestrial (by river channels) environments. Along wave-dominated coasts, storms are important sediment contributors. Storms may also change coastal geomorphology (eg., breaching of barrier, creation of new tidal inlets) and thus change hydrodynamics and sediment deposition in the lagoons. Overwash is the process, which occurs when water flow exceeds barriers, beaches and dunes. The erosion of sediment and landward deposition forms washovers. Washover defines the sediment, which was deposited during overwash. Overwash by runup and overwash by overflow can occur, depending on the height ratios of the wave runup height, the storm surge height and the dune or beach crest height (Donnelly et al. 2004). On the other hand, extreme precipitation associated with storms can induce freshwater flooding and landslides further inland (Wallace et al. 2014). Aside from these sources, sediments accumulate in lagoonal basins from rivers draining the mainland, runoff of tidal marsh and other habitats bordering the basin, and internal processes (i.e., organic carbon production, chemical precipitation, as well as erosion and resuspension of older sediments) (Kennish and Paerl 2010).

Reconstruction of coastal lagoon evolution has been carried out mainly by investigation of sedimentologic patterns. Cores from coastal lagoons worldwide have been used to investigate Holocene evolution during sea-level rise, facies associations and sediment architecture of coastal lagoon systems and have pointed out the heterogeneity and complexity of the systems (e.g., Freitas et al. 2002, 2003; Andrade et al. 2004; Stutz et al. 2006; González-Villanueva et al. 2009; Sabatier et al. 2010; Fornari et al. 2012).

In Belize, coastal lagoons represent transitional features between siliciclastic and carbonate settings. The barrier-lagoon systems show differences in size and geomorphology and thus have differences in water exchange with the sea. Belize coastal lagoons are largely fringed by mangroves. Together with geomorphology and hydrodynamics mangroves affect sedimentological processes in the lagoons.

Sea-level curves for the Western Atlantic, which are based on radiocarbon data from acroporid corals and mangrove peats (e.g., Lighty et al. 1982; Toscano and Macintyre 2003; Gischler and Hudson 2004) show a rapidly rising trend until 7000 yrs BP (Fig. 1.2). Thereafter, the rate of rise has decreased and sea level slowly approached modern level.

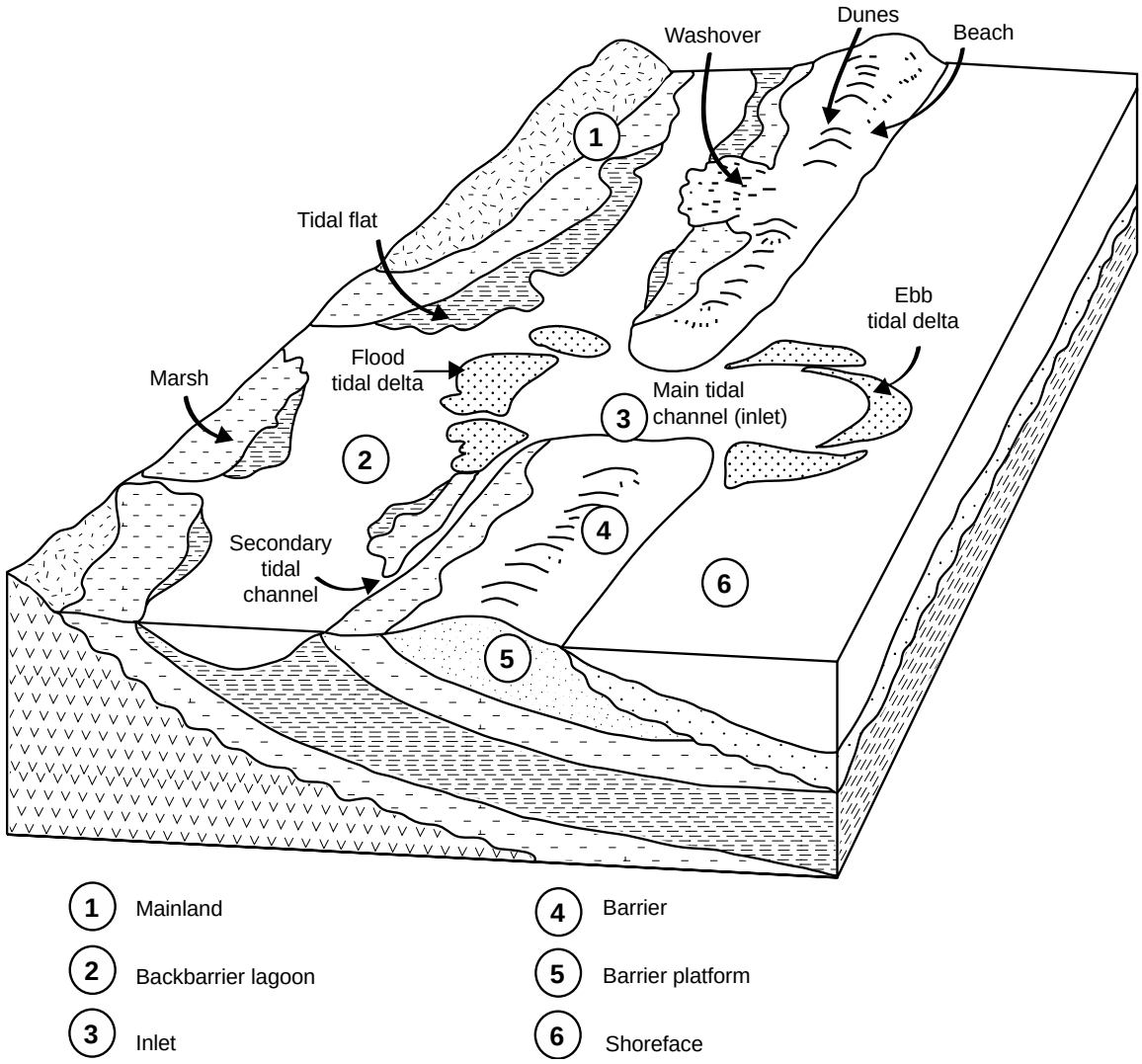

Fig. 1.1 Schematic diagram of a barrier island system showing the main depositional settings (after Reinson 1992)

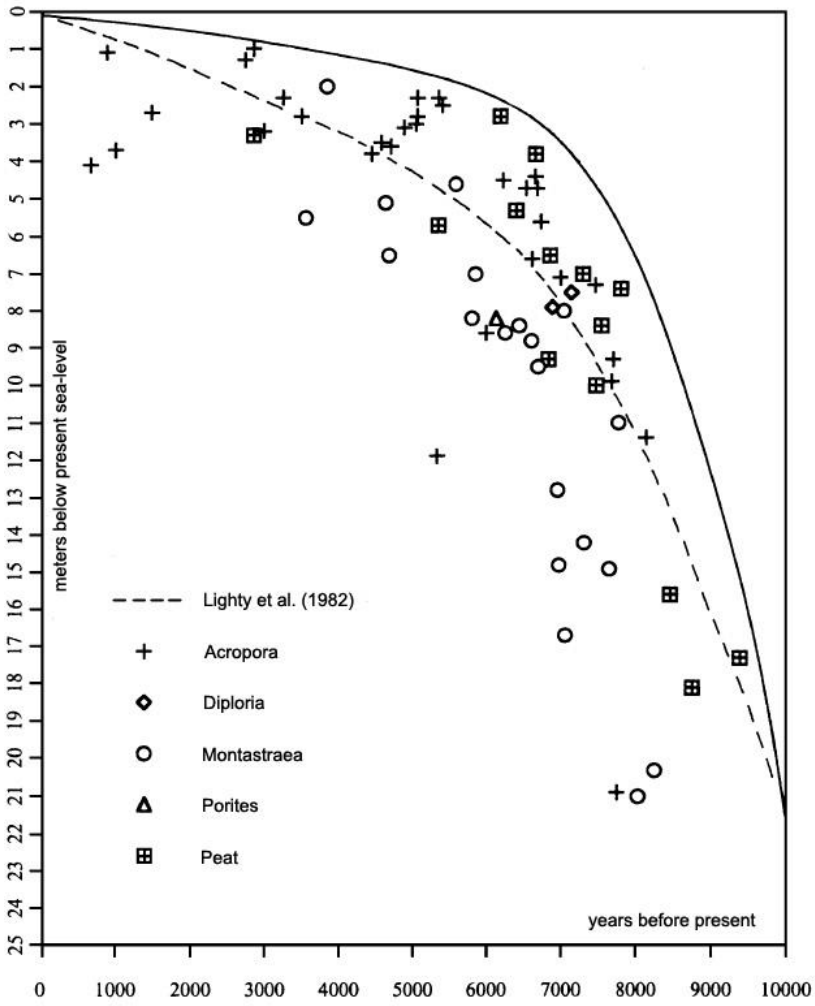

Fig. 1.2 Sea-level curves for the Western Atlantic, which are based on radiocarbon data from acroporid corals and mangrove peats (modified after Gischler and Hudson 2004)

1.3 Shell concentrations

1.3.1 Definition and genetic classification

Shell concentrations are common in the stratigraphic record and are found in fossil and recent deposits. They can be useful for the analysis of bathymetry, sedimentation rates, the hydrodynamic regime and environmental gradients (Fürsich 1990). Several studies have dealt with the definition and classification of skeletal concentrations and their significance for paleoecological, paleoenvironmental and biostratigraphic interpretations (e.g., Johnson 1960; Kidwell 1985, 1991, 2001, 2002; Kidwell et al. 1986; Fürsich 1990; Kidwell and Bosence 1991). Kidwell et al. (1986) defined the term skeletal concentration as "*any relatively dense accumulation of biologic hardparts, irrespective of taxonomic composition, state of preservation, or degree of post mortem modification*".

For the genetic classification of shell concentrations following classification schemes have been developed: A ternary diagram groups shell concentrations according to the relative

importance of biogenic, sedimentologic and diagenetic processes (Kidwell et al. 1986) (Fig. 1.3a). Based on this ternary scheme, Kidwell et al. (1986) showed the distribution of genetic types of shell concentrations along environmental gradients (Fig. 1.3b). An offshore trend of increasing biogenic and decreasing sedimentologic concentrations seaward from the coast is observed. Another classification scheme includes four types of accumulation histories, namely event, composite, hiatal and lag concentrations (Kidwell 1991) (Fig. 1.4). Each of these types has different applications to stratigraphic analysis and has different implications for the paleobiological analysis of the fauna. Event concentrations (e.g., storm, tsunami) represent single, ecologically brief episodes of concentration and are preserved as discrete events. They show a uniform preservation and taxonomic composition. Composite concentrations record multiple events and slow sedimentation. They are characterized by variable taxa and preservation states. Hiatal concentrations are the result of sediment starvation, erosion or reworking and are stratigraphically condensed. They contain highly variable preservation and variable taxonomic composition. Lag concentrations are residual concentrations, which are associated with stratigraphic truncation surfaces. The concentrations formed due to physical sorting and reworking and the shells have been subject to erosion or corrosion.

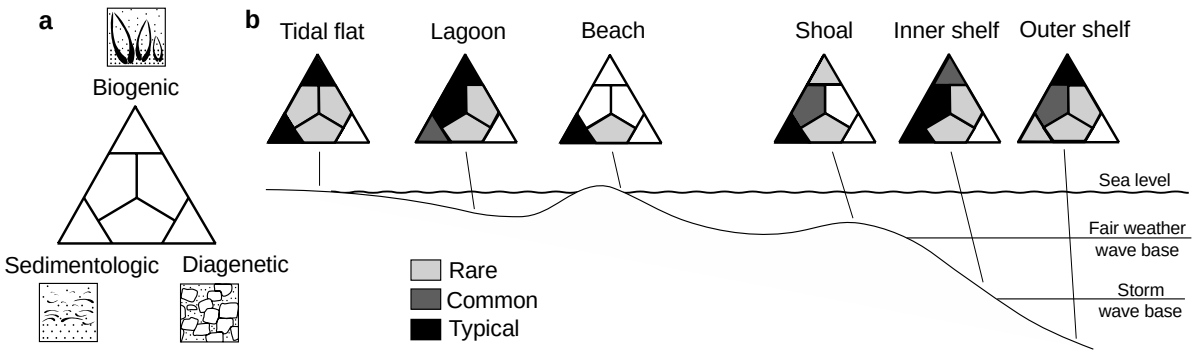

Fig. 1.3 Genetic classification of shell concentrations. **a** Ternary diagram showing genetic types of skeletal accumulations with the three end-members of concentrating processes, biogenic, sedimentologic and diagenetic. **b** Environmental distribution of skeletal concentrations along an onshore-offshore transect in a marine setting dominated by terrigenous sedimentation (modified after Kidwell et al. 1986)

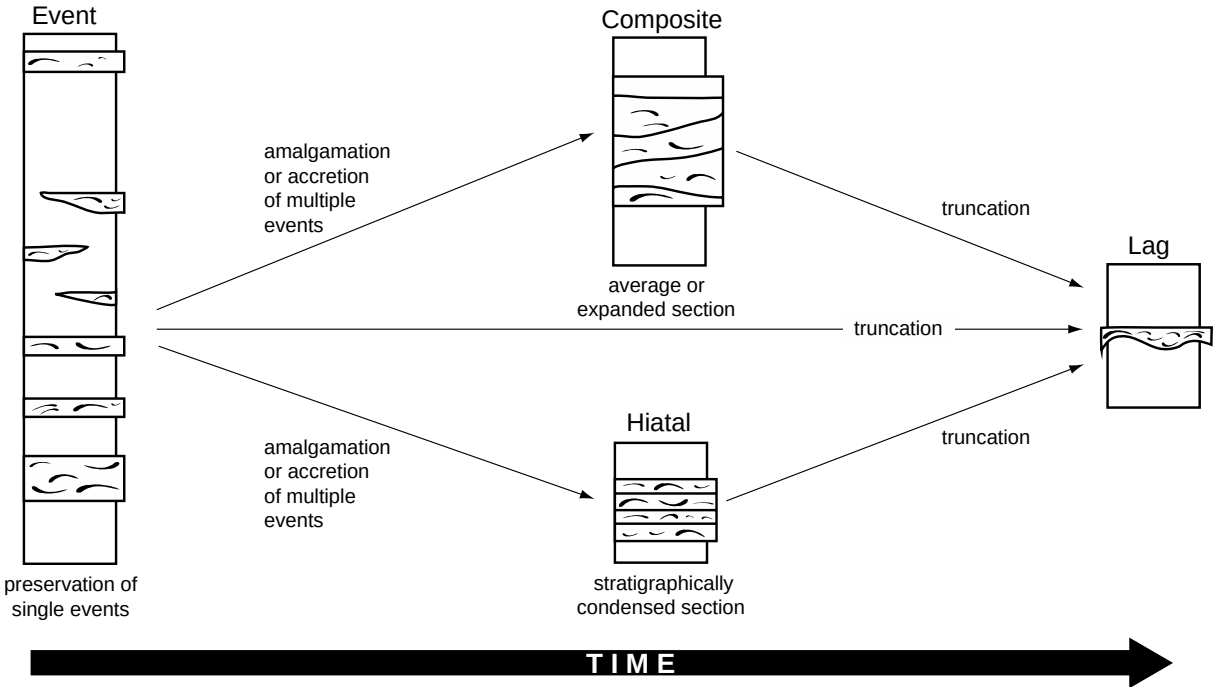

Fig. 1.4 Four categories of shell concentrations based on stratigraphy and accumulation history (modified after Kidwell 1991 and Fürsich 1995)

Biofabric, taxonomic composition and taphonomic signatures can be used to describe shell concentrations and provide information on physical and biological properties of the environment (Fürsich 1990, 1995). The biofabric, which is the three-dimensional arrangement of skeletal elements in the matrix, reflects concentration processes (Fürsich 1990, Fürsich and Oschmann 1993). Orientation of shells, grading, erosive bases, the matrix, and the modal distribution of skeletal elements give evidence for biological activity and hydrodynamic processes such as waves and currents. The taxonomic composition largely depends on the ecology of the taxa and also, but to a lesser degree, on the hydrondynamics of their accumulation (Fürsich 1990). Monotypic and polytypic concentrations can be distinguished by whether they are composed of single or several types of skeletons. A paucispecific concentration contains only few species but is strongly dominated by one species (Kidwell et al. 1986). Assemblages represent groups of specimens that occur together. A life assemblage consists of living organisms, whereas death assemblages contain preserved elements of a life assemblage after its death and decay (Fürsich 1990). Processes such as reworking and time-averaging lead to a loss of information and limits paleoecological analysis. Short-term fluctuations in species composition or environmental factors cannot be recognized in time-averaged assemblages. However, time-averaged death assemblages often record large-scale environmental conditions and may be more indicative of long-term trends than living communities (Fürsich 1990). A shell concentration may be a homogeneous or a heterogeneous assemblage, with the latter consisting of several subsidiary assemblages. Autochthonous assemblages contain specimens from the local community and are preserved in life position. Parautochthonous assemblages are composed of autochthonous

specimens that have been reworked to some degree, but have not been transported out of their original habitat. Reorientation, disarticulation and concentration by biologic agents or physical processes may have affected the specimens. Allochthonous assemblages comprise specimens that have been transported out of their life habitats (Kidwell et al. 1986). Taphonomic signatures carry information about the original environment in which the organisms lived and record the history that led to their concentration, including the hydrodynamic regime, bathymetry, residence time on the seafloor and biological activity (Fürsich 1995).

1.3.2 Studies on taxonomy and taphonomy

Variation in the taxonomic composition of shell concentrations and their taphonomic signatures can reflect paleoenvironmental gradients as shown, e.g., in modern coastal siliciclastic systems of the temperate realm in north and south America (e.g., Fürsich and Flessa 1987; Davies et al. 1989; Aguirre and Farinati 1999; Kotzian and Simões 2006; Ritter et al. 2013). Studies that focused on mollusk distribution, shell concentrations and taphonomy in the tropical Caribbean realm and surrounding regions are for the most part located in carbonate depositional environments, e.g, in south Florida, the Yucatan, the Virgin Islands, Puerto Rico, the Bahamas, and the Belize offshore atolls (Turney and Perkins 1972; Ekdale 1974, 1977; Anderson and McBride 1996; Brewster-Wingard et al. 2001; Callender et al. 2002; Parsons-Hubbard 2005; Hauser et al. 2007, 2008). Turney and Perkins (1972) recognized four environments in Florida Bay, largely defined by salinity differences, which are also characterized by the occurrences of index and common species. In a core study, Brewster-Wingard et al. (2001) recognized that the occurrence of mollusk assemblages in Florida Bay has changed over historical times, possibly due to shifts in salinity and water quality. In Puerto Rico and St. Croix, taphonomic data obtained from mollusks in cores were used to reconstruct the migration of facies over the past ca. 7 kyrs (Parsons-Hubbard 2005). In the northeastern Yucatan, Ekdale (1974) identified five mollusk assamblages ranging from the rocky intertidal zone to the open sea. Ekdale (1977) concluded that mixing of live and death assemblages is negligible. Hauser et al. (2007, 2008) used bivalve mollusk distribution and taphonomy to characterize depositional environments in atolls lagoons in Belize. In a broad platform-top to deep-water traverse in the Bahamas, Callender et al. (2002) noted that comparable taphonomic signatures on mollusk shells developed in different environments and that taphonomic processes are non-linear, thereby complicating ecological interpretations.

Few studies on mollusk taphonomy and distribution were conducted in tropical siliclastic and mixed-carbonate-siliciclastic settings in the Caribbean (e.g., Best and Kidwell 2000a, b; Best 2008). Best and Kidwell (2000a) noted that there should be significant differences in shell taphonomy among carbonate and siliciclastic settings because the latter are usually more abrasive and feature higher water turbidity and porewaters undersaturated in calcium carbonate.

However, shell preservation in fine-grained siliciclastics was found to be much better as compared to adjacent carbonate settings that included hard substrates (Best 2008; Best et al. 2007). Smaller shell loss apparently leads to lower taxonomic bias but greater time averaging in siliciclastic settings (Kidwell et al. 2005). Mollusk shell distribution and taphonomy was also used to identify event deposition in the tropical Caribbean. For example, Miller et al. (1992) studied pre- and post-hurricane distribution of mollusks in a bay at the northern coast of St. Croix and interestingly found only limited differences. Reinhardt et al. (2012) investigated taphonomic features of mollusk fauna of a distinct sand and shell sheet from beneath marine ponds of Anegada, British Virgin Islands. These authors considered the shell sheet tsunamigenic, however, noted the lack of comparative data from other Caribbean pond locations.

The distribution and composition of shell concentrations of the major mixed carbonate-siliciclastic depositional system of the Belize coast, including the factors that influence their formation, are entirely unknown. Only few studies focused on mollusks from Belize. Hauser et al. (2007, 2008) investigated modern bivalve shell assemblages from the three atolls offshore Belize. Bivalve distribution and taphonomic signatures on shells clearly reflect environmental and geomorphological differences in lagoonal environments. On the mixed-carbonate siliciclastic Belize shelf, Robertson (1963) and Purdy et al. (1975) determined distribution patterns of live mollusks and distinguished four major assemblages. They include (1) a reef and carbonate shelf community with 35 common species, (2) a deep shelf lagoon assemblage with *Nuculana cestrota* and 19 common species, (3) a nearshore lagoon assemblage with *Tivela mactroides* and 25 common species, and (4) a freshwater and brackish swamp assemblage with 5 common species. The latter comprises insufficiently sampled siliciclastic regions at and near river mouths as well as mangrove swamps and does not include fauna from coastal lagoon environments (Purdy et al. 1975).

1.4 Paleotempestology

Tropical cyclones (TCs) can cause extensive damage including coastal destruction and loss of human life (Goldenberg et al. 2001; Elsner et al. 2008). The increase in economic damage caused by TC is linked to rising coastal populations and increasing value of infrastructure in coastal areas (Pielke et al. 2008). To minimize the losses and to avoid catastrophic damage to lifes and properties, it is crucial to better understand the variability in TC activity. Therefore it is important to extend the historical and prehistorical record of TC activity. This knowledge would support the ability to predict changes in activity that may occur in the future (Liu 2004). Paleotempestology is a relatively new research field and the number of studies referring to this field has increased over the past decades. It is an approach for assessing hurricane landfall probabilities by means of geological records of past hurricane strikes (Liu 2004). Long-term paleotempestological records are important to assess risk associated with hurricane-induced

environmental impacts (e.g., Murnane 2004; Nott 2004; Elsner et al. 2008) and provide perspective on the long-term shifts in hurricane climatology (e.g., Mann et al. 2009) and the relationship between climate change and hurricane activity (Wallace et al. 2014).

1.4.1 Climate forcing

An increase in intensity and destructiveness of TCs in the North Atlantic during the past decades was observed (Emanuel 2005; Webster et al. 2005). Precise information about the underlying causes remains unclear due to the unreliability and limitations of the observational record (Landsea et al. 2010). However, North Atlantic hurricane activity has been linked to increasing sea-surface temperatures (SSTs) (Emanuel 2005; Donnelly et al. 2015), with an increase in frequency (Webster et al. 2005) and an increase in intensity of the strongest events (Elsner et al. 2008). The increase in SSTs since the late 19th century has been related to the sensitivity of Atlantic hurricanes to increasing greenhouse gasses (e.g., Emanuel et al. 2005; Hoyos et al. 2006; Saunders and Lea 2008; Webster et al. 2005; Santer et al. 2006; Gillett et al. 2008; Knutson et al. 2010). Saunders and Lea (2008) considered a 0.5 °C increase in sea surface temperature is associated with a 40% increase in hurricane frequency and activity. As likely factors for the increase in SSTs internal climate variations (Goldenberg et al. 2001; Zhang and Delworth 2006, 2009) and reduced aerosol or dust forcing (Mann and Emanuel 2006; Evan et al. 2009) have been discussed. Simulations and modeling have yielded variability and uncertainties of hurricane activities, which may be associated with different model predictions (Emanuel et al. 2008). However, most studies agree that there will be an increase in intensity and frequency of high-magnitude storms and a decrease in overall frequency of hurricanes (Bender et al. 2010; Knutson et al. 2010). Studies related changes in hurricane activity to variations in North Atlantic SST, the El Niño/Southern Oscillation (ENSO) and the North Atlantic Oscillation (NAO) (e.g., Mann et al. 2009; Donnelly and Woodruff 2007).

Several modes of climate variability influence TC activity in the North Atlantic basin. The Pacific SST has a strong influence on TC activity. It is characterized by the ENSO, an interannual mode in the tropical Pacific (Goldenberg and Shapiro 1996). North Atlantic tropical cyclone activity is also strongly related to ENSO. The anomalous westerly winds inhibit the formation of cyclones in the Caribbean and the equatorial Atlantic by increasing tropospheric vertical wind shear (Gray 1984). El Niño also inhibits Atlantic TC activity through warm upper tropospheric temperature anomalies (Tang and Neelin 2004). Pacific SST variations and associated ENSO drive changes in the upper tropospheric circulation of the tropical Atlantic through the Walker circulation, which serves as a tropospheric bridge, transferring the Pacific ENSO effects to the Atlantic sector (Arkin 1982; Wang 2005). Influence of the ENSO on climate variability has been found in proxy records from the Caribbean (e.g., Donnelly and Woodruff 2007; Woodruff et al. 2008a; Gischler et al. 2009). The North Atlantic SST impacts TC activity as a local thermodynamic effect, with warmer

North Atlantic SST supporting increased TC activity (Emanuel 2005; Webster et al. 2005). But it is unlikely that it is the only physical link to hurricane activity (Goldenberg et al. 2001). The Atlantic meridional mode (AMM) and the Atlantic multidecadal oscillation (AMO) are two prominent modes of Atlantic climate variability. The AMM is interannual to decadal and describes the meridional gradient between northern and southern tropical Atlantic SST (Kossin and Vimont 2007; Vimont and Kossin 2007). It is a coupled ocean-atmosphere mode and can be generated by external forcing such as the ENSO and NAO (e.g., Curtis and Hastenrath 1995; Nobre and Shukla 1996; Xie and Tanimoto 1998; Giannini et al. 2000). It is associated with meridional displacement of the ITCZ and associated shifts in SST and winds (Chiang and Vimont 2004). Positive phases of the AMM with warmer-than-normal SST and weaker-than-normal vertical wind shear increase TC activity in the Atlantic. Kossin and Vimont (2007) found that a positive AMM is associated with an increase in storm duration and the frequency of intense hurricanes. The AMO is multidecadal and describes North Atlantic SST variability (e.g., Landsea et al. 1999; Goldenberg et al. 2001). Goldenberg et al. (2001) explained the increase in hurricane activity in the Atlantic from 1995 to 2000 by the modulation of the main development region (MDR) by the AMO, with above-normal North Atlantic SST and a decrease in vertical wind shear.

Holocene climate variability in the region is characterized by a change from warmer/wetter conditions during the Holocene Climate Optimum (ca. 10000-5500 yrs BP) to cooler/drier conditions after ca. 5000 yrs BP (e.g., Haug et al. 2001). Another change back to warmer and wetter conditions occurred in the late Holocene (between 3000-1000 yrs BP) in the wider study area according to vegetation data (Wooller et al. 2009) and coral climate proxy data from Belize (Gischler and Storz 2009). A period of increased hurricane activity during 3500-1000 yrs BP recorded by Liu and Fearn (2000a,b) apparently correlated with a northward shift of the Intertropical Convergence Zone (ITCZ). A northern position of the ITCZ favors heavy rainfall in the southern part of the Caribbean and the Yucatán peninsula, whereas a southern position of the ITCZ causes drought in the Caribbean region (Haug et al. 2003; Hodell et al. 2005). Stronger storm activity over the Gulf coast and the inner Caribbean Sea is favored by a southern position of the ITCZ in connection with dry climatic conditions. The position of the ITCZ is associated with a shift of the Bermuda High, whose position controls the direction of hurricane paths. In addition to a longitudinal shift of the ITCZ, the role of atmospheric circulation systems have to be considered to explain the strong multidecadal variability of Caribbean hurricanes.

1.4.2 Hurricane proxies and paleohurricane records

Several geologic proxies were used as a tool in paleotempestology, ranging from sediment-based and isotope-based to micropaleontological proxies. Geologic proxies include negative ^{18}O anomalies in tree rings (Miller et al. 2006) and in speleothems (Frappier et al. 2007; Malmquist 1997; Nott et al. 2007), which are associated with hurricane-induced precipitation. ^{18}O oscillations

related boulder deposits to typhoon events (Suzuki et al. 2008). Furthermore, hurricane activity has been studied by using luminescence intensity data from corals (Nyberg et al. 2007), rainfall signatures preserved in corals (Cohen 2001; Hetzinger et al. 2008), and freshwater flood plumes (Lough 2007). Very coarse, up to boulder size, material has been interpreted to have been transported by hurricanes (Scheffers and Scheffers 2006; Spiske et al. 2008; Suzuki et al. 2008; Woodruff et al. 2009; Yu et al. 2009; Zhao et al. 2009; Toomey et al. 2013a). Hurricane-surge constructed beach ridges (Brooke et al. 2008; Nott and Hayne 2001; Nott et al. 2009; Nott 2011; Williams 2013) and scarps (Buynevich et al. 2007) served as geomorphic proxies. As biological and paleontological proxies marine foraminifera (Hippensteel and Martin 1999; Scott et al. 2003; Williams 2009, 2010) and shell-bed tempestites (Scott et al. 2003; Williams 2011) have been used. Another criterion that has been used to reconstruct storm events is coarse sediment, which is interpreted as intense terrestrial flooding events (Noren et al. 2002; Besonen et al. 2008) and which has been transported across the shelf during storms (Keen et al. 2012). The investigation of modern analogues (Hayes 1967; Nummedal et al. 1980; Kahn and Roberts 1982; Stone and Wang 1999; Sallenger et al. 2006; Morton et al. 2007; Woodruff et al. 2008a, b; Hawkes and Horton 2012) helps to interpret longer-term reconstructions (Wallace et al. 2014).

Most paleohurricane reconstructions are based on overwash deposits from the Gulf of Mexico (Liu and Fearn 1993, 2000a, b; Wallace and Anderson 2010; Lane et al. 2011; Brandon et al. 2013), the Caribbean (Bertran et al. 2004; Donnelly 2005; Donnelly and Woodruff 2007; Gischler et al. 2008; Woodruff et al. 2008b; McCloskey and Keller 2009; Malaizé et al. 2011; McCloskey and Liu 2012; Toomey et al. 2013b; van Hengstum et al. 2013) and western North Atlantic Ocean (Donnelly et al. 2001a, b, 2004; Donnelly and Webb 2004; Scileppi and Donnelly 2007; Boldt et al. 2010; Kiage et al. 2011). The records rely on the deposition of coarse-grained sediments within fine-grained background sediments. They include overwash deposits preserved in different coastal settings such as back barrier lagoons (Donnelly 2005; Donnelly and Woodruff 2007; Woodruff et al. 2008a, b; Wallace and Anderson 2010), coastal lakes (Liu and Fearn 1993, 2000a, b, 2002; Lambert et al. 2003, 2008), and marshes (Donnelly et al. 2001a, b, 2004; Scileppi and Donnelly 2007; Boldt et al. 2010). Fig. 1.5 shows a location map of overwash paleohurricane studies.

The extent of an overwash deposit is affected by many factors, such as hurricane intensity and storm surge height, coastal configuration, lake morphometry, abundance of sand supply, tide height at time of landfall, wind direction and timing and duration of landfall (Liu and Fearn 2000a). This results in a size and shape of the overwash sand fan, which is generally proportional to hurricane intensity (Liu and Fearn 2000a) (Fig. 1.6; Fig. 1.7). However, the records by Liu and Fearn (1993, 2000a, b) have been intensively criticized by Otvos (1999, 2002). According to him, most of the sand laminae, which have been related to overwash during catastrophic hurricanes by Liu and Fearn (1993, 2000a, b), have accumulated in a valley-filled estuary. As Otvos (1999) noted, other sedimentary processes than strom-surge overwash may have served as sand

sources. Also other sand sources than barrier overwash have to be considered, such as riverine floods, aeolian processes, sediment winnowing and tidal processes (Otvos 1999, 2002; Wallace et al. 2014). Furthermore, Otvos (1999, 2001, 2002) questioned the radiocarbon dates of Liu and Fearn (1993) and criticized that Liu and Fearn (2000a, b) treated the barrier as fixed although coastal barriers are dynamic systems and the sensitivity of a site to overwash may have changed over time. According to Otvos (2004), washover fan shapes are controlled by the topography, morphology, and dimensions of the associated barriers and by sand volumes delivered from eroding island dunes, beach foreshore, and offshore sand bodies. Therefore, it is important to be well versed in the coastal geologic history of the study site.

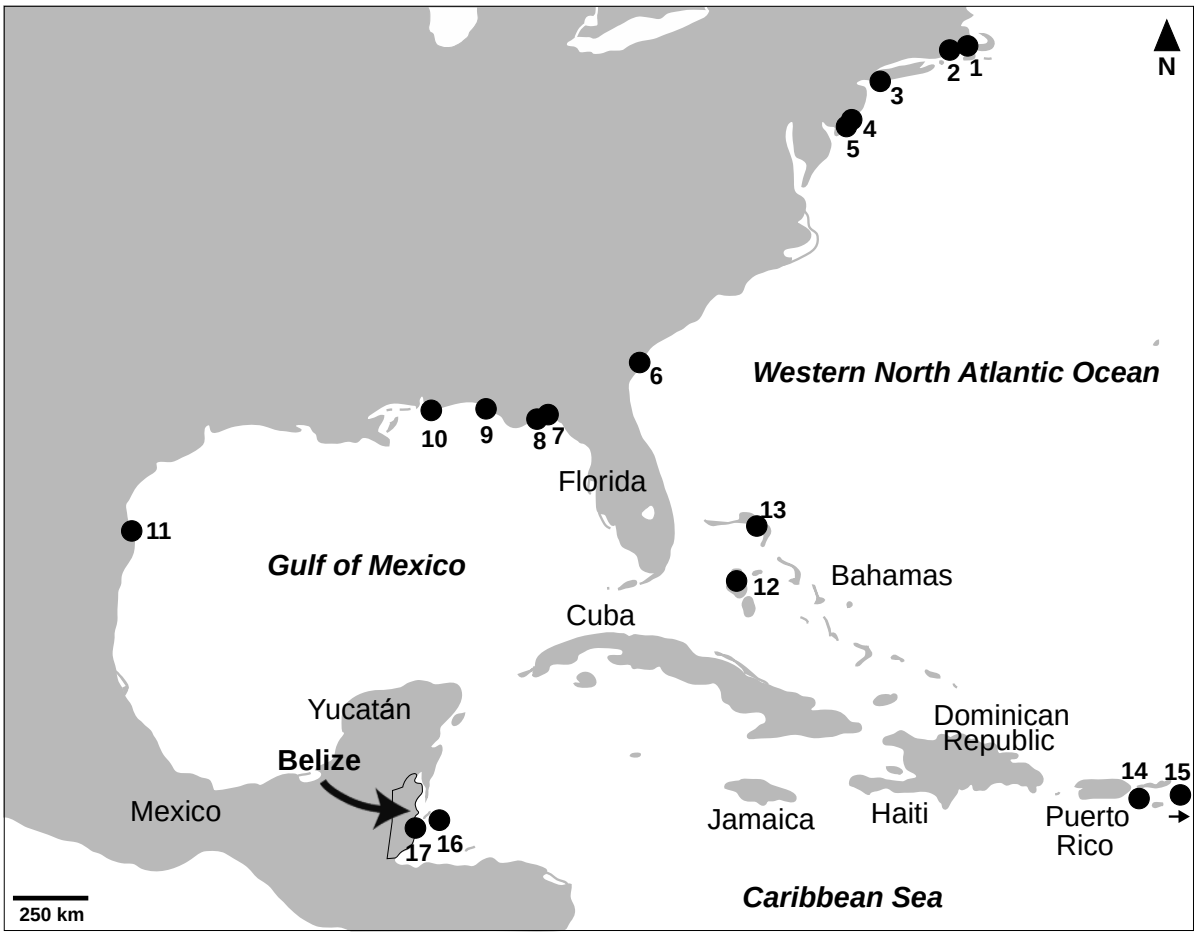

Fig. 1.5 Location map of paleohurricane studies from the Gulf of Mexico, Caribbean Sea and western North Atlantic Ocea. **1**: Mattapoisett Marsh, Buzzards Bay, Massachusetts, southwestern New England (Boldt et al. 2010). **2**: Succotash Marsh, Rhode Island, southern New England (Donnelly et al. 2001a). **3**: Western Long Island, New York (Scileppi and Donnelly 2007). **4**: Brigantine, New Jersey (Donnelly et al. 2004). **5**: Marsh at Whale Beach, southern New Jersey coast (Donnelly et al. 2001b). **6**: Wassaw Island, Georgia (Kiage et al. 2011). **7**: Spring Creek Pond, St. Marks, Florida (Brandon et al. 2013). **8**: Mullet Pond, Florida (Lane et al. 2011). **9**: Western Lake, Florida (Liu and Fearn 2000a). **10**: Lake Shelby, Alabama (Liu and Fearn 1993, 2000b). **11**: Laguna Madre, Texas (Wallace and Anderson 2010). **12**: Western Great Bahama Bank (Toomey et al. 2013). **13**: Little Bahama Bank (van Hengstum et al. 2013). **14**: Laguna Playa Grande, Vieques, Puerto Rico (Woodruff et al. 2008; Donnelly and Woodruff 2007). **15**: Grand-Case Pond, Saint-Martin, Lesser Antilles (Malaizé et al., 1011). **16**: Blue Hole, Lighthouse Reef, offshore Belize (Gischler et al. 2008, 2013; Denomee et al. 2014). **17**: Gales Point, Mullins River, Commerce Bight Lagoon, Hopkins (Belize coast) (McCloskey and Keller 2009; McCloskey and Liu 2012)

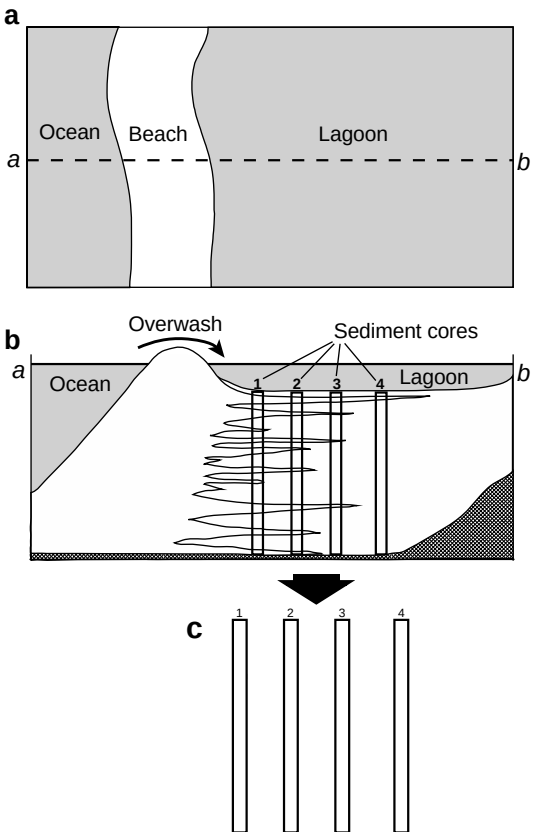

Fig. 1.6 Map view (**a**) and cross section (**b**) of overwash deposition in a coastal lake or lagoon. In the case of overtopping of the storm surge during washover, deposition of overwash fans in lagoon deposits. Landward decrease of the number and thick-ness of sand layers. The overwash deposits can be identified in sediment cores (**c**) (after Liu and Fearn 2000a; Donnelly et al. 2001a)

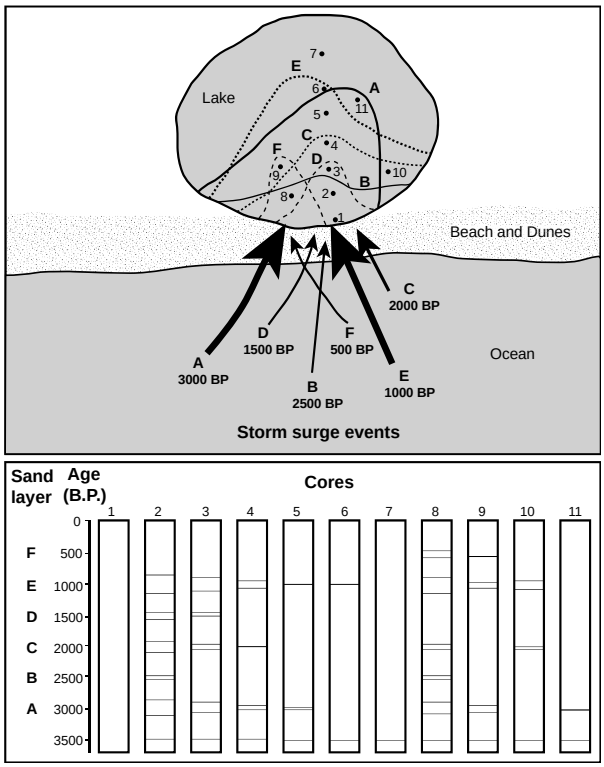

Fig. 1.7 Overwash sand deposition in a coastal lake according to hurricane tracks. Hurricanes are indicated by arrows, with thickness of the arrows being proportional to storm intensity. Cores taken close to the shoreline consist entirely of sand and individual overwash events are not distinguishable (after Liu and Fearn 2000b)

Limitations, which may reduce the completeness of a storm record, should be taken into account during study site selection. Modest sedimentation rates can limit the temporal resolution of many paleohurricane archives (Donnelly et al. 2015). Especially during low sedimentation rates, if not enough fine-grain lagoon or marsh sediment is deposited between overwash events, single deposits will be amalgamated and cannot be clearly attributed to single events (Woodruff et al. 2008a). The resulting low-resolution record thus under-represents the total number of storm events (Woodruff 2008a; Donnelly et al. 2015). However, sites with slow sedimentation rates may still be appropriate, if events are sufficiently rare (Wallace 2014). At sites with high bioturbation activity, storm deposits will be obscured (Martin 1993, 2000; Bentley et al. 2006; Hippensteel 2011). A relatively stable geomorphology is preferable because the sensitivity to overwash processes is determined by the morphology of the barrier or shoreline that separates coastal settings from the sea (Wallace et al. 2014). The decrease in the rate of sea-level rise during the past millennia resulted in shoreline stability and thus in a better preservation of overwash deposits (Woodruff et al. 2013).

The Belize coast has been subject to hurricane impacts on average every 5 years during the 20th century (Gischler et al., 2008, 2013). Atlantic hurricanes and tropical storms recorded since 1851 are provided by the hurricane data (HURDAT), maintained by the National Oceanic and Atmospheric Administration (NOAA). Storms affected northern and southern Belize more frequently than central Belize during recorded history. Density of storm tracks is highest in northern Belize and storm tracks typically run northwestward. Since 1864, five major hurricanes of category 3 or higher, according to the Saffir-Simpson scale (Simpson 1974) (Table 1.1), and 14 hurricanes of category 1 and 2 at landfall on the Belize coast have been recorded. Major hurricanes include an unnamed hurricane in 1931, Janet in 1955, Hattie in 1961, Greta in 1978 and Iris in 2001. The major hurricane Keith, which struck Belize in 2000, weakened over the offshore Belize atolls and made landfall as a tropical storm. Major hurricanes Hattie and Greta impacted the study area in the vicinity of Mullins River Beach and Colson Point. Two hurricanes struck the Belize coast close to the study area, an unnamed in 1906 and Richard in October 2010 after our fieldwork.

Table 1.1 *Saffir-Simpson Hurricane Wind Scale*

Category	Sustained Winds	Types of Damage
1	74-95 mph 64-82 kt 119-153 km/h	Very dangerous winds will produce some damage
2	96-110 mph 83-95 kt 154-177 km/h	Extremely dangerous winds will cause extensive damage
3	111-129 mph 96-112 kt 178-208 km/h	Devastating damage will occur
4	130-156 mph 113-136 kt 209-251 km/h	Catastrophic damage will occur
5	157 mph or higher 137 kt or higher 252 km/h or higher	Catastrophic damage will occur

Source: U.S. National Hurricane Center (NOAA, 2014)

1.5 Study area

Belize is situated in Central America, in the southeastern area of the Yucatán Peninsula. Its eastern border is formed by the Caribbean Sea (Fig. 1.5). The country extends from 16°N to 18°30´N latitude and from 87°30'W to 89°30´W longitude. The climate is subtropical (Wright et al. 1959). The area lies within the trade wind belt with prevailing easterly and northeasterly winds. The coast of Belize is a wave-dominated, semidiurnal microtidal area with a tidal range of 15-30 cm (Kjerfve et al. 1982). Major hurricanes made landfall on the Belize coast every 5 years during the 20th century on average (Gischler et al. 2008, 2013). Annual rainfall increases from north to south from 124 cm to 380 cm, respectively (Purdy et al. 1975), reflecting mainland topography.

Precipitation is highest during the summer months of July to September and salinity in coastal lagoons will fluctuate accordingly. Drainage density is particularly high along the coast east of the Maya Mountains (High 1975), however, there are no data available on river discharge, which is mainly dependent on rainfall pattern. Mean sea surface temperatures of the shelf range from 28.9°C during summer to 26.2°C during winter (e.g., Purdy et al. 1975). Surface water salinity decreases from ca. 35‰ at the shelf margin to ca. 18‰ near the coast, and northward into Chetumal Bay and southward into the Gulf of Honduras (Purdy 1974).

The shallow northern shelf is dominated by carbonates. The deeper southern shelf harbors a mixed siliciclastic-carbonate system with an eastward increase in carbonate content (Purdy et al. 1975; Pusey 1975; Scott 1975; Purdy and Gischler 2003). The major processes supplying sediment to coastal environments include river transport, shore erosion, longshore currents, tides, washovers and wind (Nichols and Boon 1994). The main sediment source is represented by the Maya Mountains and surrounding areas, where Paleozoic igneous, metamorphic and siliciclastic rocks and Cretaceous to Tertiary carbonates crop out. The coastal lowland is largely composed of unconsolidated Quaternary detrital sediments. A minor sediment contributor is the offshore marine realm (Adomat and Gischler 2015). Today, muddy substrate and low current velocities predominate in the coastal lagoons (Adomat and Gischler 2015). The lagoons are brackish with salinity ranging from 4 to 27‰. The coast of Belize, which has low relief, is dominated by barrier-lagoon complexes (High 1966). The coastal lagoons are usually extensively fringed by mangroves belonging to the red mangrove *Rhizophora mangle*.

1.6 Material and Fieldwork

The field trip to Belize took place from 27.07. to 06.08.2011. Five coring sites were selected along the south central coast of Belize, including the four coastal lagoons Manatee Lagoon, Colson Point Lagoon, Commerce Bight Lagoon and Sapodilla Lagoon (from N to S), as well as a swamp and marsh area north of Mullins River (Mullins River Beach). Because of a ship engine failure, the coring equipment arrived one week later than planned, on 02.08.2011. Therefore, during the first six days in the field (27.07. - 01.08.) provisional equipment was used to obtain sediment cores. A PVC-tube was used repeatedly for coring. Sediment was pushed out on the boat. Photo documentation, description and sampling occurred on the boat (twelve cores). From 02.08. to 06.08. a portable vibracorer (Lanesky et al. 1979) and 590 cm long aluminum pipes with a diameter of 7.5 cm, provided with a copper core catcher, were used for coring (Fig. 1.8). The cores were capped with plastic caps. Four to six cores were collected per day. A total of 26 cores with a total length of 73 m were obtained. The minimum length is 109 cm, the maximum length is 500 cm. The average length is 2.8 m. Water depths at the coring sites ranged between 0 and 109 m. Coordinates at the coring sites were registered using GPS.

Samples of bottom and top water for salinity measurements were collected in winter and in summer at one proximal and one distal site in each of the four lagoon sites during winter (21. 01. 2011) and summer (14. 07. 2012). Concentrations of major ions (Na^+, Mg^{2+}, Ca^{2+}, Cl^-, SO_4^{2-}, HCO_3^-) were measured at the laboratory of ALA Aachen.

The laboratory work is explained in detail in the Chapters 2, 3 and 4.

Fig. 1.8 Fieldwork. **a** Preparation of aluminum tube and Lanesky vibracorer for coring. **b** Lifting of capped core tube after coring. **c** Mangrove-fringed tidal channel. **d** Coring in the marsh environment of Mullins River Beach

1.7 Structure of the PhD thesis

This thesis comprises three manuscripts, which address the three objectives mentioned in 1.1. The three manuscripts have undergone the peer-review process of the respective journals. Two manuscripts are published (Chapter 2 and 3), the other represents the revised version of a resubmitted manuscript (Chapter 4).

Chapter 2 comprises an article entitled “Sedimentary Patterns and Evolution of Coastal Environments during the Holocene in Central Belize, Central America”, authored by Friederike Adomat and Eberhard Gischler, which has been published in the Journal of Coastal Research. The study presents sedimentary patterns of four coastal lagoon and a marsh environments covering the past 8000 years. Based on 26 sediment cores from five localities, analyses of sediment composition and texture, radiocarbon dating and mollusk shell identification were carried out to describe and correlate sedimentary facies and to shed light into the Holocene evolution of coastal lagoon environments.

Chapter 3 contains a manuscript entitled “Taxonomic and taphonomic signatures of mollusk shell concentrations from coastal lagoon environments in Belize, Central America” authored by Friederike Adomat, Eberhard Gischler and Wolfgang Oschmann, which has been published in Facies. The study comprises taxonomic and taphonomic analysis of twenty shell concentrations, which were found in cores from coastal lagoons, a mangrove-fringed tidal inlet and the marginal marine area (shallow subtidal) along the central coast of Belize. Based on the taxonomic analysis and multivariate statistical analyses ten mollusk assemblages, including seven lagoonal assemblages and three marginal marine/tidal inlet assemblages have been identified. The taphonomic analysis of bivalves gives insights into the formation of the shell concentrations.

Chapter 4 includes a manuscript by Friederike Adomat and Eberhard Gischler, entitled “Assessing the suitability of Holocene environments along the central Belize coast, Central America, for the reconstruction of hurricane records” which was resubmitted to the International Journal of Earth Sciences. The study focuses on the identification of possible storm deposits to define active and quiet periods. Furthermore, the suitability of the study area for paleotempestology reconstructions is debated by addressing both the preservation potential of event beds and the site sensitivity.

Finally, Chapter 5 presents a summary of the main results and an outlook on future work.

Chapter 2. Sedimentary patterns and evolution of coastal environments during the Holocene in central Belize, Central America

Friederike Adomat, Eberhard Gischler

Institut für Geowissenschaften, Goethe-Universität Frankfurt, Altenhoeferallee 1, 60438 Frankfurt am Main, Germany

Keywords: Coastal lagoons, lagoon sedimentology, C-14

Published in the Journal of Coastal Research 31, 802-826

Abstract: Coastal lagoons, marshes, and swamps cover large areas of the Belize coast. Twenty-six sediment cores collected along five transects along the central Belize coast and 58 radiocarbon dates from these cores reveal stratigraphic details of coastal sediment deposition. Marine inundation of the mainland and coastal lagoon formation started between 7980 calendar years before present (cal BP) and >5547 cal BP. As a response to sea-level rise during the Holocene transgression, facies retrograded toward the coast, as seen in marginal marine overlying brackish mollusk faunas. Evidence for late Holocene progradation of facies due to sea-level stagnation is largely lacking. The occurrence of landward thinning sand beds, hiatuses, and marine fauna in lagoonal successions are indications of event (overwash) sedimentation. Sediments recovered are largely of Holocene age (<7980 cal BP), overlying Pleistocene sections. Analyses of sediment composition and texture, radiocarbon dating, and mollusk shell identification were used to describe and correlate sedimentary facies. X-ray diffraction analyses have identified quartz as the dominant mineral, with the Maya Mountains as main source of coastal lagoon sediments. The most common sedimentary facies include peat and peaty sediment, mud, sand, and poorly sorted sediments. Pleistocene soil forms the basement of Holocene sediments. Holocene mud represents lagoon background permanent sedimentation. Peats and peat-rich sequences were deposited in mangrove swamp environments, whereas sandy facies mainly occur in the shoreface, beach, barriers, bars, barrier spits, and overwash deposits. Facies successions could be identified for each locality, but it has proven difficult to correlate the stratigraphic sequences, especially among localities. These differences among the five locations studied suggest that apart from regional influence such as sea-level rise, local

environmental factors such as small-scale variation in geomorphology and resulting facies heterogeneity, connectivity of the lagoon with the sea, antecedent topography, and river discharge were responsible for coastal sedimentation and lagoon development in the Holocene of Belize.

2.1 Introduction

Belize is a classical area for the study of modern carbonates and mixed carbonate-siliciclastic systems (Purdy 1974; Purdy and Gischler 2003; Purdy et al. 2003). In contrast to the offshore barrier reef and the shelf area, which are very well studied (Purdy 1974; Purdy and Gischler 2003; Purdy et al. 2003; and references therein), only a few studies deal with the coastal development of Belize, which is dominated by coastal lagoons, marshes, and mangrove swamps. High (1966, 1969, 1975) investigated sedimentation patterns in coastal lagoons, focusing on northern Belize. Studies on coastal development in central and southern Belize largely concentrated on event sedimentation (McCloskey and Keller 2009; McCloskey and Liu 2012). The definition of coastal lagoon used in this study is ‘‘a shallow coastal water body separated from the ocean by a barrier, connected at least intermittently to the ocean by one or more restricted inlets, and usually oriented shore-parallel’’ (Kjerfve 1994). These ephemeral dynamic systems are common in microtidal and low-lying coasts (Bird 1994) and cover about 13% of the world’s coastlines (Barnes 1980; Zenkovich 1969). They act as sediment traps that usually accumulate clastic sediments. Numerous studies concerning coastal lagoons and coastal environments have been published, focusing on classification (Boyd et al. 1992; Nichols and Allen 1981; Otvos 2012), Holocene evolution (Oertel et al. 1992), geomorphology (e.g., Fornari et al. 2012), ecology (Anthony et al. 2009, deWit 2011), and the use as archives of event sedimentation, i.e. hurricane activity (Donnelly and Woodruff 2007; Liu and Fearn 1993, 2000a; McCloskey and Keller 2009; McCloskey and Liu 2012). Coastal lagoons developed during the Holocene as a result of sea-level rise (Kjerfve 1994). However, Freitas et al. (2003) and González-Villanueva et al. (2009) have stressed the difficulty of deciphering evolutionary histories from sedimentary sequences of barrier-lagoon systems resulting from the complexity of these environments. In Belize, High (1969) investigated three coastal lagoons along the northern shoreline and found a regular and persistent sequence with Pleistocene limestone at the base, overlain by clay, peat, and carbonate muds at the top. He distinguished permanent processes and less frequent episodic events related to storms, both of which are important for coastal development. On the basis of preliminary investigations along the central and southern Belize coast, he could not detect a consistent stratigraphic sequence, suggesting that Holocene sedimentation is controlled by local environmental factors (High 1975). McCloskey and Keller (2009) and McCloskey and Liu (2012) studied coastal sediments at two locations in central Belize and focused on these deposits as storm archives. These authors interpreted virtually every quartz

sand layer within coastal background sedimentation as having resulted from storm events in the Holocene. Correlations of event layers among the two locations are limited. The objective of this study is the investigation of facies distribution, facies succession, and chronology within coastal lagoons and in a marsh and swamp area in central Belize. Comparisons of the different coastal settings are used to reconstruct their Holocene formation and to provide a sedimentary model. Furthermore, the significance of both local and regional forcing factors for coastal sedimentation is evaluated, and the response of coastal lagoon ecosystems to Holocene sea-level rise, climate variability, storm impact, and the possible influence of the Maya civilization are discussed.

2.2 Study area

Belize (16°N to 18°30´N; 87°30'W to 89°30´W) is situated in Central America, in the southeastern area of the Yucatán Peninsula, to the east bordered by the Caribbean Sea (Fig. 2.1). The climate is subtropical (Wright et al. 1959) and lies within the trade wind belt with prevailing easterly and northeasterly winds. Two kinds of interruptions in the normal trade wind regime may occur. First, strong northerly winds from continental North America bring cold air masses and heavy rains from October to January. Second, intense hurricanes have made landfall on the Belize coast on the average of once every 6 years between 1932 and 1961 (Stoddart 1962). The climate is influenced by the position of the intertropical convergence zone (ITCZ), which is situated over Belize during summer and moves south during winter. As a consequence, precipitation is highest during July to September. Annual rainfall increases from north to south from 124 cm to 380 cm, respectively (Purdy et al. 1975), reflecting mainland topography. The coast of Belize is a wave-dominated, semidiurnal microtidal area with a tidal range of 15-30 cm (Kjerfve et al. 1982). The surface circulation in the western Caribbean is dominated by the Caribbean current (James and Ginsburg 1979). The modern river drainage system is oriented toward E-NE north of Dangriga and toward E-SE south of Dangriga (Ferro et al. 1999). Drainage density is particularly high along the coast east of the Maya Mountains (High 1975). Major rivers such as the Belize River and the Sibun River carry high sediment loads, forming lobate deltas. Most of the other streams carry less sediment and form cuspate deltas (Ferro et al. 1999). Southerly longshore currents move considerable amounts of siliciclastic sediment that was previously transported by rivers from the hinterland to the low-lying coastal areas. Mean sea-surface temperatures of the shelf are 28.98°C during summer and 26.28°C during winter. Surface water salinity decreases from 35‰ at the shelf margin to 18‰ near the coast, and northward into Chetumal Bay and southward into the Gulf of Honduras (Purdy et al. 1975). Maximum salinity differences between surface and bottom waters of 29‰ were reported from the southern Belize coast (Purdy et al. 1975).

The oldest rocks are exposed in the Maya Mountains of southern Belize, which reach elevations of 1100 m, and include Paleozoic igneous, metamorphic, and siliciclastic rocks (Fig.

2.2). The remainder of the country is characterized by Cretaceous and Cenozoic limestone and dolostone and siliciclastics, the latter concentrated in the coastal lowlands of southern Belize. Siliciclastic muds, silts, and sands, derived from the Maya Mountains, are currently being deposited in the fluvial plain and along the coast (Esker et al. 1998). The offshore Belize Barrier Reef is situated 20–40 km from the coast. Together with the three atolls Turneffe, Lighthouse, and Glovers, this reef system is the largest in the Atlantic Ocean. The shallownorthern shelf is carbonate-dominated. The deeper southern shelf harbors a mixed system and is characterized by a siliciclastic to carbonate transition with an eastward increase of carbonate content (Purdy et al. 1975; Pusey 1975; Scott 1975). Barrier-lagoon complexes dominate the coast of Belize, which has low relief (High 1966). The central Belize coastal lowland is located south of Belize City in a 10–20-km-wide flat and low area that separates the coast from the Maya Mountains. The low coastal zone of Belize is entirely Quaternary with no outcropping rock exposures (Purdy et al. 2003).

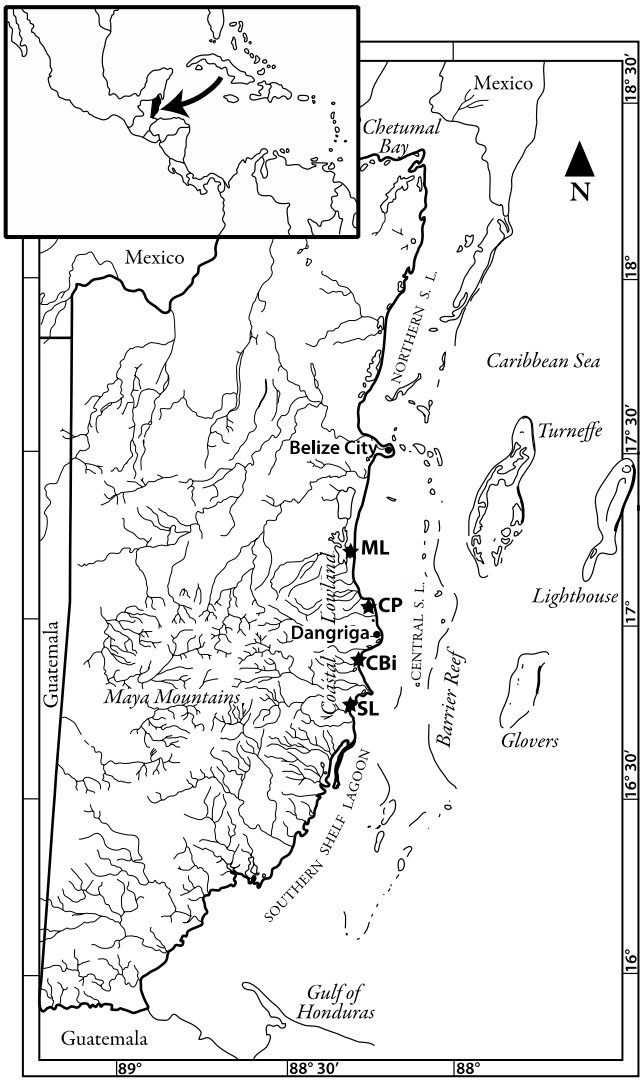

Fig. 2.1 Location map of Belize showing coring sites along the central coast of Belize. The inset map in the upper left shows the location of Belize in Central America. Asterisks mark the localities: Manatee Lagoon (ML), Mullins River Beach (MRB), Colson Point Lagoon (CP), Commerce Bight Lagoon (CBi), and Sapodilla Lagoon (SL)

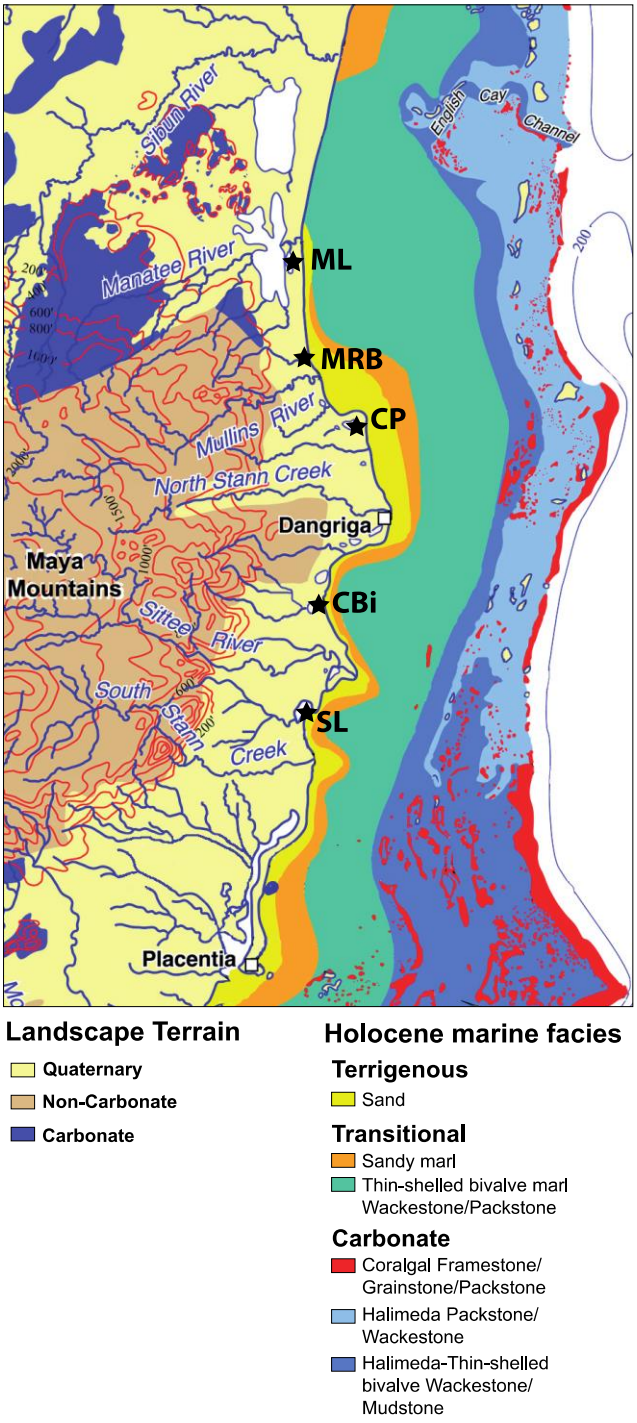

Fig. 2.2 Map of Belize showing the Holocene marine facies and mainland geology. The study area is located in the transitional zone between the mainland and the terrigenous facies belt (modified from Purdy and Gischler 2003). Asterisks mark the localities: Manatee Lagoon (ML), Mullins River Beach (MRB), Colson Point Lagoon (CP), Commerce Bight Lagoon (CBi) and Sapodilla Lagoon (SL)

The four coastal lagoons investigated show differences in their geomorphological features due to different coastal processes predominating (Figs 2.3a–e and 2.4a–e; list of cores in Table 2.1). These processes include riverine sediment input, connectivity of lagoon and shelf, waves, and longshore currents. The depositional coastal landforms observed in the study area include: lagoon, beach, barrier, barrier island, barrier spit, tidal delta, mangrove and littoral forest (mainly mangrove swamps), wetland (brackish lakes and littoral plain), and lowland savanna (short-grass savanna with scattered trees or shrubs). Vegetation is mainly composed of mangroves, which fringe lagoonal basins, swamps, and channels. The red mangrove *Rhizophora mangle* is the

most common mangrove in the study area. Some areas are affected by human activities such as agricultural use and road building.

The shape of the coastal lagoons is elongated in Manatee and Quashie Trap lagoons, and in Sapodilla Lagoon, with their long axes oriented parallel to the coastline (Figs 2.4a and 2.4 e). The shape of Commerce Bight Lagoon is subcircular (Fig. 2.4d). Colson Point Lagoon is composed of several subbasins (Fig. 2.4c). Highest salinities were measured in Sapodilla Lagoon, where a relatively wide opening in the lagoon barrier inlet allows water exchange with the open sea. The lowest salinities prevailed in Quashie Trap Lagoon, where no permanent connection to the sea exists (Table 2.2).

Sandy barriers separating lagoons from the shelf are developed at all four coastal lagoon sites. At Manatee Lagoon, the barrier is several hundred meters wide, densely vegetated, and breached by the Manatee River (Figs 2.3a and 2.4a). At Colson Point Lagoon, the barrier is densely covered by vegetation as well. A complex canal system, named Salt Creek, is oriented north to south and connects the lagoon with the open shelf lagoon (Figs 2.3c and 2.4c). At Commerce Bight Lagoon, the barrier is moderately vegetated and unbreached. It has a wavy outline on the leeward side. The lagoon is connected via a several-kilometers-long channel to the south with Freshwater Creek, which flows into the sea (Figure 2.4d). At Sapodilla Lagoon, two narrow barrier spits extend alongshore. One originates at the southern end of the lagoon (Figs 2.3e and 2.4e). The spit was breached at its southern end and thereupon a barrier island developed, leaving a narrow tidal channel between the remaining spit and the barrier island, which allows water exchange. In contrast to the smooth outline of the seaward region, the lagoonward outline of the spit and the barrier island is wavy. A second shorter but wider barrier spit extends from the northern end of the lagoon toward the south.

The lagoons receive freshwater from the mainland by rivers and creeks from the drainage system of the Maya Mountains (Fig. 2.3). Five major creeks including the Manatee River merge west of Manatee Lagoon and enter the lagoon on its western-central side region. Colson Point Lagoon receives water from Big Creek, which enters the lagoon in the SW. Commerce Bight Lagoon is fed by Back Ridge Creek in the SW. Sapodilla Lagoon receives freshwater in the southern area of the lagoon by Cabbage Haul Creek. Tidal deltas have developed in Manatee Lagoon, Colson Point Lagoon, and Commerce Bight Lagoon (Figs 2.4a, c–e). A few small tidal deltas exist in Sapodilla Lagoon (Fig. 2.4e). They developed at the lagoonward side of the tidal channel/tidal inlet.

At four localities, human activity is visible. At Mullins River Beach, a ca. 1.5- x 1.5-km-wide area was prepared for road construction. However, the swamp vegetation has recovered during the last few years. At Colson Point, Commerce Bight, and Sapodilla lagoons, artificial channels were created for aquaculture (shrimp mariculture) (Figs 2.3b–e). This is clearly visible on the satellite image of Sapodilla Lagoon (Fig. 2.3e).

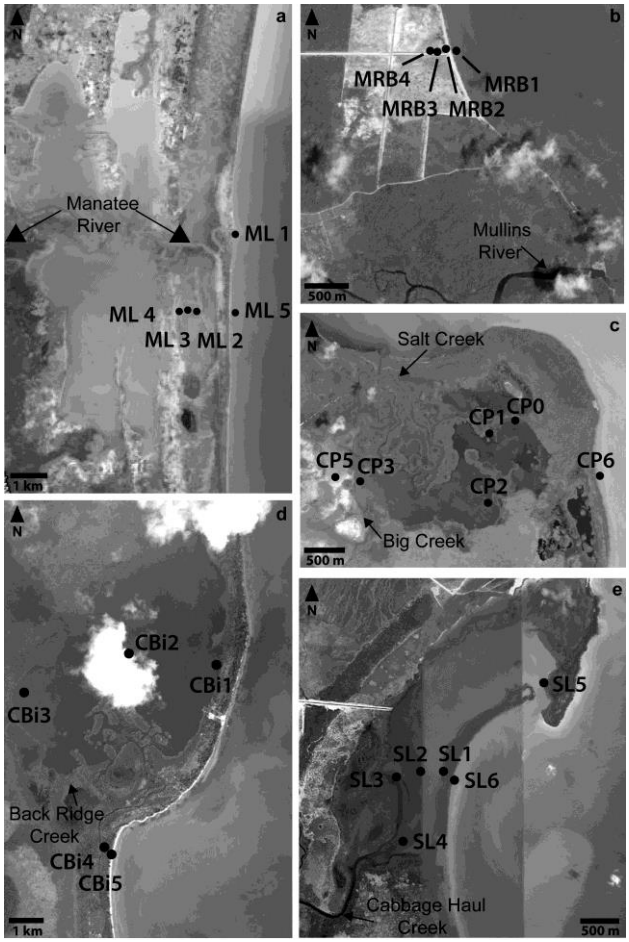

Fig. 2.3 Satellite images showing coring sites (from Google Earth). **a** Manatee Lagoon (Quasie Trap Lagoon). **b** Mullins River Beach. **c** Colson Point Lagoon. **d** Commerce Bight Lagoon. **e** Sapodilla Lagoon

Table 2.1 *List of cores drilled at Manatee Lagoon (ML), Mullins River Beach (MRB), Colson Point Lagoon (CP), Commerce Bight Lagoon (CBi), and Sapodilla Lagoon (SL)*

Core	Coordinates		Water depth (cm)	Core length (cm)	Penetration depth (cm)	Compaction (%)
	Latitude	Longitude				
ML 1	N 17° 13`50,3``	W 88° 18`13,5``	40	122.5	349	64.90
ML 2	N 17° 12`41,5``	W 88° 18`46,2``	57	452	478	5.44
ML 3	N 17° 12`41,8``	W 88° 18`53,3``	93	274	302	9.27
ML 4	N 17° 12`41,0``	W 88° 19`03,2``	73	437	464	5.82
ML 5	N 17° 12`39,8``	W 88° 18`13,8``	100	432	500	13.60
MRB1	N 17° 07`11,4``	W 88° 18`00``	81	394	499	21.04
MRB2	N 17° 07`11,6``	W 88° 18`02,2``	+100*	344	456	24.56
MRB3	N 17° 07`10,5``	W 88° 18`05,5``	0	269	305	11.80
MRB4	N 17° 07`10,6``	W 88° 18`06,6``	0	297	366	18.85
CP 0	N 17° 03`37,6``	W 88° 15`11,8``	58	318	338	5.90
CP 1	N 17° 03`25,7``	W 88° 15`22,2``	64	261	343	23.90
CP 2	N 17° 03`04,3``	W 88° 15`48,1``	88	168	257	34.60
CP 3	N 17° 03`12,9``	W 88° 16`13,6``	72	264	360	26.70
CP 5	N 17° 03`27,1``	W 88° 16`26,8``	57	99	109	9.17
CP 6	N 17° 03`15,3``	W 88° 14`37,9``	50	206	307	32.90
CBi 1	N 16° 54`04,5``	W 88° 16`55,9``	78	244	285	14.40
CBi 2	N 16° 54`08,2``	W 88° 17`17,0``	102	228	251	9.20
CBi 3	N 16° 53`55,3``	W 88° 17`42,2``	76	179	179	0.00
CBi 4	N 16° 53`18,6``	W 88° 17`22,7``	56	154	286	46.20
CBi 5	N 16° 53`18,1``	W 88° 17`21,6``	12	220	458	51.90
SL 1	N 16° 45`52,4``	W 88° 18`47,7``	109	271	366	26.00
SL 2	N 16° 45`52,5``	W 88° 18`58,3``	96	238	384	38.00
SL 3	N 16° 45`50,8``	W 88° 19`08,0``	78	325	453	28.26
SL 4	N 16° 45`22,0``	W 88° 19`05,8``	69	256	386	33.68
SL 5	N 16° 46`30,4``	W 88° 18`01,9``	94	457	489	26.18
SL 6	N 16° 45`48,4``	W 88° 18`43,7``	109	388	440	11.80

* elevation estimated

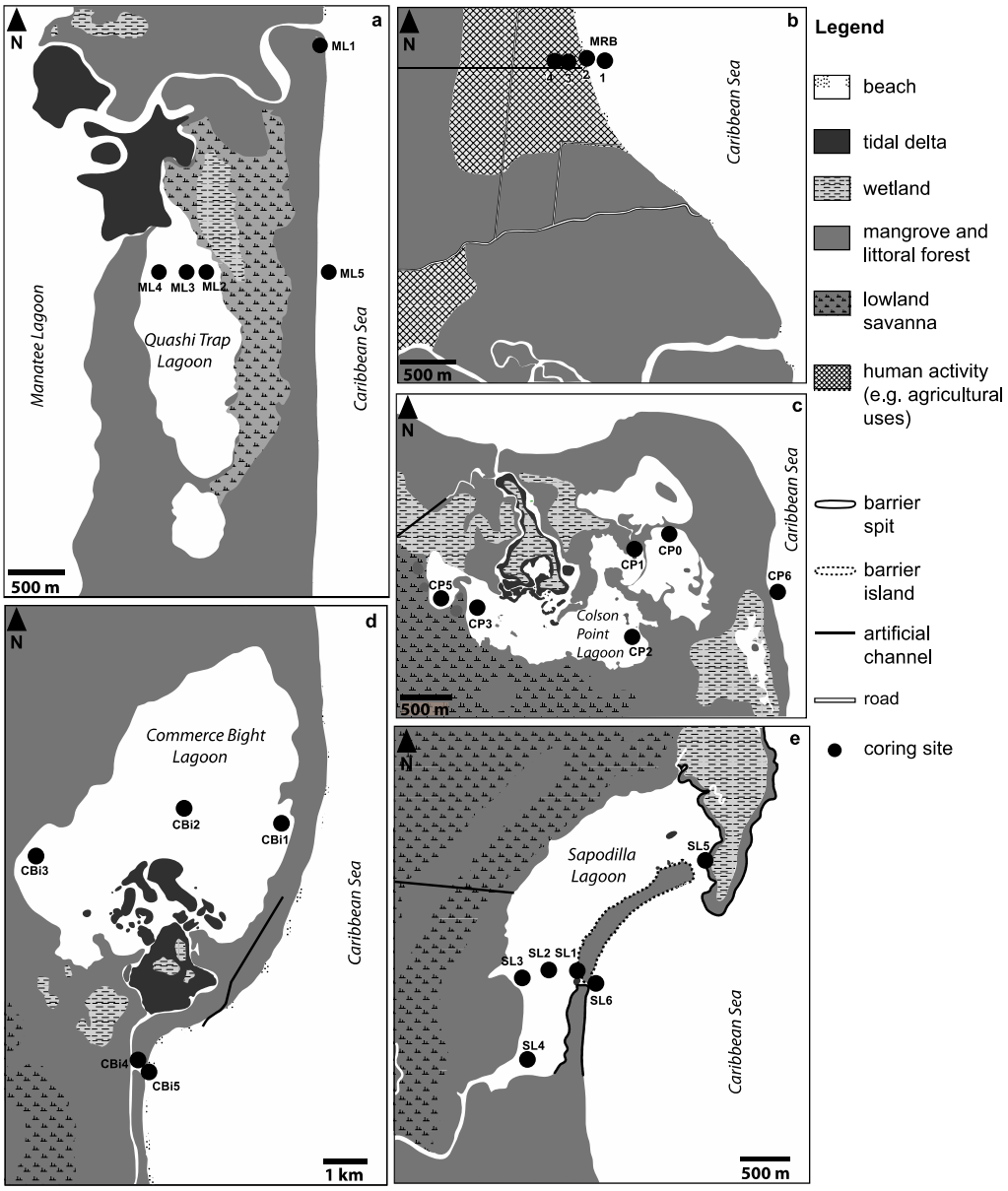

Fig. 2.4 Interpreted satellite images of the five coring sites (see Fig. 2.3)

2.3 Coring sites

As coring sites we selected the four coastal lagoons of Manatee (also called Southern Lagoon), Colson Point, Commerce Bight, and Sapodilla, and a reed swamp and salt marsh area north of Mullins River (Mullins River Beach), along the central coast of Belize (Fig. 2.1; Table 2.1). Core positions were selected to obtain transects in different coastal lagoons, more or less perpendicular to the coastline. Access was partly restricted because of high water depths and dense vegetation. The area of Mullins River Beach was selected to investigate whether or not this region comprises a former lagoon that has been filled. Also, major hurricanes in the 20th century made landfall in this area. The study sites are located between 17° 13' 50.3'' and 16° 45' 22'' N latitude and 88° 18' 13.5'' and 88° 19' 05.8'' W longitude and are situated in the Stann Creek District and the Belize District.

At Manatee Lagoon, five cores were obtained along a traverse. Three cores were taken in Quashie Trap Lagoon, which is a subbasin of Manatee Lagoon. One core was drilled in the marginal marine area and one core at the river mouth of Manatee River where a sandbar (Manatee Bar) developed (Fig. 2.3a). The subbasin of Quashie Trap Lagoon is situated about 1 km south of Manatee River. The distance between the sandy beach shoreline and the Quashie Trap Lagoon, which is connected to the Manatee Lagoon by one channel, is ca. 670 m. The Quashie Trap Lagoon covers an area with dimensions of about 2.5 x 0.95 km. Water depths at coring sites were ≤93 cm. Salinity was 8-8.1‰ during winter and 4.3-5.9‰ in the summer (Table 2.2).

At Mullins River Beach, four cores were collected perpendicular to the coast, representing a traverse of three cores on the coastal plain and one core in the marginal marine area (Fig. 2.3b). The coring sites of Mullins River Beach are located about 2 km north of the mouth of Mullins River and in an area covered by salt marsh and reed swamp behind a sandy beach. Recently, the area has been modified and prepared for building in that vegetation was bulldozed and an E-W running rubble causeway was banked up.

Colson Point Lagoon is located on a mangrove-covered headland, where a very narrow sandy beach has developed in the east; there is no beach along the northern margin of the headland. At this location, five cores were taken in the lagoon and one in the marginal marine area (Fig. 2.3c). The distance from Colson Point Lagoon to the open shelf lagoon is 0.9 km in the north and 1.2 km in the east. The connection with the ocean is made through a braided channel system that runs from the north into the lagoon. The irregularly shaped lagoon covers an area with dimensions of about 2.5 x 1.2 km. Water depths at coring sites were ≤88 cm. Salinity ranged between 3.1‰ and 7‰ in winter and 11‰and 19‰ in summer (Table 2.2).

In Commerce Bight Lagoon, which is located north of the village of Hopkins, three cores were obtained from the lagoon and two cores from the channel connecting the lagoon with the waters of the Belize shelf (Fig. 2.3d). Measured water depths were ≤102 cm. Commerce Bight Lagoon is separated from the sea by a narrow sand barrier some 130 m wide. The lagoon covers an area with dimensions of about 1.4 x 1.6 km. A ca. 1.3- km-long and ca. 10-m-wide mangrove-fringed channel that runs parallel to the coastline branches from the mouth of the Freshwater Creek and connects the lagoon with the Belize shelf. Salinity measurements were between 8‰ and 14.1‰ in winter and 14.1‰ and 20.2‰ in summer (Table 2.2).

In Sapodilla Lagoon, four cores were taken in the lagoon proper, one core in the marginal marine area and one at the northern entrance into the lagoon (Fig. 2.3e). The lagoon is separated from the sea by a 100–180-m-wide barrier sand spit. A 130–140-m-wide tidal inlet is located in the northern area of the lagoon. Water depths at the coring sites were ≤93 cm. The size of the lagoon is about 3.6 x 0.8 km. Salinity was 6.8–26.6‰ (winter) and 3.7–24.5‰ (summer) and thus higher than in the other lagoons (Table 2.2).

Table 2.2 *Salinity data from two sites each at Manatee Lagoon, Colson Point Lagoon, Commerce Bight Lagoon, and Sapodilla Lagoon. At Sapodilla Lagoon water samples were collected in the southern and in the northern areas of the lagoon in winter and in the western and eastern areas of the lagoon in summer. B, bottom water; T, surface water*

Salinity (‰)										
Season	Date	Water Depth	Manatee Lagoon		Colson Point Lagoon		Commerce Bight Lagoon		Sapodilla Lagoon	
			W	E	W	E	W	E	S/W	N/E
Winter	21 January 2012	T	8.1	8	7	3.1	8	14.1	6.8	26.6
Summer	14 July 2012	T	4.4	5	11	17.5	14.1	19.7	3.7	8
		B	4.3	5.9	16.3	19	16.5	20.2	4	24.5

2.4 Methods

Fieldwork took place in July and August 2011. A portable vibracorer (Lanesky et al. 1979) and 5.9-m-long aluminum tubes with a diameter of 7.5 cm, equipped with a copper core catcher, were used for coring. Coordinates at the coring sites were registered using GPS. Core elevation was related to mean sea level. A total of 26 cores with a total length of 73 m was obtained (Table 2.1). Core length ranged from 1.1 to 5 m. The average length is 2.8 m. Compaction ranged from 0% to 65%. Geomorphology was studied by field observations and additionally by using satellite imagery provided by Google Earth.

Water samples for salinity measurements were collected at one proximal and one distal site in each of the four lagoon sites during winter (21 January 2011) and summer (14 July 2012) (Table 2.2). Concentrations of major ions (Na^+, Mg^{2+}, Ca^{2+}, Cl^-, SO_4^{2-}, HCO_3^-) were measured at the laboratory of ALA Aachen. Salinity, which may have influence on sedimentation and ecological conditions (Bird 1994), is affected by multiple factors like precipitation, river discharge, tides, and storm surge. Brackish water conditions developed because of mixing of freshwater from river sources and marine water from the sea, which indicates a transitional ecosystem, affected by both terrestrial and marine sources.

In the laboratory, core tubes were cut in halves lengthwise using an angle grinder and knife. Photo documentation and core description were carried out, including descriptions of lithology, thickness, sedimentary structures, and sedimentary contacts. Percent compaction for each core was calculated, using core recovery and penetration depths recorded in the field. Thereon, core logs and schematic cross-sections of the lagoons were prepared. The core logs can be used for facies, and radiometric and lithological correlations. Depths given in the text refer to depths below core top corrected for compaction. Measured water depths can be referred to mean sea-level because a low tidal range of ≤30 cm can be assumed for this microtidal area. Samples were taken from each lithological unit, when possible, with 5-cm thickness. Additionally, subsamples (from within the 5-cm intervals) were collected for further sedimentological analyses. The number

of samples studied was 30 in Manatee Lagoon, 45 in Mullins River Beach, 40 in Colson Point Lagoon, 26 in Commerce Bight Lagoon, and 28 in Sapodilla Lagoon, 169 samples in total. Sediment was washed through 2-mm, 1-mm, 500-µm, 250-µm, 125-µm, and 63-µm sieves for grain size analysis and to isolate shells from the sediment for paleontological and paleoecological studies. Sediments were categorized into sediment types by combining grain size analysis and core description. Macrofossils (≥2 mm) were identified for better interpretation of facies using the descriptions and illustrations of Turney and Perkins (1972) and Abbott (1974). Subsamples of total sediment were pulverized for X-ray diffractometry and for determination of carbonate content (Milliman 1974). Carbonate content was measured with a Scheibler calcimeter (Müller 1967).

Mineralogy was determined by X-ray diffraction (XRD) using a Panalytical X'Pert Pro. Mineral phases were identified using the Panalytical-Software ''X'Pert Highscore Plus.'' Intensity measurements were carried out using the software ''MacDiff'' (Petschick et al. 1996). Mineral percentages refer to relative weight proportions determined by peak intensities of noncoincided diffraction maxima. For determination of organic matter content, the loss on ignition of peats and organic sediments was measured after heating the samples in an oven at 600°C for 3 hours. For radiocarbon dating, 58 samples of peat, organic sediment, wood, bivalve shells, and corals were selected (Table 2.3). Bivalve shells are considered to be autochthonous to parautochthonous on the basis of paleoecological investigations (Adomat et al. 2016); corals are transported fragments. Measurements were undertaken by Beta Analytic Inc., Miami, Florida, using accelerator mass spectrometry. Radiocarbon ages were converted to calendar years using Intcal09 (Talma and Vogel 1993). Calibrated ages are given with 2 σ error range. For calibration of carbonate shells the Marine09 database, and for peat and organic sediments the Intcal09 database, were applied. The variables used in the calculation for marine reservoir effect correction of carbonate shells Delta-R=120±27 and Glob res=-200 to 500.

2.5 Results

2.5.1 Sedimentary facies and minerals

The basement of the Holocene sediments is a Pleistocene soil. Pleistocene sands and silts underlying the soil were only recovered in one core. Four Holocene sedimentary facies were recognized, and are distinguished on the basis of texture and color (Figs 2.5 and 2.6). They include (1) mud (often with shells and mangrove roots), (2) sand, (3) peat/peaty sediment, and (4) transitions among facies types such as silt to fine sand and muddy sand with grain-size distribution between the mud and the sand facies. As a general spatial distribution pattern, fine-grained facies occur in the central lagoonal basins and coarser-grained facies are found at lagoonal margins.

Table 2.3 *List of accelerator mass spectrometry 14C ages reported by Beta Analytic Inc., Miami, Florida*

Core	Sample (uncorrected depth below core top, in cm)	Dated Material	Depth below sea level (corrected for compaction, in cm)	Measured age (year BP)±1σ	13C/12C ratio (‰)	Conventional age (year BP)	Calibrated calendar age, 2 σ range (year BP)	BETA No.
ML1	55-58	organic matter	201	690±30	-24.3	700±30	665±15, 575±5	325007
ML1	102-107	bivalve shell	338	1750±30	-4.6	2080±30	1500±100	348282
ML2	0-5	bivalve shell	60	124.2±0.4 (pMC)	-0.4	118.2±0.4	modern	348283
ML2	74-75	organic matter	139	3900±30	-25.5	3890±30	4330±90	325008
ML2	103-105	bivalve shell	167	5030±30	-4.3	5370±30	5620±60	348284
ML2	159-162	bivalve shell	233	1740±30	-6.4	2050±30	1470±90	325009
ML3	17-22	bivalve shell	114	3540±30	-7.7	3820±30	3610±90	348285
ML3	27-28	organic matter	123	3820±30	-26.3	3800±30	4275±5, 4195±55, 4110±20	325010
ML3	99-104	bivalve shell	205	4730±30	-4	5070±30	5315±85	325011
ML4	20-25	bivalve shell	118	109.9±0.3 (pMC)	-2.5	105±0.3	modern	348286
ML5	60-65	bivalve shell	173	290±30	-1.1	680±30	180±100	325012
ML5	425-426	organic matter	494	5920±40	-26.4	5900±40	6725±75, 6645±5	325013
MRB1	38-43	bivalve shell	132	107.5±0.3 (pMC)	+0.4	102±0.3	modern	348287
MRB1	222-223	organic matter	363	7100±40	-28.2	7050±40	7875±85	345343
MRB1	229-230	organic matter	372	7190±40	-27	7160±40	7980±40	345344
MRB2	255-256	organic matter	239	6250±30	-30.3	6160±30	7055±105	345345
MRB2	296-297	organic matter	293	6940±40	-24.4	6950±40	7910±10, 7770±90	345346
MRB3	179	organic matter	203	6310±40	-25.8	6300±40	7235±75	345347
MRB3	267-269	organic matter	304	3160±30	-26.0	3140±30	3435±5, 3370±30, 3280	345348
MRB4	243-244	organic matter	300	6070±40	-26.4	6050±40	6895±105	345349
CP0	33-38	bivalve shell	96	1730±30	-2.9	2090±30	1510±100	238280
CP0	105-110	bivalve shell	172	3940±30	-5	4270±30	4215±125	348281
CP1	70-75	bivalve shell	159	2280±30	-2.6	2650±30	2200±100	307038
CP1	86-88	organic matter	178	3610±30	-24.4	3620±30	4055±5, 3920±70	307039
CP1	187-192	bivalve shell	312	5400±30	-6.7	5700±30	5985±105	307040
CP2	5-10	bivalve shell	99	2200±30	-3.1	2560±30	2070±90	307041
CP2	20-25	bivalve shell	122	2200±30	-1.6	2580±30	2115±125	307042
CP2	40-45	organic matter	153	3420±30	-26.2	3400±30	3634±65	307043
CP3	5-10	bivalve shell	82	150±30	-2.7	520±30	modern	307044
CP6	52-57	bivalve shell	131	30±30	-1.1	420±30	modern	307045
CP6	89	coral	183	560±30	-4.7	890±30	390±90	307046
CP6	119-121	organic matter	229	4530±30	-23.8	4550±30	5295±25, 5220, 5150±30, 5085±25	307047
CP6	130-135	bivalve shell	247	4370±30	-4	4710±30	4815±45	307048
CBi1	157-160	coral	263	4500±30	-3.6	4850±30	4945±105	317594
CBi1	169-170	organic matter	276	4380±30	-27	4350±30	5025±5, 4910±60	317595
CBi1	212-213	organic matter	327	4720±30	-28.7	4660±30	5390±80	317596
CBi1	243-244	peat	363	4860±40	-25.6	4850±40	5615±35, 5525±5, 5500±20	317597
CBi2	47-48	organic matter	154	4080±30	-25.2	4080±30	4780±20, 4685±5, 4580±60, 4460±10	348278
CBi2	84-85	organic matter	195	3560±30	-26.3	3540±30	3855±45, 3760±40	317598
CBi4	38	bivalve shell	127	115.5±0.3	-3.7	110.6±0.3	modern	348279
CBi4	100-101	organic matter	243	80±30	-28	30±30	modern	317599
CBi4	107-112	coral	260	1820±30	-6	2130±30	1585±95	317600
CBi4	153-154	organic matter	342	1630±30	-22.6	1670±30	1680±10, 1570±50	317601
CBi5	125-130	coral	277	1140±30	-3	1500±30	925±65	317602
CBi5	153-158	coral	335	2810±30	-5.5	3130±30	2780±70	317603
CBi5	208-213	coral	450	1860±30	-3.2	2220±30	1675±105	317604
SL1	40-45	bivalve shell	166	320±30	-3.9	670±30	modern	348288
SL1	220-225	bivalve shell	409	3710±30	-0.1	4120±30	4005±115	320754
SL1	240-241	peat	434	5790±40	-27	5760±40	6555±105	320755
SL2	214-216	peat	442	5290±30	-26.2	5270±30	6160±20, 6050±70, 5960±20	320756
SL3	211-212	organic matter	372	5420±30	-28.1	5370±30	6255±25, 6200±20, 6130±20, 6070±10, 6035±15	320757
SL4	150-155	bivalve shell	299	1260±30	-0.8	1660±30	1080±90	320758
SL4	199-200	peat	370	5180±40	-26.4	5160±40	5975±15, 5920±30, 5795±5, 5775±5	320759
SL5	46-51	bivalve shell	146	830±30	+0.5	1250±30	680±50	320760
SL5	270-275	bivalve shell	386	5340±30	+0.9	5760±30	6040±120	348292
SL5	452-457	bivalve shell	580	3580±30	+1.9	4020±30	3880±90	320761
SL6	91-96	bivalve shell	215	1730±30	+0.6	2150±30	1600±90	320762
SL6	360-361	organic matter	516	4750±30	-26.6	4720±30	5545±35, 5465±25, 5365±45	320763

Thickness of Holocene sediments ranges from 64 to 500 cm at Manatee Lagoon, 305 to 420 cm at Mullins River Beach, 15 to 264 cm at Colson Point Lagoon, 55 to 443 cm at Commerce Bight Lagoon, and 338 to 489 cm at Sapodilla Lagoon. Ten minerals were encountered in the samples, namely quartz, microcline, albite, andalusite, muscovite, kaolinite, pyrite, aragonite, low-Mg calcite, and high-Mg calcite (Fig. 2.7; Tables 2.4 and 2.5). Additionally, ankerite was only found in concretions in core 6 from Sapodilla Lagoon (SL6). Quartz forms the most common mineral of the clastics (18-91%), followed by muscovite (0-42%) and feldspar (microcline, 0- 19%; albite, 0-6.8%). Kaolinite (0-10.7%), pyrite (0-5.4%), and andalusite (0-34.8%) occur in smaller amounts. Carbonate minerals are represented by aragonite (0-43.5%), low-Mg calcite (0-10.3%),

high-Mg calcite (0-9.5%), and ankerite (0-8.1%). No spatial patterns in mineral composition are seen among the localities investigated (Fig. 2.7).

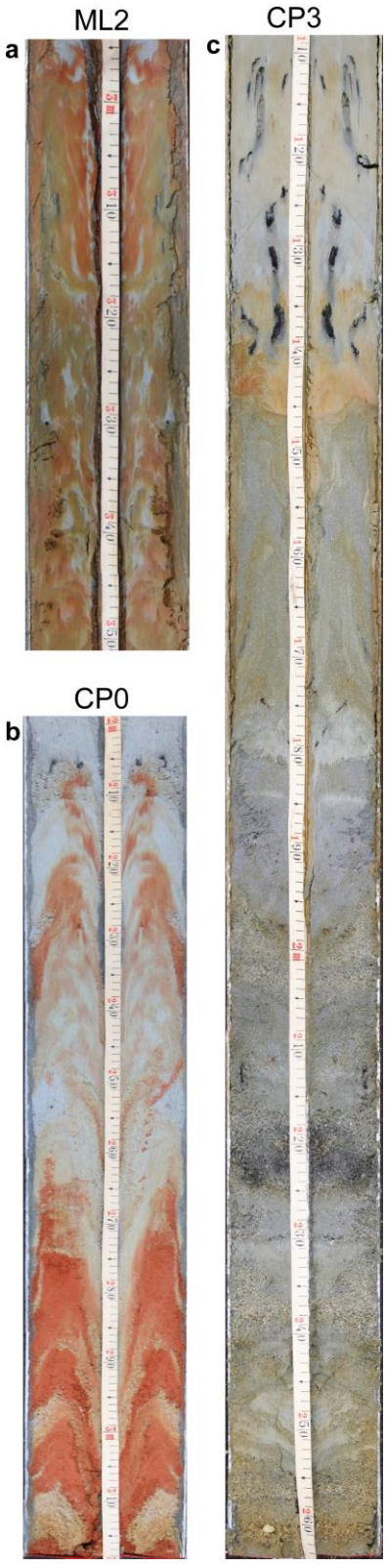

Fig. 2.5 Photographs of selected cores with representative Pleistocene facies. **a** ML2 (2.95-m to 3.5-m core depth): Soil with soft sediment deformation structures. **b** CP0 (2-m to 3.18-m core depth): Soil with soft sediment deformation structures and coarse sand. **c** CP3 (1.1-m to 2.64-m core depth): Soft sediment deformation structures in the upper half and underlying Pleistocene sands and silts

2.5.2 Pleistocene basement

A stiff bluish-gray soil, i.e., consisting of sand, silt, and clay, mostly with orange-yellow to reddish stain, forms the base in 15 of the 26 cores (Figs 2.5a,b). This facies was found at all localities (Figs 2.8–2.12). It is interpreted to have been deposited during the Pleistocene. This assumption is based on comparisons with core data from High (1975) and Gischler (2007) in Belize. Thickness amounts to at least 400 cm in core 4 from Manatee Lagoon (ML4) (Fig. 2.9). The base was only recovered in core 3 from Colson Point Lagoon (CP3), where sands and silts underlie the soil (Fig. 2.11). Grain size distribution shows a dominant mode in the <63 µm and in the fine to medium sand fractions. Mineralogically, the soil consists of 68.7% quartz, 15.7% muscovite, 3.9% kaolinite, 3.7% aragonite, 3.7% microcline, 2.5% albite, 1.5% andalusite and 0.3% pyrite. In core CBi2 a 6.5 x 4 cm-sized clast that consists of quartz and is penetrated by mangrove roots was found in the soil. No macrofauna was found. Mica flakes were observed in some cores. The Pleistocene/ Holocene-boundary deepens seaward at all locations except in Colson Point Lagoon. In some cores (ML2, ML3, ML4, CP0, CP3) from the three northern localities of Manatee Lagoon, Mullins River Beach (MRB1), and Colson Point Lagoon, deformation of sediment was observed within the soil (Fig. 2.5). Core CP0 shows deformation structures in stained sandy soil deposits. In core CP3, deformation affected micaceous silty to sandy sediments. Core ML2 exhibits deformation structures in a fine-grained stained soil. Similar structures were observed in fine-

grained soil in ML3 and in micaceous bluish soil in ML4. In core CP3, Pleistocene terrestrial or tidal sands and silts with mica flakes and wavy bedding structures underlie the bluish-gray soil (Fig. 2.5c). These sediments are composed of 74.5% quartz, 9.8% aragonite 5.8% microcline, 4.5% muscovite, 2.7% andalusite, 1.4% albite, 1.1% kaolinite, 0.2% low-Mg calcite, and 0.1% high-Mg calcite. Thickness is 160 cm.

Table 2.4 *Mineral composition of samples from Manatee Lagoon (ML), Mullins River Beach (MRB), Colson Point Lagoon (CP), Commerce Bight Lagoon (CBi),and Sapodilla Lagoon (SL) (identified and quantified using X-ray diffraction)*

Locality	Quartz (%)	Microcline (%)	Albite (%)	Andalusite (%)	Muscovite (%)	Kaolinite (%)	Pyrite (%)	Aragonite (%)	Calcite (%)	Mg-Calcite (%)
ML	62.2-88.7	3.8-8.6	0-3.1	0-5.1	0-21.1	0-3.1	0-2.4	0-19.8	0-2.0	0-1.7
MRB	29.5-90.6	3.0-19.2	0-6.2	0-34.8	0-42,4	0-10.7	0-1.9	0-5.2	0-0.7	0-0.8
CP	40.2-87.3	0-15.8	0-6.2	0-4.5	1.9-33.5	0-9.4	0-2.4	0-0.08	0-0.8	0-0.9
CBi	35.9-85.2	0-14.4	1.2-6.8	0-2.6	0-22.4	0-5.3	0-5.4	0-13.6	0-0.7	0-1.2
SL	17.8-89.1	0-18.8	0-6.7	0-2.1	1.8-29.4	0-5	0-4.4	0-43.5	0-10.3	0-9.5

Table 2.5 *Mineral composition of facies types (identified and quantified using X-ray diffraction)*

Facies type	Quartz (%)	Microcline (%)	Albite (%)	Andalusite (%)	Muscovite (%)	Kaolinite (%)	Pyrite (%)	Aragonite (%)	Calcite (%)	Mg-Calcite (%)
Soil	44.8-88.3	0-7.0	0-5.2	0-4.1	4.7-32.5	0-9.4	0-1.1	0-9.6	0	0-0.4
Mud	29.5-88.0	2.6-13.3	1.3-8.5	0-3.0	3.4-33.5	1.1-10.7	0-5.4	0-13.6	0-2.0	0-2.0
Shell concentration	17.8-84.1	0-15.8	0-3.7	0-4.1	0-18.9	0-3.9	0-2.6	3.2-42.6	0-10.3	0-1.2
Mud/silt to fine sand	33-84.9	4.3-18.9	0-7.3	0-5.3	0-41.2	0-10	0-2.4	0-43.5	0-5.3	0-1.2
Muddy sand	66.1-88.1	0-10.6	0-4.7	0-4.6	0-16	0-4.8	0-06	0-11.0	0-0.3	0-0.3
Sand	53.4-90.6	0-19.2	0-5.3	0-34.8	0-7.3	0-1.5	0-0.2	0-19.8	0-1.1	0-0.6

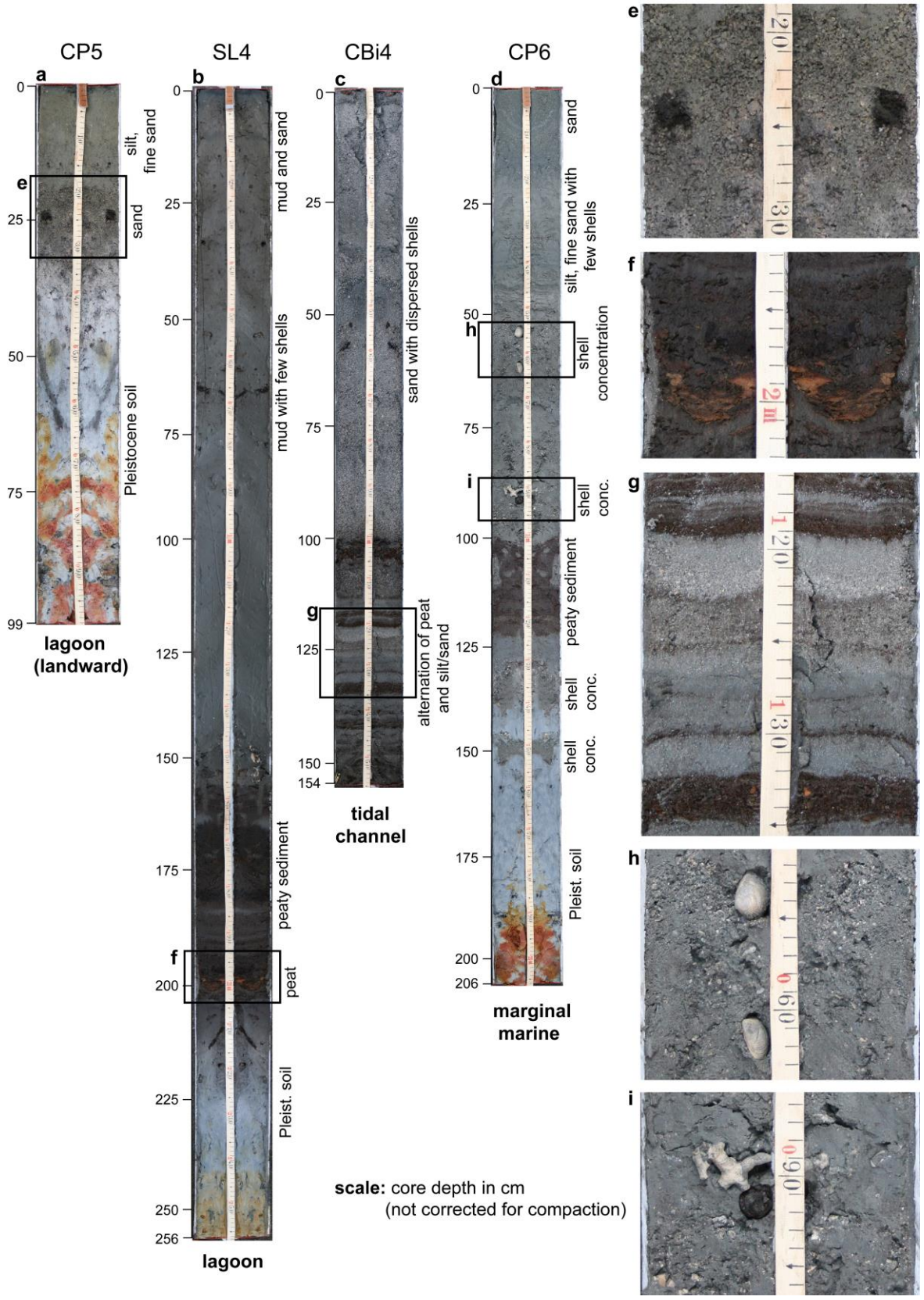

Fig. 2.6 Photographs of selected cores with representative Holocene facies. **a** CP5 from the landward area of a coastal lagoon. **b** SL4 from the center of a lagoon. **c** CBi4 from a tidal channel. **d** CP6 from the marginal marine area. **e** Quartz sand, which was transported into the lagoon by rivers. **f** Peat of the red mangrove *Rhizophora mangle*. **g** Alternation of peaty sediments and silts/sands indicating shifting facies in the tidal channel. **h** Close-up of shell concentration, which contains large specimens of the marine bivalve *Chione cancellata*. **i** Close-up of shell concentration with *Porites porites* fragments

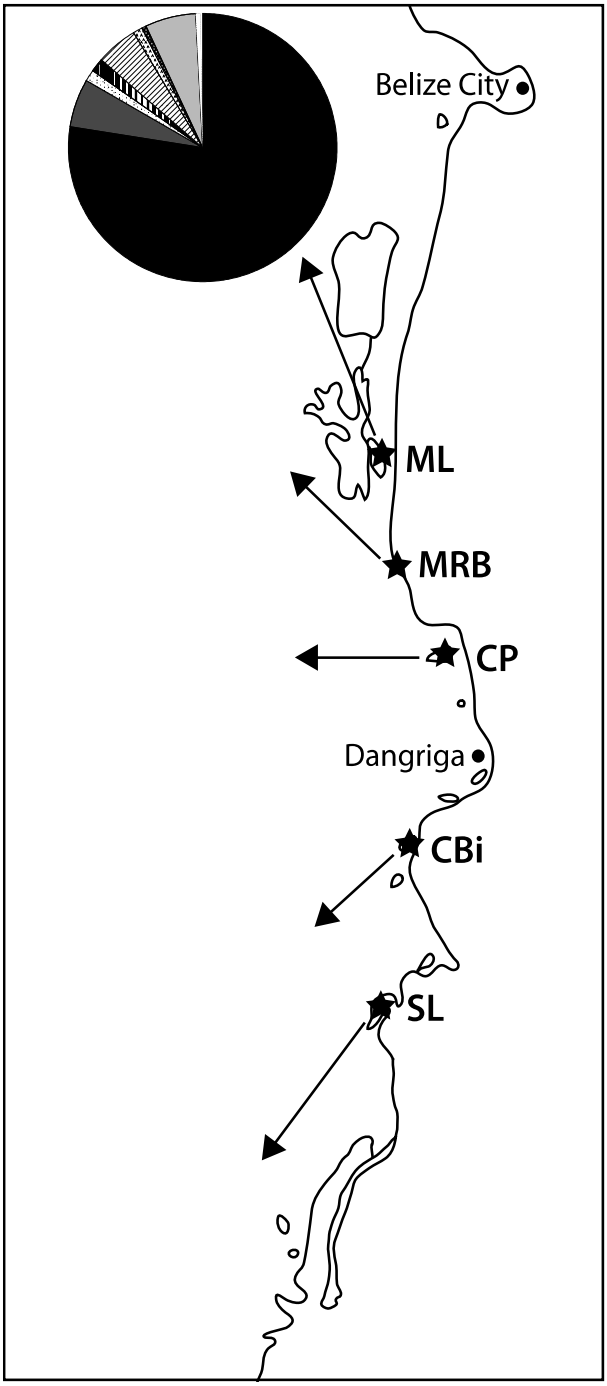

Fig. 2.7 Map of Belize coast showing mineralogic variation in Holocene sediments on pie diagrams

2.5.3 Holocene sedimentary facies

2.5.3.1 Mud

The most common sedimentary facies of Holocene deposits is a soft dark-gray mud with variable amounts of mollusk shells and mangrove roots (Fig. 2.6b). The latter originate from the

red mangrove *R. mangle*. Mud facies were recovered largely in the central basins of lagoons, but also in subsurface sediments of swamps and tidal inlet environments. Thickness of the muddy deposits ranges from 1 to 346 cm in lagoons. Grain size distribution shows a dominant mode in the <63 µm fraction. The carbonate content is ≤10% and largely derives from mollusk shells, both dispersed and concentrated in thin layers. Bivalves and gastropods are characteristic of the brackish lagoon environment and include *A. cuneimeris* and cerithid gastropods, respectively. Mineralogically, the mud consists of 60.4% quartz, 19% muscovite, 6.9% microcline, 4.5% albite, 4.3% kaolinite 2.3% aragonite, 1.6% pyrite, 0.8% andalusite, 0.2% low-Mg calcite, and 0.1% high-Mg calcite.

2.5.3.2 Sand

Sand facies occur in nearshore environments such as the transitional zone between the lagoon and the sea. The nearshore environment includes back-barrier lagoon areas (CBi1), tidal channels (CBi4, CBi5), beaches (MRB2), and marginal marine areas (ML1, ML5, MRB1, CP6, SL6). Sand facies were also found in one landward lagoon core (CP5) and as a landward thinning sand layer in MRB1 and MRB2. Sands from the nearshore area contain shells. In some of these medium to very coarse sands, a marine fauna with *Halimeda* sp., mollusk shells (bivalves: e.g., *Chione cancellata*, arcids, *Corbula* sp., *Strigilla* sp., *Donax* sp., gastropods: e.g., *Olivella* sp., *Crepidula incurva*, scaphopods: *Dentalium* sp.), and coral fragments (*Porites porites*, *Cladocora* sp.) and gravel were found. Graded sands usually did not contain any mollusk shells. Apart from the shell concentration in ML5, mollusks occur dispersed within the sands. In the sand facies of Commerce Bight Lagoon and Mullins River Beach mica particles were recognized. Thickness of sand is 8 to 324 cm. The sand facies are comprised of 77.5% quartz, 8.9% microcline, 6.4% aragonite, 2.7% andalusite, 1.8% albite, 1.8% muscovite, 0.7% kaolinite, 0.3% low-Mg calcite, 0.1% high-Mg calcite, and 0.01% pyrite. Highest quartz content was 90.6%, measured at top of core MRB2.

2.5.3.3 Silt to fine sand, muddy sand

Mixed transitional facies between the mud and sand facies were largely recovered in cores from lagoon margins, but also from marginal marine areas (Figs 2.6a,d). In the silts and fine sands mica flakes are common. They are less well sorted than the aforementioned sediments. According to the results of XRD, silt to fine sand facies are intermediate between those of the mud facies and the sand facies. They consist of 69.4% quartz, 9.2% microcline, 8.2% muscovite, 4.8% aragonite, 3.3% albite, 1.9% kaolinite, 1.7% andalusite, 0.6% low-Mg calcite, 0.5% pyrite, and 0.4% Mg calcite. Muddy sands contain 81.5% sand, 4.9% microcline, 4.6% muscovite, 4.4% aragonite, 1.7% albite, 1.4% andalusite, 1.3% kaolinite, 0.1% pyrite, 0.1% low-Mg calcite and 0.02% high-Mg calcite. These facies occur both in lagoon cores and in marginal marine cores.

2.5.3.4 Peat, peaty sediment

Sediments with an organic matter content of ≥60% were defined as peats and sediments with <60% organic matter as peaty sediments. Peat and peaty sediment occur in cores from lagoons, tidal channels, marginal marine areas, and less pronounced in cores from Mullins River Beach. They developed in vegetated shallow water environments. Thicknesses range from 1 to 69 cm (Figs 2.6b–d, f). Except for CBi1, CBi4, and MRB1, peats and peaty sediments are overlain by fine-grained sediments with low contents of organic matter. The organic matter content of peats and peaty sediments is 2.28% to 76.7%. Peat was recovered in the cores CBi1, SL1, SL2, and SL4. The color of the peat is reddish brown. Peat and peaty sediments release water upon compression. The top of the peat-rich units often shows burrows filled with overlying sediment. Some peat-rich units are interrupted by mud or sand layers.

2.6 Facies successions and radiocarbon dating

At Manatee Lagoon the thickness of Holocene sediments ranges from 64 cm (ML4) to 171 cm (ML2) in lagoon cores (Fig. 2.8). In core ML5, taken from the marginal marine area, 5 m of Holocene sediments were recovered. The base of the Holocene in the lagoon was dated to 5315 ± 85 calendar years before present (cal BP) (ML3). The succession in lagoon cores starts at the base with Pleistocene soil. Up to 4 m of this soil were recovered in the most landward core of the lagoon (ML4). This facies makes the transition to organic-rich muddy sediments (ML2, ML3). In ML2 and ML3, mollusk shell concentrations were observed between the soil and the organic-rich mud. Several distinct shell concentrations were observed in all lagoon cores. Dominant species include the bivalve *A. cuneimeris* and cerithid gastropods. In core ML5, taken in the marginal marine area, the succession starts with bioturbated peaty sediment (dated to 6720 ± 80 cal BP) and continues upward with a sharp contact to overlying mud and fine-grained sands. The 390-cm-thick fine sediments are overlain by a thin mud layer. The top of the core consists of yellowish sand that contains a marginal marine mollusk fauna at the base. Bivalves include e.g., *C. cancellata*, arcids, *Corbula* sp., *Lucina muricata*, *Strigilla* sp., and *Donax* sp. Gastropods comprise *Olivella* sp. and *C. incurva*; scaphopods are represented by *Dentalium* sp. The change from fine lagoonal sediment to coarser barrier sand, separated by a mud layer at a depth of 73 cm, was dated to 180 ± 100 cal BP. Core ML1, drilled close to the mouth of Manatee River, mainly consists of medium sand, its base dated to 1500 ± 100 cal BP. Peaty sediment, dated to 625 ± 55 cal BP, separates gray coarse sand with shells from yellowish-brown medium to coarse sand at the top of the core. Sands are coarser at the river mouth (ML1, coarse sand) than at top of ML5 (fine to medium sand).

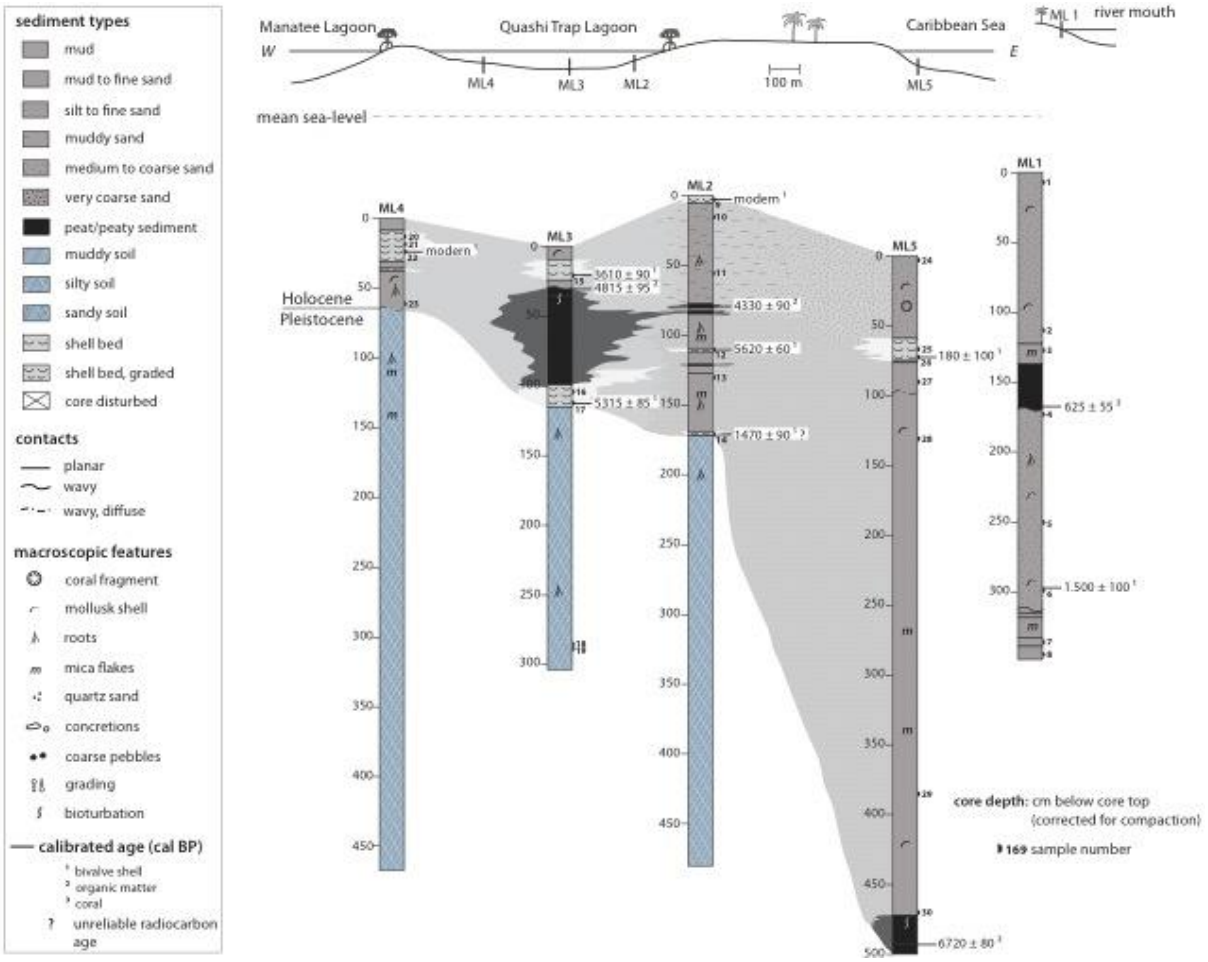

Fig. 2.8 Core logs and interpreted sedimentary facies for Manatee Lagoon. Location of coring sites is shown in Figures 2.3 and 2.4. Core logs were corrected for compaction and are arranged with reference to the sea level

The thickness of Holocene sediments at Mullins River Beach reaches 420 cm (MRB2) (Fig. 2.9). The underlying Pleistocene was recovered in three of four cores. The base of Holocene sediments was dated to 6895 ± 105 cal BP in the most landward core. The base in Holocene deposits in more seaward cores is older (7890–7980 cal BP). Sediments from Mullins River Beach are predominantly fine grained. In MRB1, MRB2, and MRB4, there is a succession of soil and organic-rich, fine-grained sediments, intercalated with distinct sand layers. The sand layers in MRB1 and MRB2 were dated to ~7900 cal BP and can be correlated. A landward decrease in thickness of the sand layer from 50.8 cm to 1.3 cm was observed. In MRB1, this sand layer shows reverse (coarsening upward) grading from medium to gravelly coarse sand. Additionally, a 125-cm-thick deposit with parallel laminations of mud and silt to sand overlying the sand layer was found in MRB1. The sand layer in MRB4 cannot be correlated with the aforementioned sand layers in MRB1 and MRB2. In core MRB3, at a depth of about 200 cm, a layer of charred organic material was detected. No shells were found in the sediments from the coastal plain. The tops of MRB1 and MRB2 consist of coarse to fine and medium to coarse sand, respectively. The sand at the top ofMRB1 from the marginal marine area contains shells of marginal marine mollusk species. Bivalves include *C. cancellata*, *Strigilla* sp., and *Donax* sp. Gastropods comprise *Olivella*

sp. and *Neritina virginea*. In addition, fragments of echinoids and *Halimeda* sp. were found. Shells and skeletons are of modern age. The underlying silt to fine sand contains bivalve shells of arcids, *Nuculana acuta*, *N. virginea*, *C. cancellata*, and subrounded gravels with a size of up to 3.5 cm.

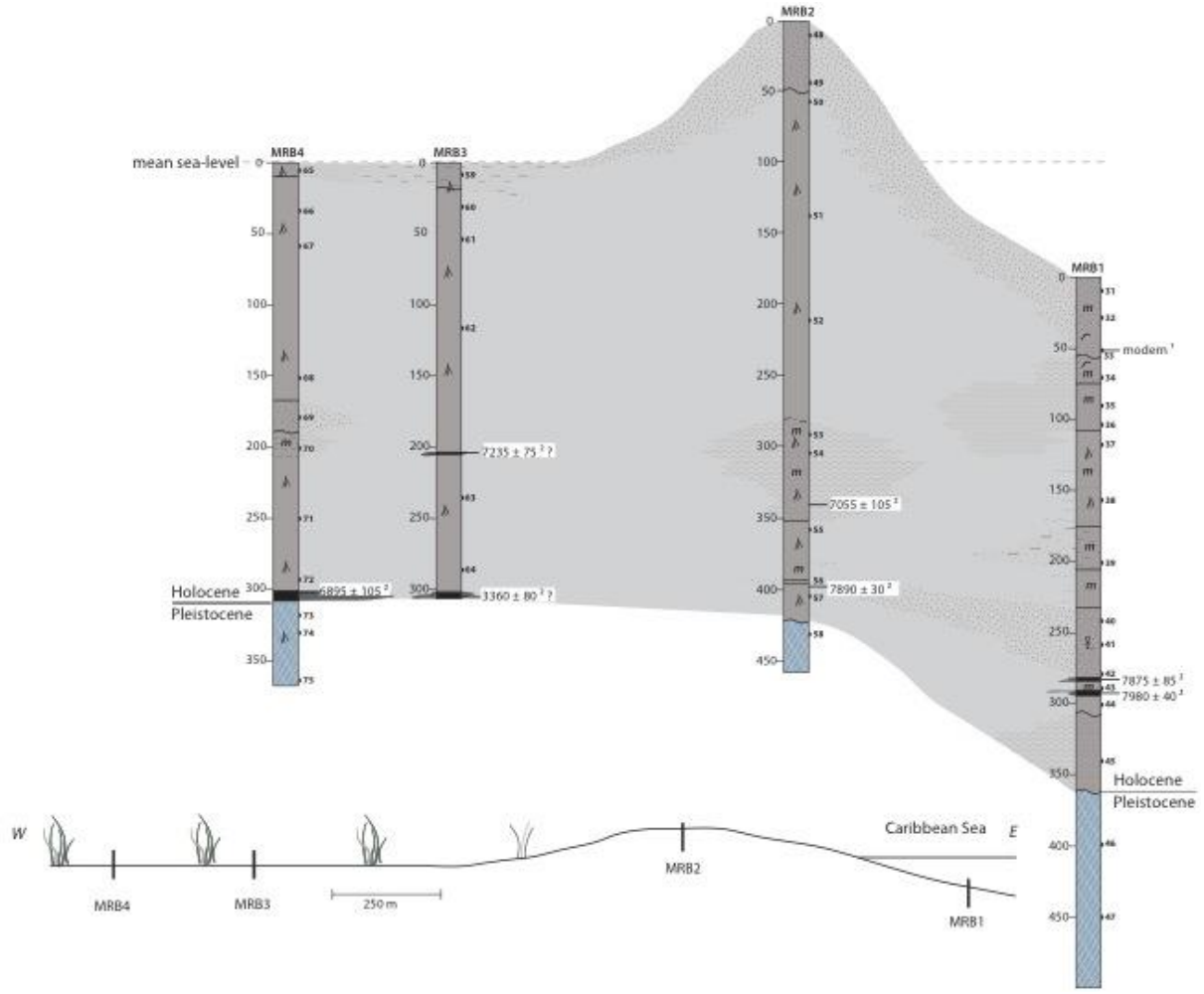

Fig. 2.9 Core logs and interpreted sedimentary facies for Mullins River Beach. Location of coring sites is shown in Figures 2.3 and 2.4. Core logs were corrected for compaction and are arranged with reference to the sea level

At Colson Point the thickness of Holocene lagoon sediments ranges from 15 cm (CP3) to 264 cm (CP1) (Fig. 2.10). The Pleistocene–Holocene boundary is irregular. The base of the Holocene was dated to 3634 ± 65 cal BP (CP2) and 5985 ± 105 cal BP (CP1). The succession of the deposits in the lagoon cores CP1, CP2, CP4, and CP5 starts at the base with Pleistocene soil with a thickness of up to 345 cm. Core CP3 shows Pleistocene sands and silts with bedding structure underlying the bluish-gray soil. Upcore, the soil is gradationally replaced by shell-rich mud (CP1, CP2, CP3) and medium sand in the most landward (CP5), which was collected in an adjacent pond, separated from the main lagoon basin. Tops of the remaining cores consist of mud with dispersed mollusk shells and mangrove roots. Peaty sediment was recovered within the

muds in the cores CP0 and CP1. Mollusk shell concentrations are common in cores from Colson Point Lagoon and mollusk diversity is similar to that in Manatee Lagoon. As in Manatee Lagoon, the dominant species in the shell concentrations are *A. cuneimeris* and cerithids. The upper shell concentrations in the cores CP1 and CP2 as well as the lower shell concentrations in the cores CP6, CP0, and CP1 can be correlated using radiometric age data. At least one shell concentration was found in each core, except for the sand-dominated core CP5. Core CP6 from the marginal marine area contains four distinct shell concentrations. The two lower shell concentrations are largely composed of the brackish species *A. cuneimeris*, comparable with the faunal composition of shell concentrations in the lagoon cores. In the upper two shell concentrations, mollusks have higher diversity and marine taxa occur. These include the bivalves *C. cancellata*, *Diplodonta* sp., *Tellina* sp., and arcids as well as echinoid spines, *Halimeda* sp. plates, worm tubes, and coral fragments of *P. porites*.

Thickness of Holocene sediments at Commerce Bight is 55 cm (CBi3) to 285 cm (CBi1) in lagoon cores and 443 cm in core CBi5 from the tidal channel (Fig. 2.11). Thickness of mud, which forms the tops of the lagoon cores, is 5 cm to 34 cm. The Pleistocene soil was recovered in the lagoon cores CBi2, CBi3, and in the channel core CBi5. It is overlain with a gradational contact by silt to fine sand. Upcore, peaty sediment and mud (CBi2) and mud (CBi3) occur, respectively. No well-defined mollusk shell concentrations were found in the cores. However, in an exploration core (CBi3´-not shown), drilled with a polyvinyl chloride tube at the same locality as CBi3, a shell concentration with *A. cuneimeris* and cerithids was observed. Facies in core CBi1, which was collected close to the barrier, differ from those in the other lagoon cores CBi2 and CBi3 in that a carbonate layer with branched corals and mollusk shells was identified at around 185-cm core depth (age of 4945 ± 105 cal BP). Further upcore, an alternation of fine-grained and coarse-grained silts and sands was deposited, overlain by normally graded sands bare of mollusk shells and sands with mangrove roots. The top of the core consists of mud with dispersed mollusk shells. Core CBi4 from the tidal channel shows frequently alternating facies of mud/silt and peaty sediment, overlain by 186 cm of sand with a marine fauna of *P. porites* fragments, *Halimeda* sp. plates, echinoid spines, and worm tubes, dated to modern times. In core CBi5, sediments consist of Pleistocene soil, silt to fine sand, and coarse sand with mollusks and corals. The change from fine-grained to coarse-grained deposits at 318 cm was dated to 2780 ± 70 cal BP. Further upcore, a coral within the sand yielded a radiocarbon age of 925 ± 65 cal BP.

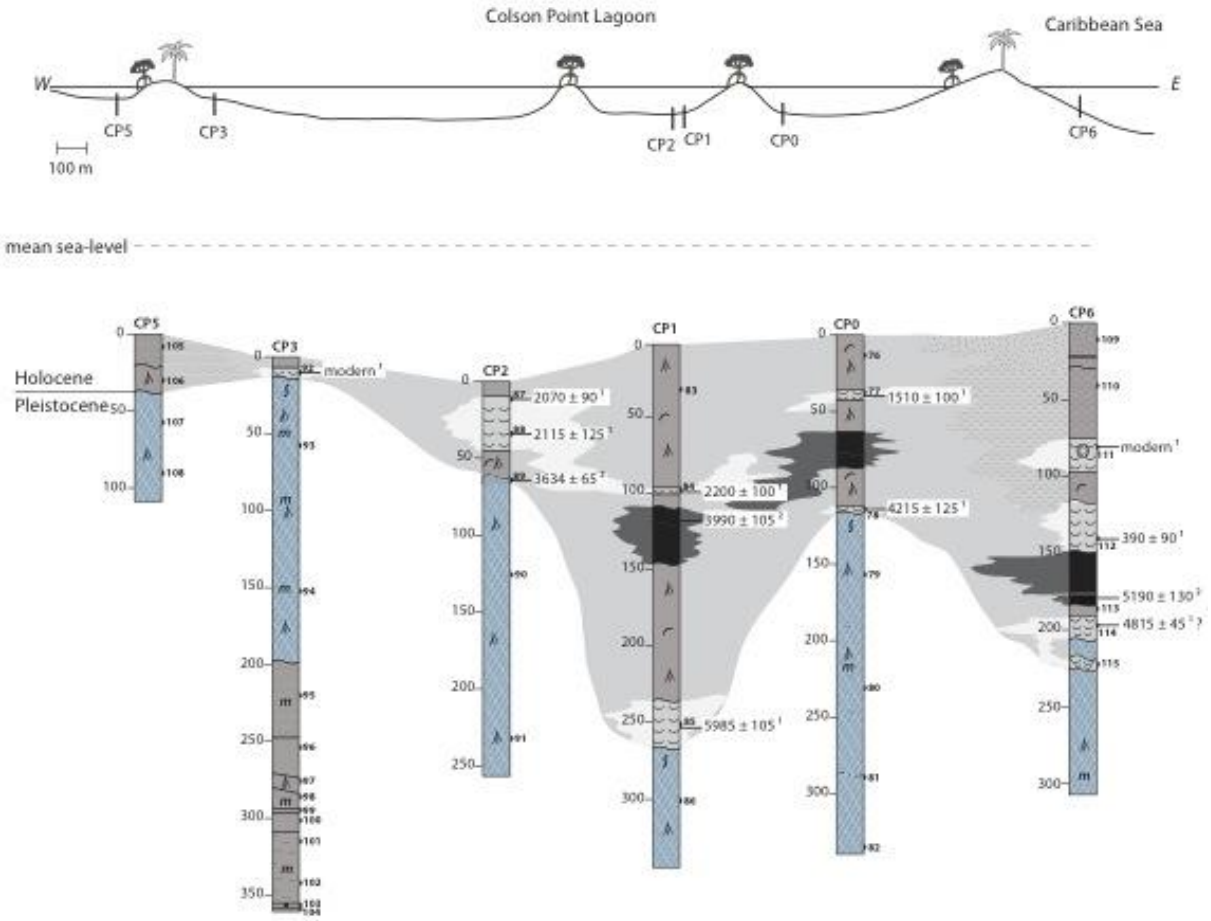

Fig. 2.10 Core logs and interpreted sedimentary facies for Colson Point Lagoon. Location of coring sites is shown in Figures 2.3 and 2.4. Core logs were corrected for compaction and are arranged with reference to the sea level

Thickness of Holocene lagoon sediments from Sapodilla Lagoon, which are predominantly fine grained, reaches 238 cm (SL4) to 384 cm (SL2) (Fig. 2.12). The base of the Holocene was dated to 5880 ± 110 cal BP (SL4) and 6150 ±130 cal BP (SL3). Pleistocene soil was only recovered in the landward cores SL3 and SL4. The cores from the lagoon show a spatially consistent stratigraphic sequence of soil, peat, and mud. Contacts between soil and the overlying peats are sharp, just like the transition from the peat-rich units to the uppermost mud facies. The Holocene basal peat began to form around 6000 cal BP. The ages of the peats, which underlie the lagoonal mud, are 6060 ± 120 cal BP (SL2) and 6555 ± 105 cal BP (SL1). The peats in the cores SL1, SL2, and SL3 can be correlated using age data. In the southern area of the lagoon, the base of the peat was dated to 5880 ± 110 cal BP (SL4). Sediments at the top of SL4 differ from the other lagoon cores in that at 74-cm core depth, a change from mud to silts and sands was observed. In the mud facies, mollusk shells with higher diversity compared with Manatee Lagoon and Colson Point Lagoon were found. There are bivalves such as *A. cuneimeris*, *L. muricata*, and *Nuculana concentrica*, and gastropods such as *Cerithium* sp., *N. viginea*, and *Bulla striata*. Distinct shell concentrations occur only in cores SL1 (4005 ± 115 cal BP) and SL5 (680 ± 50 cal BP). Core SL5, drilled at the tidal inlet adjacent to the mangrove swamp, shows an alternation of partly

laminated fine-grained and coarser-grained deposits of sand, silts, and muds. The top of the core consists of sand with mangrove roots and shells, which are mainly represented by oysters, *Corbula* sp., cerithids, *B. striata*, and *N. virginea*. In core SL6, taken from the marginal marine area east of the barrier, the succession starts with peat (5450 ± 60 cal BP), is overlain by mud (with concretions), and shows an abrupt change to coarser sandy sediment at 1600 ± 90 cal BP. The upper 100 cm exhibit an alternation of silts, fine sands, and very coarse sands with mangrove roots.

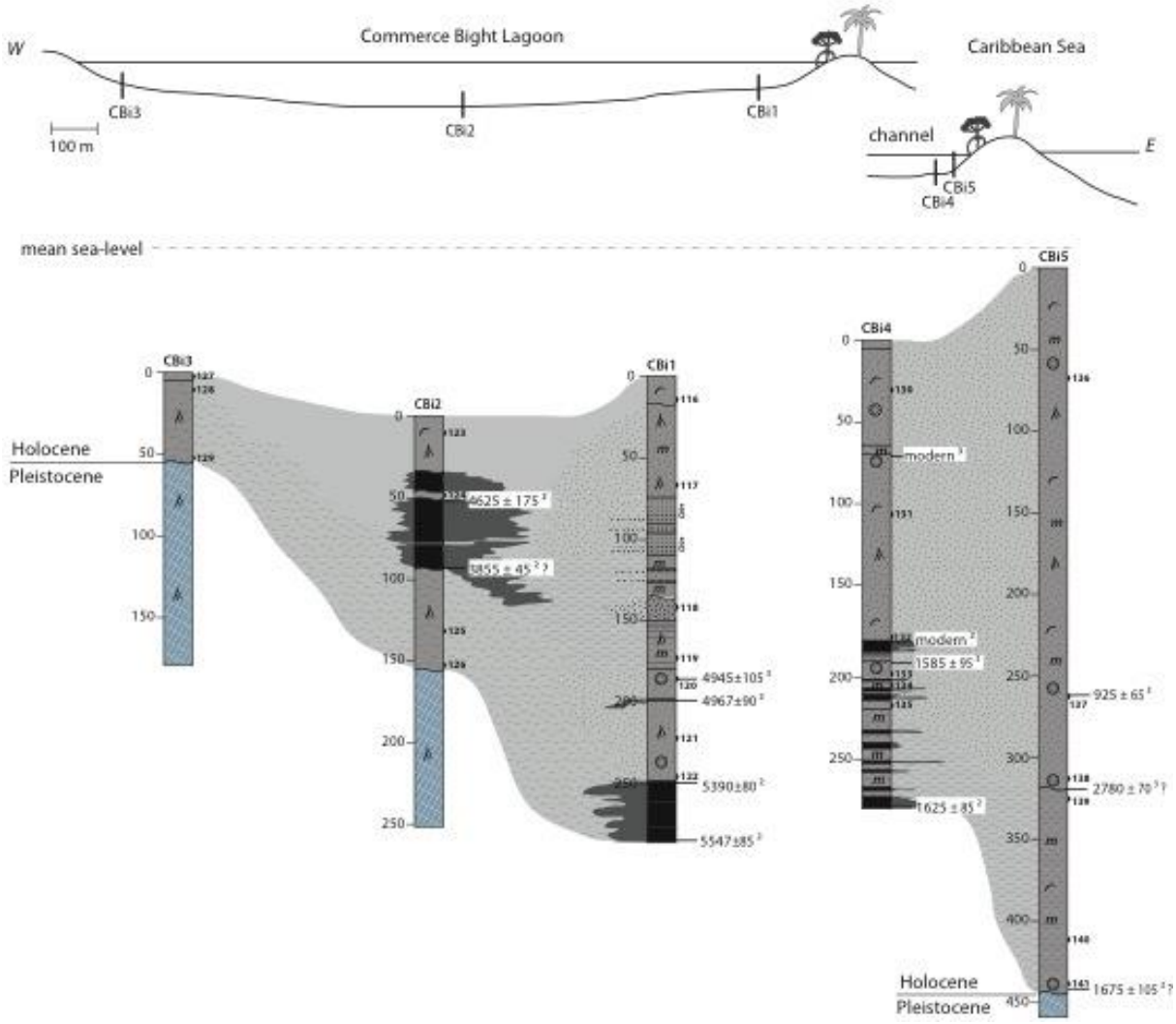

Fig. 2.11 Core logs and interpreted sedimentary facies for Commerce Bight Lagoon. Location of coring sites is shown in Figures 2.3 and 2.4. Core logs were corrected for compaction and are arranged with reference to the sea level

Six radiocarbon dates seem unreliable. The young age at the base of the Holocene in ML2 can be explained by diagenetic alteration of the measured shells. Shells differ from those in other shell concentrations by a chalky texture and by being fragmented, except for small specimens. Furthermore, mollusk shells in SL4 and the core base of SL5 seem to display too young

radiocarbon ages. The organic material that gives the upper age in MRB3 looks charred, which may be the reason why it yielded a relatively old age. A possible explanation for the age reversal in CBi2 is penetration of the peaty sediment by younger mangrove roots. The age reversal in core CP6 possibly reflects bioturbation of sediment. Bioturbation is worth considering, because shell concentrations show grading and wavy contacts. The age reversal in CBi5 probably results from reworking of older coral fragments.

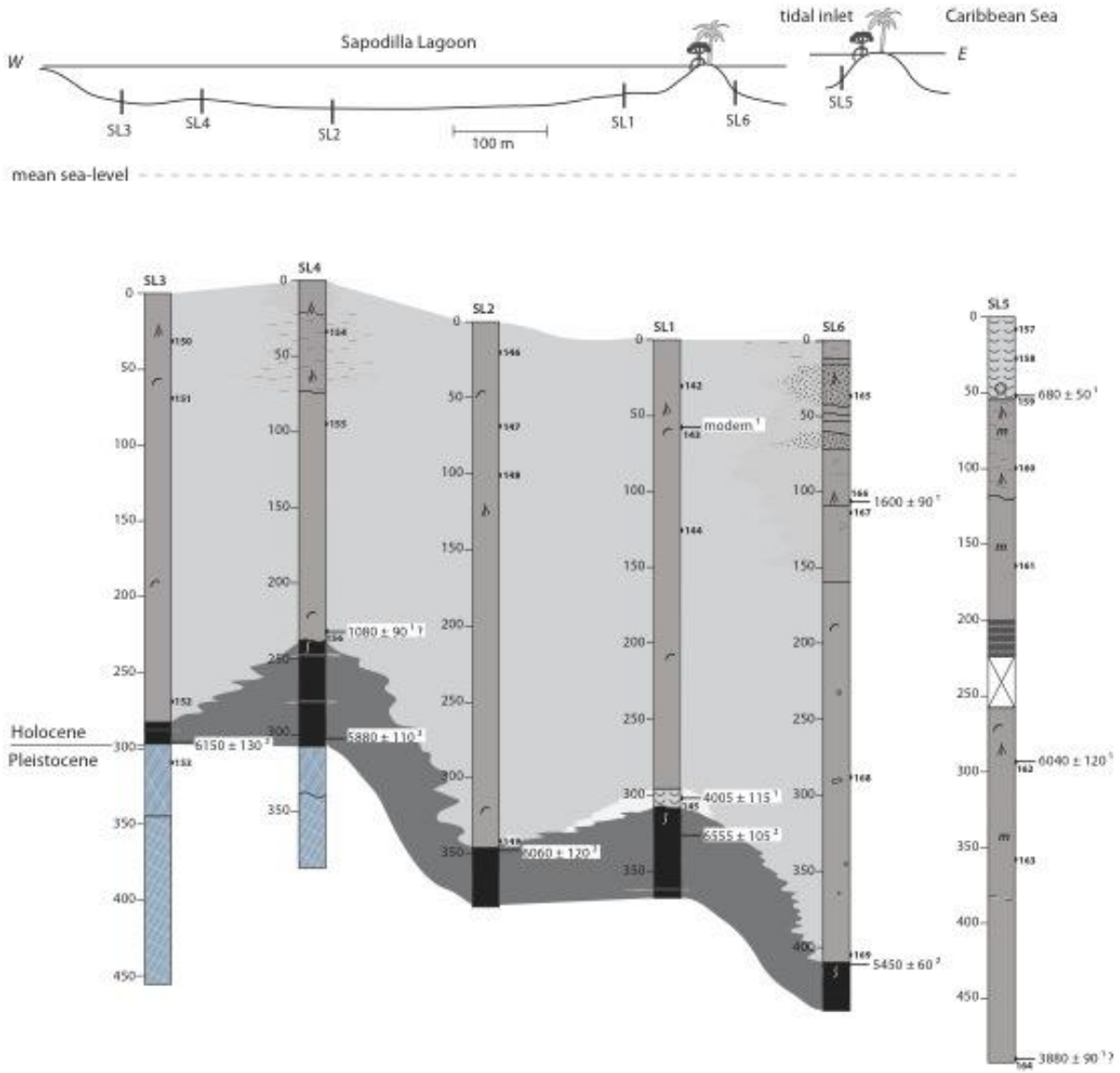

Fig. 2.12 Core logs and interpreted sedimentary facies for Sapodilla Lagoon. Location of coring sites is shown in Figures 2.3 and 2.4. Core logs were corrected for compaction and are arranged with reference to the sea level

2.7 Discussion

The particular depositional environments are characterized by different sedimentary facies (Fig. 2.13). Coarse-grained sandy facies of the coastal system represent the shoreface and foreshore, beach, barriers, barrier islands, and barrier spits. Fine-grained facies were deposited in

lagoonal basins, tidal flats, and marsh areas. Mud, containing shells of brackish water species, which forms the recent sediment surface in lagoons, reflects the background lagoon sedimentation. The sedimentation of this organic-rich, partially shell-rich mud has caused infilling of the lagoons. The muds encountered at Mullins River Beach were probably deposited in a transitional environment that was not permanently covered with water. This is indicated by the absence of the characteristic mollusk shells that were discovered from the other localities. Peat-rich sequences are the result of the existence of mangrove vegetation in intertidal environments. In the study area, peat reflects periods of growth of the red mangrove *R. mangle*, which grows at the land–sea interface. Peat of *Rhizophora* sp. Is indicative of past shoreline position and tidal range because it accumulates only within microtidal ranges (Scholl 1964a,b). Mangrove peat forms in the upper half of the tidal range (Scholl 1964a). Fibrous peat indicates autochthonous deposition. The roots of *R. mangle* are able to reduce water energy and to trap sediments. Structural adaptations like aerial roots (pneumatophores) facilitate existence in marine environments (Monacci et al. 2009). Furthermore, mangrove swamps are important for sedimentation and shape of coastal lagoons (Wanless 1974). The mud and sand overlying peat and peat-rich units indicate inundation of mangroves driven by sea-level rise, when peat accumulation was unable to keep pace with the rate of sea-level rise. Sands may have various sources, i.e terrestrial and marine. Mixing of fluvial and marine sands has occurred along the coast. Coastal landforms like barriers, spits, and beaches are formed by sand. Sand layers like those found in cores from Mullins River Beach and the backbarrier area of Commerce Bight Lagoon may be deposited by overwash during storm events. The landward lagoon sands observed in CP5 are of riverine origin, which can be explained by the proximity to a river mouth.

The Pleistocene sands and silts in core CP3 that underlie the soil are of terrestrial, i.e. riverine or tidal origin. This is indicated by the absence of shells and root penetration as well as the presence of coarse gravel and the alternation of finer and coarser micaceous sediments with wavy bedding. Wavy bedding is characteristic for tidal environments (Archer and Feldman 1995). The formation of the bluish-gray soil is not entirely clear. It could have been formed because of weathering of underlying Pleistocene substrate in a terrestrial, tidal, or salt marsh environment. The absence of mollusk shells and any other remains of marine organisms strongly suggests terrestrial formation. High (1975) described a ‘‘basal clay’’ from northern Belize that lacks shell material and shows a high montmorillonite content. This facies was considered a coastal marsh deposit associated with a residual soil. Offshore basal clay (Macintyre et al. 1995) differs in that it contains higher carbonate content and shells. High (1975) described a muddy quartz sand that is stained orange-red, which he interpreted as a residual soil developed on the underlying Pleistocene limestone. He observed this facies in cores from Commerce Bight Lagoon and it is presumably identical to the soil facies in our cores.

The soft-sediment deformation structures in the soil were most likely induced by liquefaction that could have been triggered by seismic waves of earthquakes. Earthquakes of magnitude 5 or

higher typically generate liquefaction over wide areas (Ambraseys 1988; Galli 2000). Earthquakes have occurred at the boundary of the Caribbean and North American plates, a tectonically active area (Motagua-Polochic Fault Zone) that is located about 130 km south of the study area. It remains somewhat enigmatic why the deformation structures are observed only in the cores from Manatee and Colson Point lagoons. A possible explanation could be the fact that the thickest Pleistocene sections were recovered at these two locations.

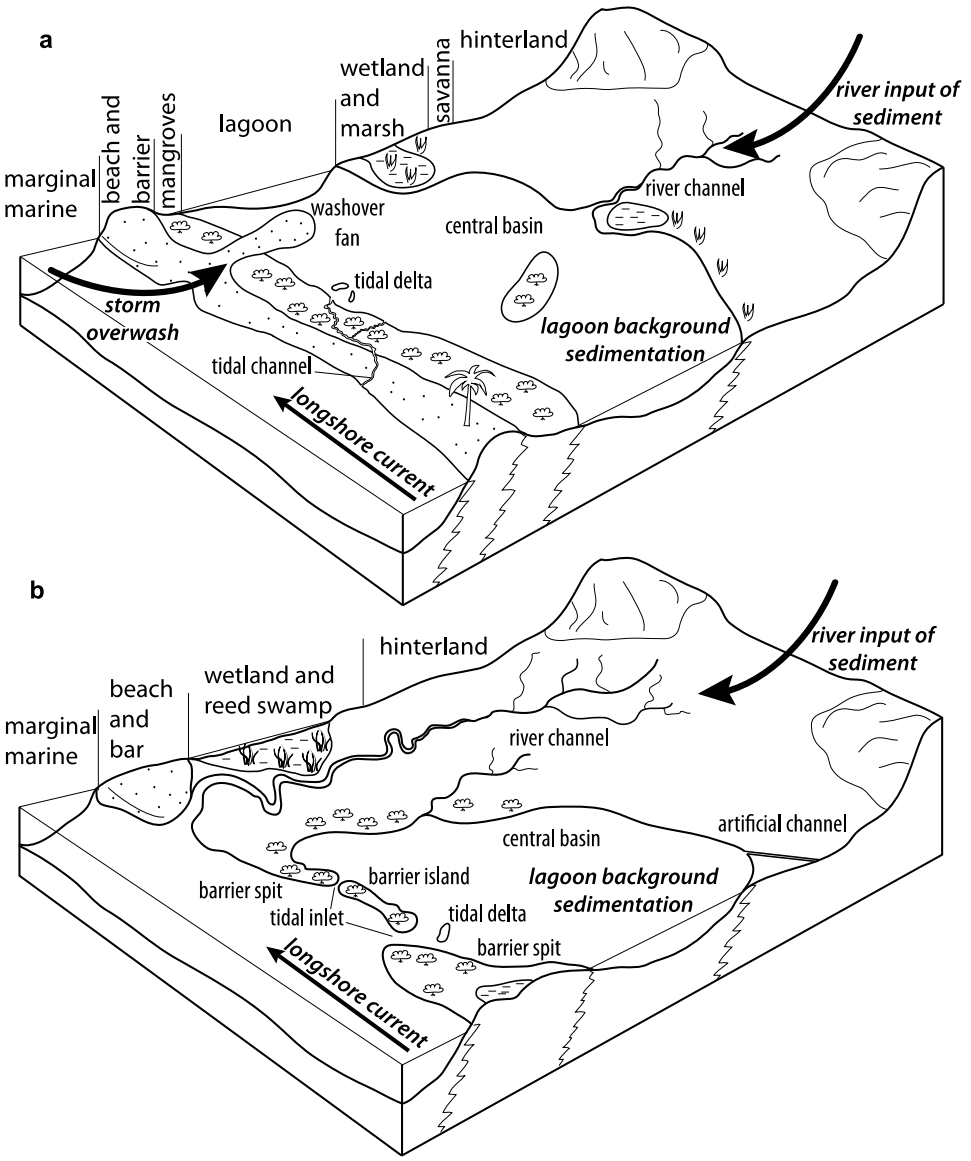

Fig. 2.13 Schematic block diagram showing the main depositional environments and facies along the Belize coast and a retrogradational shift of facies. **a** represents the environments of Manatee, Colson Point and Commerce Bight lagoons. **b** represents the environments of Mullins River Beach (left) and Sapodilla Lagoon (right)

2.7.1 Provenance of sediments and sediment supply

Quartz, microcline, albite, andalusite, muscovite, kaolinite, and low-Mg calcite originate from the hinterland. Kaolinite is a product of chemical weathering of feldspar or muscovite. These minerals are transported to the Belize coast by rivers and creeks (Krueger 1963). In contrast,

pyrite was formed autigenically in the coastal lagoons under reducing conditions. Carbonate minerals formed both in lagoons and in the marginal marine area. Carbonate may have two origins: (1) biogenic, from shells and other hard endo- or exoskeletal pieces in the lagoon and in the sea, and (2) detrital, originating from of Upper Carboniferous to Permian limestones that crop out in the Maya Mountains and from Cretaceous to Tertiary carbonates that surround the Paleozoic deposits in the Maya Mountains. Andalusite derives from contact-metamorphic rocks that enclose the Late Silurian granitoid plutons of the Maya Mountains. This heavy mineral is relatively stable and thus durable and resistant to weathering.

The major processes supplying sediment in coastal environments are river transport, shore erosion, longshore currents, tides, overwash, and wind (Nichols and Boon 1994). In our study area, all of these processes play a role, but there are differences among the localities because of different geomorphology, lagoon-to-ocean connectivity, antecedent topography, and thus different hydrologic regimes. The main sediment sources are the Maya Mountains and surrounding areas; a minor contributor is the marine realm. Coarse-grained sediments were deposited in the vicinity of river mouths, at bars, channels, and along the shoreline where water energy is high. Spits, barrier islands, and barriers are built of material transported by longshore currents that receive their load from headland and shore erosion as well as material delivered to the river mouth from the hinterland. Storm overwash processes also contribute sediment to those landforms. Fine-grained upland runoff sediments are transported in suspension and can easily be reworked by currents (Morton et al. 2000). Furthermore, fine-grained sediments may flocculate in brackish water (Bird 1994). Biogenic carbonates have their origin in shallow-water lagoons, i.e. shells of brackish fauna and on the Belize inner shallow shelf, i.e. shells of marine fauna.

2.7.2 Holocene coastal lagoon development

The geomorphology of coasts is influenced by external atmospheric, terrestrial, and marine processes such as coastal winds and climate, river outflow, and antecedent topography, as well as wave, tides, and currents (Masselink et al. 2011). The evolution of the barrier-lagoon complexes along the Belize coast has occurred during the Holocene sea-level rise. Different evolutionary models for coastal lagoon formation exist (Nichols 1989; Roy 1984). The development of long, narrow barriers including washover fans and only a few tidal inlets that can be observed in the study area is typical for microtidal areas (Hayes 1979). The shape of the lagoons is largely determined by antecedent topography. For example, the unique relief of the Pleistocene-Holocene boundary under Colson Point Lagoon may resemble a fossil lagoon-and-barrier geomorphology, or a pre-existing dune and swale system, as proposed by McCloskey and Liu (2012) to explain antecedent topography at Commerce Bight Lagoon. The soil in core CP0 located at the Pleistocene topographic high in Colson Point Lagoon contains abundant silt and sand, which would support the hypothesis of a ridge and swale morphology that may have

resulted from Pleistocene barrier formation (Figs 2.5 and 2.10). Alternatively, the high relief may also have been formed by fluvial erosion of the Pleistocene surface in this area.

Coastal lagoons may have different origins depending on local sedimentary processes. Spit formation is likely for wave-dominated coasts such as Belize, including activity of longshore currents. Spits extend from headlands parallel to the mainland shoreline, enclosing parts of the recessed mainland shore and shoreline (Oertel 2005). The existence of two narrow spits suggests that Sapodilla Lagoon has been formed because of spit progradation, as shown by Fisher (1968) and Otvos (2012). The three other coastal lagoons in the study area do not show such clear indications, but spit embayment appears to be the best model to explain their formation. Spits grow in response to a predominant littoral drift (Allen 1982). Different growth direction of the two spits is probably the result of change in direction of the net longshore drift as reported by Ferro et al. (1999). The barrier islands probably formed because of breaching of a pre-existent spit caused by a storm event. Barrier spit progradation creates lagoons with long axis perpendicular to the shoreline (Martin and Dominguez 1994), which generally accretes in shore-parallel direction (Oertel 1985). Both patterns can be observed in Sapodilla Lagoon. Breaching of the spit during storms also creates tidal inlets (FitzGerald 2005). The wavy outlines of the back-barrier region at Commerce Bight Lagoon and in the spit and barrier island at Sapodilla Lagoon possibly represent former overwash fans or flood tidal deltas behind abandoned (relict) tidal inlets.

Sediment infilling may result in lagoon segmentation (Oertel et al. 1992; Zenkovich 1967). Sediment deposited by tidal currents can form flood tidal deltas that may become subsequently vegetated by mangroves. Mangrove growth supports sediment trapping and accumulation, which leads to an increase of the size of tidal deltas. This process results in a change from single, short tidal inlets to bifurcating and branched channels, as shown at Colson Point, Commerce Bight, and Manatee lagoons (Figures 2.3 and 2.4). Finally, these processes can cause the closure of lagoons, with little or no water exchange and mixing. Contraction or expansion of lagoons is related to the balance between rate of net sediment input and the rate of sea-level rise (Cooper 1994; Morton et al. 2000; Nichols 1989). According to Barnes (1980), the typical life spans of the majority of coastal lagoons were estimated to less than 1000 years. However, the investigated coastal lagoons reached ages of several thousand years. In general, sediment infilling and amounts of sediment accumulation are related to antecedent topography (Nichols and Boon, 1994), sediment input, and basin capacity (Oertel 2005). Tidal channels formed during storm and washover events may also add to lagoon infilling (El-Ashry and Wanless 1965; Stoddart 1962; Vermeer 1963).

Facies successions allow the reconstruction of the temporal and spatial development of coastal environments. Facies distribution in the study area seems not to be controlled by the major, large-scale underlying NNE-trending tectonic structure (Purdy et al. 2003). The modern marine facies in

Belize, especially reefs and carbonate shoals, are influenced by the mesoscale structures, i.e. folds and faults affecting the basement (Esker et al. 1998; Lara 1993; Purdy 1974, 1998; Purdy and Gischler 2003; Purdy et al. 2003). According to Gischler and Hudson (2004), the start of Holocene barrier and atoll reef growth was nonsynchronous because of variations in elevation of antecedent topography along NNE-trending structures. Core data from the Belize Barrier Reef and the three offshore atolls show that along the major structures the elevation of the Pleistocene topography decreases from NNE to SSW (Gischler and Hudson 2004). Two major faults run through the study area (Purdy et al. 2003). The Northern Boundary Fault of the Maya Mountains passes Manatee Lagoon, whereas the Southern Boundary Fault crosses the study area close to Dangriga, between Colson Point and Commerce Bight lagoons (Purdy et al. 2003). However, Holocene facies do not appear to reflect the aforementioned structural fabric (Fig. 2.14). No spatial patterns such as a southward increase in accommodation space and thus increase in thickness of Holocene facies were observed in cores from our study area. An explanation might be the fact that the study area does not cover a sufficient length of coastline. In general, inundation of antecedent topography occurred along a depositional strike from south to north (Purdy et al. 2003). High (1975) suggested that the greater relief in the south prevented simultaneous flooding of wide areas. In contrast, the flat Pleistocene surface of northern Belize was flooded almost simultaneously. The facies successions discussed per location below also indicate great variability in south-central Belize.

Formation of the Quashie Trap Lagoon started 5315 ± 85 cal BP on the basis of an age date from the base of lagoon core ML3. Peaty sediments represent mangrove growth from 4815 ± 95 cal BP in the central lagoon and from 4330 ± 90 cal BP in the eastern area of the lagoon. Deposition of mud and shells in ML3 indicates unchanged conditions since 4815 ± 95 cal BP. The coarser-grained sediments in ML2, which were deposited after 4330 ± 90 cal BP, suggest interfingering of the lagoon and the adjacent barrier facies. The relatively old, uppermost age dates of cores ML2 and ML3 suggest either very low sedimentation rates or erosion, e.g., during a storm event. At the river mouth, sediments appear to be younger and sedimentation rates higher.

The absence of shells in the mud facies of Mullins River Beach suggests that no lagoon developed at this location, and the area does not represent a filled lagoon environment. The mud facies was deposited in a transitional, probably salt marsh or reed swamp environment. Root penetration of the sediment indicates vegetation in this environment. The 7–8-kyr-old sand layer observed in MRB1 and MRB2, which can be correlated by age, probably was deposited during a high-energy event. The laminated alternations of fine and coarser deposits that overlie the sand are also possibly linked to major storm events. The landward thinning of the sand bed at the core tops presumably represents a recent storm deposit. McCloskey and Keller (2009) obtained 15 cores with a maximum length of ca. 2.4 m from the coastal area about 1 km south of our study site and six cores from Gales Point, about 3.7 km north of our study site. They interpreted

interbedded sand/clay layers as storm deposits and correlated these to hurricane events. They observed landward thinning of the event deposits, which is also the case for the sand layers in the MRB cores.

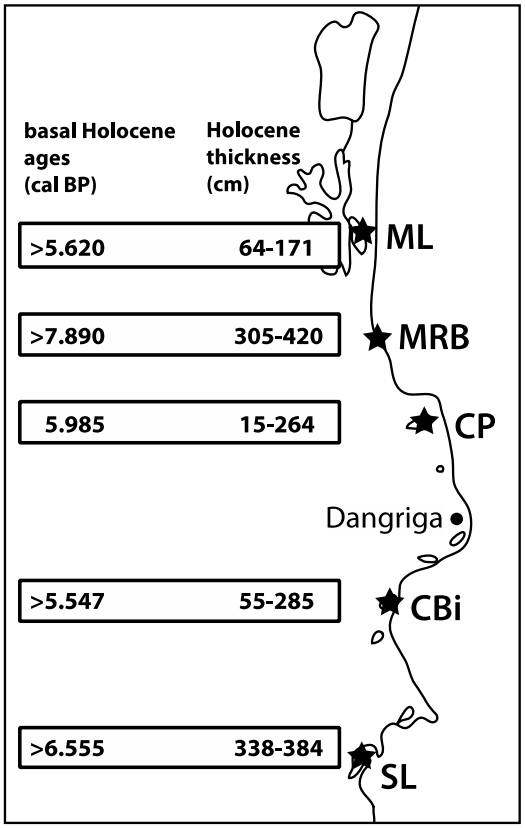

Fig. 2.14 Map of study area that shows maximum depths to Pleistocene and maximum age of Holocene deposits in cores from the study sites Manatee Lagoon (ML), Mullins River Beach (MRB), Colson Point Lagoon (CP), Commerce Bight Lagoon (CBi), and Sapodilla Lagoon (SL)

The eastern lagoon basin of Colson Point Lagoon was flooded before 5985 ± 105 cal BP. Some 2300 years later, around 3634 ± 65 cal BP, the main lagoon basin was inundated. The western margin of the lagoon was not flooded before modern times. A change in sedimentation from muddy sediments to peat and peaty sediments around 3990 ± 105 cal BP indicates sea-level stabilization. The change from peaty sediments to muds and shells occurred together with flooding of the Pleistocene soil at locality CP2. The relatively old age at the top of CP2 could be a consequence of either low sedimentation rates or erosion during a high-energy event. Faunal composition of shell layers in core CP6 from the marginal marine area suggests a retrogradational shift of facies. A lagoon mollusk assemblage dominated by *A. cuneimeris* is overlain by a marginal marine mollusk assemblage higher in diversity. The radiocarbon ages in CP6 180–140 cm downcore in CP6 indicate a hiatus between peat and shell layers. As at Manatee Lagoon, the sandy barrier at this location appears to be a recent feature.

There are several factors that may explain the origin of the shell concentrations in the lagoons. At first glance, redeposition during high-energy events seems probable. But both size frequency

diagrams and ratios of left vs. right valves of *A. cuneimeris* shells suggest that the shells are in situ or were at least not transported over long distances (Adomat et al. 2016). Still, strong precipitation events during and after major tropical storm landfalls could have caused salinity drops in the lagoon that would also have favored the episodical colonization by the brackish *A. cuneimeris* and cerithid gastropods. Holocene climate variation such as the regional change to warmer and wetter conditions in the late Holocene (e.g., Gischler and Storz 2009; Wooller et al. 2009) may only serve as an alternative explanation for the formation of the younger Holocene shell-rich beds.

After inundation of the eastern part of Commerce Bight Lagoon, mangrove growth started no later than 5547 ± 85 cal BP, reflecting sea-level stabilization. Organic-rich sediments in CBi2 are associated with adjoining tidal deltas that developed near the channel entrance into the lagoon. The modern age data at ca. 180-cm depth in core CBi4 from the channel suggests that the overlying sands are a recent event deposit. The transition from fine-grained sediment to coarser sand in CBi5 and CBi4 indicates the formation of a sandy barrier between 2780 ± 70 and 1585 ± 95 cal BP. In this core, the upper two radiocarbon ages indicate a hiatus within the barrier sands. The age reversal of the two lower age dates could be an indication of redeposition. Collectively, the occurrence of corals in cores CBi1 and CBi4 from the 180-cm-thick modern sand section in core CBi4 and the age reversal in core CBi5 support the contention of overwash deposition indicating reworking of sediment. The young ages in CBi4 and CBi5 compared with the ages of lagoon cores can be explained by erosion of older sediments due to higher energy in the tidal channel. McCloskey and Liu (2012) studied a transect of seven cores with a maximum core length of 3.1 m from the eastern area of Commerce Bight Lagoon. After ca. 2000 cal BP, a change from a wetland to a lake environment occurred, according to these authors. They interpreted clastic layers of sand as storm deposits that have been generated by storm surges and storm-induced precipitation events and distinguished between active and quiet periods lasting from several centuries to 1200 years. Moreover, they suggested that the sands and pebbles that they found at the base of all cores represent uneven antecedent topography due to a pre-existing dune and swale system. Our results show indications of storm deposition in core CBi1, taken close to the barrier. Corals and coarse sands were probably deposited during overwash events. Also, the relatively old radiocarbon age at the top of core CBi2 could be an indication of erosion. Likewise, McCloskey and Liu (2012) interpreted old ages at their core tops as the results of storm-induced erosion.

The antecedent surface of Sapodilla Lagoon was flooded between 5880 and 6555 cal BP, promoting the development of mangrove ecosystems. In the southern area of the lagoon, peat accumulation started later than at the other coring sites in the lagoon. The transition from peat toward fine-grained sediments marks the formation of the Sapodilla Lagoon. Thick lagoonal muds indicate permanent environmental conditions since the flooding of the Pleistocene soil. The occurrence of peats is an expression of mangrove growth after flooding of the Pleistocene

surface. The broad tidal inlet and the channel between the narrow spit and the barrier island allow water exchange with the open ocean, which results in water mixing and therefore increased salinity. The change from mud to silt and sand in the southern area of the lagoon (SL4) could be explained by increased river discharge at the adjacent mouth of Cabbage Haul Creek. Oyster shells indicate an intertidal mangrove environment at locality SL5 since 680 ± 50 cal BP. The absence of oysters, which are common on mangrove roots exposed at the edges of channels or ponds (Macintyre et al. 1995), in the lower core section indicates that the tidal inlet has existed only since ca. 680 cal BP. The formation of the sandy spit occurred around 1600 ± 90 cal BP, according to the age date in SL6. Coarse-grained sediments are associated with higher energy in the tidal inlet and barrier island area. The northern spit of Sapodilla Lagoon is probably of younger age. The lower andalusite content, compared with other localities, exists because Sapodilla Lagoon is located comparatively far from the metamorphic source rocks.

2.7.3 Event sedimentation

Evidence of event sedimentation along the south-central Belize coast includes landward thinning sand beds, as observed at Mullins River Beach, shell concentrations dominated by brackish taxa, as in Colson Point and Manatee lagoons, and the apparent age reversal in the stratigraphic record and sands containing marine fauna as seen in the back-barrier area of Commerce Bight Lagoon. In addition, relatively old radiocarbon ages at or close to core tops, which is the case in Manatee, Colson Point, and Commerce Bight lagoons, suggest erosion during high-energy events. Potential triggers of event sedimentation and erosion include major storms and tsunamis, with the former being the more likely candidate. Major tropical cyclones have made landfall along the Belize coast on a regular basis, i.e. every 5 years on average (Gischler et al. 2008, 2013; McCloskey and Keller 2009; McCloskey and Liu 2012; Stoddart 1962). Tsunamis that are triggered by seismic events cannot be excluded because of the nearby active Caribbean-North American plate boundary to the south. However, the frequency of major earthquakes is one to two orders of magnitude less than that of cyclone landfalls. Among the 23 true tsunamis recorded in the Caribbean during AD 1492-2000, the effects of only four events could be verified in wider Central America (Lander et al. 2002).

2.7.4 Response to sea-level change and climate variability

Western Atlantic sea-level curves (e.g., Lighty et al. 1982; Toscano and Macintyre 2003) show a rapidly rising trend until 7000 yrs BP (Fig. 2.15). Thereafter, the rate of rise has decreased and sea level slowly approached modern level. Sea-level curves are based on radiocarbon data from both acroporid corals and mangrove peats. In the following, we will refer to the local sea-level curve of Belize as best approximation of regional sea-level rise in the Holocene (Gischler 2006; Gischler and Hudson 2004). The radiocarbon ages obtained in this study have been plotted on

the Belize sea-level curve (Fig. 2.15), which is based on acroporid coral and basal peat data. The age-model with the superimposed sea-level curve shows that 50 of the 58 ages plot below and eight ages plot above the curve. On the basis of the age data, most of the dated deposits developed during the period of deceleration of the sea-level rate. Eight ages, largely from Sapodilla Lagoon, fall in the final period of rapid sea-level rise before and around 6000 cal BP. Bivalve shells largely plot below the curve, which can be explained by their subtidal habitat. *A. cuneimeris* lives infaunally in shallow water, below the sea level. Coral dates exclusively plot below the curve, probably due to dating of coral fragments that have been transported. The four peat dates that plot up to 2 m below the sea-level curve suggest that they might have undergone postdepositional compression. However, the position of the peats may result from various factors and cannot be clarified with high accuracy. Toscano and Macintyre (2003) suggest that peat dates that plot deeper than the trend line have been contaminated by younger roots or are highly compacted. Contamination by postdepositional roots give younger ages for the dated peat samples. The rooting depth of *R. mangle* can reach more than 1 m (Woodroffe 1981).

Compaction may occur naturally (dewatered or decayed) or during coring (Toscano and Macintyre 2003). According to Macintyre et al. (1995), mangrove peat dates should plot above sea-level curves, which are based on shallow-water coral ages. However, the fact that the Belize sea-level curve is a maximum curve and was drawn above existing coral and peat data by Gischler and Hudson (2004) probably explains why a few of the peat ages from this study plot at considerable depth below the curve. The organic matter dates largely plot below the curve. Seven ages plot above the curve. Of these, six derive from Mullins River Beach, where no lagoon has developed. It can be assumed that the organic matter from these samples does not derive from *R. mangle*, but from vegetation of supratidal environments.

Woodroffe (1995) and Toscano and Macintyre (2003) considered a shift in facies to more elevated environments, which have been dominated by other mangrove species, as possible explanation for peat dates that plot above the trend line. Thus, not all of the organic-matter samples serve as sea-level tracking deposits. The vertical error range caused by compaction during coring shows that the exact position of the data lies within a wide range in some cases and thus cannot be determined precisely, because sediment types have different proneness to compaction. Possible effects of neotectonic activity should also be considered to explain the scatter of the data. For instance, the activity of the Southern Boundary Fault, which runs through the area of Commerce Bight, could be responsible for the low position of the peat and organic-matter dates from this location. The area of Manatee Lagoon, from where two dates plot above the curve, is also located close to a major fault, the Northern Boundary Fault. However, this observation also cannot be seen as a firm criterion to explain the scatter of the data.

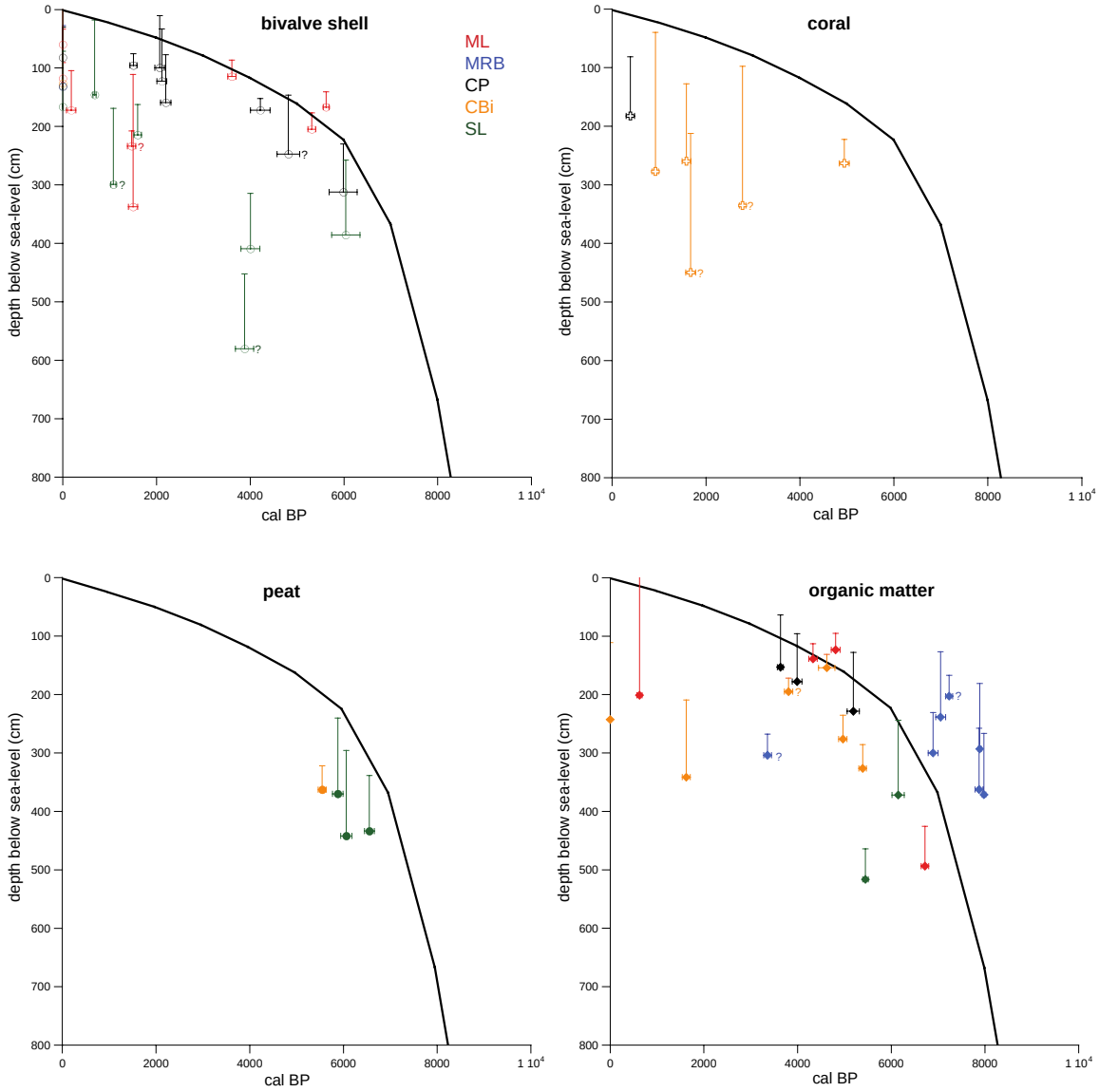

Fig. 2.15 Depth-age data from vibracores studied in this work plotted on the Holocene sea-level curve of Gischler and Hudson (2004). Vertical error bars refer to the compaction range of the dated material. For the organic matter samples with more than one calibrated calendar age (see Table 2.3), average ages are indicated. Unreliable ages are marked with question marks (see also Figs 2.8-2.12). The y-axis shows the sample elevation with respect to mean sea level

2.7.5 Comparison with previous studies

Mangrove ecosystems are very sensitive to environmental change (Covington 1988) because they thrive at the transition between the hydrosphere and the terrestrial environment and, thus, are used as indicators of sea level and environmental change (e.g., Soares 2009; Woodroffe 1990; Wooller et al. 2004). Regional changes in the rate of sea-level rise and climatic conditions occurred during the Holocene in Belize, influencing both mainland and offshore mangrove ecosystems (Monacci et al. 2011).

On the mainland, Alcalá-Herrera et al. (1994) considered sea-level rise a precondition of lagoon formation in the Cobweb Swamp in northern Belize. Results of another study in the

Cobweb Swamp area suggest that inundation of the coastal mainland occurred some 7000 yrs BP (Jacob and Hallmark 1996). Lake cores from Petén, Guatemala show that marine inundation took place around 9000 yrs BP (Curtis et al. 1998). According to Kelletat (2005), modern coastal landforms are not older than 6000–6500 yrs BP in general. In our study area, radiometric age data suggest that flooding of the mainland began between 6900 and 5300 cal BP on the basis of radiometric age data from Holocene deposits. Mangrove peat accumulated mainly between 6700 to 3900 cal BP, later than at the aforementioned offshore sites and the lacustrine sites in northern Belize and Petén, Guatemala. During marine transgression, which promoted lagoon development, mangroves probably could not keep pace with rising sea level and mangrove growth was restricted to shallower water at channel and lagoon margins. Usually, changes in the peat sedimentation rates are associated with sea-level changes according to Wooller et al. (2007) in that peat accumulation rate decreases as mangroves adapt to a decelerating rate of sea-level rise. Conversely, frequent seawater-inundation results in higher rates of peat accumulation. In contrast to offshore mangroves, mainland mangroves are able to migrate inland during marine transgression (Wooller et al. 2007). Shell accumulations directly overlying the Pleistocene soil or peat, as observed in some cores, probably indicate stable shallow-water environments. Mud deposition in the lagoons occurred during stable sea-level conditions. In general, the majority of coastal barriers have formed during deceleration of rising sea level (FitzGerald 2005).

Peat accumulation was reported to have begun around 8000 yrs BP (Monacci et al. 2009; Wooller et al., 2004, 2007) in mangrove ecosystems from the Belize shelf. Macintyre et al. (1995) detected mangrove growth since about 7000 yrs BP at Tobacco Range. At Twin Cays, the mangrove ecosystem was established about 8000 years ago (Macintyre et al. 2004). The central shelf lagoon was inundated between 10,000 and 8000 yrs BP (Esker et al. 1998; Halley et al. 1977; Shinn et al. 1982; Westphall 1986), earlier than the northern shelf lagoon, which was flooded between 6100 and 5600 yrs BP (Purdy 1974), on the basis of radiometric age data derived from basal peats.

Core data from mangrove ecosystems along the Sibun River, north of our study area, show a decrease in sedimentation rate between 6000 and 1000 cal BP, indicated by a decrease in *R. mangle* pollen and an increase in *Avicennia germinans* pollen around 6000 cal BP, as a consequence of a decrease in the rate of sea-level rise (Monacci et al., 2011). Furthermore, an environmental change was detected around 2500 cal BP, indicated by a transition from peat-dominated sections to fluvially deposited muddy sediments (Monacci et al. 2011). A similar decrease in peat accumulation rate was observed offshore at Spanish Lookout Cay (Monacci et al. 2009). Explanations include stronger erosion in the Maya Mountains caused by anthropogenic influence such as deforestation (Leyden 1987), and changes in the position of the ITCZ, leading to an increase in precipitation (Haug et al. 2001).

Deforestation and intensive land use by the Maya culture led to a substantial increase in erosion and fine-sediment deposition ("Maya Clay'') during ca. 3000–1000 yrs BP (Anselmetti et al. 2007; Jacob and Hallmark 1996). After the final decline of the classic Maya culture, triggered by a long drought during AD 1020–1100 (Kennett et al. 2012), forests grew back and erosion and sediment runoff decreased (Gischler et al. 2008). With the exception of lower sedimentation rates in upper lagoon core sections, no clear indications of these changes were detected in the cores collected during this study. Similar conclusions can be drawn when considering climate change. Holocene climate variability in the region is characterized by a change from warmer/wetter conditions during the Holocene Climate Optimum (10,000–5500 yrs BP) to cooler/drier conditions (e.g., Haug et al. 2001). Another change back to warmer and wetter conditions occurred in the late Holocene (between 3000 and 1000 yrs BP) in the wider study area according to vegetation data (Wooller et al. 2009) and coral climate proxy data from Belize (Gischler and Storz 2009). There are indications that sedimentation rates in some of the cores obtained during this study were indeed higher in lower core sections, i.e. during the mid- Holocene, than in upper core sections; however, more age data would be necessary to validate the relation between sedimentation rate and climate variability. A major problem in this context was the rarity of datable material in muds and sands.

2.8 Conclusions

The morphosedimentary elements of the studied areas along the central Belize coast include lagoon, beach, barrier, barrier island, barrier spit, and tidal delta. The coastal lagoon environments are surrounded largely by mangroves and littoral forests, but also by wetlands and lowland savannas. The principal Holocene sedimentary facies are mud, sand, and peat/peaty sediment. Additionally, transitions among these facies types occur. The recovered Holocene sections are as thick as 500 cm and overlie Pleistocene soil and sand facies. Marine inundation by the rising Holocene sea commenced some 7–5 kyrs BP. Unlike the Belize offshore realm, where temporal and spatial facies patterns have been significantly controlled by antecedent topography and by underlying tectonic structure, coastal development appears to have been controlled by a variety of additional processes. These include river discharge, lagoon-to-ocean connectivity, longshore currents, wave action, and storm events. Inherited morphology reflects mesoscale morphotectonic features of the bedrock that vary at a local scale. There are signs of coastal facies retrogradation due to Holocene sea-level rise, as indicated by changes in mollusk species composition. Late Holocene facies progradation due to stalling sea-level rise is largely absent. The diversity of the stratigraphic sequences shows that the investigated settings are complex sedimentary systems that are influenced by both local and regional features. Thus, correlation of the stratigraphic packages is difficult within one locality and also at a larger scale.

There is evidence of event (storm) deposition along the Belize coast. This includes landward thinning sand beds, hiatuses, stratigraphic reversals, redeposited marine bioclasts in coastal lagoon successions, and mollusk shell concentrations as possible expressions of storm-induced inundation and precipitation events. Indications of the influence of the rise of the Maya culture, i.e. by an increase in erosion and sediment runoff due to deforestation as well as a decrease in sediment input caused by classical Maya decline and forest regrowth reported in other studies, were not found. Likewise, correlations between coastal lagoon development and Holocene climate variability could not be drawn on the basis of the existing data.

2.9 Acknowledgements

We are grateful to the Deutsche Forschungsgemeinschaft, who funded this project (Gi222/20) and the Alfons and Gertrud Kassel-Stiftung, who funded this project. We thank Stefan Haber, Malo Jackson, David Geban, and Claire Santino for help during fieldwork. Nils Prawitz, Anja Isaack, and Lars Klostermann assisted during sample preparation in the home laboratory in Frankfurt. Dr. Rainer Petschick ran the X-ray diffractometer in Frankfurt. The critical comments of Donald McNeill, César Andrade, Marta Pérez-Arlucea, and a fourth anonymous reviewer improved this manuscript.

Chapter 3. Taxonomic and taphonomic signatures of mollusk shell concentrations from coastal lagoon environments in Belize, Central America

Friederike Adomat, Eberhard Gischler, Wolfgang Oschmann

Institut für Geowissenschaften, Goethe-Universität Frankfurt, Altenhoeferallee 1, 60438 Frankfurt am Main, Germany

Keywords: coastal lagoons, mollusk assemblages, *Anomalocardia cuneimeris*, Holocene, C-14

Accepted by Facies 62(5), 1-29

Abstract: Faunal composition and distribution patterns of mollusk assemblages from 20 shell concentrations in cores collected in coastal lagoons, a mangrove-fringed tidal inlet and the marginal marine area (shallow subtidal) along the central coast of Belize show considerable variation due to environmental heterogeneity and the interplay of several environmental factors in the course of the mid-late Holocene (ca. 6000 cal BP to modern). The investigated fauna ≥2 mm comprises 2246 bivalve, 789 gastropod and 11 scaphopod specimens. Fifty-three mollusk species, belonging to 42 families, were identified. The bivalve *Anomalocardia cuneimeris* and cerithid gastropods are the dominant species and account for 78% of the total fauna. Diversity indices are low in concentrations from lagoons and relatively high in the marginal marine and tidal inlet areas. Based on cluster analysis and nonmetric multidimensional scaling (NMDS), seven lagoonal assemblages and three marginal marine/tidal inlet assemblages were defined. A separation between lagoonal and marginal marine/tidal inlet assemblages seen in ordination indicates a lagoon-onshore gradient. The statistical separation among lagoonal assemblages demonstrates environmental changes during the Holocene evolution of the coastal lagoons, which is probably related to the formation of barriers and spits. The controlling factors of species distribution patterns are difficult to rule out, probably due to the heterogeneity of the barrier-lagoon systems and the interaction of paleoecological and paleoenvironmental factors. In addition to the taxonomic analysis, a taphonomic analysis of 1827 valves of *A. cuneimeris* from coastal lagoons was carried out. There is no relationship between depth and age of shells and their taphonomic condition. Size-frequency distributions and right-left valve ratios of *A. cuneimeris* suggest that valves were not transported over long distances but were deposited

parautochthonously in their original habitat. Shells from tidal inlet and marginal marine environments were also predominantly deposited in their original habitats.

3.1 Introduction and objectives

Skeletal concentrations are common in the stratigraphic record and are found in fossil and recent deposits. Several studies have dealt with their significance for paleoecological, paleoenvironmental and biostratigraphic interpretations (e.g., Kidwell 1985, 1991, 2001, 2002; Kidwell et al. 1986; Fürsich 1990; Kidwell and Bosence 1991). Taxonomic composition and taphonomic signatures of shell concentrations have been used to figure out paleoenvironmental conditions, e.g., in modern coastal siliciclastic systems of the temperate realm (e.g., Fürsich and Flessa 1987; Davies et al. 1989; Aguirre and Farinati 1999; Kotzian and Simões 2006; Ritter et al. 2013). Studies from the tropical Caribbean realm and surrounding regions are for the most part located in carbonate depositional environments (Turney and Perkins 1972; Ekdale 1974, 1977; Anderson and McBride 1996; Brewster-Wingard et al. 2001; Callender et al. 2002; Parsons-Hubbard 2005; Hauser et al. 2007, 2008). Index species and changes in the faunal composition have been used to define different environments (Turney and Perkins 1972), to identify physical parameters such as shifts in salinity and water quality (Brewster-Wingard et al. 2001) and to reconstruct migration of facies (Parsons-Hubbard 2005). Only few studies on mollusk distribution and taphonomy were conducted in tropical siliclastic and mixed-carbonate-siliciclastic settings in the Caribbean (e.g., Best and Kidwell 2000a, b; Best 2008). The distribution and composition of shell concentrations of the major mixed carbonate-siliciclastic depositional system of the Belize coast, including the factors that influence their formation, are entirely unknown. Hauser et al. (2007, 2008) investigated modern bivalve shell assemblages from the three atolls offshore Belize. On the Belize shelf, Robertson (1963) and Purdy et al. (1975) determined distribution patterns of live mollusks and distinguished four assemblages, including reef and carbonate, deep shelf lagoon, nearshore lagoon as well as freshwater and brackish swamp fauna. The latter comprises insufficiently sampled siliciclastic regions at and near river mouths as well as mangrove swamps. Fauna from coastal lagoon environments is not included (Purdy et al. 1975). In this study, shell concentrations found in vibracores from Belize coastal lagoon environments were examined in order to provide information about Holocene environmental changes. Taxonomic analysis of each concentration was carried out to define mollusk assemblages and to figure out if changes in abundance, distribution patterns and diversity of the species have occurred during barrier-lagoon evolution. Taphonomic analysis of valves of the most dominant species, *Anomalocardia cuneimeris* (Conrad 1846), was performed to investigate if taphonomic states changed in the record.

3.2 Geological and environmental setting

Belize is situated in Central America, in the southeastern area of the Yucatán Peninsula. Its eastern border is formed by the Caribbean Sea (Fig. 3.1). The country extends from 16°S to 18°30´S latitude and from 87°30'W to 89°30´W longitude. The climate is subtropical (Wright et al. 1959). The study area lies within the trade wind belt with prevailing easterly and northeasterly winds. The coast of Belize is a wave-dominated, semidiurnal microtidal area with a tidal range of 15-30 cm (Kjerfve et al. 1982). Major hurricanes made landfall on the Belize coast every 5 years during the 20th century on average (Gischler et al. 2008, 2013). Annual rainfall increases from north to south from 124 cm to 380 cm, respectively (Purdy et al., 1975), reflecting mainland topography. Precipitation is highest during the summer months of July to September and salinity in coastal lagoons will fluctuate accordingly. Drainage density is particularly high along the coast east of the Maya Mountains (High 1975), however, there are no data available on river discharge, which is mainly dependent on rainfall pattern. Mean sea surface temperatures of the shelf range from 28.9°C during summer to 26.2°C during winter (e.g., Purdy et al. 1975). Surface water salinity decreases from ca. 35‰ at the shelf margin to ca. 18‰ near the coast, and northward into Chetumal Bay and southward into the Gulf of Honduras (Purdy 1974).

The shallow northern shelf is dominated by carbonates. The deeper southern shelf harbors a mixed siliciclastic-carbonate system with an eastward increase in carbonate content (Purdy et al. 1975; Pusey 1975; Scott 1975; Purdy and Gischler 2003). The major processes supplying sediment to coastal environments include river transport, shore erosion, longshore currents, tides, washovers and wind (Nichols and Boon 1994). The main sediment source is represented by the Maya Mountains and surrounding areas, where Paleozoic igneous, metamorphic and siliciclastic rocks and Cretaceous to Tertiary carbonates crop out. The coastal lowland is largely composed of unconsolidated Quaternary detrital sediments. A minor sediment contributor is the offshore marine realm (Adomat and Gischler 2015). Today, muddy substrate and low current velocities predominate in the coastal lagoons (Adomat and Gischler 2015). The lagoons are brackish with salinity ranging from 4 to 27‰ (Table 3.1). The coast of Belize, which has low relief, is dominated by barrier-lagoon complexes (High 1966). The coastal lagoons are usually extensively fringed by mangroves belonging to the red mangrove *Rhizophora mangle*.

3.3 Methods

Coring was undertaken using a portable vibracorer (Lanesky et al. 1979) with aluminum core tubes of 6 m length and a diameter of 7.5 cm. Four localities along the central coast of Belize, namely Manatee, Colson Point, Commerce Bight and Sapodilla Lagoons, from north to south, were selected as core sites (Figs. 3.1, 3.2, Tables 3.1, 3.2). Percent compaction for each of the 26 cores was calculated, using core recovery and penetration depths recorded in the field.

Sediments were described visually and sub-sampled for grain-size analysis and X-ray diffractometry (XRD).

To yield a stratigraphic context and to correlate distinct concentrations twenty samples of bivalve shells, each sample comprising few valves from a shell concentration, were radiocarbon-dated using accelerator mass spectrometry. Radiocarbon ages are presented completely in Adomat and Gischler (2015). Radiocarbon ages of carbonate shells were converted to calendar years after Talma and Vogel (1993), using the Marine09 database. Calibrated ages are given with a 2 σ error range. The marine reservoir effect is ∆R=120±27 and Glob res=-200 to 500.

In most cases, samples of 5 cm thickness were taken from the concentrations. The cores, samples and data are stored in the Institut für Geowissenschaften, Goethe-Universität, Frankfurt am Main, Germany. Macrofossils larger than 2 mm mesh size, mainly mollusk shells, were identified using Parker (1959), Turney and Perkins (1972) and Abbott (1974). Mollusk shells from distinct concentrations were identified to species level where possible. For few specimens, identification was not possible due to poor preservation of diagnostic criteria. Species diversity was calculated using following indices: Species richness (R) after Margalef (1958), diversity (H) after Shannon and Wiener and evenness (E) after Pielou (1966), using the equations

$$\mathrm{R} = (\mathrm{S}-1)/\ln(\mathrm{N}) \quad (1)$$

$$\mathrm{H} = -\sum p_i \ln p_i \quad (2)$$

$$\mathrm{E} = \mathrm{H}/\ln \mathrm{S} \quad (3)$$

where S = number of species, N = total number of individuals, and p_i = S/N. For multivariate statistical analysis, cluster analysis and NMDS, an ordination method for indirect gradient analysis (Kruskal 1964a,b; Fasham 1977) were performed using the software PAST 2.17c (Hammer et al. 2001). The two methods were performed using the Bray-Curtis similarity index, which is commonly used and works well in ordination (e.g., Clarke and Warwick 2001; Mandic et al. 2002; Bush and Brame 2010). Hierarchical cluster analysis was based on species abundance data of each shell concentration and was carried out using the unweighted pair-group algorithm (UPGMA), because for ecological data (taxa-in-samples) average linkage logarithm is recommended by Hammer and Harper (2006). Other algorithms show a similar grouping of samples, indicating robustness of the groupings. NMDS was performed once for all samples and once for the lagoonal samples only. An ordination dimension of three was chosen to minimize the stress value. Stress values were around 0.1, suggesting a fair value since values below 0.1 are considered “good” (Hammer and Harper, 2006).

Skeletal mineralogy of *A. cuneimeris* was determined using XRD. Shell sizes were determined by measuring length and height of the valves with a caliper. Taxonomic analysis was undertaken on complete specimens ≥2 mm. The number of disarticulated valves of the bivalve shells was corrected by a factor of 0.5. This procedure is needed when bivalved and univalved invertebrates

like gastropods are analyzed together (Kowalewski et al. 2003). Sieving may alter preservation and disarticulation to some degree. Thin-shelled bivalves tend to break down more rapidly than thick-shelled bivalves and gastropods (Turney and Perkins 1972). The three packing categories "densely", "loosely", and "dispersed" were determined following Kidwell and Holland (1991). Scanning electron microscopy (SEM) has been applied to analyze shell microstructure of chalky and well-preserved valves of the bivalve *A. cuneimeris*.

Taphonomic analysis of 1827 valves of *A. cuneimeris* (≥2 mm) from 16 concentrations was carried out using a binocular microscope. The infaunal shallow-water bivalve *A. cuneimeris* occurs in each concentration from lagoonal environments, whereas the distribution of the remaining dominant lagoonal species *Cerithidea pliculosa* (Menke, 1829) and *Cerithium eburneum* (Bruguière, 1792) is more variable. Therefore, the study on taphonomy focuses on *A. cuneimeris*. Taphonomic attributes analyzed in this study include shell size, left-right (LR) valve ratio and the preservation states of both external and internal surfaces (Fig. 3.3). The external surfaces were scored for (1) presence of original color (glossy-cream with brownish specklings) and luster, (2) ornamentation (concentric ribs) and (3) pits. The interior was scored for (1) presence of color and luster (glossy-purple), (2) pallial line and (3) muscle scars (Fig. 3.3). It is indicated whether or not the valve had been subject to corrasion, that combines the processes of mechanical abrasion and biogeochemical corrosion (Brett and Baird 1986). Furthermore, we indicated if valves had been affected by diagenesis resulting in chalkiness, rhizoid holdfasts and bioerosion. LR-ratio and size-frequency analyses were performed to figure out if shells are *in situ* or if they have been transported. A χ^2-test was performed for evaluating the LR-ratio of valves. The null hypothesis (H_0) is that the left to right ratio is 1:1, which is an indicator of autochthony. The critical value χ_c^2=3.84 was determined by means of the degrees of freedom (df=1) and the significance level α=0.05.

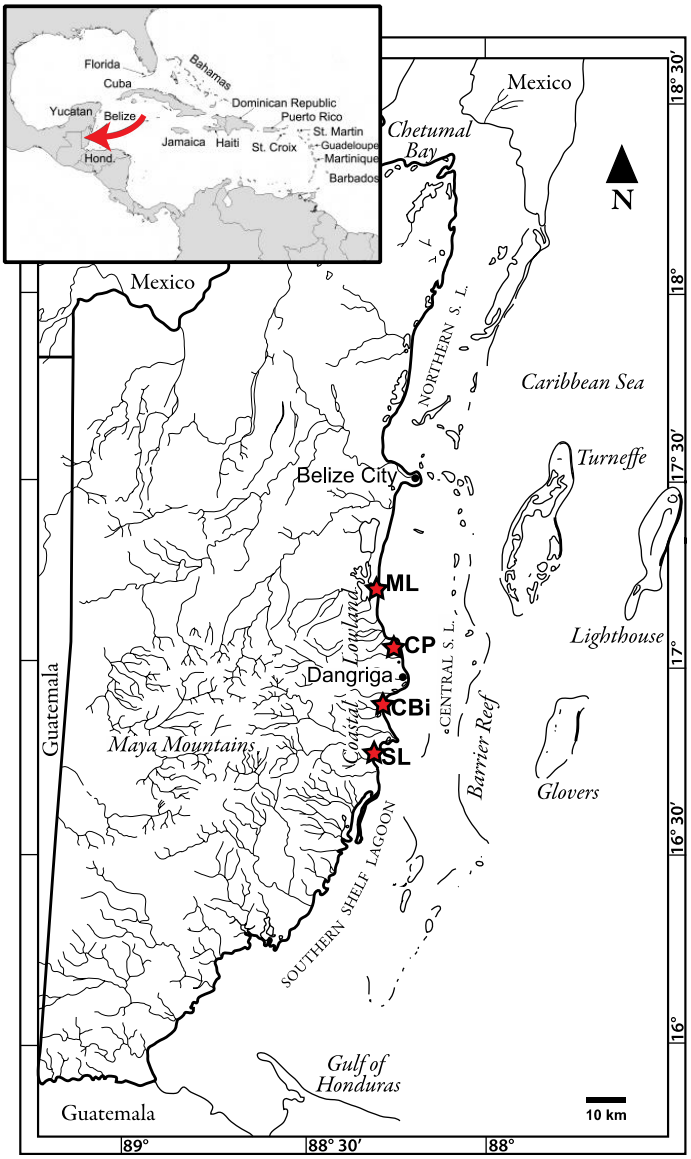

Fig. 3.1 Location map of Belize showing the study sites along the central coast of Belize. The inset map in the upper left shows the location of Belize in Central America (map after Montaggioni and Braithwaite 2009). Asterisks mark the localities: Manatee Lagoon (ML), Colson Point Lagoon (CP), Commerce Bight Lagoon (CBi) and Sapodilla Lagoon (SL)

Table 3.1 *Salinity data from two sites each at Manatee Lagoon, Colson Point Lagoon, Commerce Bight Lagoon and Sapodilla Lagoon (from north to south). At Sapodilla Lagoon water samples were collected in the southern and in the northern area of the lagoon in winter and in the western and eastern area of the lagoon in summer*

			Salinity (‰)							
Season	Date	Water Depth	Manatee Lagoon		Colson Point Lagoon		Commerce Bight Lagoon		Sapodilla Lagoon	
			W	E	W	E	W	E	S/W	N/E
Winter	21 January 2012	Surface Water	8.1	8	7	3.1	8	14.1	6.8	26.6
Summer	14 July 2012	Surface Water	4.4	5	11	17.5	14.1	19.7	3.7	8
		Bottom Water	4.3	5.9	16.3	19	16.5	20.2	4	24.5

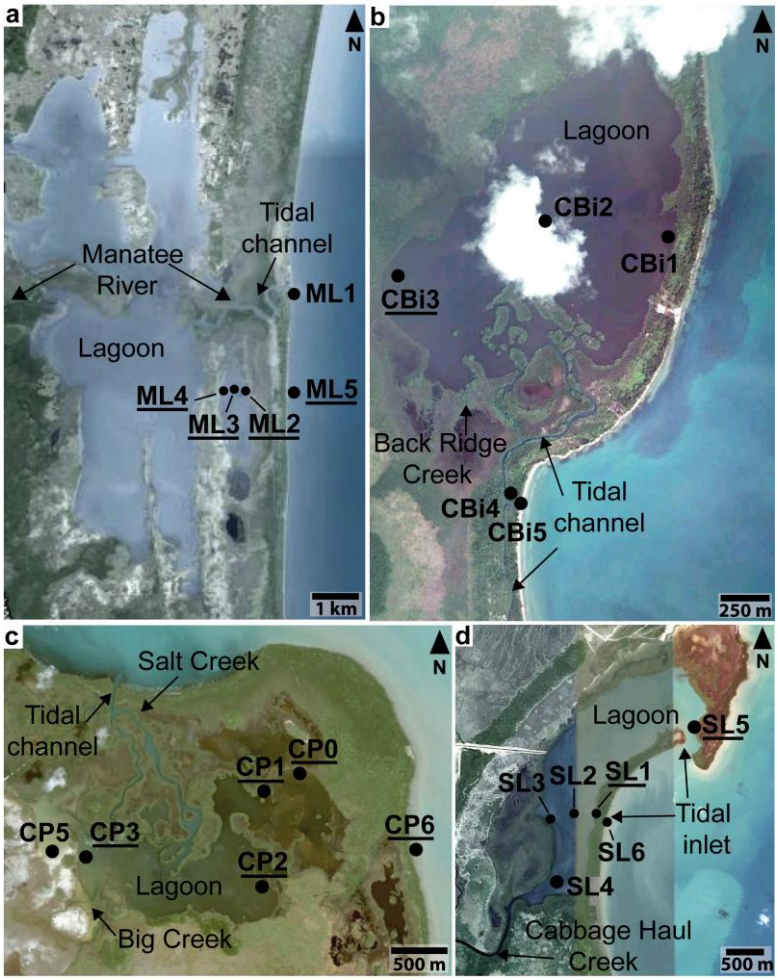

Fig. 3.2 Aerial photos showing coring sites (satellite images from Google Earth). **a** Manatee Lagoon (Quasi Trap Lagoon). **b** Commerce Bight Lagoon. **c** Colson Point Lagoon. **d** Sapodilla Lagoon. Coring sites with shell concentrations are underlined

Table 3.2 *List of cores drilled at Manatee Lagoon (ML), Colson Point Lagoon (CP), Commerce Bight Lagoon (CBi) and Sapodilla Lagoon (SL)*

Core	Coordinates		Water Depth	Core Length	Penetration	Compaction
	Latitude	Longitude	(cm)	(cm)	Depth (cm)	(%)
ML 1	N 17° 13`50.3``	W 88° 18`13.5``	40	122.5	349	64.90
ML 2	N 17° 12`41.5``	W 88° 18`46.2``	57	452	478	5.44
ML 3	N 17° 12`41.8``	W 88° 18`53.3``	93	274	302	9.27
ML 4	N 17° 12`41.0``	W 88° 19`03.2``	73	437	464	5.82
ML 5	N 17° 12`39.8``	W 88° 18`13.8``	100	432	500	13.60
CP 1	N 17° 03`25.7``	W 88° 15`22.2``	64	261	343	23.90
CP 2	N 17° 03`04.3``	W 88° 15`48.1``	88	168	257	34.60
CP 3	N 17° 03`12.9``	W 88° 16`13.6``	72	264	360	26.70
CP 5	N 17° 03`27.1``	W 88° 16`26.8``	57	99	109	9.17
CP 6	N 17° 03`15.3``	W 88° 14`37.9``	50	206	307	32.90
CBi 1	N 16° 54`04.5``	W 88° 16`55.9``	78	244	285	14.40
CBi 2	N 16° 54`08.2``	W 88° 17`17.0``	102	228	251	9.20
CBi 3	N 16° 53`55.3``	W 88° 17`42.2``	76	179	179	0.00
CBi 4	N 16° 53`18.6``	W 88° 17`22.7``	56	154	286	46.20
CBi 5	N 16° 53`18.1``	W 88° 17`21.6``	12	220	458	51.90
SL 1	N 16° 45`52.4``	W 88° 18`47.7``	109	271	366	26.00
SL 2	N 16° 45`52.5``	W 88° 18`58.3``	96	238	384	38.00
SL 3	N 16° 45`50.8``	W 88° 19`08.0``	78	325	453	28.26
SL 4	N 16° 45`22.0``	W 88° 19`05.8``	69	256	386	33.68
SL 5	N 16° 46`30.4``	W 88° 18`01.9``	94	457	489	26.18
SL 6	N 16° 45`48.4``	W 88° 18`43.7``	109	388	440	11.80

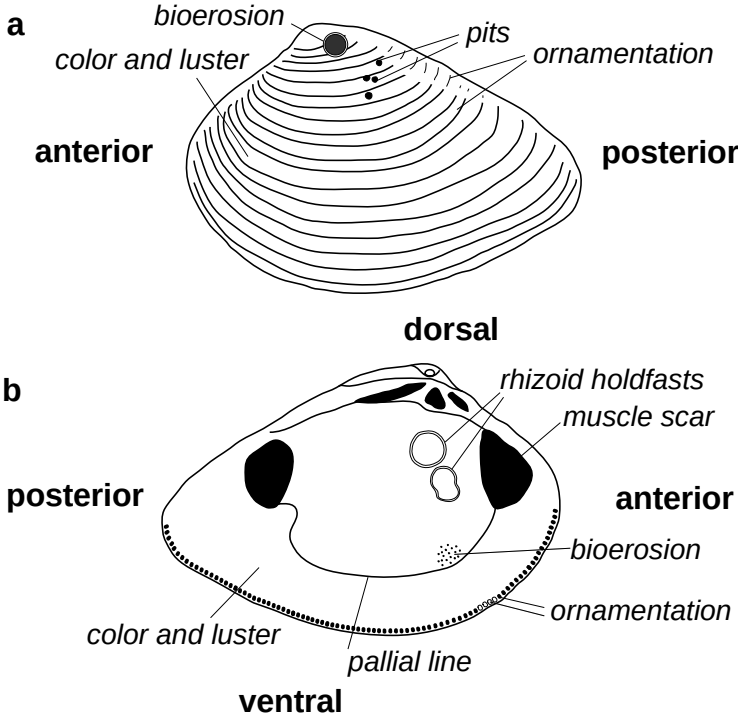

Fig. 3.3 Shell criteria, which were determined for taphonomic analysis of *Anomalocardia cuneimeris* valves. **a** External surface criteria include color and luster, ornamentation and pits. **b** Internal surface criteria include color and luster, ornamentation, pallial line and muscle scars

3.4 Results

3.4.1 Sediments

The unconsolidated siliciclastic sediments recovered in the cores were usually fine-grained in lagoons and coarser-grained at the lagoon margins and in the transitional zones between the lagoons and the sea (Figs. 3.4-3.7). Five principal facies could be distinguished. They included Pleistocene soil and Holocene peat/peaty sediment, muds, sands, and poorly sorted sediments (Adomat and Gischler 2015). However, facies successions and distribution did not show uniform patterns but strong local variation. Evolution of coastal lagoons started around 6 kyrs BP according to ^{14}C-data from Holocene organic matter and carbonate shells and skeletons. Pleistocene soil that underlay lagoonal sediments was not age-dated due to the lack of sufficient datable material.

3.4.2 Distribution of shell concentrations and radiocarbon dating

Twelve cores exhibited a total of 20 distinct shell concentrations (Figs. 3.4-3.8, Table 3.3). Fourteen concentrations derived from the coastal lagoons, one from the tidal inlet and five concentrations were found in marginal marine environments. Concentrations were most common in the two northernmost localities of Manatee (Fig. 3.4) and Colson Point Lagoons (Fig. 3.5). The former showed concentrations in four of five cores; in the latter five of six cores contained shell concentrations. The most seaward core at the Manatee locations was predominantly sandy and lacked shell concentrations. In the landward core at Colson Point, which comprised coarser-

grained deposits than the other lagoonal cores, concentrations were absent. At Commerce Bight (Fig. 3.6) and in Sapodilla Lagoon (Fig. 3.7), only one concentration was found in each, occurring at core top of the most landward lagoonal core and in the lower core portion of the most seaward lagoonal core, respectively. An additional concentration was observed at the tidal inlet to Sapodilla Lagoon.

The lateral extent of the shell concentrations is presumably low, because individual concentrations could not be correlated along individual core traverses and in many cases not even among adjacent cores that were located in a few hundred meters distance. Apart from the concentrations, mollusk shells also occurred dispersed within the cores and were abundant in some sediment types, such as in shelly sands from tidal channel and marginal marine environments. Mollusk shells in concentrations were usually mm-sized. Large cm-sized mollusk shells were found only rarely in muddy sediments.

Radiocarbon ages of concentrations ranged from 6000 cal BP to the modern (Table 3.3). One age, ML2 159-162 cm, seemed unreliable, because it was dated younger than overlying shells and peats. This could be due to diagenetic alteration of the shell material. The majority of ages of concentration from lagoons ranged from 6000 to 3500 cal BP. The concentrations from the tidal inlet (SL5) and the marginal marine realm (ML2 and the two upper concentrations in CP6) were younger than most of the concentrations from lagoonal environments.

3.4.3 Characterization of shell concentrations

The main characteristics of the shell concentrations are summarized in Table 3.3. Shell concentrations differed with respect to fabric, packing as well as species composition and relative shell abundance. The concentration from the tidal inlet area showed maximal thickness of 51 cm (SL5). The maximal thickness of concentrations from lagoonal environments was 27 cm (ML4). Fabric of concentrations from lagoons was matrix-supported, with loosely to dispersedly packed shells. Concentrations from the mangrove-fringed tidal inlet (SL5) and the marginal marine area (ML5) showed a bioclast-supported fabric and dense packing of larger shells. Core CP6 also derived from the marginal marine area, but the fabric of concentrations was similar to those of the concentrations deposited in the lagoons. In concentrations ML2 103-105 cm and ML2 159-162 cm shells were diagenetically altered and no complete shells ≥2 mm were preserved. Shelly remains in these concentrations appeared compacted and in ML2 159-162 cm enriched along the boundary between the soil and the overlying fine-grained Holocene sediment (Fig. 3.8b).

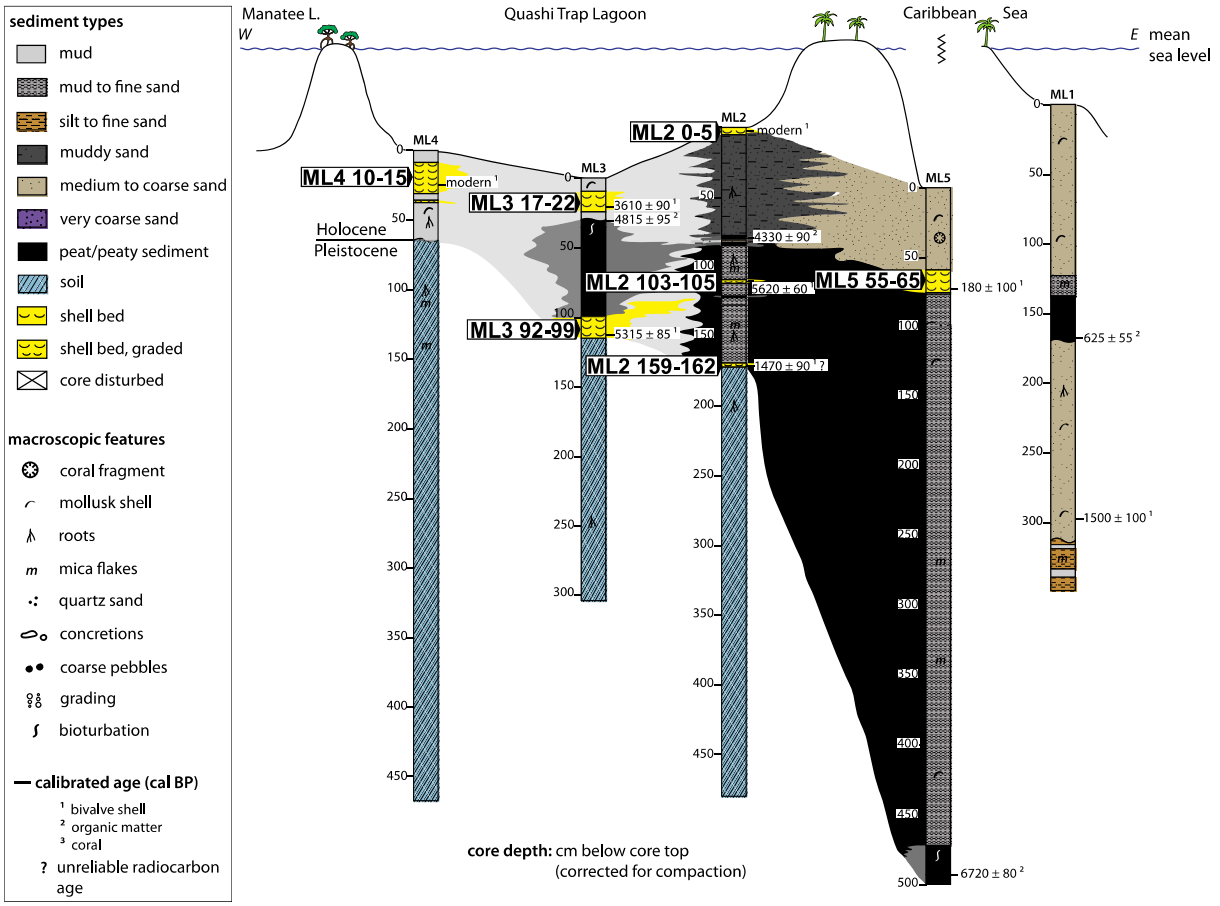

Fig. 3.4 Distribution of concentrations in cores from Manatee Lagoon. Six concentrations occur in the lagoon and one concentration in the marginal marine area. The two concentrations ML2 103-105 and ML2 159-162 are not included in Figs. 3.9, 3.10 and 3.11

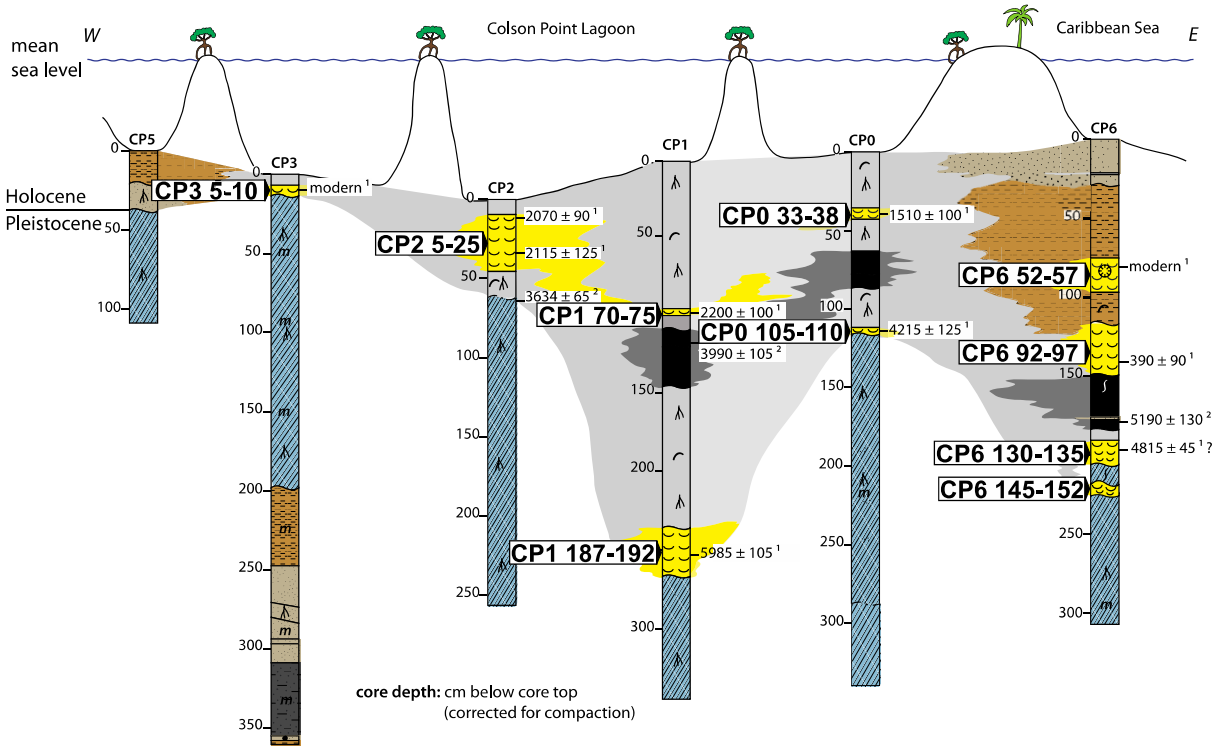

Fig. 3.5 Distribution of concentrations in cores from Colson Point Lagoon with six concentrations in the lagoonal cores and four concentrations in the marginal marine core. Legend see Fig. 3.4

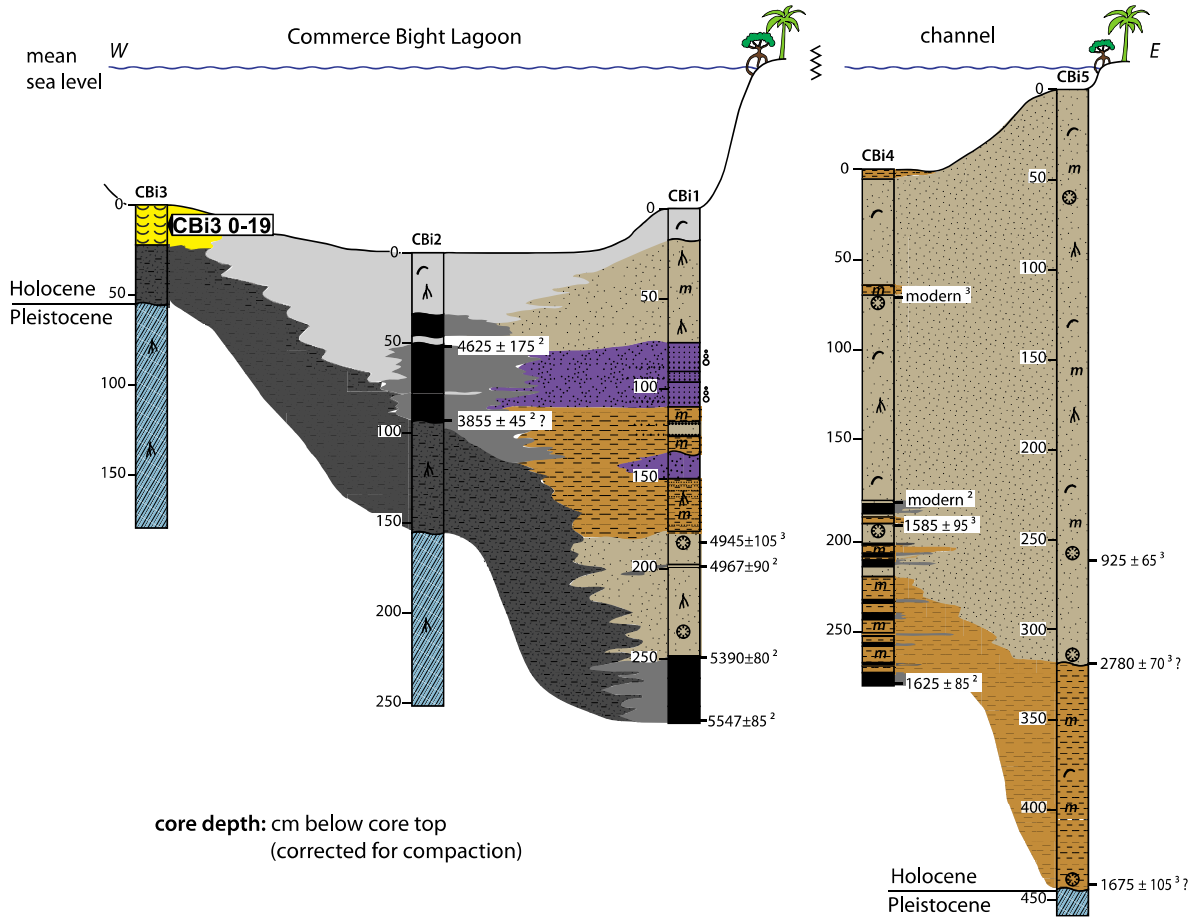

Fig. 3.6 Occurrence of one concentration in the lagoonal core CBi3 from Commerce Bight Lagoon. Legend see Fig. 3.4

Taxonomic and taphonomic analyses were not possible on shells from these accumulations. Shells were largely embedded in fine-grained sediments, which represented muddy lagoonal background sediments. In one shell accumulation from the marginal marine area, the matrix was medium grained quartz sand throughout. The quartz sand had been transported by longshore currents and formed a beach deposit. No visible changes in sediment composition and texture occurred directly below and above the concentrations in most cases. However, the concentrations overlay the Pleistocene soil or Holocene peaty sediment in some cases.

3.4.4 Taxonomic analysis of the mollusk fauna

The complete fauna comprised mainly mollusks, principally bivalves and gastropods, and rare scaphopods. In total, 53 species belonging to 42 families have been identified: 27 bivalve species, belonging to18 families, 25 gastropod species, belonging to 23 families and 1 scaphopod species, belonging to 1 family. Bivalves were more abundant than gastropods, comprising 2246 valves and 789 specimens, respectively. The number of species per

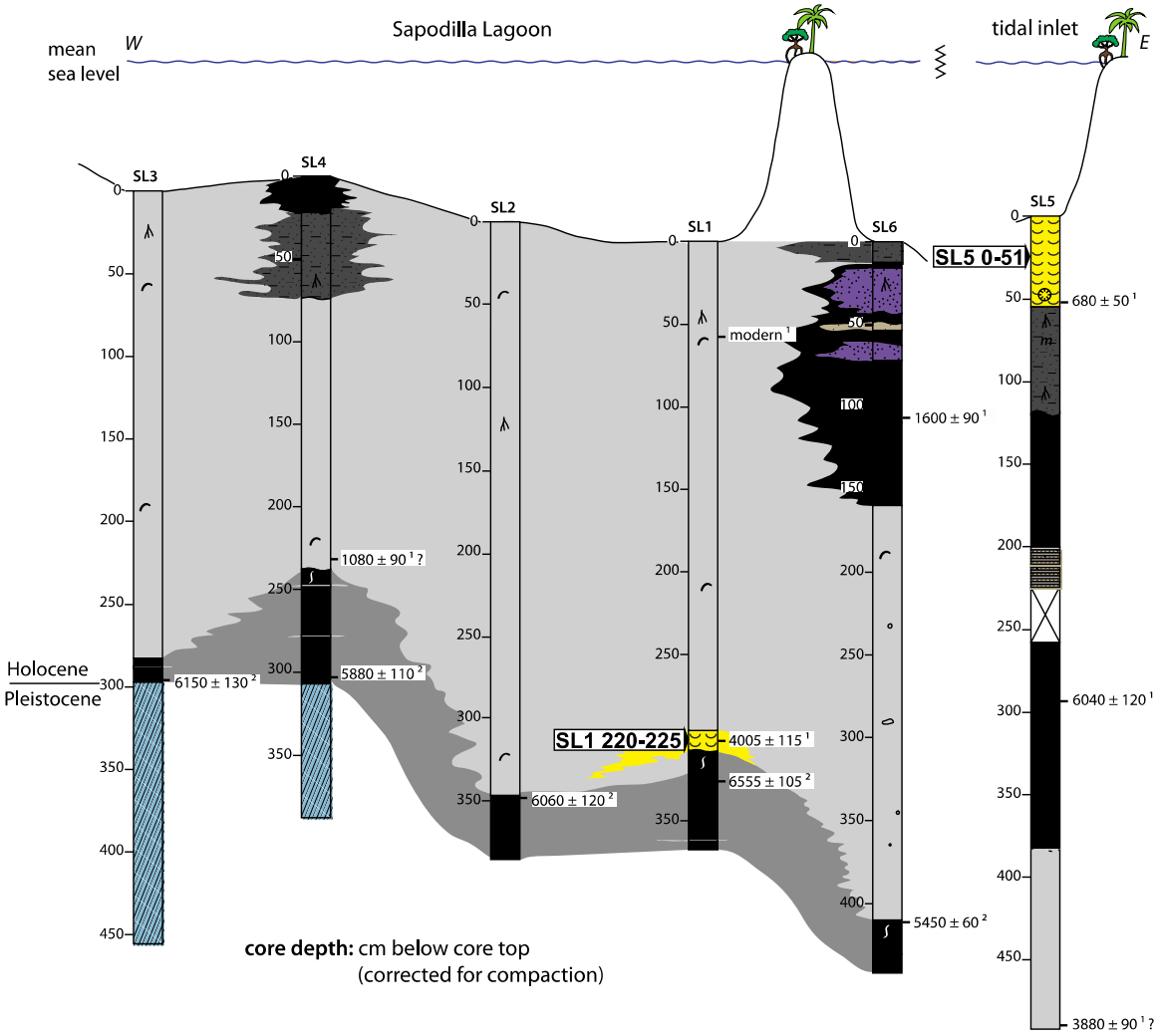

Fig. 3.7 Occurrence of one concentration in the lagoonal core SL1 and one concentration in core SL5 from the tidal inlet of Sapodilla Lagoon. Legend see Fig. 3.4

concentration ranged from 2 to 31, with fewer species in the lagoonal fauna and a relatively high number of species in the tidal inlet fauna (Table 3.4). The most common species were the bivalve *A. cuneimeris* and cerithid gastropods, which together accounted for 78% of the fauna.

Cluster analysis allowed grouping dendrogram branches into ten assemblages (Fig. 3.9). At a similarity level of 0.6 the samples formed five clusters in the dendrogram, including four clusters for the lagoon environment and one cluster for the marginal marine and tidal inlet environments (Fig. 3.9). Three samples are not fused at 0.6. This similarity level was used to define seven assemblages for lagoonal, two assemblages for marginal marine and one assemblage for tidal inlet environments. At a lower similarity level of 0.4, samples from coastal lagoons formed three clusters, and at a similarity level of 0.3, these samples could be grouped into two clusters. The NMDS ordination plots support the results obtained in the cluster analysis, in that they exhibit a similar grouping of the samples (Fig. 3.10a, b). Along the first axis (NMDS 1) of the plot, the

Table 3.3 *Characteristics of shell concentrations*

Core	Sample Depth (cm)	Thickness (cm)	Fabric	Packing	Matrix	Lower Contact	Upper Contact	Internal Structure	Calibrated Radiocarbon Age (yrs BP)
Lagoon									
ML2	0-5	5	Matrix-supported	Dispersed	Grey silt to fine sand	Gradational	None	Homogeneous	Modern
ML2	103-105	2	Matrix-supported	Dispersed	Grey mud to fine sand	Gradational	Gradational	Homogeneous, altered	5620±60
ML2	159-162	3	Matrix-supported	Loose	Grey mud to fine sand	Sharp, wavy	Gradational	Homogeneous, altered	1470±90 (Unreliable)
ML3	17-22	13	Matrix-supported	Loose	Grey mud	Gradational	Gradational	Homogeneous	3610±90
ML3	92-99	14	Matrix-supported	Loose	Grey mud	Gradational	Sharp	Mottled at base	5315±85
ML4	10-25	27	Matrix-supported	Loose to dispersed	Grey mud	Gradational	Sharp	Homogeneous	Modern
CP0	33-38	7	Matrix-supported	Dispersed	Grey mud	Gradational	Gradational	Homogeneous	1510±100
CP0	105-110	6	Matrix-supported	Loose	Grey mud	Sharp	Gradational	Bioturbation	4215±125
CP1	70-75	5	Matrix-supported	Dispersed	Grey mud	Gradational	Gradational	Homogeneous	2200±100
CP1	187-192	24	Matrix-supported	Loose	Grey mud	Gradational	Gradational	Bioturbation	5985±105
CP2	5-10,20-25	20	Matrix-supported	Loose	Grey mud	Gradational	Gradational	Homogeneous	2115±125
CP3	5-10	5	Matrix-supported	Loose	Grey mud	Gradational	Gradational	Homogeneous	Modern
CP6	130-135	11.5	Matrix-supported	Loose	Grey mud	Sharp	Gradational	Grading, bioturbation	4815±45
CP6	145-152	5.5	Matrix-supported	Loose	Grey mud	Sharp	Gradational	Grading, bioturbation	No age
CBi3	0-19	19	Matrix-supported	Loose	Grey silt to fine sand	Gradational	None	Homogeneous	No age
SL1	220-225	8	Matrix-supported	Loose	Grey mud	Sharp	Gradational	Homogeneous	4005±115
Tidal Inlet									
SL5	0-5,25-30,46-51	51	Bioclast-supported	Dense	Grey mud to fine sand	None	Gradational	Homogeneous	680±50
Marginal Marine									
ML5	55-65	14	Bioclast-supported	Dense	Yellowish brown medium sand	Gradational	Sharp	Homogeneous	180±100
CP6	52-57	14	Matrix-supported	Loose	Grey silt to fine sand	Sharp	Gradational	Homogeneous	Modern
CP6	92-97	22	Matrix-supported	Loose	Grey silt to fine sand	Gradational	Sharp	Homogeneous	390±90

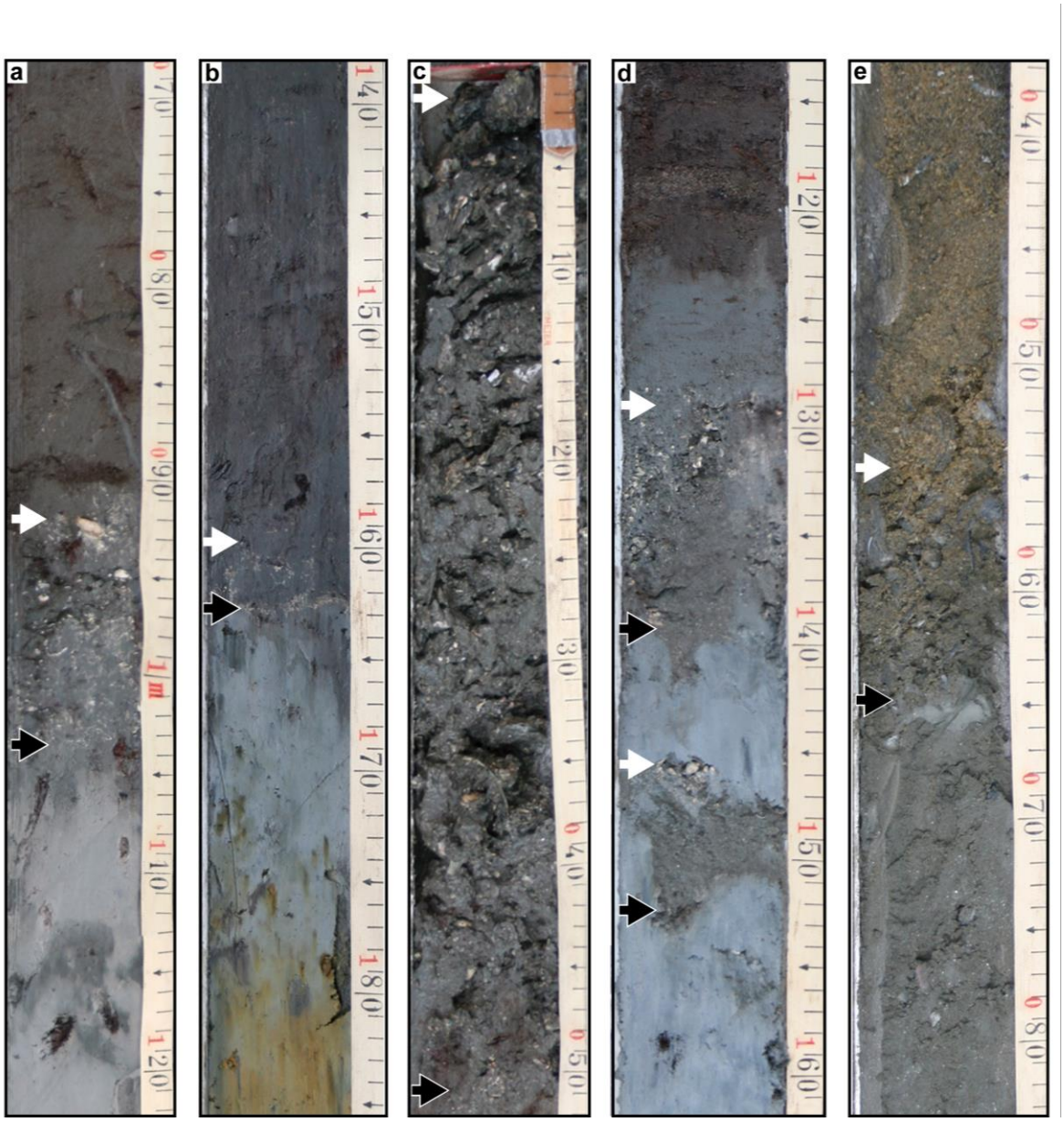

Fig. 3.8 Photos of selected cores showing concentrations from different coastal environments. White arrows mark the top, black arrows the base of concentrations. **a** Core ML3 from coastal lagoon; shells are sandwiched between Pleistocene soil and Holocene peaty mud and are more altered at the base of the concentration; the dominant species is *Anomalocardia cuneimeris*. **b** Core ML2 from coastal lagoon; shells are accumulated between Pleistocene soil and Holocene mud, at the depth of 160 cm; shells are altered and the concentration is represented by a mottled carbonate layer. **c** Core SL5 from a mangrove-fringed tidal inlet; concentration at top of core shows dense packing and a muddy matrix; shells comprise mainly *Cerithium* sp., *Bulla striata*, *Neritina virginea*, *Corbula* sp. and *Crassostrea* sp. **d** Core CP6 from the marginal marine area; the two lower concentrations in this core overlying Pleistocene soil show grading and bioturbation structures; the most common species is *A. cuneimeris*. **e** Core ML5 from the marginal marine area; densely packed concentration at the base of medium sand deposit at a depth of 50 to 65 cm, overlying a thin mud layer with sharp lower contact; shells contain mainly *Chione cancellata* and arcid bivalves

lagoonal samples are well separated from the samples from the tidal inlet and the marginal marine area (Fig. 3.10a). The NMDS plot also shows that the two basal concentrations in core CP6, which was drilled in the marginal marine area, can be assigned to lagoonal environments. In contrast, the two concentrations at the core top plot at the right hand side of the graph. The assemblages A1-A3, which formed a cluster at 0.4 (Fig. 3.9), plotted between the remaining lagoon and the marginal marine/tidal inlet assemblages along NMDS axis 1 (Fig. 3.10a,b). The NMDS plot of lagoon samples only shows the sample distribution based on a lower stress value (Fig. 3.10b).

Radiocarbon ages of the concentrations exhibited relatively narrow ranges of up to 1 kyr within most assemblages, which comprised more than one sample. In A1, ages ranged from 1510-2200 yrs cal BP. Concentrations in A4 were modern. Ages in A6 dated from 4215 to 5315 yrs cal BP. In A9, ages ranged from modern to 390 yrs cal BP. An exception is A7 where radiocarbon ages exhibited a range of almost 6 kyrs. One sample was not dated, but was assumed to be of modern or relatively young age, since the shells were found at the core top. About 3800 yrs separated the other two ages. Apart from the old radiocarbon age, CP1 187-192 also differed in that it plotted further away from the remaining samples in A7 (Fig. 3.10b). A distributional pattern of the radiocarbon ages showed that modern ages and ages up to 2200 yrs plotted more or less in the center of the ordination diagram (Fig. 3.10b). The majority of the older ages plotted in the upper section of the diagram; only one older age plotted at the bottom of the diagram.

The taxonomic composition of the assemblages A1-A10 is shown in Fig. 3.11 and in Tables 3.5 and 3.6. Assemblage A1 comprised largely *A. cuneimeris* and *C. eburneum* with proportions of 43% and 30%, respectively. *A. cuneimeris* was also the dominant species in A2, where it accounted for 67% of the fauna. Likewise, in A3, *A. cuneimeris* was the most abundant species, making up 25% of the fauna. Five other species exhibited proportion of more than 10%, of which *C. eburneum* reached the highest value of 14%. A4 was dominated by *C. pliculosa* and *A. cuneimeris*, with the former species being more frequent (59%) than the latter (33%). A5 was almost monospecific and comprised four species. The dominant species, *C. pliculosa*, accounted for 97% of the fauna. A6 and A7 both were dominated by *A. cuneimeris*, with proportions of 98% and 66%. Apart from *A. cuneimeris*, A6 comprised seven additional species, of which each species yielded proportions of less than 1%. In A7, *C. pliculosa* was the second most species with a proportion of 21%. CP1 189-192 (A7) was the only sample where the two cerithids *C. eburneum* and *C. pliculosa* co-occurred. Characteristic species found in the coastal lagoons are illustrated in Fig. 3.12.

Table 3.4 *Species richness (R), diversity (H) and evenness (E) of the mollusk fauna. The number of valves was divided by 2*

Core	Sample Depth (cm)	Number of Species (S)	Total Number of Individuals (N)	Species Richness (R)	Diversity (H)	Evenness (E)
Lagoon						
ML2	0-5	5	98	0.87	0.90	0.56
ML2	103-105	Highly altered	-	-	-	-
ML2	159-162		-	-	-	-
ML3	17-22	4	120	0.83	0.28	0.18
ML3	92-99	2	52	0.25	0.05	0.08
ML4	10-25	4	69	0.94	0.68	0.42
CP0	33-38	4	22	0.97	1.05	0.76
CP0	105-110	4	112.5	0.64	0.17	0.76
CP1	70-75	7	25	1.86	1.48	0.76
CP1	187-192	12	283.5	1.95	1.02	0.41
CP2	5-10,20-25	10	254	1.63	0.90	0.39
CP3	5-10	6	97.5	1.09	1.16	0.65
CP6	130-135	5	87.5	0.89	0.14	0.09
CP6	145-152	10	28.5	2.69	1.35	0.59
CBi3	0-19	5	254.5	0.72	0.98	0.61
SL1	220-225	12	58	2.71	2.09	0.84
Tidal Inlet						
SL5	0-5,25-30,46-51	31	254.5	5.97	2.30	0.66
Marginal Marine						
ML5	55-65	19	70	4.24	2.48	0.84
CP6	52-57	14	19.5	4.38	2.48	0.89
CP6	92-97	13	19.5	4.04	2.29	0.89

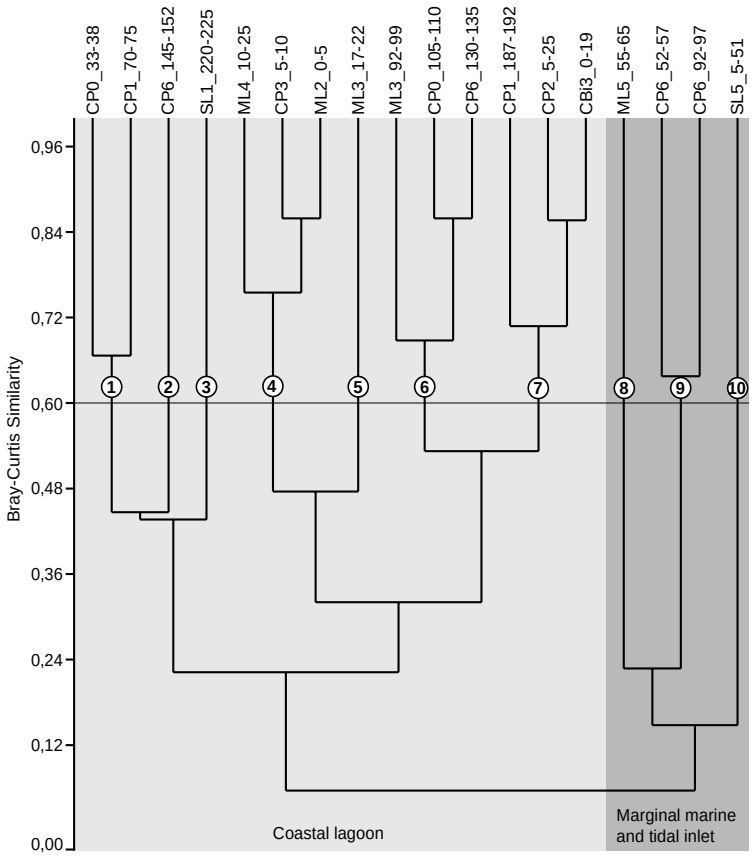

Fig. 3.9 Hierarchical Q-mode cluster analysis for concentrations from lagoonal, tidal inlet and marginal marine environments. Clustering was based on species abundance data of each shell concentration. At a similarity level of 0.6, seven lagoonal assemblages and three marginal marine and tidal inlet assemblages were defined. Clustering method: Bray-Curtis Similarity, Unweighted pair-group average (UPGMA)

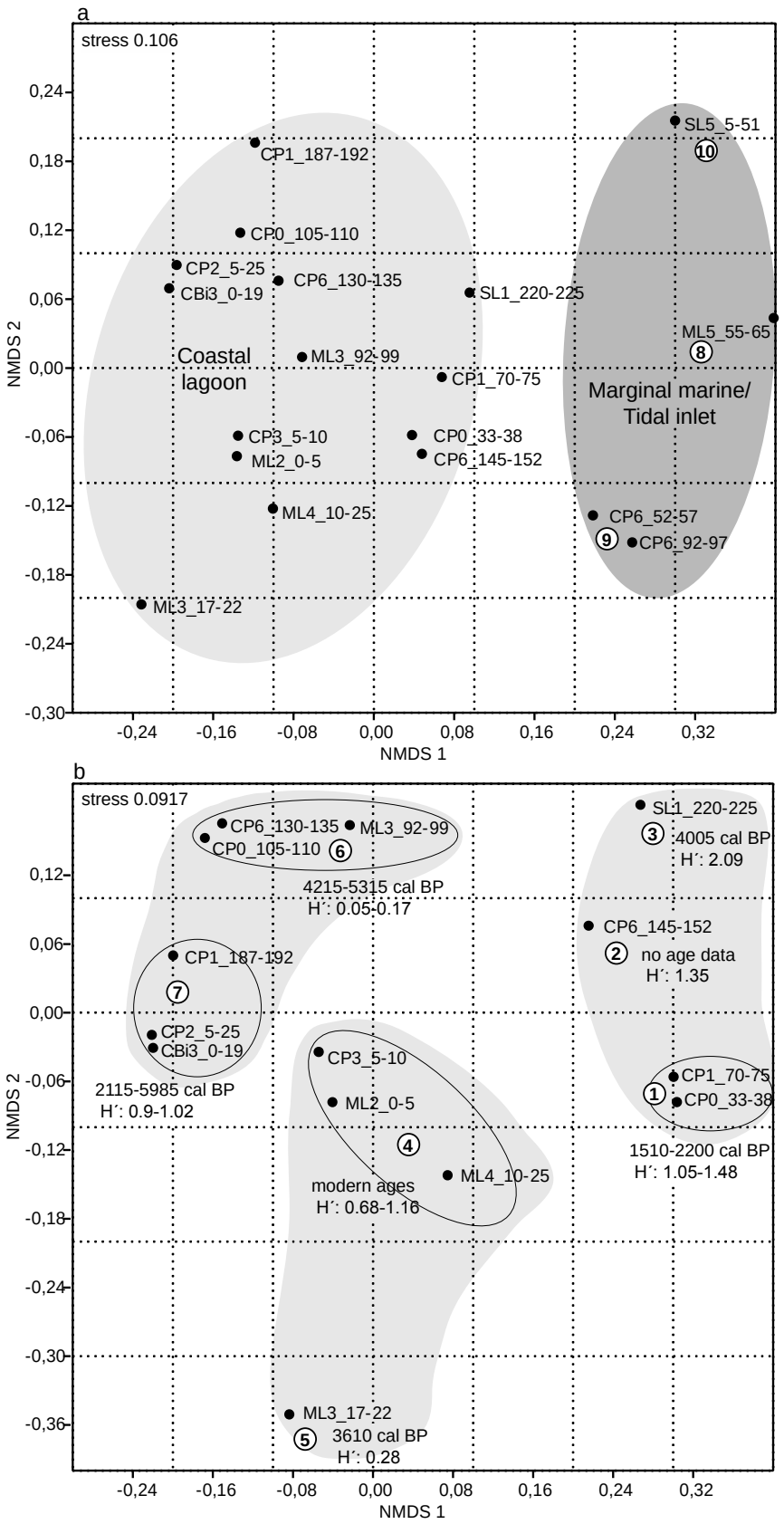

Fig. 3.10 NMDS ordination plots based on all samples (a) and by using lagoonal samples only (b). Numbering of assemblages from lagoons is based on the cluster analysis at a similarity level of 0.6. **a** Samples from lagoonal environments are well separated from samples from the marginal marine and tidal inlet areas. **b** The three clusters formed at a similarity level of 0.4 are highlighted in grey. Black ellipses group samples that form assemblages

In summary, besides the clear separation between assemblages from lagoons and assemblages from the marginal marine/tidal inlet environments, a trend in species distribution could be observed along NMDS axis 2 (Fig. 3.10b). There was a change from a nearly monospecific assemblage of *C. pliculosa* at the bottom, to *A. cuneimeris*/cerithid assemblages in the center and lastly to an almost monospecific assemblage of *A. cuneimeris* at top of the diagram. There was also an apparent trend in the distribution pattern of cerithids, with a replacement of *C. pliculosa* by *C. eburneum*. In the NMDS plot, *C. eburneum* occurred at the ends of axes NMDS 1 and NMDS 2.

Too few samples were obtained from the marginal marine and tidal inlet environments to define statistically robust associations. Assemblage A10 contained the gastropods *C. eburneum*, *Neritina virginea* (Linnaeus 1758), *Bulla striata* (Bruguière 1792), *Cerithium atratum* (Born 1778), the bivalve *Corbula* sp. (Bruguière 1797) and the oyster *Crassostrea* sp. (Guilding 1828), which lives attached on the prop roots of mangroves. Also a number of filter-feeding, attached forms such as *Brachidontes exustus* (Linnaeus 1758) and *Crepidula* sp. (Broderip 1834) were observed. *A. cuneimeris* was absent and few scaphopods of the genus *Dentalium* sp. (Linnaeus 1758) occurred.

Assemblage A8 was attributed to the marine fauna of the two topmost concentrations in the marginal marine core CP6. The bivalves *Diplodonta* sp. (Bronn 1831), *Lunarca ovalis* (Bruguière 1789), *C. cancellata* (Linnaeus 1767), *A. cuneimeris* and *Tellina* spp. (Linnaeus 1758) were common species. Gastropods were represented by *Olivella* sp. (Swainson 1831) and *Conus* sp. (Linnaeus 1758). The fauna of ML5 55-56 cm was defined as Assemblage A9. It was dominated by the bivalves *Chione cancellata*, *Corbula* sp. and arcids. Shells of these taxa were also found abundantly on the beach of Manatee Lagoon. The most common gastropod was *Olivella* sp. *Dentalium* sp. occurred in Assemblage A8, but not in A9. In contrast to the coastal lagoons, only few *A. cuneimeris* specimens were found in A9, and none in A8.

Measures of diversity were higher in marginal marine and tidal inlet environments as compared to the lagoonal settings (Table 3.4). For example, Margalef index was low in concentrations from lagoonal environments with values ranging from R=0.25 to 2.71. In contrast, mollusk fauna from the marginal marine environment showed values of R>4.0. The highest value of R=5.96 was obtained from the tidal inlet concentration. Shannon-Wiener index was low in lagoonal environments with values from H=0.05 to 2.09, and higher in the marginal marine area and tidal inlet area with values from H=2.29 to 2.48. In the ordination diagram for lagoonal samples diversity changes along NMDS axis 1 (Fig. 3.10b). Assemblages A1 and A3 exhibited high diversity. Assemblage A7 showed H' of around 1 and was intermediate; diversity measure in A4, A5, and A6 were generally low.

Dispersed mollusk shells outside the concentrations were generally more abundant in muds from Sapodilla Lagoon than in muds from other lagoons. A comparison of the concentration SL1

220-225 at the base of Holocene muds, which was dated to ~4000 cal BP (Fig. 3.7) and a sample of dispersed shells from the upper core section of the same core (not shown in Figs. 3.7, 3.9 and 3.10 because it did not originate from a concentration), indicated an upcore change in species composition. Species composition showed a replacement of *C. eburneum* by *C. pliculosa* with individual numbers of the two species of 25 and 6 specimens, respectively. Additionally, in the lower part of SL1, *Lucina muricata* (Sprengler 1798) was found, and the upper core sections contained *Lucina pectinata* (Gmelin 1791).

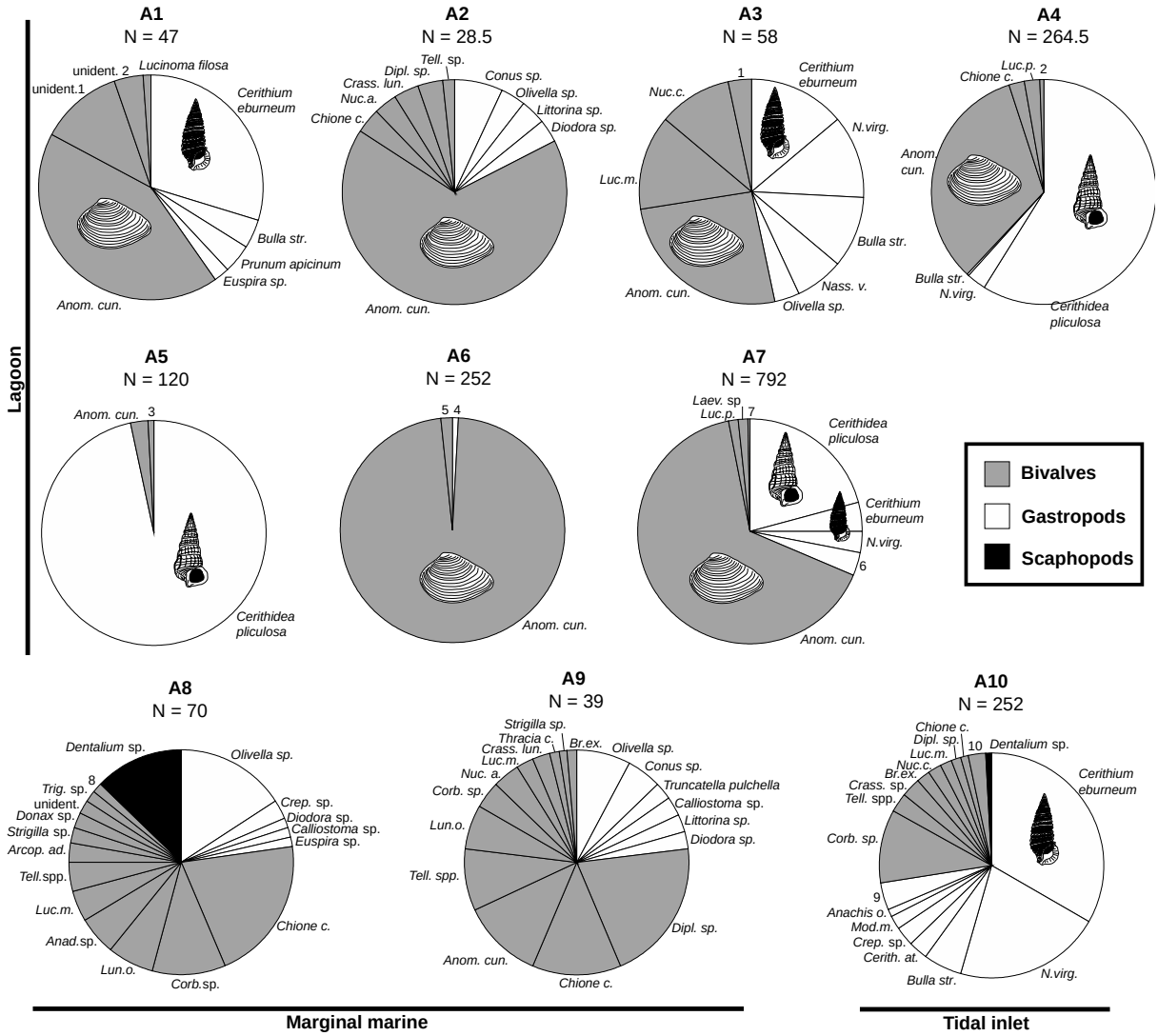

Fig. 3.11 Pie diagrams illustrating the taxonomic composition of the ten assemblages. N: Number of individuals. The two lower concentrations in ML2 are not included in the diagrams. Abbreviations are shown in Table 3.5. Taxa with proportions of < 1% in an assemblage are summarized (1-10) and shown in Table 3.6

Table 3.5 *List of abbreviations used in diagrams in Fig. 3.11*

Abbreviation	Genus/Species
Anachis o.	*Anachis obesa*
Anad sp..	*Anadara* sp.
Anom. cun.	*Anomalocardia cuneimeris*
Arcop. ad.	*Arcopsis adamsi*
Br. ex.	*Brachidontes exustus*
Bulla str.	*Bulla striata*
Cerith. at.	*Cerithium atratum*
Chione c.	*Chione cancellata*
Corb. sp.	*Corbula* sp.
Crass. lun.	*Crassinella lunulata*
Crass. sp.	*Crassostrea* sp.
*Crep.*sp.	*Crepidula* sp.
Dipl. sp.	*Diplodonta* sp.
Laev. sp.	*Laevicardium* sp.
Luc.m.	*Lucina muricata*
Luc.p.	*Lucina pectinata*
Lun.o.	*Lunarca ovalis*
Mod.m.	*Modulus modulus*
Nass. v.	*Nassarius vibex*
Nuc.a.	*Nuculana acuta*
Nuc.c.	*Nuculana concentrica*
N.virg.	*Neritina virginea*
Tell. spp.	*Tellina* spp.
Trig. sp.	*Trigoniocardia* sp.

Table 3.6 *List of taxa summarized in diagrams in Fig. 3.11*

No.	Genus/Species
1	*Brachidontes exustus*
	Nucula sp.
	Laevicardium sp.
	Tagelus divisus
2	*Brachidontes exustus*
	Lucina nassula
3	unidentified 4,5
4	*Cerithium eburneum*
	Neritina virginea
5	*Corbula* sp.
	Lucina nassula
	Tellina sp.
	Laevicardium sp.
	Crassinella lunulata
6	*Crepidula* sp.
	Prunum apicinum
	Bulla striata
	Epitonium sp.
	Cantharus sp.
	Melongena melongena
7	unidentified 3
	Tellina sp.
8	*Brachidontes exustus*
	Plicatula gibbosa
9	*Bittium reticulatum*
	Olivella sp.
	Calliostoma sp.
	Euspira sp.
	Anticlimax sp.
	Zebinella sp.
	Mangelia sp.
	Turbonilla incisa
10	*Nucula* sp.
	Arcopsis adamsi
	*Dallocardi*a *muricata*
	Crassinella lunulata
	Aequipecten exasperatus
	Hiatella sp.
	unidentified 6

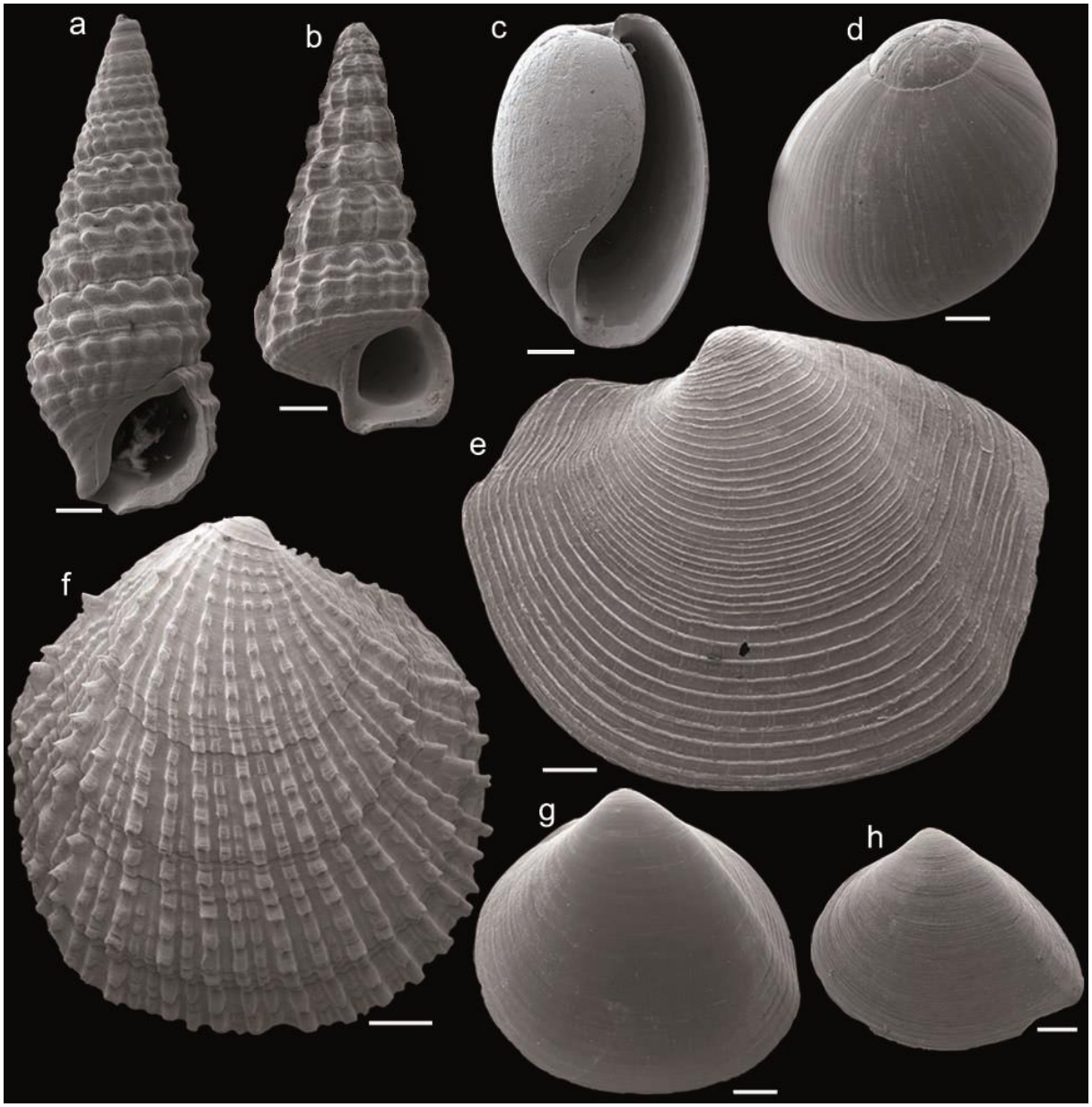

Fig. 3.12 Common species found in coastal lagoons (SEM-photographs). **a** *Cerithium eburneum*. **b** *Cerithidea pliculosa*. **c** *Bulla striata*. **d** *Neritina virginea*. **e** *Lucina pectinata*. **f** *Lucina muricata*. **g** *Laevicardium* sp. **h** unidentified bivalve. The bivalve *Anomalocardia cuneimeris* is illustrated in Fig. 3.14. Scale bar is 1 mm

3.4.5 Taphonomic analysis of shells of Anomalocardia cuneimeris

3.4.5.1 Size-frequency distributions and left-right valve ratio

Maximum valve length of *A. cuneimeris* in coastal lagoons was 16.21 mm with a mean of 6.4 mm. No visible trend in mean length and height among localities and environments was observed (Table 3.7). Most size-frequency distributions were unimodal and right-skewed (Fig. 3.13a, b, e-h, j, k, m, n) with peaks in the 4-6 mm class. Shell size in CP6 145-152 cm was left-skewed (Fig. 3.13l). Samples CP0 33-38 cm and ML4 10-25 cm showed no skewness (Fig. 3.13c, d). Both samples contained a low number of valves compared to most of the other samples. CP2 20-25 showed a distribution between bell-shaped and right-skewed (Fig. 3.13i). The mean of the left-

right valve ratio in most concentrations from lagoonal environments ranged from 1 to 1.6. Except for valves from sample CP0 105-110, the LR-ratio was not statistically different from 1:1 (H_0 could not be rejected) (Table 3.7).

3.4.5.2 Preservation

Excellent preservation of external and internal surfaces was observed in 6.7% of all investigated valves, and 4.5% of all valves exhibited chalky surfaces. The highest value of chalkiness in lagoonal cores was reached in CBi3 0-19 cm, where 77% of the valves have chalky textures (Table 3.7). The posterior margins were more affected by loss of the external ornamentation than the anterior margins. The degree of bioerosion and the number of rhizoid holdfasts was relatively low and affected 6.1% of the valves. Circular borings were attributed to predatory gastropods. Sponge borings by clionids were observed only on internal surfaces of 5.2% of the valves. The discoid rhizoid holdfasts that occurred mainly on shells from Colson Point Lagoon were only found on inner surfaces. They can be allocated to brown algae, which use the holdfasts to attach themselves to the substrate. Taphonomic signatures of valves are illustrated in Fig. 3.14.

The taphonomic grades and preservation states of external and internal surfaces of *A. cuneimeris* valves are summarized in Table 3.8. Valves with excellently preserved external surfaces generally had excellently preserved internal surfaces. In contrast, valves with poorly preserved external surfaces might have well preserved internal surfaces. Shell preservation did not show strong correlation with core depth and age. ML2 0-5, CP0 33-38 and CP1 70-75 contained the highest proportion of excellently preserved external surfaces of valves, with values between 47% and 48%. The highest value of poorly preserved external surfaces amounted to 28.8% and was reached in a concentration from the core top, in CP3 5-10. The proportion of poorly preserved valves with each of the examined criteria being met, was generally higher on external surfaces. Highest values of excellently preserved internal surfaces were observed in ML2 0-5 and CP1 70-75, with 48.5% and 42.1% excellently preserved internal surfaces, respectively. Both concentrations also exhibited high proportions of excellently preserved external surfaces. On the internal surface, muscle scars and the pallial line were more likely to be preserved than color, luster and ornamentation (Table 3.8). A correlation between shell preservation and grain size of matrix could not be observed. Matrices of concentrations from lagoonal environments were usually fine-grained and consisted of mud to fine sand.

SEM images of fractures through well-preserved valves show that the cross lamellae are clearly recognizable (Fig. 3.15a). On the contrary, in poorly preserved, chalky valves, the cross-lamellar microstructure is hardly visible and the surface is pitted (Fig. 3.15b, c). Original color of the very common lagoonal species *C. pliculosa*, which is brown with one white band on each whorl, was only preserved in two of 436 specimens. They were found in the upper sections of the cores CP2 and CP3. Shell preservation seemed not to be biased toward shell mineralogy, as

XRD analyses showed that both pristine and chalky valves were composed of 100% aragonite. Shells from the marginal marine area were not examined in detail with respect to taphonomic attributes, but most shells were affected by corrasion and few by borings and encrustations. Only shells of *Olivella* sp. showed original color and luster.

Table 3.7 *Taphonomic attributes of Anomalocardia cuneimeris valves. R: Right valve, L: Left valve; B: Both valves; Corrasion: values of valves with chalky texture indicate %-proportion. The number of affected valves is indicated for the rhizoid holdfasts and for bioerosion. For assignment of the criteria see Fig. 3.3*

Core	Sample Depth (cm)	Number of Valves	Size (mm)		(Dis)Articulation					Corrasion		
			Mean Length	Mean Height	R	L	B	LR-Ratio	χ^2	Chalkiness	Bio-erosion	Rhizoid Holdfasts
Lagoon												
ML2	0-5	66	6.2	4.8	30	36	1	1.2	0.55	0	-	2
ML2	103-105	Highly	-	-	-	-	-	-	-	-	-	-
ML2	159-162	altered	-	-	-	-	-	-	-	-	-	-
ML3	17-22	6	7.2	5.8	2	4	-	2	0.67	17	-	-
ML3	92-99	103	6.1	4.8	52	51	-	1	0.01	31	4	-
ML4	10-25	35	7	5.4	19	16	-	1.2	0.26	14	1	-
CP0	33-38	21	6.3	4.7	10	11	-	1.1	0.05	5	-	-
CP0	105-110	218	5.9	4.6	93	125	1	1.6	4.70	0	-	-
CP1	70-75	19	5.4	4.2	8	11	-	1.4	0.47	0	1	-
CP1	187-192	412	5.3	4.2	211	201	1	1	0.24	0	-	48
CP2	5-10, 20-25	347	7.1	5.4	171	176	1	1	0.07	7	2	19
CP3	5-10	73	6.1	4.8	40	33	-	1.2	0.67	41	-	1
CP6	130-135	171	6.5	5	81	90	-	1.1	0.47	1	-	9
CP6	145-152	38	7.4	5.8	21	17	-	1.2	0.42	11	1	6
CBi3	0-19	279	7.6	5.9	140	139	-	1	0.00	77	1	-
SL1	220-225	30	5.8	4.4	14	16	-	1.1	0.13	3	2	-
Tidal Inlet												
SL5	0-10,25-30,46-51	0	-	-	-	-	-	-	-	-	-	-
Marginal Marine												
ML5	55-65	0	-	-	-	-	-	-	-	-	-	-
CP6	52-57	5	6.5	5.1	3	2	-	1.5	0.20	80	2	-
CP6	92-97	4	6.8	5.5	3	1	-	3	1.00	50	1	-

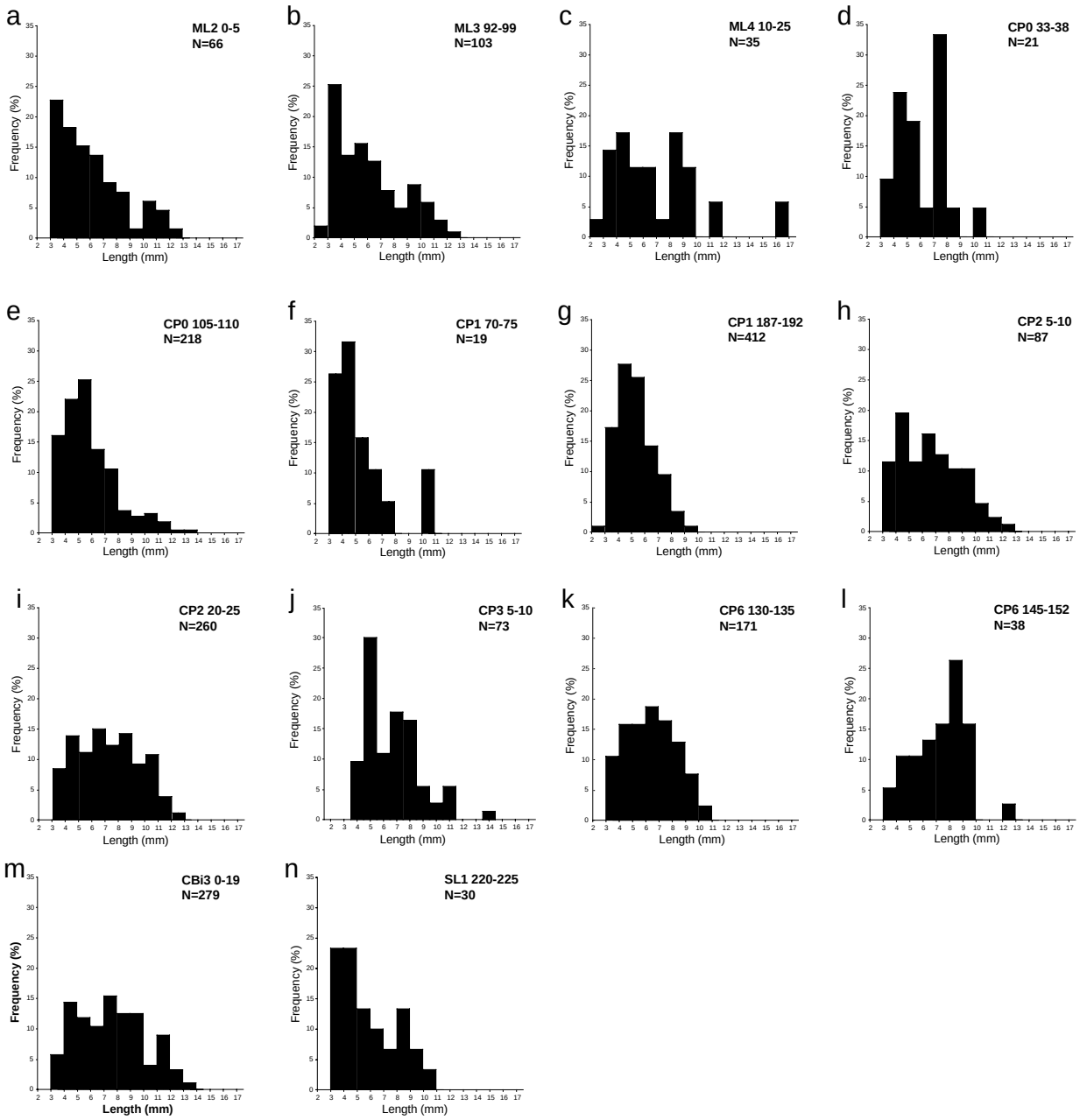

Fig. 3.13 Size-frequency diagrams of *Anomalocardia cuneimeris* valves ≥2 mm found in concentrations from lagoonal environments. N: Number of valves investigated

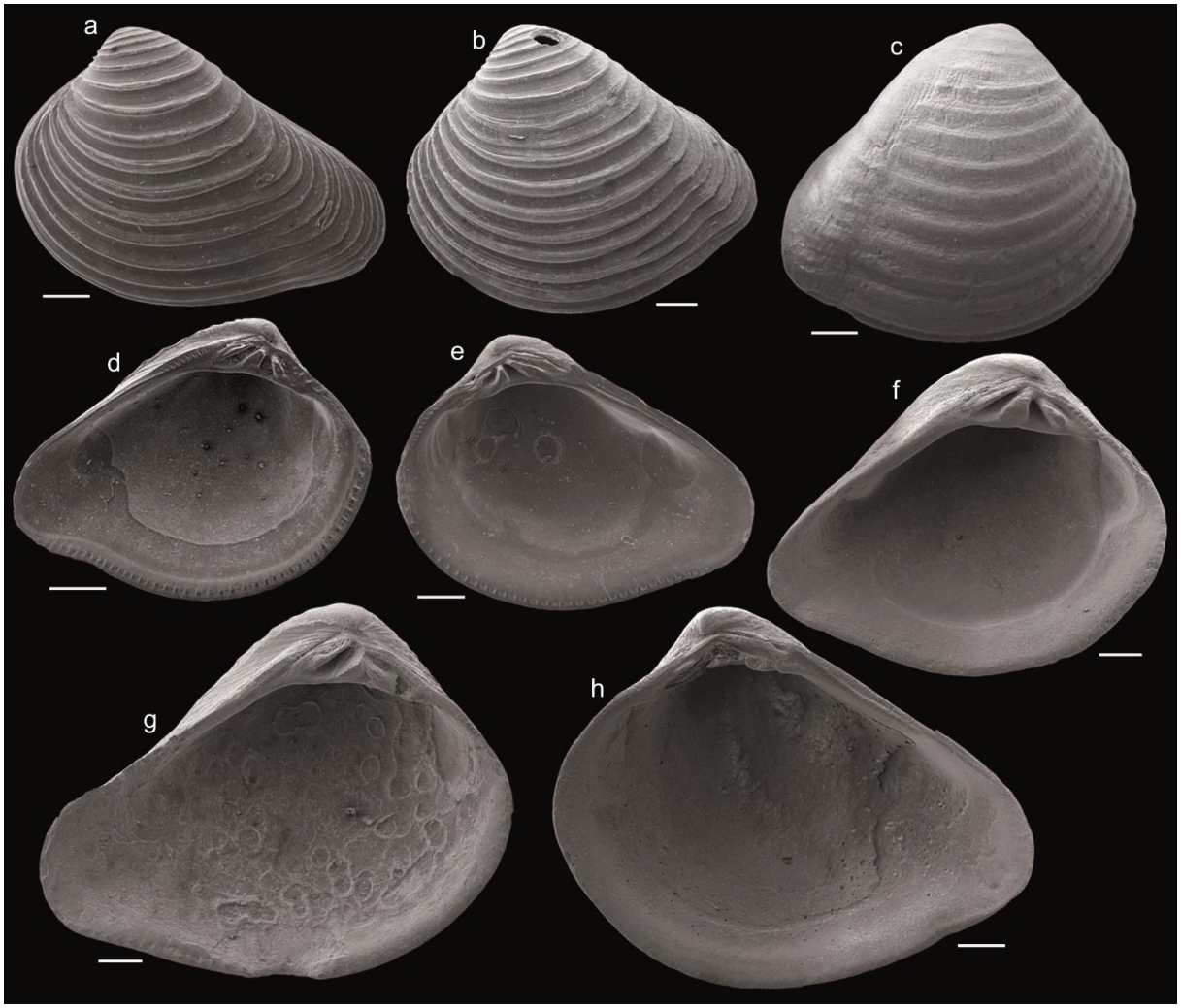

Fig. 3.14 Taphonomic signatures of external (a-c) and internal (d-h) surfaces of *Anomalocardia cuneimeris* valves (SEM-photographs). **a** Excellent preservation of left valve. **b** Well preserved of left valve with gastropod boring near the umbo. The posterior margin is affected by corrasion. **c** Fairly preserved right valve. The ornamentation, especially on the posterior margin, is affected by corrasion. The ventral region of the valve is pitted. **d** Excellently preserved left valve. **e** Excellently preserved right valve with rhizoid holdfasts. **f** Fairly preserved left valve showing loss of ornamentation. The pallial line and muscle scars are still recognizable. **g** Poorly preserved left valve with abundant rhizoid holdfasts. **h** Fairly preserved right valve with clinoid borings, which occur largely in the posterior region of this valve. Scale bar is 1 mm

Table 3.8 *Taphonomic grades and preservation states of external and internal surfaces of Anomalocardia cuneimeris valves from shell concentrations from lagoonal environments. C: Color; L: Luster; O: Ornamentation; P: Pits; PL: Pallial line; MS: Muscle scars. It is indicated if criteria are altered (x) or unaltered (-). The degree of alteration is not included. Values indicate %-proportion of valves*

Taphonomic Grade	External Surface				ML2 0-5	ML3 17-22	ML3 92-99	ML4 10-25	CP0 33-38	CP0 105-110	CP1 70-75	CP1 187-192	CP2 5-25	CP3 5-10	CP6 130 - 135	CP6 145 - 152	CBi3 0-19	SL1 220 -225
	C,L		O	P														
Excellent	-	-	-		47.0	0	4.9	2.9	47.6	9.6	47.4	36.2	10.7	12.3	0	7.9	2.5	13.3
	x	-	-		25.8	0	30.1	20.0	0	11.5	5.3	5.8	18.7	21.9	7.6	23.7	19.7	36.7
Good	-	x	-		1.5	0	0	0	4.8	25.7	0	20.6	1.7	1.4	0	18.4	0	0
	-	-	x		0.0	0	1.0	0	33.3	0	0	0.2	0.3	4.1	0	2.6	1.4	3.3
	x	x	-		7.6	33.3	34.0	14.3	0	52.3	26.3	34.0	54.5	28.8	92.4	31.6	26.5	20
Fair	-	x	x		0.0	0	0	0	0	0.5	0	0.2	0	0	0	0	0	0
	x	-	x		7.6	66.7	9.7	31.4	9.5	0.5	21.1	0	0	2.7	0	0	25.8	16.7
Poor	x	x	x		10.6	0	20.4	31.4	4.8	0	0	2.9	14.1	28.8	0	15.8	24.0	10

Taphonomic Grade	Internal Surface				ML2 0-5	ML3 17-22	ML3 92-99	ML4 10-25	CP0 33-38	CP0 105-110	CP1 70-75	CP1 187-192	CP2 5-25	CP3 5-10	CP6 130 - 135	CP6 145 - 152	CBi3 0-19	SL1 220 -225
	L,C	PL	MS	O														
Excellent	-	-	-	-	48.5	0	3.9	22.9	0	3.2	42.1	25.5	11.0	6.8	0	0	6.1	20
Good	x	-	-	-	19.7	0	27.2	17.1	47.6	21.1	26.3	21.8	18.7	6.8	0	0	11.5	23.3
	-	-	-	x	4.5	0	1.0	5.7	0	0.5	10.5	4.9	1.7	2.7	0	0	1.8	0
	x	x	-	-	1.5	0	1.9	0	0	0	0	0.2	0	0	0	0	1.8	0
	x	-	-	x	16.7	100	40.8	45.7	47.6	55.5	21.1	41.3	45.5	57.5	28.1	76.3	47.0	50
Fair	x	x	-	x	6.1	0	20.4	8.6	0	19.3	0	6.3	18.4	20.5	57.3	23.7	22.9	6.7
	x	x	x	-	0.0	0	0	0	0	0	0	0	0	0	0	0	0.7	0
	x	-	x	x	0.0	0	0	0	0	0	0	0	0	0	0	0	0.4	0
Poor	x	x	x	x	3.0	0	4.9	0	4.8	0.5	0	0	4.6	5.5	14.6	0	7.9	0

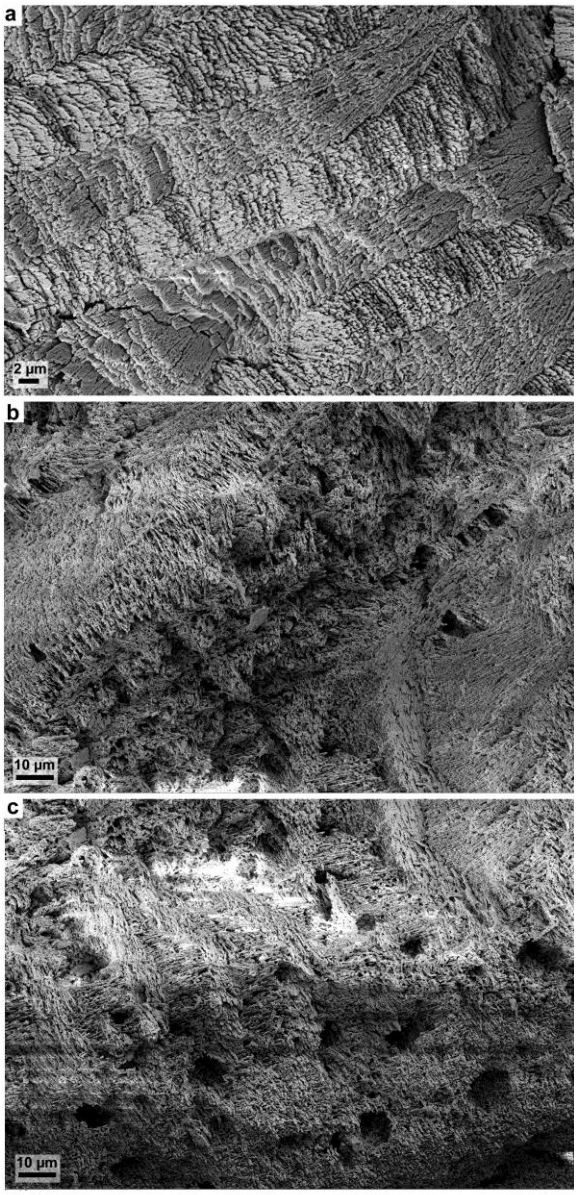

Fig. 3.15 SEM images of fractures through *Anomalocardia cuneimeris* valves, showing a pristine valve with recognizable cross lamellar microstructure (a), and a poorly preserved valve with only vaguely recognizable cross lamellae (b) and a pitted surface (c)

3.5 Discussion

3.5.1 Distribution of assemblages and their implication for paleoenvironmental reconstruction

The distribution of shell concentrations among localities, with concentrations being more frequent in cores from the northern localities than in cores from the southern localities (Figs. 3.4-3.7), probably reflects the general increase in salinity from the north to the south in the study area. Table 3.1 shows that highest values were measured in the southernmost locality. Still, a uniform trend in salinity from north to south is not recognizable. A landward decrease in salinity from east to west was measured in most cases. Salinity in the lagoons is largely controlled by geomorphology, i.e., by the connectivity of the lagoons with the open Belize shelf. For example, the broad tidal inlet to Sapodilla Lagoon allows considerable mixing of lagoon and ocean water, which results in increased salinity in the northeastern area of this site.

The separation between the marginal marine/tidal inlet assemblages and the assemblages from lagoons seen in ordination along NMDS axis 1 (Fig. 3.10a) reflects a lagoon-onshore gradient, which indicates different environmental conditions. In contrast to the coastal lagoons, the onshore area is characterized by physical characteristics such as higher water energy, sediment transport by longshore currents and higher salinity. Coastal lagoons have low flushing rates because of restricted exchange with the ocean (Anthony et al. 2009). In restricted lagoons with low flushing rates and high nutrient inputs, an increase in temperature may promote hypoxic events (D'Avanzo and Kremer 1994). The arrangement of assemblages from lagoons along NMDS axis 2 suggests that environmental changes also occurred in the lagoonal environments (Fig. 3.10b). Several climatic factors influence the processes and physical properties of coastal lagoons (Anthony et al. 2009). For example, fresh-water input during increased runoff from the mainland may result in a decrease in salinity. On the other hand, barrier breaching and overwash of saline water from the sea during storm surge cause an increase in salinity. Changes in salinity may also result from inundation. In addition to salinity, many other properties such as clastic influx, turbidity, light intensity, temperature, oxygen, nutrient supply, bottom stability and water depth may change.

Assemblages A1, A2 and A3 that are separated from the other lagoon assemblages in the NMDS plot (Fig. 3.10a, b) indicate conditions between lagoon and onshore. Maybe a less restricted circulation resulted in a higher diversity compared to A4-6 and A7. The distribution of the cerithids in the assemblages from lagoons can be used as indicator of environmental conditions, because *C. eburneum* and *C. pliculosa* show different habitat preferences. *C. eburneum*, which is a common species in A1 and A3, occurs for example, in cores CP0 and CP1, which both derive from the northeastern area at the seaward region of Colson Point Lagoon. Geomorphological features at this site, such as the proximity to the sea, the absence of a direct connection to freshwater streams and shallow water that may enhance evaporation, may indicate a preference for less restricted environments. Furthermore, *C. eburneum*, in contrast to *C. pliculosa*, was also found close to the tidal inlet in A10 (Fig. 3.11), where mixing of brackish water and seawater occurs and higher water energy prevails. On the other hand, *C. pliculosa* shows preference for areas that have low water exchange with the ocean. This species occurs in landward cores (CP2, CP3 and CBi3). In these areas, freshwater input by creeks is higher and salinity lower. The abundance of *C. pliculosa* in cores from Quashi Trap Lagoon (ML2, ML3, ML4) also suggests low salinities, which today range from 4.3 to 8.1‰. The upcore development in species composition in Sapodilla Lagoon indicates environmental changes, which probably occurred due to the evolution of the barrier spit. The upcore replacement of *C. eburneum* by *C. pliculosa* and a replacement of *L. muricata* by *L. pectinata* in core SL1 may indicate a decrease in salinity or at least a change to more restricted conditions. The fact that *L. muricata* was observed in marginal marine and tidal inlet environments (A8, A9, A10) and the common occurrence of *L. pectinata* in lagoons (A4, A7) supports this assumption.

The distribution of lagoonal mollusk assemblages can probably be explained by the Holocene evolution of the coastal lagoons. The almost monospecific *A. cuneimeris* assemblage (A6), which occurs at the base of Holocene successions, developed after the inundation of the Pleistocene surface due to sea-level rise. Species composition suggests unfavorable environmental conditions during initial stages of lagoon development between 5300 and 4200 cal BP. The absence of other species suggests inimical conditions for other species but allowed the euryhaline bivalve *A. cuneimeris* to flourish. The barrier-lagoon system had not developed during these early stages of marine transgression (Adomat and Gischler 2015). From 2200 cal BP to modern times, the *A. cuneimeris*/cerithid assemblages A1, A4, A5 and A7 were probably deposited after the formation of spits and barriers that separated lagoonal basins from the sea, which resulted in a restricted circulation.

A. cuneimeris is generally known to withstand a wide range of salinities, and it is reported to live in both enclosed and open hypersaline lagoons (Andrews 1935; Parker 1959). In Florida Bay, *A. cuneimeris* is restricted to the Northern Subenvironment, which is strongly affected by freshwater drainage from the mainland and is subject to variations in salinity (Turney and Perkins 1972). Turney and Perkins (1972, their table 5) found living *A. cuneimeris* in salinities ranging from 13 to 80‰. This species was also characteristic of lagoonal localities with restricted circulation in northeastern Yucatan assemblages (Ekdale 1977). Other species of the same genus such as *Anomalocardia brasiliana* are able to withstand hypoxic conditions (Arruda-Soares et al. 1982; Boehs et al. 2000). Along the Gulf of Mexico, *C. pliculosa* is known to live at water depths of 0-2 m, in seagrass and saltmarsh areas (Rosenberg et al. 2009) and on mudflats (Abbott 1974). Robertson (1963) assigned *C. pliculosa* to the freshwater fauna in Belize. Furthermore, along the Gulf coast, this species is frequently found in coastal salt marshes, and grazes on algae that grow on the mud at the base of the grass stalks (Rothschild 2004). Thus, it seems to be dependent on the presence of vegetation. *C. eburneum* is associated with seagrass (Tunnel et al. 2010) and was assigned to marine environments by Robertson (1963).

Shell size also may indicate specific environmental conditions. According to Abbott (1974), lengths of adult *A. cuneimeris* shells range from 12.7 to 19 mm. The average valve length of 6.4 mm in the study area is significantly lower. The relatively small shell size can be explained by hypersalinity or decreased salinities in the coastal lagoons. According to Abott (1974), brackish water specimens of *A. cuneimeris* are typically dwarfed. Environmentally suppressed specimens are usually very small and represent ecotypical dwarfs (Fürsich 1994). However, Teeter (1985) observed shell sizes of *Anomalocardia auberiana* (a synonym of *A. cuneimeris*) from San Salvador Island, which were inversely related to salinity. The influence of salinity on shell size is supported by a decrease in size of some shells from marginal marine, tidal inlet, to lagoonal areas in Belize. For instance, marine valves of *C. cancellata* are up to 29 mm long, while valves from the tidal inlets are 16 mm long at most. Some gastropod species such as *B. striata* and cerithids are larger at the tidal inlet than in lagoons. In addition to salinity fluctuations, oxygen

depletion may also cause dwarfism in bivalve mollusks (Oschmann 1993; Schöne 1999). Apart from the putrid smell, the dark color of the muddy sediments is an indicator for oxygen depletion in the Belize lagoons. XRD measurements provide evidence for the presence of pyrite, with values between 1 and 5% in samples from lagoonal muds.

In summary, because of the wide ranges of tolerances of the dominant species, one single major controlling factors for species composition cannot be identified. Rather, the composition of assemblages is probably influenced by multiple paleoecological and paleoenvironmental factors. NMDS axis 1 shows a lagoon-onshore gradient (Fig. 3.10a). The distribution of assemblages along NMDS axis 2 is based on environmental changes that occurred during the Holocene evolution of the coastal lagoons (Fig. 3.10 b). Because of the heterogeneity of the barrier-lagoon systems it is difficult to determine precisely ancient environmental conditions. Moreover, the heterogeneity may promote the development of microhabitats that show differences in their physical properties.

Assemblages A8-A10 are represented by only one sample each, precluding statistical assessment of their variability in the marginal marine and tidal inlet environments. Still, the differences in Assemblages A8 and A9 from the marginal marine area of Manatee Lagoon and that of Colson Point can be explained mainly by differences in substrate, which is finer grained at Colson Point and sandy at Manatee Bar (Fig 3.13). *Dentalium* sp., which is absent at Colson Point, but present at Manatee Bar, is an indicator for sandy substrate in the marine environment (Abbott 1974). Assemblage A10 from the mangrove-fringed tidal inlet indicates a less restricted environment compared to the lagoons. The higher faunal diversity measures and larger shell sizes in the marginal marine area, the tidal inlet and in Sapodilla Lagoon can be explained by euhaline salinity and by exchange of euhaline and brackish water through the tidal inlet, respectively. Salinity in Sapodilla Lagoon is related to geomorphological features, i.e., the broad channel connecting lagoon and open shelf (Adomat and Gischler 2015). The low diversity in the other three investigated coastal lagoons seem to be related to the restricted environmental conditions, which are only favorable for euryhaline species such as *A. cuneimeris*. Apart from salinity and substrate variation, water depth and hydrodynamic conditions may have to be considered as well for variable species composition and the presence/absence of *A. cuneimeris*.

The results presented here show differences to those of other mollusk studies from the Belize shelf and offhore atolls. Robertson (1963) mapped a living *Tivela mactroides* community along the coast of central Belize. Only one specimen of the index species *T. mactroides* was found in our study area, i.e., in fine-grained sediments underlying the concentration in the marginal marine core ML5. Probably due to insufficient sampling of the brackish-water habitats, the abundance of *A. cuneimeri*s and *C. pliculosa* in the coastal lagoons was not mentioned by Robertson (1963), but both can be found on his list of taxa. *A. cuneimeri*s was identified as characteristic species in the brackish Chetumal bay fauna of northernmost Belize (Robertson 1963). Hauser et al. (2007)

investigated mollusks in offshore atolls and found a high number of species, only few of which were found in the marginal marine environments along the coast. These include *C. cancellata*, *Arcopsis adamsi*, *Crassinella lunulata*, *Diplodonta* sp., and *Tellina* sp. None of the species from the coastal lagoons were found in the offshore area by Hauser et al. (2007).

3.5.2 Taphonomic attributes as indicators of depositional conditions

The shells from the Belize coastal lagoons are not preserved in life position, but deposited in the original substrate, in a habitat characteristic for the species. They are considered to be parautochthonous. According to Kidwell et al. (1986), parautochthonous assemblages are composed of autochthonous specimens that have been reworked to some degree but not transported out of the original life habitat. No allochthonous exotic taxa from the offshore area were found within the mollusk assemblages from the lagoons. Thus, these shells can be considered as belonging to the indigenous fauna. The concentrations recovered from the mangrove-fringed tidal inlet are interpreted as being largely parautochthonous. The shells that were found in marginal marine environments also have been accumulated in their preferred substrate, because they comprise species typical for these habitats.

Post-mortem transportation of lagoonal shells over wide distances is not probable because in most parts of the Belize lagoons circulation is restricted and they represent low-energy environments. Warme (1969) concluded that the distribution of recurrent assemblages indicate that widespread mixing has not occurred. This is also the case for the *A. cuneimeris*/cerithid assemblages, which occur at several localities and in various core depths in the study area. At the tidal inlet and the marginal marine area, higher tidal current velocities than in other parts of the lagoon prevail. In these areas mixing of parautochthonous and allochthonous individuals probably has occurred to some degree. However, species from Assemblage 5 mostly seem to be deposited in their original habitat. This is supported by the occurrence of species, such as oysters, which live with the left valve attached to mangroves that fringe the inlet. A high number of oyster fragments indicates higher water energy, which is associated with tidal currents. Indications for transport by high-energy (storm) events were found at Commerce Bight, with coral fragments of *Porites porites* (Pallas 1766) in the tidal channel and the backbarrier lagoonal area indicating transport and displacement from the original habitat.

A rapid burial of the shells is unlikely because most shells show signs of alteration (Table 8). Physical reworking, bioturbation and processes such as bioerosion, dissolution, maceration and encrustation may occur in the mixed layer of the seafloor (Kidwell 2013). Most dissolution of carbonates occurs in the taphonomically active zone, defined by Aller (1982) as the zone near the sediment-water interface, where pore waters are under-saturated with respect to aragonite and calcite. The degree of bioerosion of the shells investigated is not very high, suggesting that they did not undergo long exposure on the sediment surface. DeFrancesco and Hassan (2008)

noted that encrustation degrees are small in lagoonal environments, because the main encrusting organisms typically live in marine settings. This may also be the case for the coastal lagoons in Belize where no encrustations were found on shells. The fact that the discoid rhizoid holdfasts were only observed on shells from Colson Point Lagoon and two specimens from Manatee Lagoon, indicates either longer exposure on the sea-floor or that the producers of these structures, probably brown algae, only lived at these sites.

The fact that internal surfaces are generally better preserved than the external surfaces is associated with the relative good preservation potential of the muscle scars and the pallial line. The good preservation of these two characteristics can be attributed to their position in the more protected area of the valve. Corrosion is the result of early diagenetic processes and carbonate dissolution. These processes gave some of the concentrations a compacted appearance and the affected shells a friable nature. This is strongly pronounced in the two basal concentrations in core ML2 where shells are highly altered (Fig. 3.8b). Those shells show chalky surfaces and reveal unreliable radiocarbon ages due to alteration of the original shell microstructure. Oxidation of organic matter may lower the pore-water pH and promote shell-carbonate dissolution (e.g., Best and Kidwell 2000a). Also, the slightly acidic nature of brackish water promotes shell surface alteration such as pitting and chalkiness (Trewin and Welsk 1976; Alexandersson 1979). Therefore, a mixture of taphonomic states is expected within concentrations that represent longer periods of accumulation (Tomašových et al. 2006).

Interpretation of size-frequency distributions is challenging because their shape in living and dead populations depends on several factors such as (1) varying growth and mortality rates, (2) sorting by currents and waves, (3) removal, destruction and breakage by predators or scavengers, and (4) selective breakage during transport (e.g. Boucot 1953; Craig and Hallam 1963; Craig and Oertel 1966; Fagerstrom 1964; Trewin 1973). The fidelity of size-frequency distributions is relatively high in low-energy and soft-bottom environments as compared to high-energy and hard-bottom settings (Tomasovych 2004). Right-skewness is described as typical size-frequency distributions of life assemblages (Boucot 1953) and as characteristic of in situ populations with constant death rates (Richards and Bambach 1975). The shape of most size-frequency distributions suggests that they display former life assemblages, which have been altered to some degree due to time-averaging and other taphonomic processes. Left-skewness in CP6 145-152 cm seems to be associated with bioturbation processes, during which valves of juveniles were reworked and preferentially destroyed by burrowing organisms. The base of the two basal concentrations in CP6 show downward reworking of muddy sediment, producing wavy lower contacts, and enrichment of large shells at the top of the concentration (Fig. 3.8d).

3.5.3 Formation of shell concentrations

In the study area, different origins of coastal lagoon and marginal marine shell concentrations have to be considered. Generally, accumulation of shells during high-energy events seems probable, since hurricanes have made landfall in Belize once every five years on average during the 20th century (Gischler et al. 2008, 2013). Such sedimentologic concentrations, which include storm lags, flood deposits and distal washover deposits are associated with barrier beaches (Kidwell et al. 1986). However, the taxonomic composition of the concentrations from lagoonal environments excludes deposition by wash-over during storm events because taxa from lagoon and offshore habitats are not mixed. Shell beds would be more densely packed and grain-supported after reworking by storms (Dattilo et al. 2008). In addition, occurrence within a graded deposit and sharp erosional bases would be expected (Kidwell 1991). Furthermore, the investigated concentrations lack sediment structures such as grading and imbrication of shells. Sharp bases may also result from changes in the hydrodynamic regime, such as sea-level fluctuations and changing river discharge. Coarsening upward grading in the two basal concentrations in core CP6 is not explained by storm influence, but by reworking of shells by bioturbators such as crustaceans. The size-frequency distributions also do not show strong transport-related sorting of shells, which would be expected in storm deposits (Flügel 2004). Still, storm events may have promoted the formation of concentrations indirectly. Increased precipitation and river drainage associated with storms could have influenced lagoonal environmental conditions such as a decrease in salinity and elevated nutrient supply, creating favorable conditions for species tolerating reduced salinity such as *A. cuneimeris* and cerithids. Conversely, storm surges may have increased salinity in the lagoons. Thus, the Belize concentrations from lagoons formed as a result of both biologic and sedimentologic processes, typical for shell accumulations in these settings (Kidwell et al. 1986; their fig. 5). Biogenic processes in the coastal lagoons of Belize may include high biological productivity, e.g., colonization events of opportunistic species. Sedimentological processes such as hydraulic reworking of initially dispersed shells, removal of sediment and accumulation of shells during periods of sediment starvation may have contributed to the formation of the lagoonal shell accumulations. Sediment input in the coastal lagoons has fluctuated due to increased river drainage after precipitation events. Conversely, during dry periods, sediment input by creeks decreased, resulting in sediment starvation. Most of the concentrations from lagoonal environments in Belize exhibit comparably loose shell packing (Table 3.3), as described by Kidwell (1991) for biostratigraphically condensed concentrations. Repeated cycles of shell burial, exhumation, winnowing and recolonization, as reporteded by Kidwell and Aigner (1985) in shallow-water environments, would explain the mixing of taphonomic states within the concentrations.

Origin of marginal marine concentrations may result from several processes including the accumulation, reworking and redeposition of shells in this high-energy environment. The densely

packed and bioclast-supported concentration in ML5 from the marginal marine area of Manatee Lagoon was deposited at the base of beach sands (Fig. 3.3e). The sharp basal contact of the coarse-grained beach sands and the thin mud layer at its base possibly indicate deposition during a high-energy event. Graded storm beds often show shells concentrated near their bases (Anderson and McBride 1996), which was also observed in core ML5. Dense packing and bioclast-supported fabric in concentration from SL5, collected in a channel right behind the beach ridge, is also associated with increased water-energy, compared to the concentrations from lagoonal environments.

Death assemblages mostly represent time-averaged relics of life assemblages with mixing of skeletal elements of non-contemporaneous populations or communities (Fürsich 1990). The mollusk assemblages from the Belize coast do not represent snapshots of life assemblages, but contain individuals that lived together in the same habitat. A mixing of generations has probably occurred. Moreover, shell survival of multiple reworking events can increase temporal mixing (Kowalewski 1997). Time-averaging within concentrations from Belize probably concerns "within-habitat time-averaging", that is assemblages composed of multiple generations (e.g., Kidwell and Bosence 1991; Kowalewski and Bambach 2003). Skeletal concentrations can form within a short period of time of a few minutes to hundreds of thousands of years (Kidwell 1985). To answer the question of how much time is represented by one concentration, many radiocarbon dates are required. Although reworking and mixing of shells in death assemblages may limit their utilization as indicator for past lagoonal environments (DeFrancesco and Hassan 2008), the present study shows that it is possible to decipher changes in their distribution patterns by studying mollusk assemblages.

3.6. Conclusions

1. A total of 20 concentrations with 53 mollusk species were detected in twelve sediment cores from coastal lagoons, a mangrove-fringed tidal inlet and the marginal marine environments of central Belize. The most frequent species in lagoons are the bivalve *A. cuneimeris* and cerithid gastropods *C. eburneum* and *C. pliculosa*.

2. Species richness and diversity are low in coastal lagoons and higher in the mangrove-fringed tidal inlet and the marginal marine area.

3. Seven assemblages were distinguished in coastal lagoons: A1 comprises mainly *A. cuneimeris* and *C. eburneum*. In A2 and A3, the dominant species is *A. cuneimeris*. A4 is a *C. pliculosa*/*A. cuneimeris* assemblage with the former being the most abundant species. A5 is an almost monospecific assemblage, with of *C. pliculosa* and *A. cuneimeris* being as dominant species. A6 comprises largely *A. cuneimeris*. A7 is an *A. cuneimeris*/*C. pliculosa* assemblage with the former being more abundant.

4. The NMDS ordination shows a lagoon-onshore gradient along the first axis. NMDS axis 2 indicates changes in environmental conditions during the Holocene evolution of the barrier-lagoon complexes.

5. No species from the offshore habitats occur in the concentrations from lagoons, demonstrating that taxa from different environments are not mixed.

6. Species composition, size-frequency distributions and the left-right valve ratio of *A. cuneimeris* indicate that the shells are parautochthonous, have not been transported over long distances and were deposited in their original habitat. The matrix of the concentrations corresponds to the substrate preferences of the dominant species.

7. Variation in the taphonomic signatures indicated that valves in concentrations from coastal lagoons show different taphonomic signatures, but preservation does not show temporal or spatial trends.

8. Formation of the concentrations in the coastal lagoons occurred due to both biogenic and sedimentologic processes and environmental conditions that have been favorable for few tolerant (euryhaline) species that occurred abundantly. The concentration in a marginal marine core was probably formed during a high-energy event.

3.7 Acknowledgements

We are grateful to the Deutsche Forschungsgemeinschaft (Gi222/20) and the Alfons and Gertrud Kassel-Stiftung, who funded this project. We thank Stefan Haber, Malo Jackson, David Geban and Claire Santino for help during fieldwork. Nils Prawitz, Anja Isaack and Lars Klostermann assisted during sample preparation. Dr. Rainer Petschick ran the X-ray diffractometer, Wolfgang Schiller and Claudia Franz operated the SEM. Two reviewers whose useful comments helped to improve the manuscript are gratefully acknowledged.

Chapter 4. Assessing the suitability of Holocene environments along the central Belize coast, Central America, for the reconstruction of hurricane records

Friederike Adomat, Eberhard Gischler

Institut für Geowissenschaften, Goethe-Universität Frankfurt, Altenhoeferallee 1, 60438 Frankfurt am Main, Germany

Keywords: paleotempestology, tropical storms, storm record, overwash, coastal lagoons, shell concentrations

Resubmitted to the International Journal of Earth Sciences

Abstract: Since the Belize coast was repeatedly affected by hurricanes and the paleo-hurricane record for this region is poor, sediment cores from coastal lagoon environments along the central Belize coast have been examined in order to identify storm deposits. The paleohurricane record presented in this study spans the past 8000 years and exhibits three periods with increased evidences of hurricane strikes occurring at 6000-4900 cal yr BP, 4200-3600 cal yr BP and 2200-1500 cal yr BP. Two earlier events around 7100 and 7900 cal yr BP and more recent events around 180 cal yr BP and during modern times have been detected. Sand layers, redeposited corals and lagoon shell concentrations have been used as proxies for storm deposition. Additionally, hiatuses and reversed ages may indicate storm influence. While sand layers and corals represent overwash deposits, the lagoon shell concentrations, which mainly comprise the bivalve *Anomalocardia cuneimeris* and cerithid gastropods, have been deposited due to changes in lagoon salinity during and after storm landfalls. Comparison with other studies reveals similarities with one record from Belize, but hardly any matches with other published records. The potential for paleotempestology reconstructions of the barrier-lagoon complexes along the central Belize coast differs depending on geomorphology, and deposition of washovers in the lagoon basins is limited, probably due to the interplay of biological, geological and geomorphological processes.

4.1 Introduction and aims

The increase in intensity and destructiveness of hurricanes over the past few decades has been subject of discussions in a number of publications (e.g., Goldenberg et al. 2001; Emanuel 2005; Webster et al. 2005). The underlying causes for this phenomenon are not entirely clear, however, North Atlantic hurricane activity has been linked to increasing sea-surface temperatures (SSTs) (Emanuel 2005; Hoyos et al. 2006; Saunders and Lea 2008; Donnelly et al. 2015), with an increase in frequency (Webster et al. 2005), and an increase in intensity of the strongest events (Elsner et al. 2008). The increase in SSTs since the late 19th century has been related to the sensitivity of Atlantic hurricanes to increasing atmospheric concentrations of greenhouse gasses (e.g., Emanuel et al. 2005; Webster et al. 2005; Santer et al. 2006; Gillett et al. 2008; Knutson et al. 2010), internal climate variations (Goldenberg et al. 2001; Zhang and Delworth 2006, 2009), and reduced aerosol or dust forcing (Mann and Emanuel 2006; Evan et al. 2009). Simulations and modeling have yielded variability and uncertainties of hurricane activities, which may be associated with different model predictions (Emanuel et al. 2008). However, most studies agree that there will be century-scale increases in Atlantic tropical cyclone activity (e.g., Mann and Emanuel 2006; Holland and Webster 2007) and an increase in intensity and frequency of high-magnitude storms and a decrease in overall frequency of hurricanes by the end of the twenty-first century (Bender et al. 2010; Knutson et al. 2010).

As the most active area for tropical hurricanes in the North Atlantic (Donnelly 2005), the Caribbean, is an area of interest for paleotempestology studies. The Belize coast, located in the western Caribbean, is vulnerable to hurricanes. The hurricane data (HURDAT), maintained by the National Oceanic and Atmospheric Administration (NOAA), provides Atlantic hurricanes and tropical storms recorded since 1851 (Fig. 4.1; Table 4.1). The terms major hurricane and intense hurricane refer to storms of category 3 or higher, according to the Saffir-Simpson scale. Storms affected northern and southern Belize more frequently than central Belize during recorded history. Density of storm tracks is highest in northern Belize and storm tracks typically run northwestward (Fig. 4.1). Since 1864, five major hurricanes of category 3 or higher and 14 hurricanes of category 1 and 2 made landfall on the Belize coast. Major hurricanes include an unnamed hurricane in 1931, Janet in 1955, Hattie in 1961, Greta in 1978 and Iris in 2001. The major hurricane Keith, which struck Belize in 2000, weakened over the offshore Belize atolls and made landfall as a tropical storm. Major hurricanes Hattie and Greta impacted the study area in the vicinity of Mullins River Beach and Colson Point. Two hurricanes struck the Belize coast close to the study area, an unnamed in 1906 and Richard in October 2010 after our fieldwork.

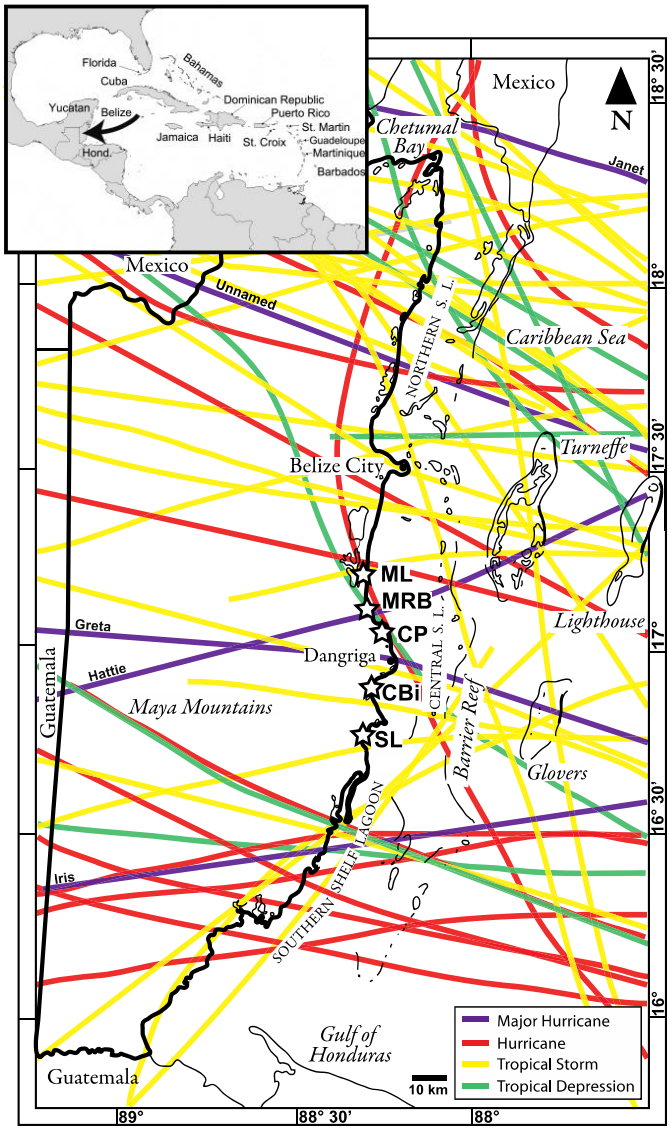

Fig. 4.1 Location map of Belize showing coring sites along the central coast of Belize. The inset map in the upper left shows the location of Belize in the Caribbean region (map after Montaggioni and Braithwaite 2009). Asterisks mark the localities Manatee Lagoon (ML), Colson Point Lagoon (CP), Commerce Bight Lagoon (CBi) and Sapodilla Lagoon (SL). Lines indicate approximate storm tracks recorded since 1851. Storm type refers to strength of storms during landfall at the coast. Storms are listed in Table 1. Source: U.S. National Hurricane Center (NOAA, 2014)

Paleotempestology is an approach for assessing hurricane landfall probabilities by means of geological records of past hurricane strikes (Liu 2004). Storm records can be used to identify changes in hurricane climatology over the past years, also for the unrecorded time before 1851. Extending the historical and prehistoric record of tropical cyclone activity would support the ability to predict activity changes, including characteristics such as frequency, track, intensity and size that may occur in the future (Murnane 2004). Several geologic proxies have been used in paleotempestology. These include sediment-based proxies such as overwash deposits, wave- or flood-generated structures or deposits (tempestites) as well as micropaleontological proxies such as microfossils, and climatic proxies such as tree rings, oxygen isotherms from speleothems and corals (Liu 2004, and references therein). Paleohurricane records have mainly been generated by

means of identification and analysis of overwash sand layers in sediment cores obtained from coastal wetlands, typically from coastal lakes, lagoons, and marshes along the Atlantic U.S. coast (e.g., Donnelly et al. 2001a, b, 2004; Scott et al. 2003), the Gulf of Mexico (Liu and Fearn 1993, 2000a, b; Liu 2004; Lane et al. 2011; Brandon et al. 2013), and the Caribbean (Donnelly and Woodruff 2007; McCloskey and Keller 2009; Malaizé et al. 2011; McCloskey and Liu 2012). These records provide evidence of hurricane strikes dating back up to several thousand years and imply alternating periods of intense and reduced hurricane activity (e.g., Liu and Fearn 1993; Donnelly and Woodruff 2007; McCloskey and Liu 2012). However, storm records may be inconsistent among different regions (e.g., Mann et al. 2009). Stoddart (1962) and High (1969) documented geomorphological and sedimentological effects of hurricanes on Belize reefs and cays. Gischler et al. (2008, 2013) and Denommee et al. (2014) used coarse-grained layers intercalated in the muddy, annually laminated deposits of the offshore Blue Hole (Lighthouse Reef) to develop highly resolved storm records reaching back some 1.4 kyrs. But up to now only few studies have presented paleohurricane records obtained from the Belize coast (McCloskey and Keller 2009; McCloskey and Liu 2012). Aim of this study is the identification of storm deposits in cores from the central Belize coast, to figure out active and quiet periods and to assess the results in comparison with other records in order to evaluate the suitability of barrier-lagoon complexes for paleotempestology reconstructions.

4.2 Study area

Belize (16°S to 18°30´S; 87°30'W to 89°30´W) is situated in Central America, in the southeastern area of the Yucatán Peninsula, to the east bordered by the Caribbean Sea (Fig. 4.1). The climate is subtropical (Wright et al. 1959) and lies within the trade wind belt with prevailing easterly and northeasterly winds. The coast of Belize is a wave-dominated, semidiurnal microtidal area with a tidal range of 15-30 cm (Kjerfve et al. 1982). Annual rainfall increases from north to south from 124 cm to 380 cm, respectively (Purdy et al. 1975), reflecting mainland topography. Precipitation is highest during the summer (July-September). Drainage density is particularly high along the coast east of the Maya Mountains (High 1975), however, there are no systematical data available on river discharge. Mean sea surface temperatures of the shelf range from 28.9°C during summer to 26.2°C during winter (e.g., Purdy et al. 1975). Surface water salinity decreases from ca. 35‰ at the shelf margin to ca. 18‰ near the coast, and northward into Chetumal Bay and southward into the Gulf of Honduras (Purdy et al. 1975). Sedimentary facies of the shallow northern shelf are carbonate-dominated. The deeper southern shelf harbors a mixed system and is characterized by a siliciclastic to carbonate transition with an eastward increase in carbonate content (Pusey 1975; Scott 1975; Purdy et al. 1975; Purdy and Gischler 2003). The coast of Belize, which has low relief, is dominated by barrier-lagoon complexes (High 1966). The coastal lagoons are usually extensively fringed by the red mangrove *Rhizophora*

Table 4.1 *Storms that struck the Belize coast recorded since 1851. Tracks of storms are shown in Fig. 4.1*

Year	Date	Name	Area of Belize	Type (at landfall)	Wind (kt; max.)	Category
1864	Aug 26-Sep 1	-	Northern Belize	Hurricane	70	1
1870	Oct 30-Nov 30	-	Northern Belize	Hurricane	70	1
1892	Oct 5-16	-	Northern Belize	Hurricane	85	2
1893	Jul 4-7	-	Northern Belize	Hurricane	85	2
1898	Sep 12-22	-	Northern Belize	Tropical Storm	50	-
1898	Oct 27-Nov 4	-	Northern Belize	Tropical Storm	51	-
1904	Sep 28-Oct 4	-	Northern Belize	Tropical Storm	70	-
1906	Oct 8-23	-	Northern, Central B.	Hurricane	105	3
1916	Aug 27-Sep 2	-	Northern Belize	Tropical Storm	70	1
1917	Jul 6-14	-	Central Belize	Tropical Depression	45	-
1918	Aug 22-26	-	Southern Belize	Hurricane	90	2
1921	Jun 16-26	-	Northern Belize	Tropical Storm	80	1
1924	Jun 18-21	-	Northern Belize	Tropical Storm	40	-
1926	Oct 3-5	-	Southern Belize	Tropical Depression	35	-
1931	Jul 11-17	-	Northern Belize	Tropical Depression	60	-
1931	Aug 10-19	-	Central Belize	Tropical Storm	50	-
1931	Sep 6-13	-	Northern Belize	Major Hurricane	115	4
1931	Sep 8-16	-	Northern Belize	Tropical Storm	85	2
1931	Nov 11-16	-	Northern Belize	Tropical Storm	45	-
1932	Sep 25-Oct 2	-	Southern Belize	Tropical Storm	125	-
1932	Oct 7-15	-	Northern Belize	Tropical Storm	60	-
1933	Jul 14-24	-	Northern Belize	Tropical Storm	45	-
1933	Sep 16-25	-	Northern Belize	Tropical Storm	140	4
1934	Jun 4-18	-	Southern Belize	Tropical Storm	85	2
1938	Oct 10-17	-	Northern Belize	Tropical Storm	50	-
1940	Sep 18-25	-	Northern Belize	Tropical Storm	45	-
1941	Sep 23-30	-	Southern Belize	Hurricane	105	3
1942	Sep 15-22	-	Central Belize	Tropical Storm	45	-
1942	Nov 5-11	-	Northern Belize	Hurricane	85	2
1943	Oct 20-23	-	Southern Belize	Tropical Storm	40	-
1945	Aug 29-Sep 1	-	Northern Belize	Tropical Storm	50	-
1945	Oct 2-5	-	Southern Belize	Hurricane	85	2
1954	Sep 24-27	Gilda	Central Belize	Tropical Storm	60	-
1955	Sep 21-30	Janet	Northern Belize	Major Hurricane	150	5
1956	Sep 21-25	Flossy	Northern Belize	Tropical Depression	80	1
1960	Jul 10-16	Abby	Southern Belize	Hurricane	85	2
1961	Jul 20-24	Anna	Central Belize	Hurricane	100	3
1961	Oct 27-Nov 1	Hattie	Central Belize	Major Hurricane	140	5
1964	Nov 5-10	-	Northern Belize	Tropical Depression	35	-
1969	Aug 29-Sep 4	Francelia	Southern Belize	Hurricane	100	3
1971	Sep 5-18	Edith	Northern Belize	Tropical Storm	140	5
1971	Nov 12-22	Laura	Southern Belize	Tropical Storm	60	-
1974	Sep 14-22	Fifi	Southern Belize	Hurricane	95	2
1977	Oct 16-19	Frieda	Northern Belize	Tropical Depression	40	-
1978	Sep 13-20	Greta	Central Belize	Major Hurricane	115	4
1980	Sep 20-26	Hermine	Northern Belize	Tropical Storm	60	-
1993	Sep 14-21	Gert	Northern Belize	Tropical Storm	85	2
1999	Oct 28-Nov 1	Katrina	Northern Belize	Tropical Depression	35	-
2000	Sep 28-Oct 6	Keith	Northern Belize	Tropical Storm	120	4
2001	Aug 14-22	Chantal	Northern Belize	Tropical Storm	60	-
2001	Oct 4-9	Iris	Southern Belize	Major Hurricane	125	4
2008	May 31-Jun 1	Arthur	Northern Belize	Tropical Storm	40	-
2010	Jun 25-Jul 2	Alex	Northern Belize	Tropical Storm	95	2
2010	Sep 23-26	Matthew	Southern Belize	Tropical Storm	50	-
2010	Oct 20-25	Richard	Central Belize	Hurricane	85	2
2011	Aug 19-22	Harvey	Central Belize	Tropical Storm	55	-
2013	Jun 17-20	Barry	Southern Belize	Tropical Depression	-	-

Source: U.S. National Hurricane Center (NOAA, 2014)

mangle. The major processes supplying sediment to coastal environments include river transport, shore erosion, southerly longshore currents, tides, washovers and wind (Nichols and Boon 1994). Sediments delivered to the coast from the sea are mainly transported by longshore and tidal currents. Material from the hinterland is transported into coastal lagoons by creeks. The main sediment source are the Maya Mountains and surrounding areas, where Paleozoic igneous, metamorphic and siliciclastic rocks and Cretaceous to Tertiary carbonates crop out. The coastal lowland is largely composed of unconsolidated Quaternary detrital sediments. A minor contributor is the offshore marine realm.

Today, muddy substrate and low current velocities predominate in the coastal lagoons selected for this study. Salinity in the lagoons, which hardly get deeper than about 1 m, is brackish and ranges from 4‰ to 27‰ (Adomat and Gischler 2015). (1) Manatee Lagoon is more than 10 km long and part of an even larger coastal lagoon system that is separated from the Belize shelf by an up to 2 km wide swampy area with mangroves, bordered by a sand ridge with palm tree and palmetto vegetation and a seaward beach (Fig. 4.2a). The lagoon is connected with the sea by Manatee River. Quashi Trap Lagoon is a 2 km long, shallow basin between Manatee Lagoon and the Belize shelf and connected to Manatee Lagoon by a shallow, ca. 500 m long channel. (2) The Mullins River Beach area includes a swampy area bordered on the seaside by a sandy beach ridge (Fig. 4.2b). Much of the vegetation of the backshore area has recently been cleared for construction and connected with the Northern Highway to the west by an artificial causeway. (3) Colson Point Lagoon has a complex outline and is about 2 km wide (Fig. 4.2c). It is fed from the west by Big Creek, and connected to the sea to the north by a complex system of strongly meandering and bifurcating creeks. A ca. 500 m wide mangrove area separates the lagoon from the Belize shelf towards the east. (4) Commerce Bight has a more or less circular outline with an approximate diameter of 1.3 km and a pronounced tidal delta in the south (Fig. 4.2d). To the south, a ca. 2 km long, small creek connects the lagoon basin with the adjacent Belize shelf. The width of the densely vegetated sandy ridge separating the lagoon from the sea is ca. 100 m. (5) Sapodilla Lagoon is an elongated, ca. 3 km long lagoon with a ca. 135 m wide inlet in the northeast that connects to the Belize shelf (Fig. 4.2e). It is separated from the shelf by a ca. 200 m wide spit densely vegetated by mangroves. The lagoon is fed by Cabbage Haul Creek entering at the southwestern lagoon margin.

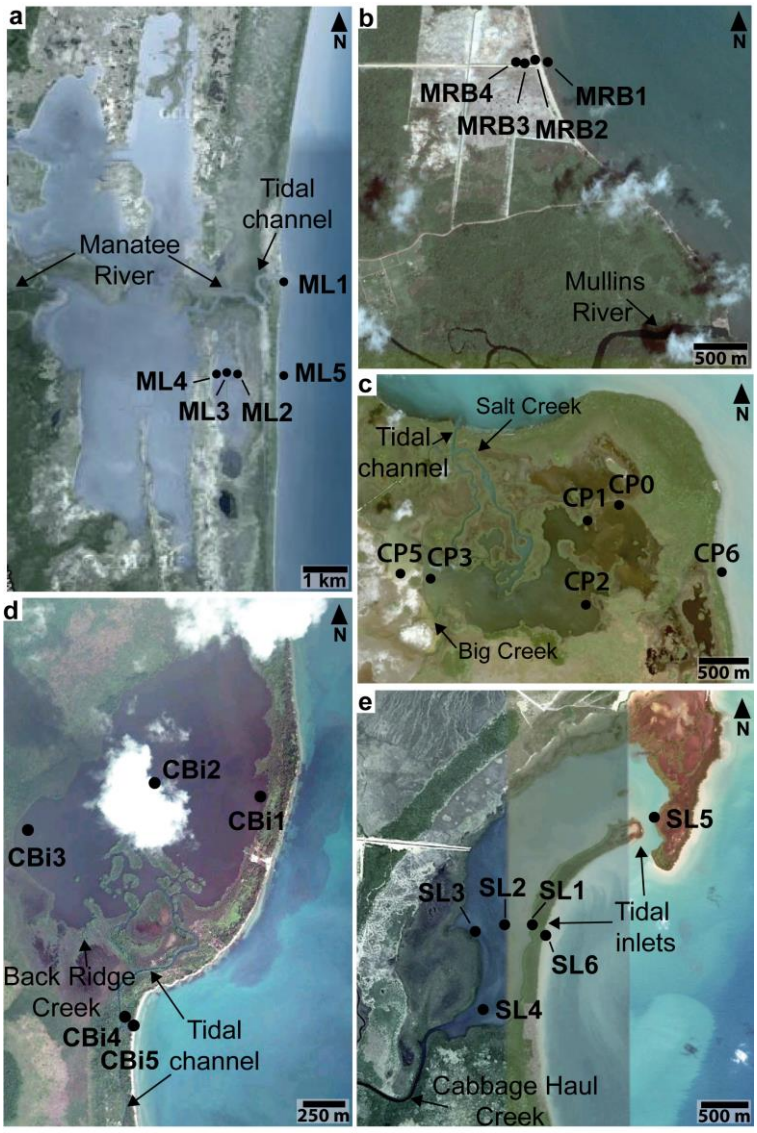

Fig. 4.2 Aerial photos showing coring sites (satellite images from Google Earth). **a** Manatee Lagoon (Quashi Trap Lagoon). **b** Mullins River Beach. **c** Colson Point Lagoon. **d** Commerce Bight Lagoon. **e** Sapodilla Lagoon

4.3 Methods

Fieldwork took place in July and August 2011. A portable vibracorer (Lanesky et al. 1979) and 5.9 m long aluminum tubes with a diameter of 7.5 cm, equipped with a copper core catcher, were used for coring. The five coring sites are located along the central Belize coast (Figs. 4.1, 4.2; Table 4.2). A total of 26 cores with a total length of 73 m were obtained. Core length ranged from 1.1 to 5 m. Compaction of sediment ranged between 0 and 65%, with an average of 23%. In the following, core depths are corrected for compaction by multiplying thicknesses of all sediment types with the compaction factor obtained from core depth and penetration depth (Table 4.2). One compaction factor was calculated for each core. In the laboratory, core tubes were cut in halves lengthwise using an angle grinder and knife. Photo documentation and core description were carried out, including descriptions of lithology, thickness, sedimentary structures and sedimentary contacts. Potential event deposits were identified by visual examination of cores and

based on sediment texture (sieve analysis). Sediment was washed through 2 mm, 1 mm, 500 µm, 250 µm, 125 µm and 63 µm sieves for grain size analysis and to isolate shells from the sediment. Samples of organic matter, bivalve shells and corals were selected to date possible event deposits. Age-dating was undertaken by Beta Analytic Inc., Miami, Florida, using accelerator mass spectrometry (AMS). Radiocarbon ages were converted to calendar years using Intcal09 (Talma and Vogel 1993). Calibrated ages are given with a 2 σ error range. For calibration of carbonate shells the Marine09 database, and for peat and organic sediments the Intcal09 database was applied. The variables used in the calculation for marine reservoir effect correction of carbonate shells are Delta-R=120±27 and Glob res=-200 to 500. In this publication, only age data of potential event deposits are listed. A complete list of the radiocarbon ages is published in Adomat and Gischler (2015; their table 5).

Table 4.2 *List of all cores drilled at Manatee Lagoon (ML), Mullins River Beach (MRB), Colson Point Lagoon (CP), Commerce Bight Lagoon (CBi) and Sapodilla Lagoon (SL)*

Core	Coordinates		Water Depth (cm)	Core Length (cm)	Penetration Depth (cm)	Compaction (%)
	Latitude	Longitude				
ML 1	N 17° 13`50,3``	W 88° 18`13,5``	40	122.5	349	64.90
ML 2	N 17° 12`41,5``	W 88° 18`46,2``	57	452	478	5.44
ML 3	N 17° 12`41,8``	W 88° 18`53,3``	93	274	302	9.27
ML 4	N 17° 12`41,0``	W 88° 19`03,2``	73	437	464	5.82
ML 5	N 17° 12`39,8``	W 88° 18`13,8``	100	432	500	13.60
MRB1	N 17° 07`11,4``	W 88° 18`00``	81	394	499	21.04
MRB2	N 17° 07`11,6``	W 88° 18`02,2``	+100*	344	456	24.56
MRB3	N 17° 07`10,5``	W 88° 18`05,5``	0	269	305	11.80
MRB4	N 17° 07`10,6``	W 88° 18`06,6``	0	297	366	18.85
CP 0	N 17° 03`37,6``	W 88° 15`11,8``	58	318	338	5.90
CP 1	N 17° 03`25,7``	W 88° 15`22,2``	64	261	343	23.90
CP 2	N 17° 03`04,3``	W 88° 15`48,1``	88	168	257	34.60
CP 3	N 17° 03`12,9``	W 88° 16`13,6``	72	264	360	26.70
CP 5	N 17° 03`27,1``	W 88° 16`26,8``	57	99	109	9.17
CP 6	N 17° 03`15,3``	W 88° 14`37,9``	50	206	307	32.90
CBi 1	N 16° 54`04,5``	W 88° 16`55,9``	78	244	285	14.40
CBi 2	N 16° 54`08,2``	W 88° 17`17,0``	102	228	251	9.20
CBi 3	N 16° 53`55,3``	W 88° 17`42,2``	76	179	179	0.00
CBi 4	N 16° 53`18,6``	W 88° 17`22,7``	56	154	286	46.20
CBi 5	N 16° 53`18,1``	W 88° 17`21,6``	12	220	458	51.90
SL 1	N 16° 45`52,4``	W 88° 18`47,7``	109	271	366	26.00
SL 2	N 16° 45`52,5``	W 88° 18`58,3``	96	238	384	38.00
SL 3	N 16° 45`50,8``	W 88° 19`08,0``	78	325	453	28.26
SL 4	N 16° 45`22,0``	W 88° 19`05,8``	69	256	386	33.68
SL 5	N 16° 46`30,4``	W 88° 18`01,9``	94	457	489	26.18
SL 6	N 16° 45`48,4``	W 88° 18`43,7``	109	388	440	11.80

* elevation estimated

4.4 Results

4.4.1 Sediments

Holocene and Pleistocene sediments were recovered in the vibracores (Adomat and Gischler 2015). Facies successions and distribution do not show uniform patterns but strong local variation. Sediments comprise Holocene peat and peaty sediment, mud, sand, and poorly sorted sediments. Pleistocene soils form the basement of Holocene sediments. Coastal lagoon evolution started around 6 kyrs BP. Lagoon cores are predominantly composed of mud and peat units with mangrove roots and occasional shell concentrations. From north to south, the major characteristics of the sedimentary successions are as follows. In Manatee Lagoon, the Pleistocene basement dips towards the sea and is overlain by mud with shell concentrations (Fig. 4.3). Silt to fine sand and muddy sand occurs in the most seaward lagoon core. Cores from the marginal area show barrier sand, which overlie mud to fine sand. At Mullins River Beach, mud predominates, which may have been deposited in a reedswamp (Fig. 4.4). In some core sections, sand and laminated sediment were observed. Holocene sediments from Colson Point Lagoon predominantly comprise mud with shell concentrations, which is intercalated by mangrove peats and peaty sediments (Fig. 4.5). The underlying Pleistocene deposits exhibit considerable relief. In Commerce Bight Lagoon, mud overlies muddy sands (Fig. 4.6). In the backbarrier core, sand alternates with silt to fine sand. The channel deposits comprise largely medium to coarse sand, which overlie micaceous silt to fine sand. Sediments from Sapodilla Lagoon consist of thick lagoonal muds and Holocene basal peats and peaty sediments (Fig. 4.7). Close to the river mouth (SL4) and the tidal inlets (SL5, SL6), coarse-grained sediments occur.

4.4.2 Possible storm deposits and radiocarbon dating

Possible storm deposits have been identified in 18 cores from the five localities. These include sand layers marine fauna, shell concentrations, hiatuses and reversed ages (Table 4.3, Table 4.4). Radiocarbon dating of the sand layers has proven difficult because no appropriate material for radiocarbon dating was found. To obtain an approximate age of the sand deposits, organic matter from the top of the underlying sediments was selected for dating. This way, four of five sand layers have been dated. Further radiocarbon ages have been obtained from five corals and from bivalves from 15 of 17 shell concentrations. The basal concentration in CP6 and the concentration in CBi3 were not age-dated. Articulated bivalve shells and corals preserved in situ potentially to be used for dating were not available.

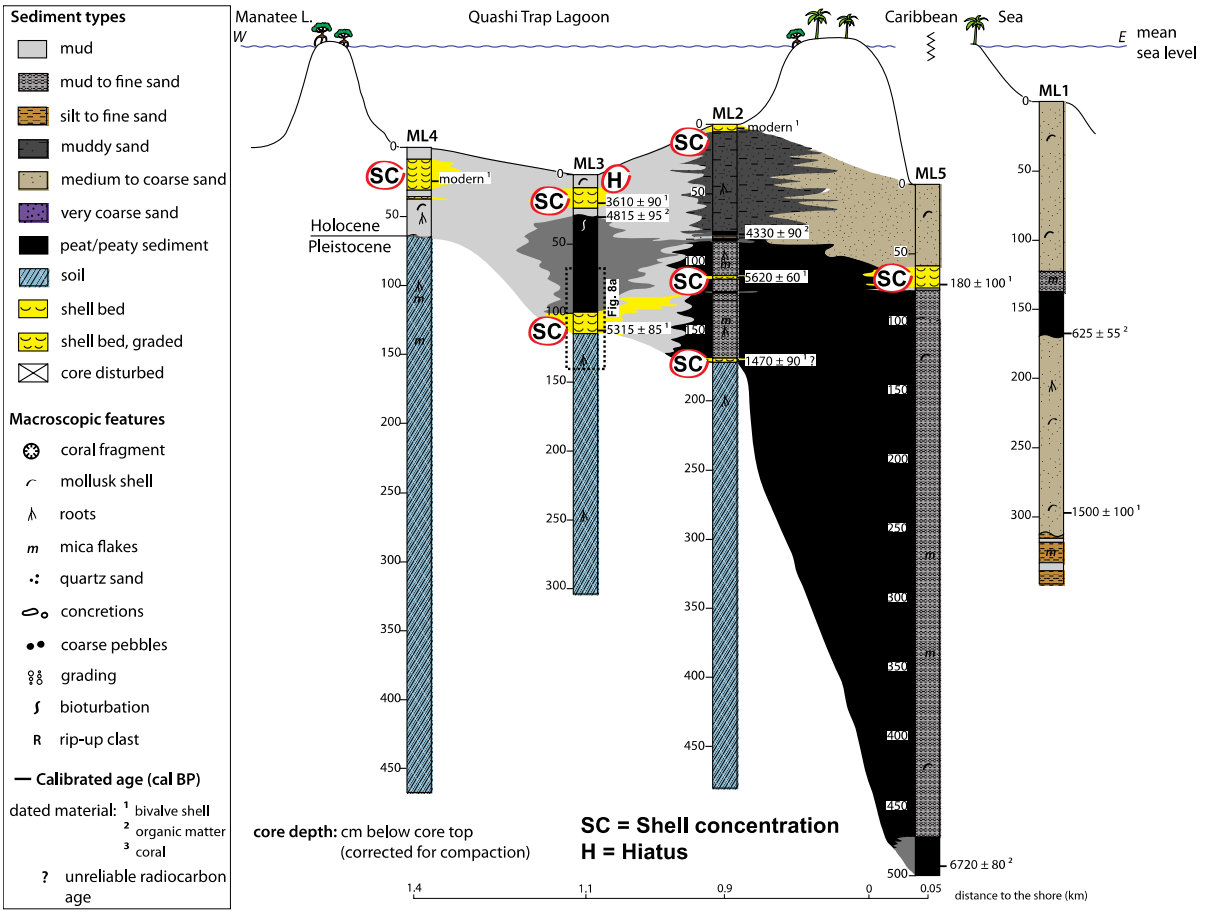

Fig. 4.3 Core logs and interpreted sedimentary facies at Manatee Lagoon. Location of coring sites is shown in Fig. 4.2. Core logs were corrected for compaction and are arranged with reference to the sea level. Abbreviations highlight deposits, which are interpreted to be related to hurricanes. SC: Shell concentration; H: Hiatus. Dashed rectangle in ML3 highlights core section shown in Fig. 4.8

4.4.2.1 Manatee Lagoon

In cores from Manatee Lagoon, seven shell concentrations were observed in the lagoonal cores ML2, ML3 and ML4 (Fig. 4.3; Fig. 4.8a). Mollusk fauna within the lagoonal shell concentrations mainly comprise the bivalve *Anomalocardia cuneimeris* and cerithid gastropods (Adomat et al. 2016). Seven assemblages were distinguished in the lagoons. Assemblage A1 comprises mainly *A. cuneimeris* and *C. eburneum*. In A2 and A3, the dominant species is *A. cuneimeris*. Assemblage A4 is a *C. pliculosa*/*A. cuneimeris* assemblage with the former being the most abundant species. Assemblage A5 is an almost monospecific assemblage, with of *C. pliculosa* and *A. cuneimeris* being as dominant species. A6 comprises largely *A. cuneimeris*. A7 is an *A. cuneimeris*/*C. pliculosa* assemblage with the former being more abundant. Contacts between the shell concentrations and the under- and overlying sediments vary from sharp to gradational. The matrix of the lagoonal shell concentrations is fine-grained throughout and includes grey mud to fine sand. The shell concentration in the marginal marine core ML5, found at the base of a sand deposit close to the core top, contains marine mollusk fauna, shows a bioclast-supported fabric and a sharp contact to the underlying mud layer. One hiatus was found in core ML3 with a relatively old age of 3610±90 cal yr BP close to the core top. Hiatuses are

indicated by relatively old radiocarbon ages at or close to core tops. The striking age reversal in core ML2 is presumably due to diagenetic alteration of the dated mollusk shells thereby producing a relatively young age at the base of the Holocene section.

4.4.2.2 Mullins River Beach

A distinct sand layer was found in two cores from Mullins River Beach (Fig. 4.4; Fig. 4.8b, c). It extends for at least 62 m; from core MRB1 obtained about 57 m offshore to core MRB2 collected about 5 m west of the coastline (Fig. 4.2b). Thickness of the sand layer decreases landward. The samples yielded radiocarbon ages of 7875±85 cal yr BP in MRB1 and 7890±30 cal yr BP in MRB2 (Table 4.3). In the remaining two cores of the transect, MRB3 and MRB4, a similar sand layer could not be identified.

The 51 cm thick sand layer in core MRB1 was found at a corrected core depth of 232 to 283 cm. The medium to very coarse sand is inversely graded and its color ranges from light olive brown to yellowish brown. Like the grain size, the content of the most abundant mineral quartz increases upwards from 76 to 89%. In contrast, the second most common mineral microcline decreases upwards from 19 to 4%. No shell material was found in the sand. The contacts to the underlying and overlying deposits are sharp. The sand layer is overlain by an alternation of grey mud and silt of about 120 cm thickness. The lamination in the lower 27 cm of this deposit is regularly spaced; further upcore the lamination is less regularly spaced.

The 1 cm thick sand layer in core MRB2 was found at a corrected core depth of 394 to 395 cm and consists of light yellowish brown medium to coarse sand. The quartz and microcline content of the sand layer is 53% and 9%, respectively. Furthermore, this sand shows an andalusite content of 34%, which is high compared to beach sands at the core top with less than 3% andalusite and an andalusite content of the sand layer in core MRB1 of less than 6%. The sand layer also lacks shells. Both contacts, to the underlying organic-rich grey mud to silt and to the overlying grey mud, are sharp. The overlying mud contains a 2 cm thick silt layer. This deposit is similar to a deposit overlying the sand layer in core MRB1. In core MRB2, the planar laminated unit of grey mud and silt is about 41 cm thick and thus, like the sand layer, this deposit also shows landward thinning. It is overlain by another sand layer, a 65 cm thick micaceous silt to fine sand deposit, which shows a sharp but wavy lower contact and gradually merges into laminated fine-grained sediments. The lower portion of this micaceous silt to fine sand contains rip-up clasts from the underlying grey mud (Fig. 4.8b). The micas observed in these deposits are flaky and have larger grain sizes than the surrounding components.

4.4.2.3 Colson Point Lagoon

As in Manatee Lagoon, shell concentrations are common in cores from Colson Point Lagoon. Ten shell concentrations were observed in the cores CP0, CP1, CP2, CP3 and CP6, of which eight have been interpreted as possible storm deposits (Fig. 4.5; Fig. 4.8d). Faunal composition is similar to that of the lagoonal concentrations in Manatee Lagoon. The two basal shell

concentrations in core CP6, which was collected in the marginal marine area, have probably been deposited in a lagoon environment (Adomat et al. 2016). These two shell concentrations in core CP6 are graded. In contrast to the basal concentrations, the two shell concentrations further upcore represent marginal marine deposits. In core CP2 a hiatus was found, showing an age of 2070±90 cal yr BP close to core top. In core CP6 from the marginal marine area east of Colson Point, a sand layer of 3 cm thickness is interbedded with mangrove peat (Fig. 4.8e).

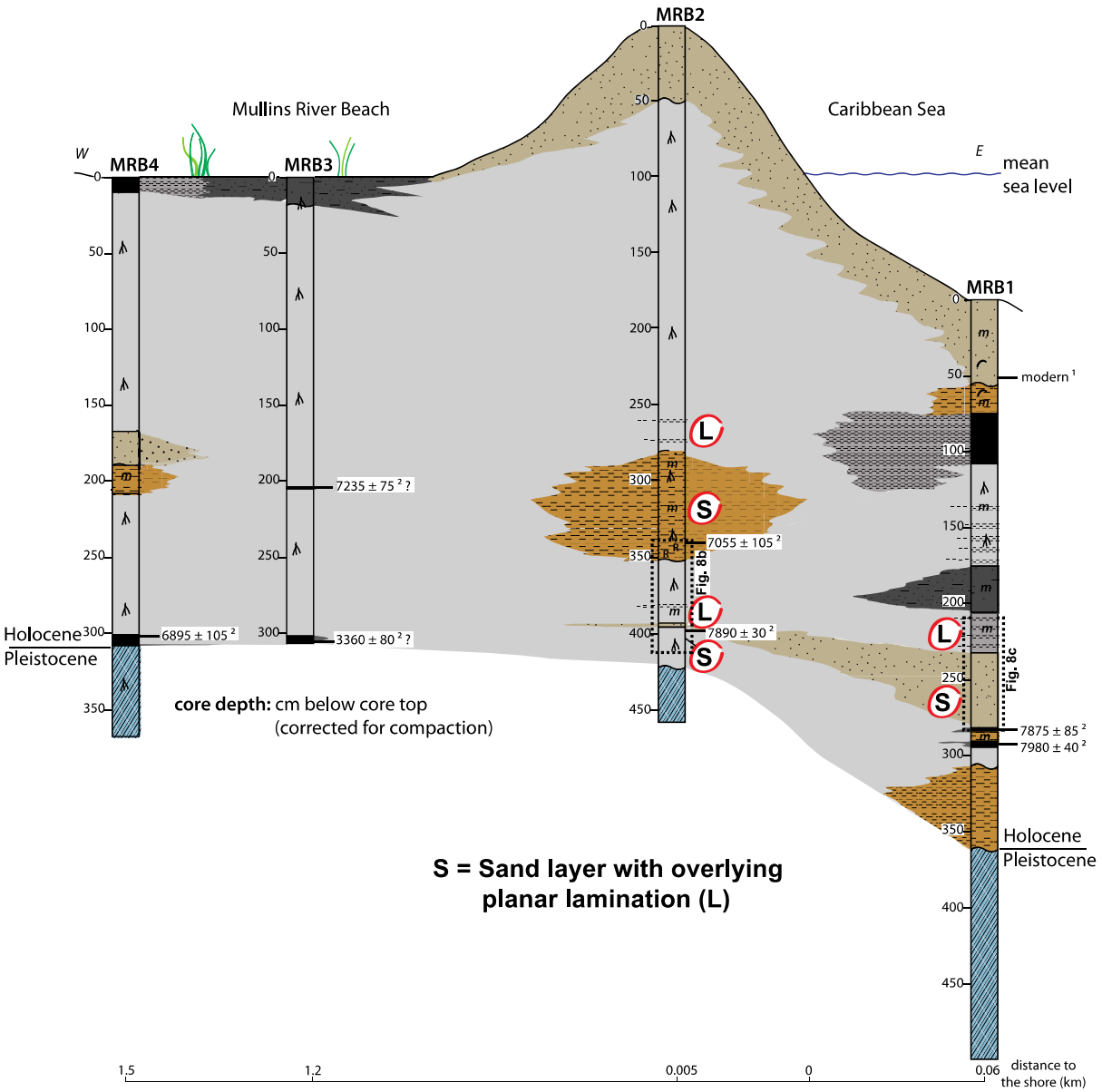

Fig. 4.4 Core logs and interpreted sedimentary facies at Mullins River Beach. Location of coring sites is shown in Fig. 4.2. Core logs were corrected for compaction and are arranged with reference to the sea level. Abbreviations highlight deposits, which are interpreted to be related to hurricanes. L: Planar lamination; S: Sand. Dashed rectangles in MRB1 and MRB2 highlight core sections shown in Fig. 4.8

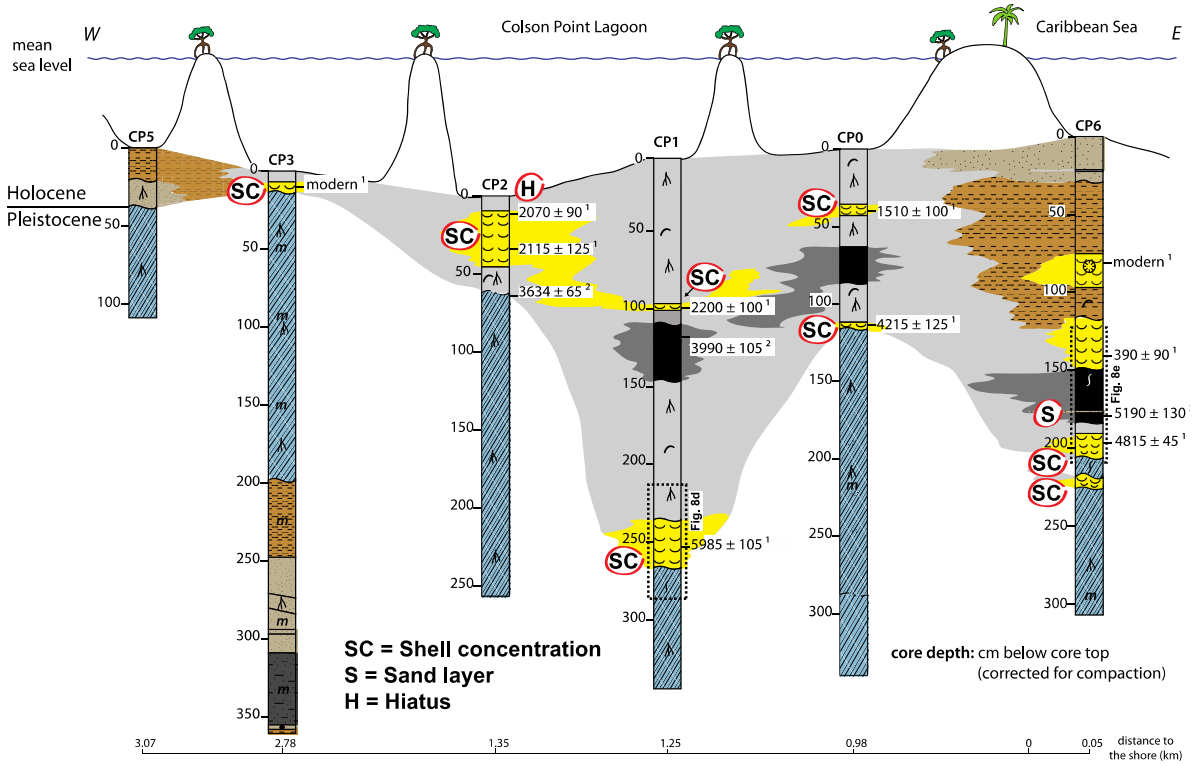

Fig. 4.5 Core logs and interpreted sedimentary facies at Colson Point Lagoon. Location of coring sites is shown in Fig. 4.2. Core logs were corrected for compaction and are arranged with reference to the sea level. Abbreviations highlight deposits, which are interpreted to be related to hurricanes. SC: Shell concentration; H: Hiatus. Dashed rectangles in CP1 and CP6 highlight core sections shown in Fig. 4.8

4.4.2.4 Commerce Bight Lagoon

Different possible storm deposits occur in cores from Commerce Bight Lagoon (Fig. 4.6). At the top of the lagoonal core CBi3, a shell concentration, dominated by *A. cuneimeris* and cerithids, was found. In the lagoonal core CBi2, a hiatus with an age of 4625±175 cal yr BP in 50 cm core depth was observed. The backbarrier core CBi1 shows medium to very coarse sand deposits and marine fauna that is represented by fragments of the branched coral *Porites porites*. The coral fragments and few mollusk fragments are embedded in a ca. 5 cm thick bed within medium to very coarse sands (Fig. 4.8f). Underlying and overlying sediments comprise mainly quartz sands without shells, and are partially graded and sporadically intercalated with fine-grained sediments. One coral yielded an age of 4945±105 cal yr BP (Table 4.3). The peat layer, which is located about 12 cm below the coral-bearing sand deposit was dated to 4967±90 cal yr BP. Only in the uppermost 20 cm of the backbarrier core, normal lagoon sediments of dark mud with brackish shells were found. *P. porites* fragments were also found in cores CBi4 and CBi5 from the tidal channel of Commerce Bight, where they occur in fine to coarse sands, together with dispersed brackish to marine and marine mollusk shells, respectively. In the lower section core CBi5 exhibits an age reversal with older deposits overlying deposits of younger age.

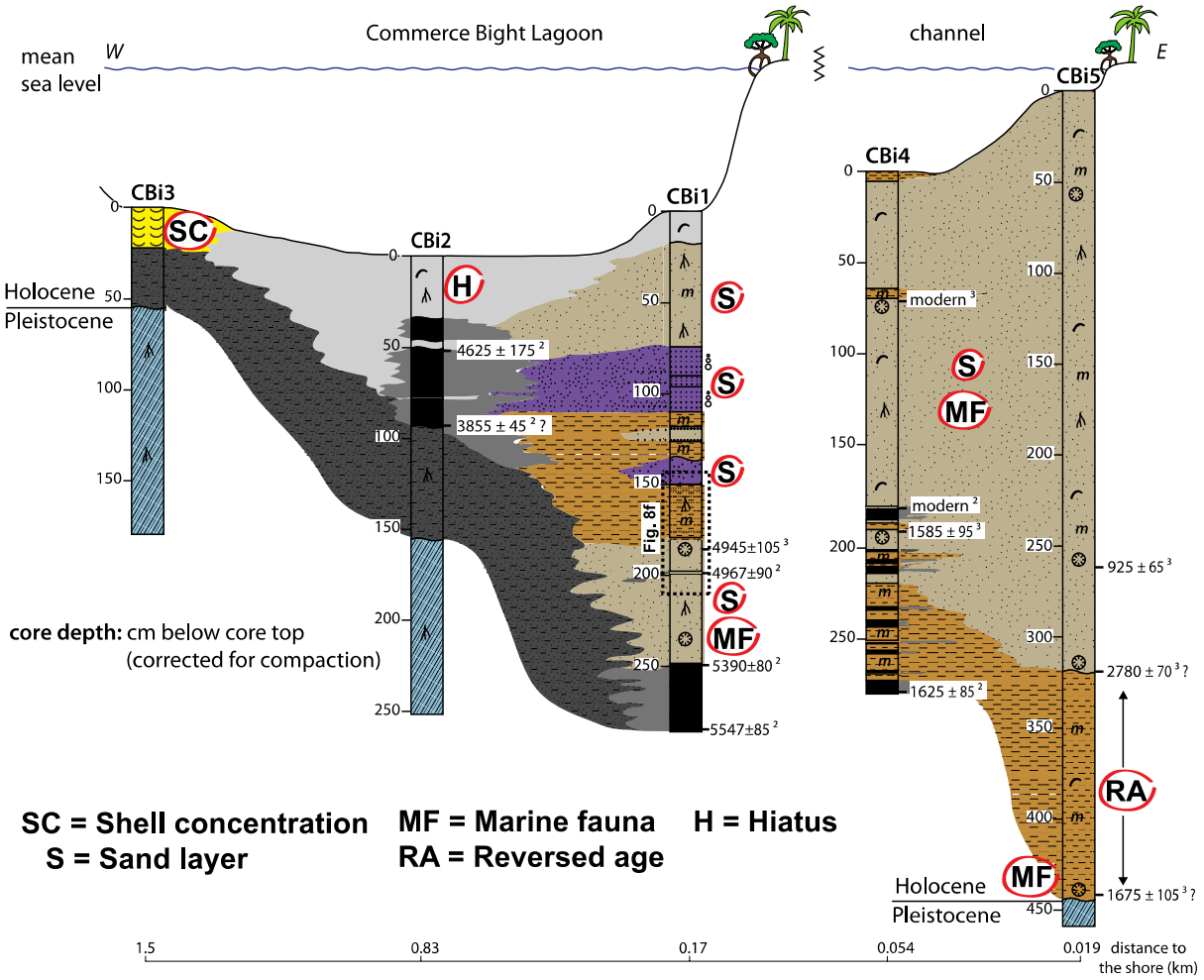

Fig. 4.6 Core logs and interpreted sedimentary facies at Commerce Bight Lagoon. Location of coring sites is shown in Fig. 4.2. Core logs were corrected for compaction and are arranged with reference to the sea level. Abbreviations highlight deposits, which are interpreted to be related to hurricanes. SC: Shell concentration; S: Sand; MF: Marine fauna; RA: Reversed age. Dashed rectangle in CBi1 highlights core section shown in Fig. 4.8

4.4.2.5 Sapodilla Lagoon

At the base of Holocene sediments the lagoonal core SL1 shows a shell concentration with abundant specimens of *A. cuneimeris* and cerithids. The shell concentration in core SL5 is not interpreted to be storm-generated. Core SL5 contains a 32 cm thick sand layer, which is overlain by more consolidated fine-grained sediments with planar lamination (Fig. 4.8g). Sediment structures could not be identified due to sediment loss during cutting the core.

In summary, the following deposits have been interpreted to be related to storm events: (1) Five sand layers, of which three occur in two cores from Mullins River Beach, one in a core from Colson Point and one in a core from Sapodilla Lagoon; additionally, multiple sand deposits occur in the backbarrier and in the two tidal channel cores from Commerce Bight Lagoon. (2) Marine fauna identified in sands from the lower section of the backbarrier core and from two channel cores from Commerce Bight Lagoon (3) Sixteen lagoonal shell concentrations and one marginal marine shell concentration found in eleven cores from Manatee, Colson Point, Commerce Bight

and Sapodilla lagoons. (4) Three hiatuses occurring in lagoon cores from Manatee, Colson Point and Commerce Bight lagoons, and one reversed age in one core from Commerce Bight Lagoon.

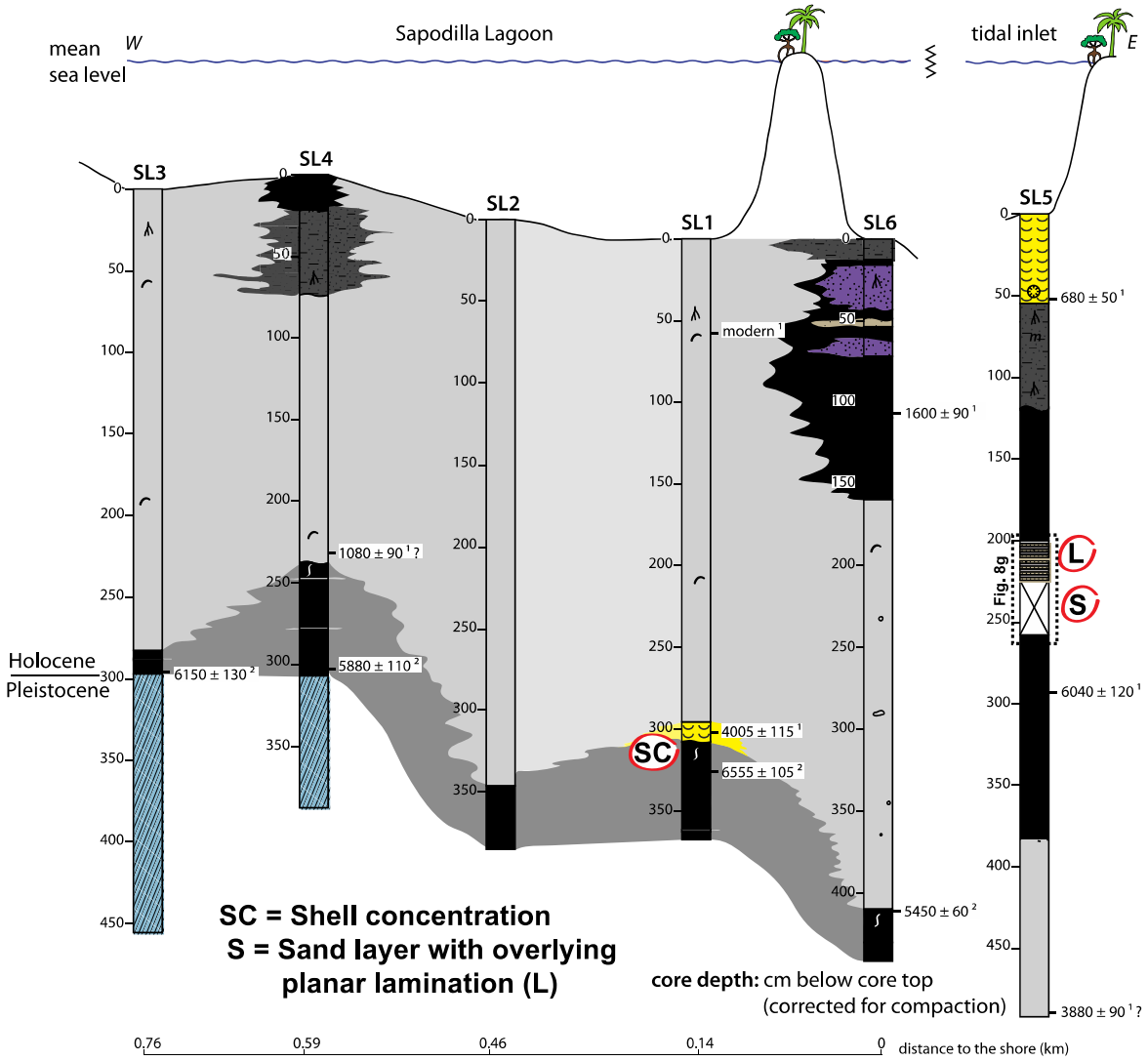

Fig. 4.7 Core logs and interpreted sedimentary facies at Sapodilla Lagoon. Location of coring sites is shown in Fig. 4.2. Core logs were corrected for compaction and are arranged with reference to the sea level. Abbreviations highlight deposits, which are interpreted to be related to hurricanes. SC: Shell concentration; S: Sand; L: Lamination. Dashed rectangle in SL5 highlights core section shown in Fig. 4.8

Table 4.3 *Characteristics and radiocarbon dates of possible overwash deposits including sand layers, marine fauna, hiatuses and reversed ages*

Core	Corrected Thickness (cm)	Type	Sediment	Lower Contact	Upper Contact	Sediment Structures	Dated Material	Conventional Age (yr BP)	Calibrated Age (cal yr BP, 2 σ range)	Calibrated Age (cal yr BP)	BETA No.
MRB1	51	Sand layer	Medium to very coarse sand	Sharp, planar	Sharp, planar	Inverse grading, landward thinning, overlain by laminated fine-grained sediments	Organic matter of underlying organic mud	7050±40	7960-7790	7875±85	345343
MRB2	1	Sand layer	Medium to coarse sand	Sharp, planar	Sharp, planar	Landward thinning, overlain by laminated fine-grained sediments	Organic matter of underlying organic mud	6950±40	7920-7900, 7860-7680	7910±10, 7770±90	345346
MRB2	27	Sand layer	Silt to fine sand	Sharp, wavy	Gradational	Rip-up clasts at base, micaceous, overlain by laminated fine-grained sediments	Organic matter within sand deposit	6160±30	7160-6950	7055±105	345345
CP6	3	Sand layer	Medium to coarse sand	Sharp, planar	Sharp, planar	Sandwiched between mangrove peat	Underlying mangrove peat	4550±30	5320-5270,5220-5220, 5180-5120,5110-5060	5295±25, 5220, 5150±30, 5085±25	307047
SL5	32	Sand layer	Fine sand	Sharp, wavy*	Sharp, planar*	Overlain by laminated fine-grained sediments	No age	No age	No age	No age	No age
CBi1	248	Marine fauna	Coral fragments, coarse to very coarse sand	Gradational	Gradational	Overlying sands partially normally graded	Coral fragment	4850±30	5050-4840	4945±105	317594
CBi4	11	Marine fauna	Coral fragments, brackish to marine mollusks, coarse to very coarse sand	Gradational	Gradational	None	Coral fragment	2130±30	1680-1490	1585±95	317600
CBi5	447	Marine fauna	Coral fragments, marine mollusks, coarse to very coarse sand	Gradational	Gradational	None	Three coral fragments from various core depths	1. 1500±30 2. 3130±30 3. 2220±30	1. 990-860 2. 2850-2710 3. 1780-1570?	1. 925±65 2. 2780±70 3. 1675±105?	1. 317602 2. 317603 3. 317604
ML3	0-21	Hiatus	Mud overlying shell conc.	Gradational	None	None	Bivalve shell	3820±30	3700-3520	3610±90	348285
CP2	0-11	Hiatus	Mud overlying shell conc.	Gradational	None	None	Bivalve shell	2560±30	2160-1980	2070±90	307041
CBi2	0-52	Hiatus	Mud overlying muddy peat	Gradational	None	None	Organic matter	4080±30	4800-4760, 4690-4680, 4646-4520, 4470-4450	4780±20, 4685±5, 4580±60, 4460±10	348278
CBi5	323-438	Reversed Age	Change from silt to fine sand to medium to coarse sand	Sharp, wavy	Gradational	None	Two coral fragments	1. 3130±30 2. 2220±30	1. 2850-2710 2. 1780-1570?	1. 2780±70 2. 1675±105?	1. 317603 2. 317604

* Vague due to sediment loss
? Unreliable radiocarbon age

Table 4.4 *Characteristics and radiocarbon dates of 16 lagoon and one marginal marine (ML5) shell concentrations. Packing categories were determined following Kidwell and Holland (1991). Lagoon concentrations are interpreted to have been formed due to salinity changes in the lagoons related to storm events. The concentration in ML5 was probably formed during a storm event*

Core	Corrected Thickness (cm)	Fabric	Packing	Matrix	Lower Contact	Upper Contact	Internal Structure	Conventional Age (yr BP)	Calibrated Age (cal yr BP, 2 σ range)	Calibrated Age (cal yr BP)	BETA No.
ML2	5	Matrix-supported	Dispersed	Grey silt to fine sand	Gradational	None	Homogeneous	118.2±0.4	Modern	Modern	348283
ML2	2	Matrix-supported	Dispersed	Grey mud to fine sand	Gradational	Gradational	Homogeneous, altered	5370±30	5680-5560	5620±60	348284
ML2	3	Matrix-supported	Loose	Grey mud to fine sand	Sharp, wavy	Gradational	Homogeneous, altered	2050±30?	1560-1380?	1470±90?	325009
ML3	13	Matrix-supported	Loose	Grey mud	Gradational	Gradational	Homogeneous	3820±30	3700-3520	3610±90	348285
ML3	14	Matrix-supported	Loose	Grey mud	Gradational	Sharp	Mottled at base	5070±30	5400-5230	5315±85	325011
ML4	27	Matrix-supported	Loose to dispersed	Grey mud	Gradational	Sharp	Homogeneous	105±0.3	Modern	Modern	348286
ML5	14	Bioclast-supported	Dense	Yellowish brown med. sand	Sharp	Gradational	Homogeneous	680±30	280-80	180±100	325012
CP0	7	Matrix-supported	Dispersed	Grey mud	Gradational	Gradational	Homogeneous	2090±30	1610-1410	1510±100	238280
CP0	6	Matrix-supported	Loose	Grey mud	Sharp	Gradational	Bioturbation	4270±30	4340-4090	4215±125	348281
CP1	5	Matrix-supported	Dispersed	Grey mud	Gradational	Gradational	Homogeneous	2650±30	2300-2100	2200±100	307038
CP1	24	Matrix-supported	Loose	Grey mud	Gradational	Gradational	Bioturbation	5700±30	6080-5890	5985±105	307040
CP2	20	Matrix-supported	Loose	Grey mud	Gradational	Gradational	Homogeneous	2580±30	2240-1990	2115±125	307042
CP3	5	Matrix-supported	Loose	Grey mud	Gradational	Gradational	Homogeneous	520±30	Modern	Modern	307044
CP6	11.5	Matrix-supported	Loose	Grey mud	Sharp	Gradational	Grading, bioturbation	4710±30	4860-4770	4815±45	307048
CP6	5.5	Matrix-supported	Loose	Grey mud	Sharp	Gradational	Grading, bioturbation	No age	No age	No age	No age
CBi3	19	Matrix-supported	Loose	Grey silt to fine sand	Gradational	None	Homogeneous	No age	No age	No age	No age
SL1	8	Matrix-supported	Loose	Grey mud	Sharp	Gradational	Homogeneous	4120±30	4120-3890	4005±115	320754

? Unreliable radiocarbon age

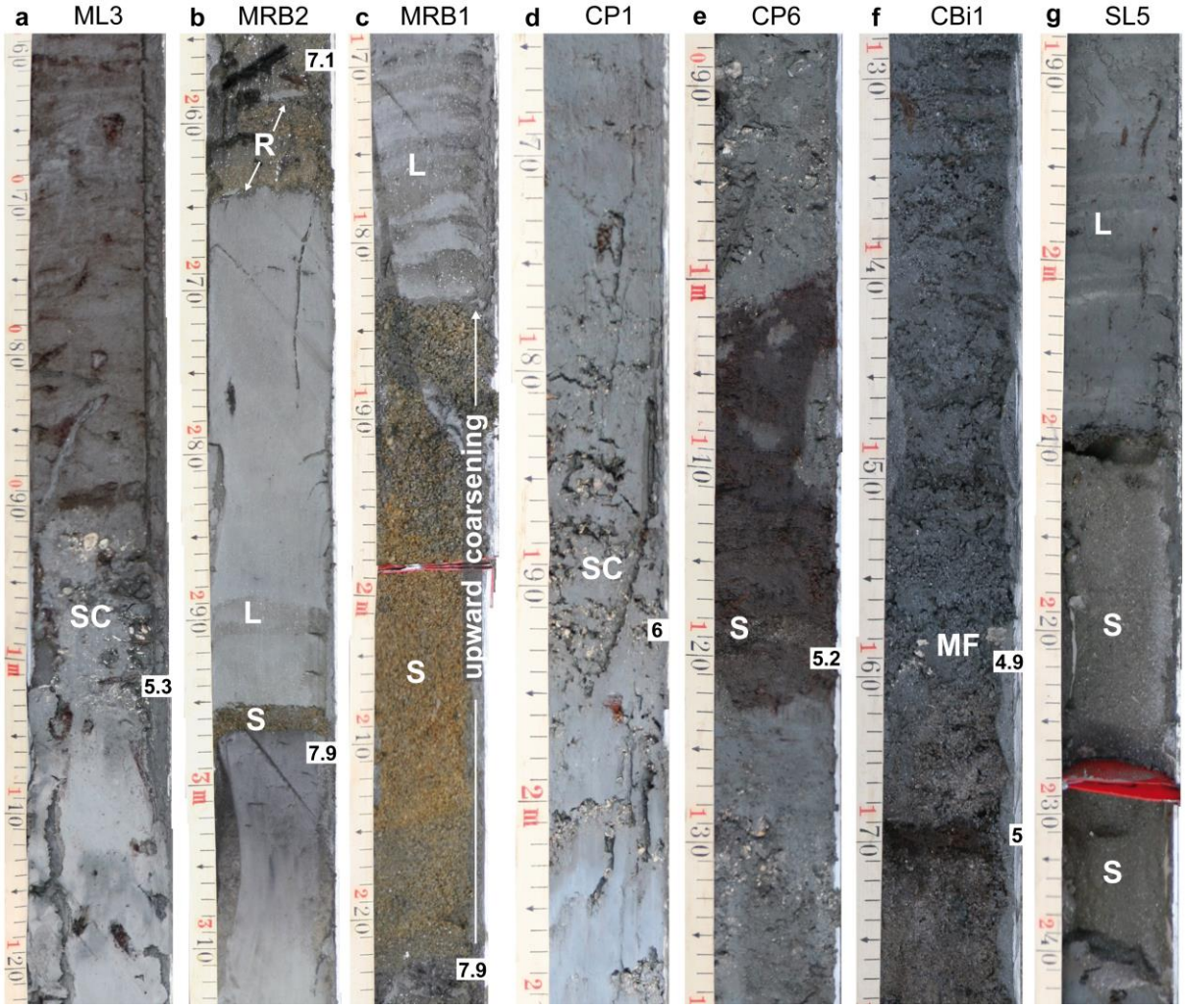

Fig. 4.8 Close ups of selected cores showing possible storm deposits. Numbers indicate rounded calibrated radiocarbon ages in kyrs BP. Note that the tape measure indicates uncorrected core depths. Location of cores is shown in Fig. 4.2. **a** ML3; Lagoon shell concentration (SC) overlying Pleistocene soil. **b** MRB2; Sand layer (S) with sharp contacts, overlain by laminations (L) of mud and silt. At top of the core micaceous sand layer with sharp lower contact and rip-up clasts (R). **c** MRB1; Upward coarsening sand layer (S) with sharp contacts, overlain by a planar lamination (L) of mud and silt. The thickness of the sand layer increases from MRB1 to MRB2. **d** CP1; Lagoon shell concentration (SC) between Pleistocene soil and lagoonal mud. **e** CP6; Sand layer (S) in the basal portion of the mangrove peat. Bioturbation is recognizable in the upper portion of the peat and the lower lagoon shell concentration underlying the peat. Marine fauna with corals in the upper shell concentration overlying the peat. **f** CBi1; Coral fragments (MF) embedded in medium to coarse sand. **g** SL5; Sand layer (S), overlain by planar lamination (L). Fine sand was lost during cutting the core tube.

4.5 Discussion

4.5.1 Interpretation of possible storm deposits

4.5.1.1 Sand layers

Overwash deposits in coastal lagoons are reported as grain size anomalies or sand layers in the fine-grained background sedimentation (e.g., Liu and Fearn 1993, 2000a; Lane et al. 2011). During overwash, storm surge and waves overtop the barrier crest and transport sediments landward. Overwash deposits consist of locally derived material from foredune, beach and nearshore environments and are typically well to poorly sorted fine to coarse sands (Donnelly and

Webb 2004). In the study area, coarse-grained sediments are limited to the shoreface and foreshore, beach, barriers, barrier islands and barrier spits, whereas fine-grained facies were deposited in lagoon basins, tidal flats and marsh areas (Adomat and Gischler 2015). Thus, we interpret the sand layers in cores MRB1, MRB2, CP6, SL5 to have been deposited during high-energy events. At the Mullins River Beach location, the beach separates the marsh environment from the sea. There is no evidence for the existence of a barrier or beach during time of deposition of the sand layer, but the geomorphological setting of this site has changed in the past. The absence of mollusk shells in the muddy sediments, compared to muds from the other locations, suggest that a lagoon did not develop during the Holocene. Rather, a salt marsh or reed swamp environment persisted at this location (Adomat and Gischler 2015). Due to retrogradation of facies during Holocene sea-level rise, which is indicated by marine shells overlying lagoon shells in core CP6, it can be assumed that at Colson Point the barrier had a more seaward position in the past, and at Mullins River Beach a beach existed further seaward during early stages of coastal development. The barrier and the beach probably served as source for washover sands. At site SL5, the sand spit may have served as source for washover sands. More radiocarbon ages would be necessary to clarify whether or not the spit already existed during the time of deposition of the sand layer. Some sand deposits in the cores have not been interpreted as storm deposits, because they lack typical textural and compositional indications. Deposition of coarse-grained layers may be explained by other mechanisms such as riverine floods, aeolian processes, sediment winnowing and tidal processes (Otvos 1999; 2002; Wallace et al. 2014). A landward retreat of barriers due to rising sea level and marine transgression may be an alternative explanation for these sand deposits.

Several diagnostic criteria suggest storm origin of the sand layers in cores MRB1, MRB2, CP6 and SL5. The gradual upward coarsening of the sand deposit in MRB1 indicates deposition during a high-energy event. Generally, upward-fining trends of hurricane overwash deposits are observed, but inverse grading was also found in some places (Morton et al. 2007; Williams 2010). Spiske and Jaffe (2009) observed normal grading during setup and inverse grading during return flow and attributed them to decelerating and accelerating flow, respectively. According to Ferm et al. (1972), transgressive backbarrier deposits are generally coarsening upward sequences. The landward fining of the sand layer from core MRB1 to core MRB2 indicates marine rather than fluvial origin (Switzer and Jones 2008, and references therein). The landward thinning of the deposit is indicative of overwash deposits (Liu and Fearn, 2000a; Liu, 2004), but thickness is dependent on local topography (Peters and Jaffe 2010). The unimodal but predominantly poor sorting suggests deposition during a storm event. Generally, storm deposits have a unimodal particle size distribution, whereas a bimodal (e.g., Goff et al. 2001, 2004; Switzer and Jones 2008) and polymodal (e.g., Morton et al. 2008; Spiske and Jaffe 2009) grain size distribution is considered as being indicative of tsunami deposits. Modality, however, is site and source dependent. The similar ages and the fact that thickness and grain size increase from the proximal

to the distal end of the overwash fan suggest deposition of the two sand layers during the same event. A sharp contact with the underlying sediments, as observed in the sand deposits in cores MRB1, MRB2, CP6 and SL5, is another characteristic of overwash deposits (Donnelly et al. 2001a, b; Morton et al. 2007). According to Williams (2010), who used the presence of foraminifera as evidence for an offshore origin, the absence of foraminifera in sand layers does not necessarily rule out a marine origin of inshore deposits. Likewise, the lack of macrofauna and foraminifera in the sand layers in cores MRB1, MRB2, CP6 and SL5 also does not exclude a storm origin of the deposits. The recent beach sand at the top of core MRB2 does not contain shells either.

Rip-up clasts composed of the underlying sediment, as found in the upper sand deposit in core MRB2, are generally attributed to erosion of underlying sediment by tsunamis due to higher velocity and energy of these events (Gelfenbaum and Jaffe 2003; Switzer and Jones 2003; Morton et al. 2007) and seem to be rare in storm deposits (Jaffe et al. 2008). However, Donnelly and Webb (2004) encountered rip-up clasts at the basal contacts of backbarrier hurricane overwash deposits and assessed them as indicative of high-velocity currents.

Characteristics of both storm and tsunami deposits depend on available source material, offshore bathymetry, onshore topography and depositional environment (Kortekaas and Dawson 2007). In the study area, tsunamis that are triggered by seismic events cannot be excluded due to the nearby active Caribbean-North American plate boundary to the south. However, in the Caribbean the frequency of major earthquakes is 1-2 orders of magnitude less than that of cyclone landfalls, and of the tsunami events recorded during AD 1492-2000 only four events could be verified (Lander et al. 2002). In general, islands of the eastern Caribbean (Greater and Lesser Antilles) seem to be more frequently affected by tsunamis than the continental areas in the west (Lander et al. 2002; O´Loughlin and Lander 2003). Tsunami deposits have been reported from many regions including the wider Caribbean, Australia, and the Mediterranean (e.g., Lander et al. 2002; Scheffers and Kelletat 2003; Kelletat et al. 2004; Dominey-Howes et al. 2006; Scheffers 2006; Switzer and Jones 2008). However, Morton et al. (2008) and Spiske et al. (2008) have questioned several published Caribbean examples of tsunami deposits and reinterpreted them as storm features. Several diagnostic criteria for the distinction of storm and tsunami deposits have been proposed (e.g., Scheffers and Kelletat 2003; Morton et al. 2007; Switzer and Jones 2008), but many signatures are applicable to both storm and tsunami deposits (Switzer and Jones 2008).

Lamination of sediment was described as common diagnostic criterion for storm deposits and occurs as planar stratification with thin, often graded laminae and laminasets, or as foreset bedding (Schwartz 1975; Morton et al. 2007; Switzer and Jones 2008). The laminated sediments overlying sand layers as observed in cores MRB1, MRB2 and SL5 (Fig. 4.8 b, c, g) are interpreted to be associated with storm events. Only one of the five sand layers in the cores, core CP6, lacks overlying laminated sediments, due to deposition in mangrove peat (Fig. 4.8e). The

recurring stratigraphy of a sand layer with overlying laminated sediments probably reflects hydrodynamic inundation characteristics of a storm surge. In contrast to tsunamis, storms are limited only to unidirectional landward flow. However, Spiske and Jaffe (2009) described a complete hurricane surge sequence from a carbonate environment of Bonaire, Netherlands Antilles, which shows bidirectional storm directions and consists of three sedimentary units corresponding to setup, peak and return flow of the storm surge. Storm-induced sediment deposition takes place under primarily laminar flow conditions, during a period of hours to days (Tuttle et al. 2004). According to Morton et al. (2007), the absence of mud in most sandy storm deposits is the result of persistent high velocity and nearly unidirectional flow during the storm. Fine-grained sediments in storm deposits result from late-stage deposition from suspension. Williams (2010) detected two sedimentation styles in one storm surge deposit. The author distinguished a thick sand fan that was deposited by traction load and a thinner, finer and more organic-rich blanket that was deposited from suspension. Laminasets of alternating coarse and fine textures are indicative of high-frequency waves (Morton et al. 2007) and thin graded laminae are reported to be the result of individual waves during storm deposition (e.g., Sedgewick and Davis 2003; Switzer and Jones 2008). Laminations may be destroyed by bioturbation (Hennessy and Zarillo 1987). Due to their flaky shape, micas that occur within the laminated deposits may be easily suspended and transported in water and successively settled from suspension (Jagodziński et al. 2009). Jagodziński et al. (2009) detected abundant mica flakes in the uppermost portion of a tsunami deposit, which probably have been transported by suspension. The authors explained their absence in the lower part of the deposit by bedload transport. Several inundation pulses during storms (sensu Switzer and Jones 2008) can be regarded as possible cause for the deposition of sand layers and overlying laminated sediments encountered during this study. Generally, the thickness of sandy tsunami deposits rarely exceeds 25 cm, whereas sandy storm deposits can be up to 10 times thicker (Morton et al. 2007; Bryant 2008).

4.5.1.2 Marine fauna

The coral fragments in core CBi1 indicate a marine source and are interpreted as overwash deposits. The medium to very coarse sands found in the core also were transported during overwash processes. Sedimentation of coarse sands with corals and dispersed marine mollusk shells in cores CBi4 and CBi5 also results from barrier overwash. The narrow sandy barrier is situated about 100 m from CBi1. Distance from coring sites CBi4 and CBi5 to the barrier is 55 m and 20 m, respectively. Interfingering of muddy and sandy deposits indicates that lagoon background sedimentation was repeatedly interrupted by overwash. Sedimentation of mud with brackish shells at the top of the core demonstrates a return to lagoonal conditions. According to Hippensteel (2010), overwash deposits are the product of reworking, and therefore, dates obtained from fossils of those deposits may represent the age of the fossils but not the time of storm deposition. Morton et al. (2008) also considered problems concerning the dating of specific events because there can be substantial time elapsed between the death of an organism and the

incorporation of its skeletal material into the sediment. Hence, the ages of the corals obtained do not necessarily reflect the ages of the storm events, particularly if they are not supported by other proxies. However, the radiocarbon age of the coral found in CBi1 seems to be a fairly reliable datum of overwash, because the age of the underlying peat was dated to be only 500 years younger.

4.5.1.3 Shell concentrations

The accumulation of shells in the lagoons may have different origins: (1) Deposition of shells by overwash during high storm-surges, (2) formation of storm lags as a product of sediment winnowing during storms and subsequent accumulation of shells and (3) thriving of tolerant mollusk species due to changes in environmental conditions.

If the shells had accumulated during overwash events, both nearshore and marine mollusk species would be expected in the deposit. Overwash of marine species, mainly microfossils, into lagoons and lakes during storms is common (e.g., Hippensteel and Martin 1999; Morton et al. 2007; Hippensteel 2011; Pilarczyk and Reinhardt 2011; Hippensteel and Garcia 2014). However, the dominant species in the shell concentrations, *A. cuneimeris*, is known to tolerate a wide range of salinities. Turney and Perkins (1972) reported a salinity range of 13-80‰ in which living *A. cuneimeris* were found. *A. cuneimeris* lives in both enclosed and open hypersaline lagoons (Andrews 1935; Parker 1959). In Florida Bay, *A. cuneimeris* is restricted to the Northern Subenvironment, defined by only one species, which is greatly affected by freshwater drainage from the mainland (Turney and Perkins 1972). In Belize, taxonomic analysis including composition and diversity of mollusk species show differences between the lagoonal shell concentrations and shell concentrations from the marginal marine area. Taphonomic analysis of *A. cuneimeris*, such as numbers of left and right valves (LR-ratio) and size-frequency diagrams, suggest parautochthonous life assemblages, which have not been transported over wide distances and which have been deposited in their original brackish habitat. These observations indicate that the shells have not been deposited during overwash processes, and a marine origin can be excluded.

The second hypothesis is also invalid because the matrix of the shell concentrations is fine-grained and similar to lagoon background sediments. Storm lags typically lack fine matrix and have erosive bases (Brenner and Davies 1973). Only some contacts are sharp and changes in composition between the underlying deposits and the shell concentrations were not found except for under-and overlying peats and soils. Furthermore, no taphonomic features that would reflect storm events, such as preferred orientation of valves, bioclast-supported fabric and dense packing were observed in the shell concentrations. Grading in two shell concentrations is attributed to bioturbation. Separate dating of several shells from one shell concentration would help to elucidate time-averaging within the accumulation.

Since the shells are parautochthonous, they are interpreted to have accumulated episodically in the lagoons, probably during periods of favorable environmental conditions. Episodic favorable conditions may have resulted from increased river drainage associated with storm landfall precipitation events lowering salinity. Alternatively, an increase in salinity due to marine inundation and low air pressure associated with storm surges is possible. High water levels inshore of the barriers after storms caused either by floodwater runoff from the mainland or remnants of the storm surge (Morton 2002). Generally, an increase in salinity as a result of inundation is postulated (Li et al. 2009). According to Liu (2004), a hurricane-induced storm surge can cause saltwater intrusion into low-salinity lakes thereby producing abundance peaks of marine microfossils such as foraminifera, dinoflagellates and diatoms, even without significant overwash deposition (Li 1994; Hemphill-Haley 1996; Zhou 1998; Collins et al. 1999; Hippensteel and Martin 1999; Liu et al. 2003). But the contrary has also been demonstrated. Hoese (1960) showed that heavy rainfall after drought led to a rapid decrease in salinity of more than 30‰, causing a mortality of stenohaline mollusks in the bay fauna of Mesquite Bay on the central Texas coast. A decrease of salinity after landfall of a hurricane was reported from a brackish water coastal backbarrier lake separated from the Gulf of Mexico and related to freshwater input from surrounding marsh area as a result of heavy rain (Liu et al. 2011). The prolonged low salinity after hurricanes is considered to be the result of slow drainage through constricted tidal channels (Li et al. 2009; Liu et al. 2011). Constrictions are probably related to the formation of barriers and spits during Holocene evolution of the lagoons. Unfavorable conditions that allowed tolerant species such as *A. cuneimeris* and cerithids to flourish may have promoted the formation of shell concentrations. Storm events may have caused environmental variation such as salinity changes. In an area with highly variable precipitation such as in Belize, heavy rainy season or rain events during a dry season are to be considered as alternative explanations for environmental changes. The record by McCloskey and Liu (2012) from Belize also exhibits a dual sensitivity to both wind and rain. The authors considered both seaward and landward input and discussed the link between hurricane activity and strong precipitation events. Profiles of terrestrial elements such as Fe, Ti, Cr, Mn, Zn and Ti and marine elements such as S, Cl and Br served as environmental proxies, and helped the authors to distinguish between inland and seaward origin of sediments. In contrast to the lagoonal shell concentrations, which are considered to represent indirect evidence of storm events, the concentration together with the overlying sand deposit in the marginal marine core ML5 may represent direct evidence of storm deposition. This is suggested by its position at the base of the sand deposit, the densely packed, bioclast-supported nature, and the sharp contact to the underlying mud layer. Origin of the shell concentration at the top of core SL5 from the tidal inlet to Sapodilla Lagoon is probably not storm-related but rather formed due to higher energy in the tidal channel and the presence of a more diverse fauna related with mangrove vegetation.

4.5.1.4 Hiatuses and age reversals

The relatively old radiocarbon ages at or close to core tops, as observed in three cores from Manatee, Colson Point and Commerce Bight Lagoons, suggest erosion during high-energy events. McCloskey and Liu (2012) also recognized relatively old ages at top of cores from Commerce Bight Lagoon and interpreted them as the results of storm-induced erosion.

Age reversals, as observed in six cores from Mullins River Beach (MRB3) and Manatee, Colson Point, Commerce Bight and Sapodilla Lagoons (ML2, CP6, CBi2, CBi5 and SL5), also may indicate storm influence. However, only the age reversal in core CBi5 is interpreted to be storm-influenced, since the dated corals are likely redeposited and further indications for storms such as coarse sands occur in the core. In the other five cores age reversal are due to diagenetic alteration of dated material, young root penetration from above and bioturbation? Erosion and sediment mixing resulting in reversed ages may also be caused by other processes, such as river floods or tsunamis. However, in the study area a storm origin is quite likely. Limitations in radiocarbon dating may also be a conceivable explanation for reversed ages. Dated bivalve shell material may have undergone diagenetic alteration, which resulted in reversed ages as observed in cores ML2 and SL5. Radiocarbon dating of organic matter from peats and peaty sediments may produce too young ages due to contamination by younger roots. This could explain the reversed ages in core CBi2. The relatively old date in MRB3 may be attributed to the charred nature of the dated organic material, resulting in a too old age. Bioturbation processes, which are indicated by reworking of sediment, wavy lower contacts and grading of shells, probably caused the reversed age in core CP6.

4.5.2 Comparison with other studies

In this study, some thirty potential event beds have been identified along the central Belize coast during a time interval of 8 kyrs (Tables 4.3 and 4.4). Sand layers, shell concentrations and marine fauna, represented by corals, are interpreted as storm event beds and included in the diagram on Figure 9. Due to the fact that ^{14}C-ages from corals might be considerably older than the event deposits in which they occur, ages not supported by additional evidence have not been interpreted as being related to hurricane activity. Hiatuses, age reversals and the unreliable age of the shell concentration in ML2 are not figured because they exhibit a wide range of the ages and ages do not obligatorily indicate the time of hurricane landfall. A number of event deposits can be grouped into three phases occurring from 6000 to 4900, from 4200 to 3600 and from 2200 to 1500 cal yr BP. In addition, there are two earlier events positioned around 7900 and 7100 cal yr BP and more recent events centered around 180 cal yr BP and during modern times (Fig. 4.9). The fact that 5 major storms have been recorded in the study area during the past 150 years, but only one storm deposit during 250-300 year periods on average during the studied time interval of the past 8 kyrs clearly suggests incompleteness of the record. However, it is the best storm

record there is from the studied interval in the area. The clustering of events during certain time periods furthermore allows to approximately contrast active and inactive storm intervals, thereby permitting comparisons with other paleotempestology studies. It has to be kept in mind, however, that determination of active and inactive periods based on the identified event deposits is debatable due to the low number of event deposits, the use of different proxies and the fact that the event deposits originate from several sites along the coast.

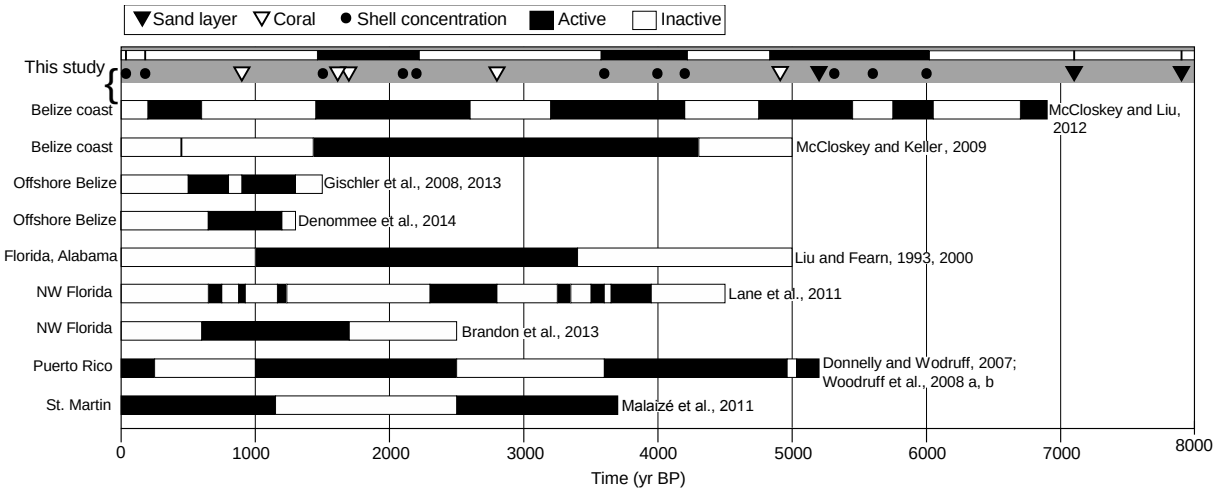

Fig. 4.9 Ages of possible event deposits identified in the study area, compared with paleohurricane records from the Belize coast, offshore Belize, the Gulf Coast and the Antilles archipelago. Three periods with event deposits being more frequent can be recognized. Ages of different proxies, including sand layers, shell concentrations and corals, are shown in the diagram. Coral ages were only included if supported by other proxies as there is a possibility that they are older than the surrounding sediment

A comparison with storm activity data from other studies shows both coincidences and differences (Fig. 9). Identified storm events match best with data from McCloskey and Liu (2012) from south-central Belize. Furthermore, some temporal correlations with hurricane activity periods from Puerto Rico (Donnelly and Woodruff 2007; Woodruff et al. 2008 a, b) exist. The hurricane frequency records from the Gulf of Mexico and the Antilles archipelago exhibit differences to the Belize records (Fig. 4.9). The comparison with the shorter high-resolution storm records from offshore Belize of Gischler et al. (2008, 2013) and Denommee et al. (2014) shows that correlation between storm layers, even in one region, is difficult. However, small discrepancies even exist between these two offshore records.

Along the Belize coast, McCloskey and Keller (2009) obtained 15 cores with a maximum length of ca. 2.4 m from the coastal area about 1 km south of our study site, and six cores from Gales Point, about 3.7 km north of our study site. They interpreted interbedded sand and clay layers as storm deposits, correlated these to hurricane events and identified a period of clustered hurricane events ranging from 4500 to 2500 yr BP and one extreme event around 450 yr BP. McCloskey and Liu (2012) studied a transect of seven cores with a maximum core length of 3.1 m from the eastern area of Commerce Bight Lagoon. After ca. 2000 yr BP, a change from a wetland to a lake

environment occurred, according to these authors. They interpreted clastic layers of sand as storm deposits, being generated by storm surges and storm-induced precipitation events, and distinguished between active and quiet periods, lasting from several centuries to 1200 years. Within the 7000 year record, they identified six active periods: 6900-6700 yr BP, 6050-5750, 5450-4750, 4200-3200, 2600-1450 and 600-200 yr BP. High-resolution data for the last 1500 years from the Belize Blue Hole sinkhole, located on the Lighthouse Reef Atoll, suggest intense hurricane activity from 500 to 800 yr BP, from 900 to 1300 yr BP (Gischler et al. 2008, 2013) and from 650 yr BP to 1200 yr BP (Denommee et al. 2014). Deviations between the two records are based on the fact that different minimal grain-sizes have been used to define event layers, which resulted in different numbers of storm deposits.

Further studies from the Gulf Coast and the Caribbean have documented hurricane activity spanning the last 7000 years. As proxy for the paleohurricane reconstructions, coarser grained deposits in fine-grained background sediments have been used. Lane et al. (2011) detected grain size anomalies in sediments from a coastal sinkhole at Apalachee Bay, NW Florida, and constructed both low and high threshold event chronologies with seven intervals in the high threshold series that exhibit event frequencies at or above three events per century. Brandon et al. (2013) yielded a period of increased intense hurricane frequency between 1700 and 600 yr BP from an adjacent area at Appalachee Bay. Sand layers in coastal lake and marsh sediments from Alabama and NW Florida indicate a hyperactive phase from 3400 to 1000 yr BP and quiescent phases from 5000 to 3400 yr BP and from 1000 yr BP to present (Liu and Fearn 1993, 2000a). However, the records by Liu and Fearn (1993, 2000a, b) have been intensively criticized by Otvos (1999, 2002). According to this author, most of the sand laminae, which have been related to overwash during catastrophic hurricanes by Liu and Fearn (1993, 2000a, b), have accumulated in a valley-filled estuary. As Otvos (1999) noted, other sedimentary processes than strom-surge overwash may have served as sand sources. Furthermore, Otvos (1999, 2001, 2002) questioned the radiocarbon dates of Liu and Fearn (1993) and criticized that Liu and Fearn (2000a, b) treated the barrier as fixed although coastal barriers are dynamic systems and the sensitivity of a site to overwash may have changed over time. The record of intense hurricane activity established by Donnelly and Woodruff (2007) and Woodruff et al. (2008a, b) in Puerto Rican lagoons demonstrates intervals of relatively frequent intense hurricane strikes from 2500 to 1000 yr BP, 4000-3600 yr BP and from 1000 to 0 yr BP. Fewer intense strikes have been recorded around 5000 yr BP, between 3600 and 2500 yr BP and between 1000 and 250 yr BP. Malaizé et al. (2011) investigated lacustrine pond sediments from Saint Martin (northern part of Lesser Antilles archipelago) and identified two relatively dry climatic periods from 3700 to 2500 yr BP and from 1150 yr BP to the present with predominantly carbonate mud deposition, droughts and hurricane events. In contrast, during a humid period from 2500 to 1150 yr BP, deposition of black organic mud occurred during pond highstand.

In the studied region, Holocene climate variability in the region is characterized by a change from warmer/wetter conditions during the Holocene Climate Optimum (ca. 10000-5500 yrs BP) to cooler/drier conditions after ca. 5000 yrs BP (e.g., Haug et al. 2001). Another change back to warmer and wetter conditions occurred in the late Holocene (between 3000-1000 yrs BP) in the wider study area according to vegetation data (Wooller et al. 2009) and coral climate proxy data from Belize (Gischler and Storz 2009). A period of increased hurricane activity during 3500-1000 yrs BP recorded by Liu and Fearn (2000a) apparently correlated with a northward shift of the Intertropical Convergence Zone (ITCZ). A northern position of the ITCZ favors heavy rainfall in the southern part of the Caribbean and the Yucatán peninsula, whereas a southern position of the ITCZ causes drought in the Caribbean region (Haug et al. 2003; Hodell et al. 2005). Stronger storm activity over the Gulf coast and the inner Caribbean Sea is favored by a southern position of the ITCZ in connection with dry climatic conditions. The position of the ITCZ is associated with a shift of the Bermuda High, whose position controls the direction of hurricane paths. Therefore, differences in hurricane frequency can be observed in the Caribbean as shown in the records in Figure 9. Data from localities positioned in the same region such as e.g., Puerto Rico and St. Martin or coastal lagoons and offshore sinkholes in Belize also differ, suggesting that the preservation of hurricane deposits plays an important role as well.

4.5.3 Suitability of Belize barrier-lagoon complexes for reconstruction of storm events

The preservation potential of sandy storm deposits appears to be higher in beach and marginal marine settings than in coastal lagoons. The cores investigated during this study that contain sandy storm deposits derive from the beach (core MRB2), the marginal marine area (cores MRB1 and CP6) and the tidal inlet (core SL5) (Fig. 4.2). Core CBi1 is the only core from a lagoonal basin that contains washover sands, which is attributed to the adjacency to the barrier. Along the Belize coast, which has been hit by hurricanes on a regular basis, a higher number of overwash deposits in lagoons may be expected. Still, in the cores that contain sand layers, the storm record is poor when considering the frequency of historical hurricane landfalls. Liu (2004) stated that in coastal lake sites, which are repeatedly impacted by landfalling hurricanes, sediment cores are expected to contain multiple layers of overwash deposits sandwiched between normal organic lake sediments. The fact that cores taken from the central lagoon basin do not contain washovers may be attributed to several factors. According to Sedgwick and Davis (2003), the preservation potential of individual storm deposits is highly variable and depends on factors such as the rate of bioturbation, frequency of overwash, thickness of the units as well as the magnitude and rate of sea-level change. Liu (2004) noted that the preservation potential of sediments deposited at the bottom of coastal lakes, which are isolated from the sea, is higher than in shallow-water marine environments, because overwash deposits will not be removed by tidal scouring or reworking. According to this author, shallow marine environments are inappropriate for providing high-resolution records because of reworking and obliteration by subsequent storm events. The

relatively poor record in the Belize lagoon cores may result from biological and physical processes in the lagoons. Bioturbation is a common process in the lagoons and evidence of bioturbation was also found in several cores (Fig. 4.8e). In mangrove-vegetated environments, the benthic fauna is typically dominated by burrowing decapods such as crabs (Kristensen 2008). They dig and maintain burrows in the sediment, affecting sediment topography by physical displacement of particles. The burrowing activity may destroy sediment structures and hampers the identification of event deposits. Erosion of sands by tidal flushing is limited because the Belize coast is a microtidal area with a tidal range of max. 30 cm. The coastal lagoons in the study area are tidally connected to the sea. However, they represent restricted, not open lagoons (Fig. 4.2). Manatee, Colson Point and Commerce Bight lagoons are connected with the sea by relatively long bifurcating and branched tidal channels. An exception is Sapodilla Lagoon, which is less restricted than the other lagoons. Here, the permanent broad tidal inlet, which is interpreted to have been formed by spit progradation (Adomat and Gischler 2015), and the channel between the narrow spit and the barrier island allow water exchange with the open ocean. The core sites of MRB1, CP6 and SL5, which contain event sand layers, are today located in areas with increased water energy, compared to the lagoon basins. But during time of deposition of the sand layers, low water energy prevailed at the sites, which is supported by the predominant fine-grained sediments in the cores.

In addition to bioturbation and tidal flushing, some other aspects need to be considered, which may reduce the fidelity of the sediment archive: After two or more events that occurred in a relative short time interval, the lack of enough material for erosion and deposition may cause that no depositional evidence was left in the record after an event. Furthermore, event beds that have been deposited back-to-back may not be registered as single events. The top of the first event bed may not be covered by background sediments and thus is vulnerable to erosion. During deposition of the subsequent event bed, partial removal of the top of the earlier event deposit may occur, producing amalgamated event beds, as observed by Keen et al. (2004) and McCloskey and Keller (2009). Not all variations in faunal composition may be preserved in the record. Evidences of minor changes in faunal composition that occur in the time period until the conditions return to the initial level (e.g., until the barrier got reestablished) may not be registered in the record. Hence, it has to be taken into account for how long the conditions such as barrier breaching or freshwater input that caused the variations prevailed.

Besides the reduction of the preservation potential, the occurrence of storm deposits is also dependent on the sensitivity of a site to storm deposition (Hippensteel et al. 2013). The paleotempestological sensitivity of a lake or lagoon, which is enclosed by a barrier, in turn depends on meteorological factors, long-term changes in sea level and geomorphological factors (Liu 2004). These factors may have changed over time and thus also the sensitivity may have changed over time. Sea-level rise may have a strong influence on site sensitivity, especially on low-lying coastal areas as in Belize. Only intense storms produce high storm surges that are able

to overtop the barrier. Sand deposition is also possible during less intense storms via active channels and inlets (Donnelly et al. 2001a). Geomorphological factors such as offshore bottom slope, coastline configuration, supply of floodwater from river discharge as well as stochastic meteorological factors influence the relationship between storm surge height and hurricane intensity (Jarvinen and Neumann 1985; Hubbert and McInnes 1999). Whether a storm surge will overtop a barrier depends primarily on two factors, the storm surge height and the barrier height (Liu 2004). Storm surges of weaker hurricanes possibly were not able to exceed the barrier. According to Malaizé et al. (2011), only high-intensity hurricanes significantly contribute to event sedimentation. Most sites only record hurricanes that make landfall in the immediate vicinity at major hurricane strength (category 3) or above) (Donnelly and Webb 2004; Liu 2004; Elsner et al. 2008; Liu et al. 2008; McCloskey and Keller 2009; McCloskey and Liu 2012). According to Morton et al. (2007), the highest storm surges of tropical cyclones are generally restricted to a few tens of kilometers adjacent to the eye, although elevated water levels can encompass more than 600 km of coast. The characteristics of hurricanes lead to different hurricane effects of the two sides of the storm track. Vortex winds that flow counterclockwise around the eye, and much slower regional winds that move the storm system forward. On the right side of a hurricane the winds are stronger, because the two winds move in the same direction and are additive (Coch 1994). Thus, low correlation of event beds from the study area to published records from areas in greater distance from the study area is not surprising.

Mangrove vegetation, which densely fringes the coastal lagoons in the study area since ca. 6 kyrs BP, acts as a protective barrier against erosion during storm or flood events (e.g., Danielsen et al. 2005; Kathiresan and Rajendran 2005), tends to reduce the magnitude of erosion (Morton 2002) and may also prevent a complete storm record. Mangroves are able to attenuate storm surges by reducing the surge amplitude and by reducing the inundation distances (e.g., Zhang et al. 2012; Liu et al. 2013). It has been shown that mangroves are more effective at reducing surges from hurricanes with a rapid forward speed than those of hurricanes with a slow forward speed (Zhang et al. 2012). Because of their dense stilt roots, trees of *R. mangle* are effective in dissipating the energy of low surges (McIvor et al. 2012; Zhang et al. 2012)

In summary, the following features can be regarded as favorable for paleotempestology reconstructions in the coastal lagoons: The situation behind a sandy barrier and the proximity to the sea, which is the case for Manatee and Commerce Bight Lagoons, and, with a slightly larger distance to the sea, for Colson Point Lagoon, makes the coastal lagoons susceptible to overwash. In contrast, several processes may impede reconstruction of a hurricane record: Bioturbation is a common process in the lagoons. Tidal flushing, although the coast is microtidal, plays a minor role and is strongest in Sapodilla Lagoon, where the tidal inlet is relatively broad. Due to the connections of the coastal lagoons to major rivers, the record in coastal lagoons may be complicated by fluvial events unrelated to hurricane strikes. Sea-level rise and transgression of the sediment complexes during the Holocene may have a negative effect, because in

transgressive settings storm records will be destroyed or obscured through time (Hippensteel 2010). The dynamic nature of coastal environments complicates the interpretation of sedimentary records (Donnelly et al. 2001a). Dense mangrove growth, which is found at all localities except for Mullins River Beach, is able to prevent hurricane impacts in the lagoons to some degree and thus reduces the sensitivity of the sites for overwash.

4.6 Conclusions

1. Five proxies of possible event deposits including sand layers, marine fauna represented by corals embedded in coarse sands, lagoon shell concentrations, hiatuses and age reversals could be identified in 17 cores from coastal lagoon environments in central Belize.

2. The 8000 year record allows grouping of event deposits from 6000 to 4900, 4200 to 3600 and from 2200 to 1500 cal yr BP. Two events occurred earlier, around 7900 cal yr BP and 7100 cal yr BP. Further events have been dated to around 180 cal yr BP and to modern times.

3. The sand layers and corals have a marine origin and probably represent washover deposits. The shell concentrations presumably reflect periods of lowered salinity, which may have resulted from increased river discharge, associated with hurricane landfalls, or increased salinity after inundation by seawater during storms.

4. Sand layers have been observed in cores from a marsh area, the marginal marine area, the tidal inlet and the backbarrier area of a lagoon, but not in cores from the lagoon basins, suggesting a low preservation potential in the lagoons. The preservation potential of storm deposits depends on physical and biological processes such as bioturbation and tidal flushing. Additionally, deposits of severe, infrequent events are more likely to be preserved because they are thicker, contain coarser clasts and extend more landward.

5. The record displays sediments of certain events on one hand and sediments of time spans that passed between the events on the other hand. Evidence for event deposits that have occurred within short time periods and small events that have happened between severe events may not be stored in the record due to insufficient resolution of the archive. The sensitivity of the study area to overwash deposition has changed over time due to the dynamic nature of coastal environments. There is evidence of single event deposits in coastal environments and a potential influence on the lagoon fauna due to hurricane-induced salinity changes. However, the suitability of the study area for paleohurricane reconstructions is limited, which is indicated by the scarcity of overwash deposits in lagoon basins and the moderate correlation and consistency of identified event deposits among cores and localities.

4.7 Acknowledgements

We are grateful to the Deutsche Forschungsgemeinschaft (Gi222/20) and the Alfons and Gertrud Kassel-Stiftung, who funded this project. We thank Stefan Haber, Malo Jackson, David Geban and Claire Santino for help during fieldwork. Nils Prawitz, Anja Isaack and Lars Klostermann assisted during sample preparation in the home laboratory. Rainer Petschick ran the X-ray diffractometer. Michaela Spiske and an anonymous reviewer whose useful comments helped to improve the manuscript are gratefully acknowledged.

Chapter 5. Conclusions and Outlook

5.1 Conclusions

The comprehensive sedimentological, paleoecological and paleotempestological analysis of 26 sediment cores from five localities along the central Belize coast provides insights into the past 8000 years of Holocene evolution of the coastal environments, changes in species composition during the evolution of lagoon-barrier complexes and allows an evaluation of the suitability of coastal lagoon environments for paleohurricane reconstructions.

1. Sedimentary patterns and radiocarbon dates show that evolution of the coastal lagoons started around 6 kyrs BP, due to marine inundation during Holocene sea-level rise. Facies patterns have been controlled by a variety of processes, including river discharge, lagoon-to-ocean connectivity, longshore currents, wave action, and storm events. The Holocene sediments overlie a stiff bluish-grey Pleistocene soil that exhibits deformation structures in some cores, which can be attributed to liquefaction that may have been triggered by seismic waves of earthquakes.

The main Holocene sediments include (1) mud (often with mangrove roots and mollusk shells), (2) sand, (3) peat/peaty sediment, and (4) transitions among facies types such as silt to fine sand and muddy sand with a grain-size distribution between the mud and the sand facies. The grey mud represents lagoonal background sedimentation. The coarser sediments occur mainly in the peripheral areas of the lagoons, on barriers, bars, barrier spits and washover deposits, and on the shoreface and the beach. XRD identified quartz as the most common mineral. Additional minerals are microcline, albite, andalusite, muscovite, kaolinite, pyrite, aragonite, low-Mg calcite, and high-Mg calcite. Ankerite was only found in concretions in core SL6. No spatial patterns in mineral composition can be recognized among the localities investigated.

The Maya Mountains served as the main supplier of the coastal sediments. Sediment is moved by several processes such as river transport, shore erosion, longshore currents, tides, overwash, and wind. However, there are differences among the localities because of variable geomorphology, lagoon-to-ocean connectivity, antecedent topography, and thus different hydrologic regimes.

Core transects reveal the sediment architecture and facies successions for each locality:

In Manatee Lagoon the up to 4 m thick recovered Pleistocene soil is overlain by Holocene mud, shell concentrations and peaty sediments. The base of Holocene sediments, which marks the beginning of lagoon formation, was dated to 5.3 kyrs BP. Landward, inundation of the Pleistocene surface occurred later.

At Mullins River Beach the base of Holocene sediments was dated to ~7 kyrs BP in the landward core and >8 kyrs BP in more seaward cores. No indications, e.g. shells, were found for the existence of a lagoon during earlier stages of coastal development. The predominantly fine-grained sediments probably have been deposited in a swamp environment. Sand layers, overlain by micaceous planar laminations, of which one can be traced along two cores and which can be correlated by age, were attributed to storm events.

Sediments in Colson Point Lagoon are similar to those obtained from Manatee Lagoon and comprise mainly mud with shell concentrations and peaty sediments. Inundation of the Pleistocene started ~6 kyrs BP in the eastern area and later, ~3.6 kyrs BP to modern, in the western area of the lagoon. Species composition of the shell concentrations in core CP6 indicates retrogradation due to sea-level rise. The irregular relief of the Pleistocene–Holocene boundary is attributed to a ridge and swale morphology that may have resulted from Pleistocene barrier formation.

Mangrove vegetation at Commerce Bight Lagoon started before 5.5 kyrs BP in the backbarrier area and presumably later in central and western areas of the lagoon. Cores from the lagoon contain fine-grained sediments. Compared to Manatee Lagoon and Colson Point Lagoon, shell concentrations are rare and were only observed in one core. Coarse-grained deposits in the most seaward lagoonal core indicate interfingering of lagoonal and barrier sediments and are evidence of overswash. The presence of marine fauna in the backbarrier core and the channel cores also suggests overwash of marine sediments into the lagoon.

The Pleistocene surface of Sapodilla Lagoon was flooded between 6 and 7 kyrs BP. Peats and peaty sediments that overlie the Pleistocene soil indicate mangrove vegetation during early stages of lagoon formation. The lagoonal cores consist of a spatially consistent stratigraphic sequence of peat and mud. The comparatively thick muddy sediments suggest permanent environmental conditions since the flooding. Coarser-grained deposits occur only close to river mouths and tidal inlets where the water energy is higher. Owing to the broad tidal inlet Sapodilla Lagoon is less restricted than the other lagoons and therefore exhibits higher salinities. The mangrove vegetation close to the tidal inlet exists since ˜680 ± 50 cal BP, which is indicated by the occurrence of oysters. Sapodilla Lagoon probably has been formed due to spit progradation. The onset of sandy deposits, which were dated to ~1.6 kyrs BP, marks the initiation of the formation of the narrow southern spit.

Correlation of facies successions between the five localities is difficult due to the heterogeneity and complexity of the coastal environments.

2. Species composition and distribution patterns of mollusk shell concentrations suggest changes in paleoenvironmental conditions during Holocene coastal lagoon evolution. Taxonomic analysis of the mollusk fauna was performed for the 16 lagoonal, one tidal inlet and three marginal marine (shallow subtidal) shell concentrations. Dominant taxa in the lagoons are the

bivalve *A. cuneimeris* and cerithid gastropods, which together account for 78% of the total fauna. Cerithid gastropods comprise largely *C. pliculosa* and *C. eburneum*. Custer analysis allows the distinction of ten assemblages, including seven lagoonal, one tidal inlet and two marginal marine assemblages. The two basal concentrations in core CP6 can be assigned to lagoonal environments, whereas the overlying two concentrations at core top have a marginal marine origin. Proportions of the dominant taxa for each of the lagoonal assemblages A1-A7 are as follows:

A1: *A. cuneimeris* (43%) and *C. eburneum* (30%)

A2: *A. cuneimeris* (67%)

A3: *A. cuneimeris* (25%)

A4: *C. pliculosa* (59%) and *A. cuneimeris* (33%)

A5: *C. pliculosa* (97%)

A6: *A. cuneimeris* (98%)

A7: *A. cuneimeris* (66%) and *C. pliculosa* (21%); only co-occurrence of the two cerithid species *C. pliculosa* and *C. eburneum*

Species richness and diversity exhibit generally lower values for lagoonal samples and higher values for marginal marine/tidal inlet samples. Too few samples were obtained from the marginal marine and tidal inlet environments to define statistically robust assemblages. A8 from the tidal inlet exhibits higher faunal diversity measures and larger shell sizes. Differences in species composition of the marginal marine assemblages A9 and A10 are attributed to varying substrate.

NMDS supports grouping of samples obtained from cluster analysis. Distribution along NMDS axis 1 shows a lagoon/onshore gradient, separating lagoon assemblages from the marginal marine and tidal inlet assemblages. The distribution of assemblages along NMDS axis 2 is based on environmental changes that occurred during the Holocene evolution of the coastal lagoons. Changes in environmental conditions are considered as being related to storm events and changes in geomorphology. Storm events may have caused an increase in salinity in the lagoons due to marine inundation or a decrease in salinity due to increased precipitation. Geomorphological changes are probably related to the development of barriers and spits that separate the lagoon from the sea. The controlling factors of species distribution patterns are difficult to figure out, probably due to the heterogeneity of the barrier-lagoon systems and the interaction of paleoecological and paleoenvironmental factors.

Taphonomic analysis was carried out on 1827 valves of *A. cuneimeris*. Size-frequency distributions, right-left valve ratios and the absence of exotic fauna suggest that the shells are parautochthonous. Lagoonal shell concentrations formed as a result of both biologic and sedimentologic processes. Shells from tidal inlet and marginal marine environments were also

predominantly deposited in their original habitats. No relationship between the core depth and the age of shells and their taphonomic condition was observed.

3. Five different proxies for storm activity, including sand layers, marine fauna, shell concentrations, hiatuses and age reversals were found in 17 sediment cores and were considered as potential event deposits. The sand layers and corals have a marine origin and probably represent washover deposits. In contrast to sand layers, corals, hiatuses and age reversals, which are interpreted to be direct evidences of hurricane impact, the shell concentrations represent indirect evidence of storms. The accumulation of shells presumably reflects changes in paleoenvironmental conditions. Periods of lowered salinity may have resulted from increased river discharge associated with hurricane landfalls. Increased salinity can be explained by seawater inundation after storms. The potential storm deposits accumulate in three periods, from 6000 to 4900, from 4200 to 3600 and from 2200 to 1500 cal yr BP. Two events occurred earlier, around 7900 cal yr BP and 7100 cal yr BP. Further events have been dated to around 180 cal yr BP and to modern times.

Bearing in mind the hurricane frequency of the Belize coast, the hurricane record obtained from the 26 sediment cores is poor. Also, the correlation and consistency of storm deposits is moderate. The suitability of the sites for paleohurricane reconstructions depends on a number of processes. The preservation potential of single event beds can be limited by physical and biological processes such as bioturbation, tidal flushing, amalgamation of discrete event beds, and the lack of material for erosion and deposition after multiple hurricane events or a severe event. The vulnerability of a site to overwash during storm events is dependent on several factors such as geomorphology, the direction and intensity of hurricanes, and the presence of mangrove vegetation. Mangroves, which are able to attenuate storm surges, are common along the Belize coast. Site sensitivity has probably changed over time due to the dynamic nature of coastal environments.

5.2 Outlook

In order to predict future responses to environmental changes it is important to detect changes in depositional environments in the sediment record and to understand the controlling factors. Analysis of further vibracores from other locations along the Belize coast would be interesting for comparison and to support the conclusions drawn in this study. Future studies should concentrate on providing a more detailed chronological framework including extended radiocarbon dating. This would also be helpful to calculate sedimentation rates more precisely. Further analyses may be useful, such as elemental profiles of sediments X-ray fluorescence (XRF) scans for better interpretation of the provenance of lagoon sediments (terrestrial or marine) and to assign them to different coastal processes. Fe, Ti, Cr, Mn, Zn and V have been used as indicators for terrestrial, and S, Cl and Br as indicators for marine origin (McCloskey and Liu

2012). Further radiocarbon dating of shells, especially dating of several shells from one shell concentration, would help to elucidate time averaging within the shell concentrations. For onshore depositional environments optically stimulated luminescence (OSL) dating of quartz may be an additional dating technique, because in these setting shells commonly show signs of reworking. Additional paleohurricane records for the area are needed to identify mechanisms that cause hurricane variability and trends. Records of similar environments would help to reveal the vulnerability of coastal lagoon environments and to test the suitability of these records. Moreover, for improved correlation of paleohurricane records between study sites, uniform methodology for the identification and interpretation of possible storm deposits and their relation to local features as well as the dating methods of storm deposits should be developed. For example, a relatively new method for reconstructing hurricane records from coastal environments uses organic geochemical proxies of $\partial^{15}N$ and $\partial^{13}C$ that are independent of sand layers (Lambert et al. 2008). $\partial^{15}N$ and $\partial^{13}C$ values of organic matter alter due to severe storms. These isotope signatures are indicators of current velocity and duration of storm-driven, fertilizing seawaters (Lambert et al. 2003, 2008; Otvos 2009).

References

Abbott RT (1974) American Seashells. Van Nostrand Reinhold Company, New York

Adomat F, Gischler E (2015) Sedimentary patterns and evolution of coastal environments during the Holocene in central Belize, Central America. Journal of Coastal Research 31: 802-826

Adomat F, Gischler E, Oschmann W (2016) Taxonomic and taphonomic signatures of mollusk shell concentrations from coastal lagoon environments in Belize, Central America. Facies 62(5), 1-2

Aguirre ML, Farinati EA (1999) Taphonomic processes affecting late Quaternary molluscs along the coastal area of Buenos Aires province (Argentina, Southwestern Atlantic). Palaeogeography Palaeoclimatology Palaeoecology 149: 283-304

Alcalá-Herrera JA, Jacob JS, Machain Castillo ML, Neck, RW (1994) Holocene palaeosalinity in a Maya wetland, Belize, inferred from the microfaunal assemblage. Quaternary Research 41: 121-130

Alexandersson ET (1979) Marine maceration of skeletal carbonates in the Skagerrak, North Sea. Sedimentology 26: 845-852

Allen JRL (1982) Spits. In: Schwartz ML (ed) The Encyclopedia of Beaches and Coastal Environments, Hutchinson Ross Publishing, Stroudsburg, Pennsylvania, pp 789-792

Aller RC (1982) Carbonate dissolution in nearshore terrigenous muds: the role of physical and biological reworking. The Journal of Geology 90: 79-95

Ambraseys N (1988) Engineering seismology. Earthquake Engineering and Structural Dynamics 17: 1-105

Andrade C, Freitas MC, Moreno J, Craveiro SC (2004) Stratigraphical evidence of Late Holocene barrier breaching and extreme storms in lagoonal sediments of Ria Formosa, Algarve, Portugal. Marine Geology 210: 339-362.

Anderson LC, McBride RA (1996) Taphonomic and paleoenvironmental evidence of Holocene shell-bed genesis and history on the northeastern Gulf of Mexico shelf. Palaios 11: 532-549

Andrews EA (1935) Shell repair by the snail, Neritina. *Journal of Experimental Zoology* 70: 75-107

Anselmetti FS, Ariztegui D, Brenner M, Hodell D, Rosenmeier MF (2007) Quantification of soil erosion rates related to ancient Maya deforestation. Geology 35: 915-918

Anthony A, Atwood J, August P, Byron C, Cobb S, Foster C, Fry C, Gold A, Hagos K, Heffner L, Kellogg DQ, Lellis-Dibble K, Opaluch JJ, Oviatt C, Pfeiffer-Herbert A, Rohr N, Smith L, Smythe T, Swift J, Vinhateiro N (2009) Coastal lagoons and climate change: ecological and social ramifications in U.S. Atlantic and Gulf coast ecosystems. Ecology and Society 14: 8

Archer AW, Feldman HR (1995) Incised valleys and estuarine facies of the Douglas Group (Virgilian): Implications for similar Pennsylvanian sequences in the U.S. Mid-Continent. In: Hyne NJ (ed) Sequence Stratigraphy of the Mid-Continent, Tulsa Geological Society, pp 119-140

Arkin PA (1982) The relationship between interannual variability in the 200-mb tropical wind field and the Southern Oscillation. Monthly Weather Review 110: 1393-1404

Arruda-Soares H, Schaeffer-Novelli Y, Mandelli J (1982) *Anomalocardia brasiliana* (Gmelin, 1791) bivalve comestível da região do Cardoso, Estado de São Paulo: aspectos biológicos de interesse para a pesca commercial. Bol Inst Pesca 9: 21-38

Bao R, Alonso A, Delgado C, Pages JL (2007) Identification of the main driving mechanisms in the evolution of a small coastal wetland. Palaeogeography Palaeoclimatology Palaeoecology 247: 296-312

Barnes RSK (1980) Coastal lagoons: the natural history of a neglected habitat. Cambridge University Press, Cambridge

Bender MA, Knutson TR, Tuleya RE, Sirutis JJ, Vecchi GA, Garner ST, Held IM (2010) Modeled impact of anthropogenic warming on the frequency of intense Atlantic hurricanes. Science 327: 454-458

Bentley SJ, Sheremet A, Jaeger JM (2006) Event sedimentation, bioturbation, and preserved sedimentary fabric: field and model comparisons in three contrasting marine settings. Continental Shelf Research 26: 2108-2124

Bertran P, Bonnissent D, Imbert D, Lozouet P, Serrand N, Stouvenot C (2004) Paléoclimat de Petites Antilles depuis 4000 ans BP: l'enregistrement de la lagune de Grand-Case à Saint-Martin. Comptes Rendus Geoscience 336: 1501–1510

Besonen MR, Bradley RS, Mudelsee M, Abbott MB, Francus P (2008) A 1,000-year, annually-resolved record of hurricane activity from Boston, Massachusetts. Geophysical Research Letters 35: L14705

Best MMR (2008) Contrast in preservation of bivalve death assemblages in siliciclastic and carbonate tropical shelf settings. Palaios 23: 796-809

Best MMR, Kidwell SM (2000a) Bivalve taphonomy in tropical mixed siliciclastic-carbonate settings. I. Environmental variation in shell condition. Paleobiology 26: 80-102

Best MMR, Kidwell SM (2000b) Bivalve taphonomy in tropical mixed siliciclastic-carbonate settings.II. Effect of bivalve life habits and shell types. Paleobiology 26: 103-115

Best MMR, Ku TCW, Kidwell SM, Walther LM (2007) Carbonate preservation in shallow marine environments: unexpected role of tropical siliciclastics. The Journal of Geology 115: 437-456

Bird ECF (1994) Physical setting and geomorphology of coastal lagoons. In: Kjerfve B (ed.) Coastal lagoon processes, Elsevier Amsterdam, pp 9-39

Boehs G, Absher TM, Cruz-Kaled AC (2000) Composition and distribution of benthic mollusk on intertidal flats of Paranaguá Bay (Paraná, Brazil). Scientia Marina 64: 537-543

Boldt KV, Lane P, Woodruff JD, Donnelly JP (2010) Calibrating a sedimentary record of overwash from Southeastern New England using modeled historic hurricane surges. Marine Geology 275:127–139

Boucot AJ (1953) Life and death assemblages among fossils. American Journal of Science 251: 25-40

Boyd R, Dalrymple R, Zaitlin BA (1992) Classification of clastic coastal depositional environments. Sedimentary Geology 80: 139-150

Brandon CM, Woodruff JD, Lane P, Donnelly JP (2013) Tropical cyclone wind speed constraints from resultant storm surge deposition: A 2500 year reconstruction of hurricane activity from St. Marks, FL. Geochemistry Geophysics Geosystems 14: 2993-3008

Brenner RL, Davies DK (1973) Storm-generated coquinoid sandstone: genesis of high-energy marine sediments from the Upper Jurassic of Wyoming and Montana. Geological Society of America Bulletin 84: 1685-1698

Brett CE, Baird GC (1986) Comarative Taphonomy: A key to paleoenvironmental interpretation based on fossil preservation. Palaios 1: 207-227

Brewster-Wingard GL, Stone JR, Holmes CW (2001) Molluscan faunal distribution in Florida Bay, past and present. An integration of down-core and modern data. Bulletins of American Paleontology 361: 199-231

Brooke B, Ryan D, Pietsch T, Olley J, Douglas G, Packett R, Radke L, Flood P (2008) Influence of climate fluctuations and changes in catchment land use on Late Holocene and modern beach-ridge sedimentation on a tropical macrotidal coast: Keppel Bay, Queensland, Australia. Marine Geology 251: 195-208

Bryant E (2008) Tsunami: The underrated hazard. Springer, Berlin, Heidelberg

Bush AM, Brame RI (2010) Multiple paleoecological controls on the composition of marine fossil assemblages from the Frasnian (Late Devonian) of Virginia, with a comparison of ordination methods. Paleobiology 36:573–591

Callender WR, Staff GM, Parsons-Hubbard KM, Powell EN, Rowe GT, Walker SE, Brett CE, Raymond A, Carlson DD, White S, Heise EA (2002) Taphonomic trends along a fore reef slope: Lee Stocking Island, Bahamas. I. Location and water depth. Palaios 17: 50-65

Chiang JCH, Vimont DJ (2004) Analogous Pacific and Atlantic meridional modes of tropical atmosphere-ocean variability. Journal of Climate 17: 4143-4158

Clarke KR, Warwick RM (2001) Change in marine communities: an approach to statistical analysis and interpretation. Primer-E Ltd, Plymouth

Coch NK (1994) Geologic effects of hurricanes. Geomorphology 10: 37-63

Cohen A (2001) Hurricane tracking with chemistry: exploring the coral archive. Workshop on Atlantic Basin Paleohurricane Reconstructions from High Resolution Records, March 25–27, 2001. University of South Carolina, Columbia, South Carolina.

Collins ES, Scott DB, Gayes PT (1999) Hurricane records on the South Carolina coast: Can they be detected in the sediment record? Quaternary International 56: 15-26f

Cooper JAG (1994) Lagoons and microtidal coasts. In: Carter RWG, Woodroffe CD (eds) Coastal Evolution. Late Quaternary Shoreline Morphodynamics, Cambridge Cambridge University Press, pp 219-265

Covington DJ (1988) Mangrove peats of Belize. Dissertation, A&M University, College Station, Texas

Craig GY, Hallam A (1963) Size-frequency and growth-ring analyses of *Mytilus edulis* and *Cardium edule*, and their palaeoecological significance. Palaeontology 6: 731–750

Craig GY, Oertel G (1966) Deterministic models of living and fossil populations of animals. Quarterly Journal of the Geological Society of London 122: 315-355

Curtis JH, Brenner M, Hodell DA, Balser RA, Islebe GA, Hooghiemstra H (1998) A multi-proxy study of Holocene environmental change in the Maya lowlands of Peten, Guatemala. Journal of Paleolimnology 19: 139-159

Curtis S, Hastenrath S (1995) Forcing of anomalous sea surface temperature evolution in the tropical Atlantic during Pacific warm events. Journal of Geophysical Research 100: 15835-15847

Danielsen F, Sorensen MK, Olwig MF, Selvam V, Parish F, Burgess ND, Hiraishi T, Karunagaran VM, Rasmussen MS, Hansen LB, Quarto A, Suryadiputra N (2005) The Asian tsunami: a protective role for coastal vegetation. Science 310: 643

Dattilo BF, Brett CE, Tsujita CJ, Fairhurst R (2008) Sediment supply versus storm winnowing in the development of muddy and shelly interbeds from the Upper Ordovician of the Cincinnati region, USA. Canadian Journal of Earth Sciences 45: 243-265

D'Avanzo C, Kremer JN (1994) Diel oxygen dynamics and anoxic events in an eutrophic estuary of Waquoit Bay, Massachusetts. Estuaries 17: 131-139

Davies DJ, Powell EN, Stanton RJ Jr (1989) Taphonomic signatures as a function of environmental process: shells and shell beds in a hurricane-influenced inlet on the Texas coast. Palaeogeography Palaeoclimatology Palaeoecology 72: 317-356

DeBeaumont E (1845) Leons de geologie practique. In: Bertrand P (ed.) Septieme Lecon Paris France, pp 223 252

DeFrancesco CG, Hassan GS (2008) Dominance of reworked fossil shells in modern estuarine environments: Implications for paleoenvironmental reconstructions based on biological remains. Palaios 23: 14-23

Denommee KC, Bentley SJ, Droxler AW (2014) Climatic controls on hurricane patterns: a 1200-y near-annual record from Lighthouse Reef, Belize. Scientific Reports 4: 3876

DeWit R (2011) Biodiversity of coastal lagoon ecosystems and their vulnerability to global change. In: Grillo O, Venora G (eds.) Ecosystems Biodiversity, InTech, Rjieka, pp 209-240

Dominey-Howes DTM, Humphreys GS, Hesse PP (2006) Tsunami and paleotsunami depositional signatures and their potential value in understanding the late- Holocene tsunami record. Holocene 16: 1095–1107

Donnelly C, Kraus NC, Larson M (2004) Coastal overwash: Part 1, Overview of processes. Regional Sediment Management Demonstration Program Technical Note, ERDC/RSM-TN-14, U.S. Army Engineer Researcher and Development Center, Vicksburg, MS

Donnelly JP (2005) Evidence of past intense tropical cyclones from backbarrier salt pond sediments: A case study from Isla de Culebrita, Puerto Rico, USA. Journal of Coastal Research 42: 201-210

Donnelly JP, Webb T (2004) Backbarrier sedimentary records of intense hurricane landfalls in the northeastern United States. In: Murnane R, Liu K (eds) Hurricanes and Typhoons: Past Present and Potential, Columbia Press, New York, pp 58-96

Donnelly JP, Woodruff JD (2007) Intense hurricane activity over the past 5,000 years controlled by El Nino and west African monsoon. Nature 447: 465-468

Donnelly JP, Bryant SS, Butler J, Dowling J, Fan L, Hausmann N, Newby P, Shuman B, Stern J, Westover K, Webb T (2001a) 700 yr sedimentary record of intense hurricane landfalls in southern New England. Geological Society of America Bulletin 113: 714–727

Donnelly JP, Roll S, Wengren M, Butler J, Lederer R, Webb T (2001b) Sedimentary evidence of intense hurricane strikes from New Jersey. Geology 29: 615–618

Donnelly JP, Butler J, Roll S, Wengren M, Webb T (2004) A backbarrier overwash record of intense storms from Brigantine, New Jersey. Marine Geology 210: 107-121

Donnelly JP, Hawkes AD, Lane P, MacDonald D, Shuman BN, Toomey MR, van Hengstum PJ, Woodruff J D (2015) Climate forcing of unprecedented intense-hurricane activity in the last 2000 years. Earth's Future 3: 1-17

Ekdale AA (1974) Marine molluscs from shallow-water environments (0 to 60 meters) off the northeast Yucatán coast, Mexico. Bulletin of Marine Science 24: 638-668

Ekdale AA (1977) Quantitative paleoecological aspects of modern marine mollusk distribution, northeast Yucatán coast, Mexico. In: Frost SH, Weiss MP, Saunders JB (eds) Reefs and related carbonates: ecology and sedimentology. American Association of Petroleum Geologists, Studies in Geology 4: 195–207

El-Ashry MT, Wanless HR (1965) Birth and early growth of a tidal delta. Journal of Geology 73: 404-406

Elsner JB, Kossin JP, Jagger TH (2008) The increasing intensity of the strongest tropical cyclones. Nature 455: 92-95

Emanuel K (2005) Increasing destructiveness of tropical cyclones over the past 30 years. Nature 436: 686-689

Emanuel K, Sundararajan R, Williams J (2008) Hurricanes and global warming: Results from downscaling IPCC AR4 simulations. Bulletin of the American Meteorological Society 89: 347-367

Esker D, Eberli GP, McNeill D (1998) The structural and sedimentological controls on the reoccupation of Quaternary incised valleys, Belize Southern Lagoon. American Association of Petroleum Geologists Bulletin 82: 2075–2109

Evan AT, Vimont DJ, Heidinger AK, Kossin JP, Bennartz R (2009) The role of aerosols in the evolution of tropical North Atlantic Ocean temperature anomalies. Science 324: 778–781

Fagerstrom JA (1964) Fossil communities in paleoecology: their recognition and significance. American Association of Petroleum Geologists 75: 1197–1216

Fasham M JR (1977) A comparison of nonmetric multidimensional scaling, principal components analysis and reciprocal averaging for the ordination of simulated coenoclines and coenoplanes. Ecology 58: 551-561

Ferm JC, Milici RC, Eason JE (1972) Carboniferous depositional environments in the Cumberland Plateau of Southern Tennessee and Northern Alabama. Geological Society of America, Southeast Section, Field Guide

Ferro C, Droxler AW, Anderson JB, Mucciarone D (1999) Late Quaternary shift of mixed siliciclastic-carbonate environments induced by glacial eustatic sea-level fluctuations in Belize. In: Harris PM, Saller AH, Simo JA (eds) Advances in carbonate sequence stratigraphy: application to reservoirs, outcrops and models, SEPM Special Publications 63, pp 385-411

Fisher JJ (1967) Origin of barrier island chain shorelines, Middle Atlantic states. Geological Society of America Special Papers 115: 66-67

Fisher JJ (1968) Barrier island formation: Discussion. Geological Society of America Bulletin 79: 1421-1426

FitzGerald DM (2005) Tidal inlets. In: Schwartz M (ed) Encyclopedia of Coastal Science, Springer Dordrecht, pp 958-964

Flügel E (2004) Microfacies of carbonate rocks: Analysis, Interpretation and Application. Springer, Berlin, Heidelberg

Fornari M, Giannini PCF, Nascimento DR Jr (2012) Facies associations and controls on the evolution from a coastal bay to a lagoon system, Santa Catarina Coast, Brazil. Marine Geology 323-325: 56-68

Frappier AB, Sahagian D, Carpenter SJ, González LA, Frappier BR (2007) Stalagmite stable isotope record of recent tropical cyclone events. Geology 35: 111–114

Freitas MC, Andrade C, Cruces A (2002) The geological record of environmental changes in southwestern Portuguese coastal lagoons since the Lateglacial. Quaternary International 93-94: 161-170

Freitas MC, Andrade C, Rocha F, Tassinari C, Munhá JM, Cruces A, Vidinha J, da Silva CM (2003) Lateglacial and Holocene environmental changes in Portuguese coastal lagoons 1. The sedimentological and geochemical records of the Santo André coastal area. The Holocene, 13: 433-446

Fornari M, Giannini PCF, Nascimento DR Jr (2012) Facies associations and controls on the evolution from a coastal bay to a lagoon system, Santa Catarina Coast, Brazil. Marine Geology 323-325: 56-68

Fürsich FT (1990) Fossil concentrations and life and death assemblages. In: Briggs DEG, Cowther PR (eds) Palaeobiology: A Synthesis, Blackwell Scientific Publications, Oxford, pp 235-239

Fürsich FT (1994) Paleoecology and evolution of Mesozoic salinity-controlled benthic macroinvertebrate associations. Lethaia 26: 327-346

Fürsich FT (1995) Shell concentrations. Eclogae Geologicae Helvetiae 88: 643-655

Fürsich FT, Flessa KW (1987) Taphonomy of tidal flat molluscs in the northern Gulf of California: Paleoenvironmental analysis despite the perils of preservation. Palaios 2: 543-559

Fürsich FT, Oschmann W (1993) Shell beds as tools in basin analysis: the Jurassic of Kachchh, western India. Journal of the Geological Society of London 150: 169-185

Galli P (2000) New empirical relationships between magnitude and distance for liquefaction. Tectonophysics 324: 169-187

Gelfenbaum G, Jaffe B (2003) Erosion and Sedimentation from the 17 July, 1998 Papua New

Guinea Tsunami. Pure and Applied Geophysics 160: 1969–1999

Giannini A, Kushnir Y, Cane MA (2000) Interannual variability of Caribbean rainfall, ENSO, and the Atlantic Ocean. Journal of Climate 13: 297–311

Gilbert GK (1885) The topographic features of lake shore. Fifth Annual Report US Geological Survey: 69-123

Gilbert GK (1890) Lake Bonneville US Geological Survey, Monograph I

Gillett NP, Stott PA, Santer BD (2008) Attribution of cyclogenesis region sea surface temperature change to anthropogenic influence. Geophysical Research Letters 35: L09707

Gischler E (1994) Sedimentation on three Caribbean atolls: Glovers Reef, Lighthouse Reef and Turneffe Islands, Belize. Facies 31: 243-254

Gischler E (2002) Holocene lagoonal development in isolated carbonate platforms of Belize. Sedimentary Geology 159: 113-132

Gischler E (2006) Comment on "Corrected western Atlantic sea-level curve for the last 11,000 years based on calibrated ^{14}C dates from *Acropora palmata* framework and intertidal mangrove peat" by Toscano and Macintyre, Coral Reefs 22, 257-270 (2003), and their response in Coral Reefs 24: 187-190 (2005). Coral Reefs 25: 273-279

Gischler E (2007) Pleistocene facies of Belize barrier and atoll reefs. Facies 53: 27-41

Gischler E (2008) Accretion patterns in Holocene tropical coral reefs: do massive coral reefs with slowly growing corals accrete faster than branched coral (acroporid) reefs with rapidly growing corals? International Journal of Earth Sciences 97: 851-859.

Gischler E, Ginsburg RN (1996) Cavity dwellers (coelobites) under rubble in southern Belize barrier and atoll reefs. Bulletin of Marine Science 58: 570-589

Gischler E, Hudson JH (2004) Holocene development of the Belize Barrier Reef. Sedimentary Geology 164: 223–236

Gischler E, Storz D (2009) High-resolution windows into Holocene climate using proxy data from Belize corals (Central America). Palaeobiodiversity and Palaeoenvironments 89: 211-221

Gischler E, Hudson JH, Storz D (2009) Growth of Pleistocene massive corals in south Florida: low skeletal extension rates and possible ENSO, decadal, and multi-decadal cyclicities. Coral Reefs 28: 823–830

Gischler E, Shinn EA, Oschmann W, Fiebig J, Buster NA (2008) A 1,500 year Holocene Caribbean climate archive from the Blue Hole, Lighthouse Reef, Belize. Journal of Coastal Research 24: 1495-1505

Gischler E, Ginsburg RN, Herrle JO, Prasad S (2010) Mixed carbonates and siliciclastics in the Quaternary of southern Belize: Pleistocene turning points in reef development controlled by sea-level change. Sedimentology 57: 1046-1068

Gischler E, Anselmetti FS, Shinn EA (2013) Seismic stratigraphy of the Blue Hole (Lighthouse Reef, Belize), a late Holocene climate and storm archive. Marine Geology 344: 155-162

Goff JR, Chague-Goff C, Nichol S (2001) Palaeotsunami deposits: a New Zealand perspective. Sedimentary Geology 143: 1-6

Goff JR, McFadgen BG, Chague-Goff C (2004) Sedimentary differences between the 2002 Easter storm and the 15thcentury Okoropunga tsunami, southeastern North Island, New Zealand. Marine Geology 204: 235–250

Goldenberg SB, Shapiro LJ (1996) Physical mechanisms for the association of El Niño and West African rainfall with Atlantic major hurricane activity. Journal of Climate 9: 1169-1187

Goldenberg SB, Landsea CW, Mestas-Nuñez AM, Gray WM (2001) The recent increase in Atlantic hurricane activity: Causes and implications. Science 293: 474–479

González-Villanueva R, Pérez-Arlucea M, Alejo I, Goble R (2009) Climatic-related factors

controlling the sedimentary architecture of a barrier-bagoon complex in the context of the Holocene transgression. In: da Silva CP (ed) Proceedings of the 2009 International Coastal Symposium (ICS), Journal of Coastal Research, Special Issue 56, pp 627-631

Gray WM (1984) Atlantic seasonal hurricane frequency. Part I: El Niño and 30 mb quasibiennial oscillation influences. Monthly Weather Review 112: 1649–1668

Halley RB, Shinn EA, Hudson JH, Lidz B (1977) Recent and relict topography of Boo Bee Patch Reef, Belize. Proceedings of the Third International Coral Reef Symposium 2: 29-35

Hammer Ø, Harper DAT (2006) Paleontological Data Analysis. Blackwell, Malden, Oxford, Carlton

Hammer Ø, Harper DAT, Paul DR (2001) PAST: Paleontological Statistics Software Package for education and data analysis. Palaeontologica Electronica 4: 4–9, 178 kb

Harris PT, Heap AD (2003) Environmental management of clastic coastal depositional environments: inferences from an Australian geomorphic database: Ocean and Coastal Management 46: 457-478

Haug GH, Hughen KA, Sigman DM, Peterson LC, Röhl U (2001) Southward migration of the intertropical convergence zone through the Holocene. Science 293: 1304-1308

Haug GH, Gunther D, Peterson LC, Sigman DM, Hughen KA, Aeschlimann B (2003) Climate and the collapse of Maya civilization. Science 299: 1731-1735

Hauser I, Oschmann W, Gischler E (2007) Modern bivalve shell assemblages on three atolls offshore Belize (Central America, Caribbean Sea). Facies 53: 451-478

Hauser I, Oschmann W, Gischler E (2008) Taphonomic signatures on modern Caribbean bivalve shells as indicators of environmental conditions (Belize, Central America). Palaios 23: 586-600

Hawkes AD, Horton BP (2012) Sedimentary record of storm deposits from Hurricane Ike, Galveston and San Luis Islands, Texas. Geomorphology 171–172: 180–189

Hayes MO (1967) Hurricanes as geological agents: case studies of Hurricanes Carla, 1961, and Cindy, 1963. Bureau of Economic Geology Report of Investigation 61: 1–54

Hayes MO (1979) Barrier island morphology as a function of tidal and wave regime. In: Leatherman SP (ed) Barrier Islands, Academic Press, New York pp 1-27

Hayes MO, FitzGerald DM (2013) Origin, Evolution, and Classification of Tidal Inlets. Journal of Coastal Research, Special Issue: 14-33

Hayes MO, Kana T (1976) Terrigenous clastic depositional environments. Technical Report 11 - CRD, Department of Geology, University of South Carolina, Columbia, SC

Hemphill-Haley E (1996) Diatoms as an aid in identifying late-Holocne tsunami deposits. Holocene 6: 439-448

Hennessy JT, Zarillo GA (1987) The interrelation and distinction between flood-tidal delta and washover deposits in a transgressive barrier island. Marine Geology 78: 35–56

Hetzinger S, Pfeiffer M, Dullo W-C, Keenlyside N, Latif M, Zinke J (2008) Caribbean coral tracks Atlantic multidecadal oscillation and past hurricane activity. Geology 36: 11-14

High LR Jr (1966) Recent coastal sediments of British Honduras. Dissertation, Rice University, Houston

High LR Jr (1969) Storms and sedimentary processes along the northern British Honduras coast. Journal of Sedimentary Petrology 39: 235-245

High LR Jr (1975) Geomorphology and sedimentology of Holocene coastal deposits, Belize. In: Wantland KF, Pusey WC (eds) Belize shelf-carbonate sediments, clastic sediments, and ecology, American Association of Petroleum Geologists, Studies in Geology 2, pp 53–96

Hippensteel SP (2010) Paleotempestology and the Pursuit of the Perfect Paleostorm Proxy. GSA Today 20: 52-53

Hippensteel SP (2011) Spatio-lateral continuity of storm overwash deposits in back barrier marshes. Geological Society of America Bulletin 123: 2277-2294

Hippensteel SP, Garcia WJ (2014) Micropaleontological Evidence of Prehistoric Hurricane Strikes from Southeastern North Carolina. Journal of Coastal Research 30: 1157-1172

Hippensteel SP, Martin RE (1999) Foraminifera as an indicator of overwash deposits, barrier island sediment supply, and barrier island evolution: Folly Island, South Carolina. Palaeogeography Palaeoclimatology Palaeoecology 149: 115–125

Hippensteel SP, Eastin MD, Garcia WJ (2013) The geological legacy of Hurricane Irene: Implications for the fidelity of the paleo-storm record. GSA Today 23: 4-10

Hodell DA, Brenner M, Curtis JH (2005) Terminal Classic drought in the northern Maya Lowlands inferred from multiple sediment cores in Lake Chichancanab (Mexico). Quaternary Science Reviews 24: 1413-1427

Hoese HD (1960) Biotic changes in a bay associated with the end of a drought. Limnology and Oceanography 5: 326-336

Holland GJ, Webster PJ (2007) Changes in tropical cyclone number, duration, and intensity in a warming environment. Philos. Trans. R. Soc 365: 454-458

Hoyos CD, Agudelo PA, Webster PJ, Curry JA (2006) Deconvolution of the factors contributing to the increase in global hurricane intensity. Science 312: 94-97

Hoyt JH (1967) Barrier island formation Geological Society of America Bulletin: 78: 1125-1136

Hubbert G, McInnes K (1999) A storm surge inundation model for coastal planning and impact studies. Journal of Coastal Research 15: 168-185

Hurricane Database (HURDAT) (2014) Hurricane Research Division. National Oceanic and Atmospheric Administration. Re-analysis Project. Data (http://www.aoml. noaa. gov/hrd/ hurdat/Data_Storm.html)

Jacob JS, Hallmark CT (1996) Holocene stratigraphy of Cobweb Swamp, a Maya wetland in northern Belize. Geological Society of America Bulletin 108: 883-891

Jaffe BE, Morton RA, Kortekaas S, Dawson AG, Smith DE, Gelfenbaum G, Foster IDL, Long D, Shi S (2008) Reply to Bridge (2008) Discussion of articles in “Sedimentary features of tsunami deposits”. Sedimentary Geology 211: 95-97

Jagodziński R, Sternal B, Szczuciński W, Lorenc S (2009) Heavy minerals in 2004 tsunami deposits on Kho Khao Island, Thailand. Polish Journal of Environmental Studies 18: 103–110

James NP, Ginsburg RN (1979) The geological setting of Belize reefs. In: James NP, Ginsburg RN (eds) The seaward margin of Belize barrier and atoll reefs, Special Publication 3, International Association of Sedimentologists. Blackwell Scientific Publications, Oxford, London, pp 1-15

Jarvinen BJ, Neumann CJ (1985) An evaluation of the SLOSH storm surge model. Bulletin of the American Meteorological Society 66: 1408-1411

Johnson RG (1960) Models and methods for analysis of the mode of formation of fossil assemblages. Geological Society of America Bulletin 71: 1075-1086

Kahn JH, Roberts HH (1982) Variations in storm response along a microtidal transgressive barrier island arc. Sedimentary Geology 33: 129–146

Kathiresan K, Rajendran N (2005) Coastal mangrove forests mitigated tsunami. Estuarine Coastal and Shelf Science 65: 601–606

Keen TR, Bentley SJ, Vaughan WC, Blain CA (2004) The generation and preservation of multiple hurricane beds in the northern Gulf of Mexico. Mar Geol 210: 79-105

Keen TR, Slingerland RL, Bentley SJ, Furukawa Y, Teague WJ, Dykes JD (2012) Sediment transport on continental shelves: storm bed formation and preservation in heterogeneous sediments. In: Li MZ, Sherwood CR, Hill PR (eds) Sediments, Morphology and Sedimentary

Processes on Continental Shelves: Advances in Technologies, Research, and Applications, International Association of Sedimentologists, Special Publications 44, pp 295–310

Kelletat D (2005) Holocene coastal geomorphology. In: Schwartz M (ed) Encyclopedia of Coastal Science, Springer, Dordrecht, pp 527-528

Kelletat D, Scheffers A, Scheffers A (2004) Holocene tsunami deposits on the Bahaman islands of Long Island and Eleuthera. Zeitschrift für Geomorphologie 48: 519-540

Kennett DJ, Breitenbach SFM, Aquino VV, Asmerom Y, Awe J, Baldini UL, Bartlein P, Culleton BJ, Ebert C, Jazwa C, Macri MJ, Marwan N, Polyak V, Prufer KM, Ridley HE, Sodemann H, Winterhalder B, Haug G (2012) Development and disintegration of Maya political systems in response to climate change. Science 338: 788-791

Kennish MJ, Paerl HW (2010) Coastal Lagoons: Critical Habitats of Environmental Change. Chapter 1. In: Kennish M, Paerl H (eds.) Coastal Lagoons: Critical Habitats of Environmental Change, CRC Press, Boca Raton, pp 1-16

Kiage LM, Deocampo D, McCloskey TA, Bianchette TA, Hursey M (2011) A1900-year paleohurricane record from Wassaw Island, Georgia, USA. Journal of Quaternary Science 26: 714-722

Kidwell SM (1985) Palaeobiological and sedimentological implications of concentrations. Nature 318: 457-460

Kidwell SM (1991) The stratigraphy of concentrations. In: Allison PA, Briggs DEG (eds.) Taphonomy: Releasing the data locked in the fossil record, Plenum Press, New York, pp 211-290

Kidwell SM (2001) Ecological fidelity of molluscan death assemblages. In: Aller JY, Woodin SA, Aller RC (eds) Organism-sediment interactions, University of South Carolina Press, Columbia, pp 199-221

Kidwell SM (2002) The stratigraphy of skeletal concentrations: Testing for broad-scale trends. In: DeRenzi M, Pardo Alonso MV, Belinchón M, Peñalver E, Montoya P, Márques-Aliaga A (eds) Current topics on taphonomy and fossilization, Ayuntamiento de Valencia, Valencia, pp 179-186

Kidwell SM (2013) Time-averaging and fidelity of modern death assemblages: Building a taphonomic foundation for conservation palaeobiology. Palaeontology 56: 487-522

Kidwell SM, Aigner T (1985) Sedimentary dynamics of complex shell beds: Implications for ecologic and evolutionary patterns. In: Bayer U, Seilacher A (eds) Sedimentary and Evolutionary Cycles, Springer, Berlin, pp 382-395

Kidwell SM, Bosence DWJ (1991) Taphonomy and time-averaging of marine shelly faunas. In: Allison PA, Briggs DEG (eds) Taphonomy: Releasing the data locked in the fossil record, Plenum Press, New York, pp 115-210

Kidwell SM, Holland SM (1991) Field description of coarse bioclastic fabrics. Palaios 6: 426-434

Kidwell SM, Best MMR, Kaufman DS (2005) Taphonomic trade-offs in tropical marine death assemblages: Differential time averaging, shell loss, and probable bias in siliciclastic vs. carbonate facies. Geology 33: 729-732

Kidwell SM, Fürsich FT, Aigner T (1986) Conceptual framework for the analysis and classification of fossil cencentrations. Palaios 1: 228-238

Kjerfve B (1994) Coastal lagoon processes. In: Kjerfve B (ed.) Coastal lagoon processes, Elsevier Amsterdam, pp 1-8

Kjerfve B, Ruetzler K, Kierspe GH (1982) Tides at Carrie Bow Cay, Belize. Smithsonian Contributions to the Marine Sciences 12: 47-52

Knutson TR, McBride JL, Chan J, Emanuel K, Holland G, Landsea C, Held I, Kossin JP, Srivastava AK, Sugi M (2010) Tropical cyclones and climate change. Nature Geoscience 3: 157–163

Kortekaas S, Dawson AG (2007) Distinguishing tsunami and storm deposits: An example from Martinhal, SW Portugal. Sed Geol 200: 208-221

Kotzian CB, Simões MG (2006) Taphonomy of recent freshwater molluscan death assemblages, Touro Passo Stream, Southern Brazil. Revista Brasileira de Paleontologia 9: 243-260

Kowalewski M (1997) The reciprocal taphonomic model. Lethaia 30: 86-88

Kowalewski M, Bambach RK (2003) The limits of paleontological resolution. In: Harries PJ (ed) Approaches in High-Resolution Stratigraphic Paleontology, Kluwer Academic/Plenum Publishers, New York, pp 1-48

Kowalewski M, Carroll M, Casazza L, Gupta NS, Hannisdal B, Hendy A, Krause RA, LaBarbera M, Lazo DG, Messina C, Puchalski S, Rothfus TA, Salgeback J, Stempein J, Terry AC, Tomašových A (2003) Quantitative fidelity of brachipod-mollusk assemblages from modern subtidal environments of San Juan Islands, USA. Journal of Taphonomy 1: 43-65

Kossin JP, Vimont DJ (2007) A more general framework for understanding Atlantic hurricane variability and trends. Bulletin of the American Meteorological Society 88: 1767-1781

Kristensen E (2008) Mangrove crabs as ecosystem engineers; with emphasis on sediment processes. Journal of Sea Research 59: 30-43

Krueger WC Jr (1963) Mineralogical composition and textural properties of river sediments from British Honduras. Dissertation, Rice University, Houston

Kruskal JB (1964a) Multidimensional scaling by optimizing goodness of fit to a nonmetric hypothesis. Psychometrika 29: 1- 27

Kruskal JB (1964b) Nonmetric multidimensional scaling: a numerical method. Psychometrika 29: 115-129

Lander JF, Whiteside LS, Lockridge PA (2002) A brief history of tsunamis in the Caribbean Sea. Science of Tsunami Hazards 20: 57-94

Landsea CW, Pielke RA Jr, Mestas-Nuñez AM, Knaff JA (1999) Atlantic basin hurricanes: Indices of climatic changes. Climate Change 42: 89-129

Landsea CW, Vecchi GA, Bengtsson L, Knutson TR (2010) Impact of Duration Thresholds on Atlantic Tropical Cyclone Counts. Journal of Climate 23: 2508-2519

Lambert WJ, Aharon P, Rodriguez AB (2003) An assessment of the Late Holocene record of severe storm impacts from Lake Shelby, Alabama. Gulf Coast Association of Geological Societies Transactions 53: 443–452

Lambert WJ, Aharon P, Rodriguez AB (2008) Catastrophic hurricane history revealed by organic geochemical proxies in coastal lake sediments: a case study of Lake Shelby, Alabama (USA). Journal of Paleolimnology 39: 117-131

Lane P, Donnelly JP, Woodruffe JD, Hawkes AD (2011) A decadally-resolved paleohurricane record archived in the late Holocene sediments of a Florida sinkhole. Marine Geology 287: 14-30

Lanesky DE, Logan BW, Brown RG, Hine AC (1979) A new approach to portable vibracoring underwater and on land. Journal of Sedimentary Petrology 49: 654-657

Lara ME (1993) Divergent wrench faulting in the Belize southern lagoon: implications for Tertiary Caribbean plate movements and Quaternary reef distribution. American Association of Petroleum Geologists Bulletin 77: 1041-1063

Leyden BW (1987) Late Quaternary aridity in the Lake Valencia Basin (Venezuela) – reply. Ecology 68: 1553-1555

Li X (1994) A 6200-year environmental history of the Pearl River Marsh, Louisiana. Dissertation, Louisiana State University

Li C, Weeks E, Rego J (2009) In situ measurements of saltwater flux through tidal passes of Lake Pontchartrain estuary by Hurricanes Gustav and Ike in September 2008. Geophysical

Research Letters 36: L19609

Lighty RG, Macintyre IG, Stuckenrath R (1982) Acropora palmata reef framework: a reliable indicator of sea-level in the western Atlantic for the past 10,000 years. Coral Reefs 1: 125-130

Liu H, Zhang K, Li Y, Xie L (2013) Numerical study of the sensitivity of mangroves in reducing storm surge and flooding to hurricane characteristics in southern Florida. Cont Shelf Res 64: 51-65

Liu K-B (2004) Paleotempestology: Principles, methods, and examples from Gulf coast lake-sediments. In: Murnane R, Liu K (eds) Hurricanes and Typhoons: Past Present and Potential, Columbia Press, New York, pp 13-57

Liu K-B, Fearn ML (1993) Lake-sediment record of late Holocene hurricane activities from coastal Alabama. Geology 21: 793-796

Liu K-B, Fearn ML (2000a) Reconstruction of prehistoric landfall frequencies of catastrophic hurricanes in northwestern Florida from lake sediment records. Quaternary Research 54: 238-245

Liu K-B, Fearn ML (2000b). Holocene history of catastrophic hurricane landfalls along the Gulf of Mexico coast reconstructed from coastal lake and marsh sediments. In: Ning ZH, Abdollahi KK (eds) Current stresses and potential vulnerabilities: Implications of Global Change for the Gulf Coast Region of the United States, Gulf Coast Regional Climate Change Council. Franklin Press, Baton Rouge, pp 38-47

Liu K-B, Li C, Bianchette TA, McCloskey TA, Yao Q, Weeks E (2011) Storm deposition in a coastal backbarrier lake in Louisiana caused by hurricanes Gustav and Ike. Journal of Coastal Research, Special Issue 64: 1866-1870

Liu K-B, Lu H, Shen C (2003) Assessing the vulnerability of the Alabama Gulf coast to intense hurricane strikes and forest fires in the light of long-term climatic changes. In: Ning ZH, Turner RE, Doyle T, Abdollahi K (eds) Integrated assessment of the consequences of climate change for the Gulf Coast region, Environmental Protection Agency, Baton Rouge, pp 223-230

Lough JM (2007) Tropical river flow and rainfall reconstructions from coral luminescence: Great Barrier Reef, Australia. Paleoceanography 22: 2218-2234

Macintyre IG, Littler MM, Littler DS (1995) Holocene history of Tobacco Range, Belize, Central America. Atoll Research Bulletin 430 1-18

Macintyre IG, Toscano MA, Lighty RG, Bond GB (2004) Holocene history of the mangrove islands of Twin Cays, Belize, Central America. Atoll Research Bulletin 510: 1-16

Malaizé B, Bertran P, Carbonel P, Bonnissent D, Charlier K, Galop D, Limbert D, Serrand N, Stouvenot C, Pujol C (2011) Hurricanes in the Caribbean during the past 3700 years BP. Holocene 21: 911-924

Malmquist DL (1997) Oxygen isotopes in cave stalagmites as a proxy record of past tropical cyclone activity. In: 22nd Conference on Hurricanes and Tropical Meteorology. American Meteorological Society: 393-394

Mandic O, Harzhauser M, Spezzaferri S, Zuschin M (2002) The paleoenvironment of an early Middle Miocene Paratethys sequence in NE Austria with special emphasis on paleoecology of mollusks and foraminifera. Geobios 24: 193-206

Mann ME, Emanuel K (2006) Atlantic hurricane trends linked to climate change. Eos 87: 233-241

Mann ME, Woodruff JD, Donnelly JP, Zhang Z (2009) Atlantic hurricanes and climate over the past 1,500 years. Nature 460: 880-885

Margalef DR (1958) Information theory in ecology. International Journal of General Systems 3: 36-71

Martin L, Dominguez JM (1994) Geological history of coastal lagoons. In: Kjerfv B (ed) Coastal lagoon processes, Elsevier, Amsterdam, pp 41-68

Martin RE (1993) Time and taphonomy: actualistic evidence for time-averaging of benthic foraminiferal assemblages. In: Kidwell SM, Behrensmeyer AK (eds) Taphonomic Approaches to Time Resolution in Fossil Assemblages, Paleontological Society, Short Course in Paleontology 6, pp 34-56

Martin RE (2000) Environmental Micropaleontology: The Application of Microfossils to Environmental Geology. Kluwer Press, New York

Masselink G, Hughes MG, Knight J (2011) Introduction to coastal processes and geomorphology. Taylor & Francis, New York

McCloskey TA, Keller G (2009) 5000 year sedimentary record of hurricane strikes on the central coast of Belize. Quaternary International 195: 53-68

McCloskey TA, Liu K-B (2012) A 7000 year record of paleohurricane activity from a coastal wetland in Belize. The Holocene 23: 278-291

McGee WJ (1890) Enchroachment of the sea. The Forum 9: 437-449

McIvor AL, Möller I, Spencer T, Spalding M (2012) Reduction and wind and swell waves by mangroves. NCP Report 1. Cambridge Coastal Research Unit Working Paper 40: 1-27

Medina-Gómez I, Herrera-Silveira JA (2003) Spatial characterization of water quality in a karstic coastal lagoon without anthropogenic disturbance: a multivariate approach. Estuarine Coastal and Shelf Science 58: 455-465

Miller AI, Llewellyn G, Parsons KM, Cummins H, Boardman MR, Greenstein BJ, Jacobs DK (1992) Effect of hurricane Hugo on molluscan skeletal distributions, Salt River Bay, St. Croix, U.S. Virgin Islands. Geology 20: 23-26

Miller DL, Mora CI, Grissino-Mayer HD, Mock CJ, Uhle ME, Sharp Z (2006) Tree-ring isotope records of tropical cyclone activity. Proceedings of the National Academy of Sciences of theUnited States of America 103: 14294-14297

Milliman JD (1974) Marine carbonates. Springer, New York

Monacci NM, Meier-Grünhagen U, Finney BP, Behling H, Wooller MJ (2009) Mangrove ecosystem changes during the Holocene at Spanish Lookout Cay, Belize. Palaeogeography Palaeoclimatology Palaeoecology 280: 37-46

Monacci NM, Meier-Grunhagen U, Finney BP, Behling H, Wooller MJ (2011) Paleoecology of mangroves along the Sibun River, Belize. Quaternary Research 76: 220-228

Montaggioni L, Braithwaite CJR (2009) Quaternary Coral Reef Systems. Developments in Marine Geology 5. Elsevier, Amsterdam

Morton RA (2002) Factors controlling storm impacts on coastal barriers and beaches-a preliminary basis for near real-time forecasting. Journal of Coastal Research 18: 486-501

Morton RA, Gelfenbaum G, Jaffe BJ (2007) Physical criteria for distinguishing sandy tsunami and storm deposits using modern examples. Sedimentary Geology 200: 184-207

Morton RA, Richmond BM, Jaffe BE, Gelfenbaum G (2008) Coarse-clast ridge complexes of the Caribbean: a preliminary basis for distinguishing tsunami and storm-wave origins. Journal of Sedimentary Research 78: 624-637

Morton RA, Ward GH, White WA (2000) Rates of sediment supply and sea-level rise in a large coastal lagoon. Marine Geology 167: 261-284

Müller G (1967) Methods in sedimentary petrology. Part 1. Schweizerbart, Stuttgart

Murnane RJ (2004) Introduction. In: Murnane RJ, Liu K-B (eds) Hurricanes and Typhoons: Past Present and Potential, Columbia Press, New York, pp 1-10

National Oceanic and Atmospheric Administration (NOAA) (2014) National Hurricane Center. NHC Data Archive. Past Track Seasonal Maps. Atlantic Basin (http://www.nhc.noaa.gov/data/)

National Oceanic and Atmospheric Administration (NOAA) (2014) National Hurricane Center.

Saffir-Simpson Hurricane Wind Scale (http://www.nhc.noaa.gov/aboutsshws.php)

Nichols MM (1989) Sediment accumulation rates and relative sea-level rise in lagoons. Marine Geology 88: 201-219

Nichols MM, Allen G (1981) Sedimentary processes in coastal lagoons. Coastal lagoon research, present and future. UNESCO Technical Papers in Marine Science 33: 27-80

Nichols MM, Boon JD (1994) Sediment transport processes in coastal lagoons. In: Kjerfve B (ed) Coastal lagoon processes, Elsevier, Amsterdam, pp 157-219

Nobre P, Shukla J (1996) Variations of sea surface temperature, wind stress, and rainfall over the tropical Atlantic and South America. Journal of Climate 9: 2464–2479

Noren AJ, Bierman PR, Steig EJ, Lini A, Southon J (2002) Millennial-scale storminess variability in the northeastern United States during the Holocene epoch. Nature 419(6909): 821-824

Nott J (2004) Palaeotempestology: The study of prehistoric tropical cyclones– a review and implications for hazard assessment. Environment International 30: 433-447

Nott J (2011) A 6000 year tropical cyclone record from Western Australia. Quaternary Science Reviews 30: 713–722

Nott J, Hayne M (2001) High frequency of 'supercyclones' along the Great Barrier Reef over the past 5,000 years. Nature 413: 508–512

Nott J, Haig J, Neil H, Gillieson D (2007) Greater frequency variability of landfalling tropical cyclones at centennial compared to seasonal and decadal scales. Earth and Planetary Science Letters 255: 367–372

Nott J, Smithers S, Walsh K, Rhodes E (2009) Sand beach ridges record 6000 year history of extreme tropical cyclone activity in northeastern Australia. Quaternary Science Reviews 28: 1511-1520

Nummedal D, Penland S, Gerdes R, Schramm W, Kahn J, Roberts H (1980) Geologic response to hurricane impact on low-profile Gulf Coast Barriers. Transactions Gulf Coast Association of Geological Societies 30: 183-195

Nyberg J, Malmgren BA, Winter A, Jury MR, Kilbourne KH, Quinn TM (2007) Low Atlantic hurricane activity in the 1970s and 1980s compared to the past 270 years. Nature 447: 698-701

Oertel GF (1985) The barrier island system. Marine Geology 63: 1-18

Oertel GF (2005) Coastal lakes and lagoons. In: Schwartz M (ed) Encyclopedia of coastal science, Springer, Dordrecht, pp 263-265

Oertel GF, Kraft JC, Kearney MS, Woo HJ (1992) A rational theory for barrier-lagoon development. In: Fletcher CH, Wehmiller JF (eds) Quaternary Coasts of the United States, SEPM (Society for Sedimentary Geology) *48,* Tulsa, pp 77–87

O´Loughlin KF, Lander JF (2003) Caribbean tsunamis. A 500 year history from 1498-1998. Advances in Natural and Technological Hazards Research, Kluwer Academic Publishers, Dordrecht

Oschmann W (1993) Environmental oxygen fluctuations and the adaptive response of marine benthic organisms. Journal of the Geological Society 150: 187-191

Otvos EG (1999) Quaternary costal history, basin geometry and assumed evidence for hurricane activity, northeastern Gulf of Mexico coastal plain. Journal of Coastal Research 15: 438-43

Otvos EG (2001) Assumed Holocene highstands, Gulf of Mexico. Basic issues of sedimentary and landform criteria. Journal of Sedimentary Research 71: 645-647

Otvos EG (2002) Discussion of "Prehistoric landfall frequences of catastrophic hurricanes" (Liu and Fearn, 2000). Quaternary Research 57: 425-428

Otvos EG (2004) Holocene Gulf levels: Recognition issues and an updated sea-level curve.

Journal of Coastal Research 20: 680-699

Otvos EG (2012) Coastal barriers-Nomenclature, processes, and classification issues. Geomorphology 139-140: 39-52

Parker RH (1959) Macro-invertebrate assemblages of central Texas coastal bays and Laguna Madre. American Association of Petroleum Geologists Bulletin 43: 2100-2166

Parsons-Hubbard K (2005) Molluscan taphofacies in recent carbonate reef/lagoon systems and their application to sub-fossil samples from reef cores. Palaios 20: 174-191

Peters R, Jaffe BE (2010) Identification of tsunami deposits in the geologic record; developing criteria using recent tsunami deposits. U.S. Geological Survey Open-File Report 2010-1239

Petschick R, Kuhn G, Gingele F (1996) Clay mineral distribution in surface sediments of the South Atlantic - sources, transport, and relation to oceanography. Marine Geology 130: 203-229

Pielke RA Jr, Gratz J, Landsea CW, Collins D, Saunders MA, Musulin R (2008) Normalized hurricane damages in the United States: 1900-2005. Natural Hazards Review 9: 29-42

Pielou EC (1966) The measurement of diversity in different types of biological collections. Journal of Theoretical Biology 13: 131-144

Pilarczyk JE, Reinhardt EG (2011) *Homotrema rubrum* (Lamarck) taphonomy as an overwash indicator in marine ponds from Anegada, British Virgin Islands. Natural Hazards 63: 85-100

Purdy EG (1974) Karst-determined facies patterns in British Honduras: Holocene carbonate sedimentation model. American Association of Petroleum Geologists Bulletin, 58: 825-855

Purdy EG, Gischler E (2003) The Belize margin revisited: 1. Holocene marine facies. International Journal of Earth Sciences, 92: 532-551

Purdy EG, Gischler E, Lomando AJ (2003) The Belize margin revisited: 2. Origin of Holocene antecedent topography. International Journal of Earth Sciences 92: 552-572

Purdy EG, Pusey WC, Wantland KF (1975) Continental shelf of Belize: regional shelf attributes. In: Wantland KF, Pusey WC (eds) Belize shelf-carbonate sediments, clastic sediments, and ecology, American Association of Petroleum Geologists, Studies in Geology 2, pp 1-40

Pusey WC (1975) Holocene carbonate sedimentation on northern Belize shelf. In: Wantland KF, Pusey WC (eds) Belize shelf-carbonate sediments, clastic sediments, and ecology, American Association of Petroleum Geologists, Studies in Geology 2, pp 131-233

Reinson GE (1992) Transgressive barrier island and estuarine systems. In: Walker RG (ed) Facies Models. Response to Sea Level Change, Geological Association of Canada, pp 179-194

Richards RP, Bambach RK (1975) Population dynamics of some Paleozoic brachiopods and their paleoeecological significance. Journal of Paleontology 49: 775-798

Ritter MN, Erthal F, Coimbra JC (2013) Taphonomic signatures in molluscan fossil assemblages from the Holocene lagoon system in the northern part of the coastal plain, Rio Grande do Sul State, Brazil. Quaternary International 305: 5-14

Robertson R (1963) The mollusks of British Honduras. Philadelphia Shell Club 1: 15-20

Rosenberg G, García EF, Moretzsohn F (2009) Gastropods (Mollusca) of the Gulf of Mexico. In: Felder DL, Camp, DK (eds) The Gulf of Mexico: Origins, Waters and Marine Life, A&M University Press, Texas, pp 579-699

Rothschild SR (2004) Beachcomber´s guide to Gulf Coast marine life. Taylor Trade Publishing, Houston

Roy PS (1984) New South Wales estuaries: origin and evolution. In: Thom BG (ed) Coastal Geomorphology in Australia. Academic Press, Sydney, pp 99-121

Roy PS, Cowell MA, Ferland MA, Thom BG (1994) Wave-dominated coasts. In: Carter WG,

Woodroffe CD (eds) Coastal evolution: Late Quaternary shoreline morphodynamics, Cambridge University Press, Cambridge, pp 121-186

Sabatier P, Dezileau L, Barbier M, Raynal O, Lofi J, Briqueu L, Condomines M, Bouchette F, Certain R, Von Grafenstein U, Jorda C, Blanchemanche P (2010) Late-Holocene evolution of a coastal lagoon in Gulf of Lions (South of France). Bulletin de la Société Geologique de Française 181: 27-36

Sallenger AH, Stockdon HF, Fauver L, Hansen M, Thompson D, Wright CW, Lillycrop J (2006) Hurricanes 2004: an overview of their characteristics and coastal change. Estuaries and Coasts 29: 880-888

Santer BD, Wigley TML, Gleckler PJ, Bonfils C, Wehner MF, AchutaRao K, Barnett TP, Boyle JS, Brüggemann W, Fiorino M, Gillett N, Hansen JE, Jones PD, Klein SA, Meehl GA, Raper SCB, Reynolds RW, Taylor KE, Washington WM (2006) Forced and unforced ocean temperature changes in Atlantic and Pacific tropical cyclogenesis regions. Proceedings of the National Academy of Sciences 103: 13905–13910

Saunders MA, Lea AS (2008) Large contribution of sea surface warming to recent increase in Atlantic hurricane activity. Nature 451: 557-560

Scheffers A (2006) Sedimentary impacts of Holocene tsunami events from the intra Americas seas and southern Europe: a review. Zeitschrift für Geomorphologie 146: 7-37

Scheffers A, Scheffers S (2006) Documentation of the impact of Hurricane Ivan on the coastline of Bonaire (Netherlands Antilles). Journal of Coastal Research 22: 1437-1450

Scheffers A, Kelletat D (2003) Sedimentologic and geomorphologic tsunami imprints worldwide - a review. Earth-Sci Rev 63: 83-92

Scholl DW (1964a) Recent sedimentary record in mangrove swamps and rise in sea level over the southwestern coast of Florida: Part I. Marine Geology 1: 344-366

Scholl DW (1964b) Recent sedimentary record in mangrove swamps and rise in sea level over the southwestern coast of Florida: Part II. Marine Geology 2: 343-364

Schöne BR (1999) Sclerochronology: Implications for ecotypical dwarfism in oxygen-restricted environments (Middle Devonian, Rheinisches Schiefergebirge). Senckenbergiana Lethaea 79: 35-41

Schwartz RK (1975) Nature and genesis of some washover deposits. U.S. Army Coastal Engineering Research Center Technical Memo 61, Ft. Belvoir, VA

Scileppi E, Donnelly JP (2007) Sedimentary evidence of hurricane strikes in western Long Island, New York. Geochemistry Geophysics Geosystems 8: 25

Scott MR (1975) Distribution of clay minerals on Belize shelf. In: Wantland KF, Pusey WC (eds) Belize shelf-carbonate sediments, clastic sediments, and ecology, American Association of Petroleum Geologists, Studies in Geology 2 pp 97–130

Scott DB, Collins ES, Gayes PT, Wright E (2003) Records of prehistoric hurricanes on the South Carolina coast based on micropaleontological and sedimentological evidence, with comparison to other Atlantic Coast records. Geological Society of America Bulletin 115: 1027–1039

Sedgwick PE, Davis RA (2003) Stratigraphy of washover deposits in Florida: Implications for recognition in the stratigraphic record. Marine Geology 200: 31-48

Shinn EA, Hudson JH, Halley RB, Lidz B, Robbin DM, Macintyre IG (1982) Geology and sediment accumulation rates at Carrie Bow Cay, Belize, I, Structure and Communities, Smithonian Contributions to Marine Science 12: 63-75

Simpson RH (1974) The hurricane disaster potential scale. Weatherwise 27: 169-186

Soares MLG (2009) A conceptual model for the response of mangrove forests to sea-level rise. In: da Silva CP (ed) International Coastal Symposium (ICS) 2009 Proceedings, Journal of Coastal Research, Special Issue 56, pp 267-271

Spiske M and Jaffe BE (2009) Sedimentology and hydrodynamic implications of a coarse-grained hurricane sequence in a carbonate reef setting. Geology 37: 839-842

Spiske M, Böröcz Z, Bahlburg H (2008) The role of porosity in discriminating between tsunami and hurricane emplacement of boulders: a case study from the Lesser Antilles, southern Caribbean. Earth and Planetary Science Letters 268: 384-396

Stoddart DR (1962) Catastrophic storm effects on the British Honduras reefs and cays. Nature 196: 512-515

Stone GW, Wang P (1999) The importance of cyclogenesis on the short-term evolution of Gulf Coast barriers. Transactions Gulf Coast Association of Geological Societies 49: 478-487

Stutz S, Prieto AR, Isla FI (2006) Holocene evolution of the Mar Chiquita coastal lagoon area (Argentina) indicated by pollen analysis. Journal of Quaternary Science 21: 17-28

Suzuki A, Yokoyama Y, Kan H, Minoshima K, Matsuzaki H, Hamanaka N, Kawahata H (2008) Identification of 1771 Meiwa tsunami deposits using a combination of radiocarbon dating and oxygen isotope microprofiling of emerged massive Porites boulders. Quaternary Geochronology 3: 226-234

Switzer AD, Jones BG (2008) Setup, deposition and sedimentation characteristics of two storm overwash deposits, Abrahams Bosom Beach, southeastern Australia. Journal of Coastal Research 24: 189-200

Talma AS, Vogel JC (1993) A simplified approach to calibrating ^{14}C dates. Radiocarbon 35: 317-322

Tang BH, Neelin JD (2004) ENSO influence on Atlantic hurricanes via tropospheric warming. Geophysical Research Letters 31: L24204

Teeter JW (1985) Holocene lacustrine depositional history. In: Curran HA, White B (eds) Pleistocene and Holocene carbonate environments on San Salvador Island, Bahamas, Geological Society of America, Special Papers 300, pp 133-145

Tomašových A (2004) Postmortem durability and population dynamics affecting the fidelity of brachiopod size-frequency distributions. Palaios 19: 477-496

Tomašových A, Fürsich FT, Wilmsen M (2006) Preservation of autochthonous shell beds by positive feedback between increased hardpart-input rates and increased sedimentation rates. Journal of Geology 114: 287-312

Toomey MR, Donnelly JP, Woodruff JD (2013a) Reconstructing mid–late Holocene cyclone variability in the Central Pacific using sedimentary records from Tahaa, French Polynesia. Quaternary Science Reviews 77: 181-189

Toomey MR, Curry WB, Donnelly JP, van Hengstum PJ (2013b) Reconstructing 7000 years of North Atlantic hurricane variability using deep-sea sediment cores from the western Great Bahama Bank. Paleoceanography 28: 31-41

Toscano MA, Macintyre IG (2003) Corrected western Atlantic sea-level curve for the last 11,000 years based on calibrated C-14 dates from Acropora palmata framework and intertidal mangrove peat. Coral Reefs 22: 257–270

Trewin NH (1973) Sorting of bivalve populations in a beach environment. Geological Journal 8: 307-316

Trewin NH, Welsk W (1976) Formation and composition of a graded estuarine shell bed. Palaeogeography Palaeoclimatology Palaeoecology 19: 219-230

Tunnel JW Jr, Andrews J, Barrera NC, Moretzsohn F (2010) Encyclopedia of Texas Seashells: Identification, Ecology, distribution, and history. A&M University Press, Texas

Turney WJ, Perkins BF (1972) Molluscan distribution in Florida Bay. Sedimenta III, University of Miami, Miami

Tuttle MP, Ruffman A, Anderson T, Jeter H (2004) Distinguishing tsunami from storm deposits in

eastern North America: the 1929 Grand Banks Tsunami versus the 1991 Halloween Storm. Seismological Research Letters 75: 117-131

van Hengstum PJ, Donnelly JP, Toomey MR, Albury NA, Lane P, Kakuk B (2013) Heightened hurricane activity on the Little Bahama Bank from 1350 to 1650 AD. Continental Shelf Research 86: 103-115

Vermeer DE (1963) The effects of Hurricane Hattie, 1961, on the cays of British Honduras. Zeitschrift für Geomorphologie 7: 332-354

Vimont DJ, Kossin JP (2007) The Atlantic meridional mode and hurricane activity. Geophysical Research Letters 34: L07709

Wallace DJ, Anderson JB (2010) Evidence of similar probablility of intense hurricane strikes for the Gulf of Mexico over the late Holocene. Geology 38: 511–514

Wallace DJ, Woodruff JD, Anderson JB, Donnelly JP (2014) Palaeohurricane reconstructions from sedimentary archives along the Gulf of Mexico, Caribbean Sea and western North Atlantic Ocean margins. In: Martini IP, Wanless HR (eds) Sedimentary coastal zones from high to low latitudes: Similarities and Differences, Geological Society, Special Publications 388, London, pp 481-502

Wang C (2005) ENSO, Atlantic climate variability, and the Walker and Hadley circulations. In: Diaz HF, Bradley RS (eds) The Hadley Circulation: Present, Past and Future, Kluwer Academic Publishers, Dordrecht, pp 173-202

Wanless HR (1974) Mangrove sedimentation in geological perspective. In: Gleason PJ (ed) Environments of south Florida: present and past, Memoir 2. Miami, Florida: Miami Geological Society, pp 190-200

Warme JE (1969) Live and dead molluscs in a coastal lagoon. Journal of Paleontology 43: 141-150

Webster PJ, Holland GJ, Curry JA, Chang HR (2005) Changes in tropical cyclone number, duration, and intensity in a warming environment. Science 309: 1844-1846

Westphall MJ (1986) Anatomy and history of a ringed reef complex, Belize, Central America. Dissertation, University of Miami, Florida

Williams HFL (2009) Stratigraphy, sedimentology and microfossil content of Hurricane Rita storm surge deposits in southwest Louisiana. Journal of Coastal Research 25: 1041-1051

Williams HFL (2010) Storm surge deposition by Hurricane Ike on the McFaddin National Wildlife Refuge, Texas: implications for paleotempestology studies. Journal of Foraminiferal Research 40: 210-219

Williams HFL (2011) Shell bed tempestites in the Chenier Plain of Louisiana: late-Holocene example and modern analogue. Journal of Quaternary Science 26: 199-206

Williams HFL (2013) 600-Year sedimentary archive of hurricane strikes in a prograding beach ridge plain, southwestern Louisiana. Marine Geology 336: 170-183

Woodroffe CD (1990) The impact of sea-level rise on mangrove shorelines. Progress in Physical Geography 14: 483-520

Woodruff JD, Donnelly D, Emanuel K, Lane P (2008a) Assessing sedimentary records of paleo-hurricane activity using modeled hurricane climatology. Geochemistry Geophysics Geosystems 9: Q09V10

Woodruff JD, Donnelly D, Mohrig D, Geyer WR (2008b) Reconstructing relative flooding intensities responsible for hurricane-induced deposits from Laguna Playa Grande, Vieques, Puerto Rico. Geology 36: 391-394

Woodruff JD, Donnelly JP, Okusu A (2009) Exploring typhoon variability over the mid-to-late Holocene: evidence of extreme coastal flooding from Kamikoshiki, Japan. Quaternary Science Reviews 28: 1774-1785

Woodruff JD, Irish JL, Camargo SJ (2013) Coastal flooding by tropical cyclones and sea-level rise. Nature 504: 44-52

Wooller MJ, Behling H, Guerrero JL, Jantz N, Zweigert ME (2009) Late Holocene hydrologic and vegetation changes at Turneffe atoll, Belize, compared with records from mainland central America and Mexico. Palaios 24: 650-656

Wooller MJ, Behling H, Smallwood BJ, Fogel M (2004) Mangrove ecosystem dynamics and elemental cycling at Twin Cays, Belize, during the Holocene. Journal of Quaternary Science 19: 703-11

Wooller MJ, Morgan R, Fowell SJ, Behling H, Fogel M (2007) A multi-proxy peat record of Holocene mangrove paleoecology from Twin Cays, Belize. The Holocene 17: 1129-1139

Wright ACS, Romney DH, Arbuckle RH, Vial DE (1959) Land in British Honduras. Colonial Research Publications 24, London

Xie S-P, Tanimoto Y (1998) A pan-Atlantic decadal climate oscillation. Geophysical Research Letters 25: 2185-2188

Yu K-F, Zhao J-X, Shi Q, Meng Q-S (2009) Reconstruction of storm/tsunami records over the last 4000 years using transported coral blocks and lagoon sediments in the southern South China Sea. Quaternary International 195: 128-137

Zenkovich VP (1967) Processes of Coastal Development. Interscience Publishers, New York

Zenkovitch VP (1969) Origin of barrier beaches and lagoon coast. In: Castanares AA, Phleger FB (eds) Coastal Lagoons, a Symposium, Universidad Nacional Autónoma, Mexico, pp 27-38

Zhang R, Delworth TL (2006) Impact of Atlantic multidecadal oscillations on India/Sahel rainfall and Atlantic hurricanes. Geophysical Research Letters 33: L17712

Zhang R, Delworth TL (2009) A new method for attributing climate variations over the Atlantic Hurricane basin's main development region. Geophysical Research Letters 36: L06701

Zhao J-X, Neil DT, Feng Y-X, Yu K-F, Pandolfi JM (2009) High-precision U-series dating of very young cyclone-transported coral reef blocks from Heron and Wistari reefs, southern Great Barrier Reef, Australia. Quaternary International 195: 122-127

Zhou X (1998) A 4,000-year pollen record of vegetation changes, sea-level rise, and hurricane disturbance in Atchafalaya Marsh of Southern Louisiana. Dissertation, Louisiana State University

Zusammenfassung

Die vorliegende Arbeit umfasst sedimentologische, paläoökologische und paläotempestologische Untersuchungen an insgesamt 26 Sedimentkernen, die von fünf Lokalitäten entlang der Küste von Belize stammen. Die erbohrten Sedimentkerne umfassen Sedimente der letzten 8000 Jahre und liefern Einblicke in die Entwicklung von Küstenlagunen während des Holozäns. Belize liegt in Zentralamerika, im Osten der Karibik und ist Teil der Halbinsel Yucatán, wo es das südöstliche Gebiet einnimmt. Das Land liegt zwischen 16°N und 18°30´N geographischer Breite und 87°30'W und 89°30´W geographischer Länge innerhalb des Passatwindgürtels. Das Klima ist subtropisch (Wright et al. 1959). Der jährliche Niederschlag nimmt von Norden nach Süden zu und erreicht Werte von jeweils 124 cm und 380 cm (Purdy et al. 1975). Die höchsten Niederschläge sind in den Monaten Juli bis September zu verzeichnen. In der Geschichte wurde die Küste von Belize wiederholt von Hurrikanen getroffen, die mit Überflutungen der flachen Küstengebiete einhergehen. Schwere Hurrikane trafen Belize durchschnittlich alle fünf Jahre im Laufe des 20. Jahrhunderts (Gischler et al. 2008, 2013). Die Küste von Belize ist geprägt von Küstenlagunen, welche von dichten Mangroven der Art *Rhizophora mangle* umsäumt werden. Die Lagunen sind durch sandige Barrieren oder Nehrungen vom offenen Meer getrennt. Wasseraustausch zwischen den Lagunen und dem Meer findet durch ein oder mehrere lange, z.T. verzweigte, meist natürliche Kanäle („tidal channels“) oder kürzere Einlässe („tidal inlets“) statt. Die Gezeiten sind halbtägig und der Tidenhub ist mit 15-30 cm relativ gering (Kjerfve et al. 1982). Das Hinterland ist geprägt vom Gebirgszug der Maya Mountains, die eine Höhe von ca. 1100 m erreichen und aus paläozoischen Magmatiten, Metamorphiten und siliziklastischen Gesteinen bestehen. Daneben kommen kreidezeitliche und känozoische Kalksteine und Dolomite vor. Die Küste von Belize bildet eine Übergangszone zwischen siliziklastisch geprägten Gebieten und dem von Karbonaten dominiertem Schelfbereich. Vor allem der flachere nördliche Schelfbereich ist durch Karbonate charakterisiert, während der tiefere südliche Schelf sowohl siliziklastische als auch karbonatische Sedimente aufweist. Der Küste vorgelagert sind ein Barriereriff, welches sich küstenparallel über eine Länge von ca. 250 km erstreckt, sowie die drei Atolle Turneffe Islands, Lighthouse Reef und Glovers Reef.

Während eines Geländeaufenthalts vom 27.07. 2011 bis zum 06.08.2011 wurden mithilfe eines Lanesky-Vibrationsbohrers (Lanesky et al. 1979) und 590 cm langen Aluminiumrohren mit einem 7,5 cm Durchmesser Sedimentkerne gebohrt. Das Arbeitsgebiet erstreckt sich über eine Distanz von ca. 50 km entlang der mittleren belizischen Küste. Für die Geländearbeit wurden die fünf Lokalitäten Manatee Lagoon, Mullins River Beach, Colson Point Lagoon, Commerce Bight Lagoon und Sapodilla Lagoon ausgewählt. Bis auf die Lokalität Mullins River Beach, bei welcher es sich um ein Sumpfgebiet handelt, entstammen alle Sedimentkerne Küstenlagunen und deren Umgebung. Insgesamt wurden 26 Sedimentkerne mit einer Gesamtlänge von 72,95 m gebohrt.

Die einzelnen Kerne weisen Längen von 109 cm bis 500 cm auf. Die durchschnittliche Kernlänge beträgt 2,8 m. Die Wassertiefe an den einzelnen Kernstationen, deren Koordinaten mit einem GPS-Gerät registriert wurden, betrug 0 bis 109 m. Die Kompaktion der Sedimente innerhalb der Aluminiumrohre wurde aus der Differenz der Penetrationstiefe und der tatsächlichen Sedimentmächtigkeit ermittelt und liegt im Bereich zwischen 0 und 65%. Zur Bestimmung der Salinität der Küstenlagunen wurden im Januar 2011 und im Juli 2012 Wasserproben entnommen und zur Analyse zu ALA Aachen geschickt. Die Salinitäten in den Lagunen lagen im brackischen Bereich, zwischen 3,1 und 26,6‰.

Die Laborarbeit fand in Laboren des Instituts für Geowissenschaften der Goethe-Universität Frankfurt statt. Zuerst würden die Sedimentkerne geöffnet und fotografiert. Eine Kernhälfte diente zur Probennahme, die andere Kernhälfte, die Archivhälfte, wurde in Sedimentkern-Lagerrohren („D-Tubes“) gelagert. Die Sedimente der Kerne wurden beschrieben und anschließend Sedimentproben entnommen. Insgesamt wurden 169 Proben, nach Möglichkeit von 5 cm Mächtigkeit entnommen. Zur Korngrößenanalyse wurden diese durch 2 mm-, 1 mm-, 500 µm-, 250 µm-, 125 µm-, und 63 µm-Siebe „geschlämmt“. Der Karbonatgehalt wurde mit einem Scheibler-Kalzimeter gemessen. Organikgehalt der Torfe und torfigen Sedimente wurde mit der Methode des Glühverlusts ermittelt. Dazu wurden die gemahlenen Proben nach dem Trocknen und Wiegen für drei Stunden bei 600°C im Muffelofen erhitzt und anschließend nach dem Abkühlen erneut gewogen. Mithilfe der Röntgendiffraktometrie (XRD; engl.: X-ray diffraction) wurde die Mineral-zusammensetzung der zuvor gemahlenen Proben bestimmt. Insgesamt 58 Proben, bestehend aus Organik torfiger Sedimente, Muschelschalen und Korallen, wurden mit der Beschleuniger-Massenspektrometrie (AMS; engl.: Accelerator Mass Spectrometry) bei Beta Analytic Inc., Miami datiert.

Der Schwerpunkt der Arbeit liegt auf folgenden Fragestellungen:

1. Die Untersuchung der Faziesverteilung, der Faziesabfolge und der Chronologie, um die Evolution der Küstenlagunen während des Holozäns zu rekonstruieren

2. Taxonomische Auswertung der Molluskenfauna der Schalenlagen, um herauszufinden, ob sich Änderungen in der Häufigkeit, den Verteilungsmustern und der Diversität im Laufe der Entstehung der Barrieren-Lagunen Komplexe ereignet haben

Taphonomische Auswertung, um die Entstehung der Schalenlagen zu klären und um zu ermitteln, ob die taphonomische Schalenzustände innerhalb des Sedimentberichts Änderungen aufweisen

3. Identifizierung von Sturmablagerungen, um aktive und ruhige Zeiträume zu definieren und um die Eignung des Untersuchungsgebietes für Paläo-Hurrikan Rekonstruktionen zu bewerten

1. Die Sedimentverteilung und Radiokarbondatierungen zeigen einen Beginn der Entstehung der Küstenlagunen vor ca. 6000 Jahren infolge der marinen Überflutung während des holozänen Meerestiegelanstiegs. Die Fazies-Verteilungsmuster werden durch eine Vielzahl von Prozessen gesteuert, wozu Flusseintrag, die Verbindung zwischen Lagune und dem offenen Ozean, küstenparallele Ströme, Wellenaktivität und Sturmereignisse zählen. Die holozänen Sedimente liegen über einem festen blaugrauen pleistozänem Boden, der in einigen Kernen Deformationsstrukturen aufweist, welche Liquefaktion zugerechnet werden können, die wohl durch Erdbebenwellen ausgelöst wurde.

Die vorwiegend holozänen Sedimente beinhalten (1) Schlamm (oft mit Mangrovenwurzeln und Molluskenschalen), (2) Sand, (3) Torf/torfige Sedimente und (4) Sedimente, deren Korngrößen im Übergangsbereich zwischen der Schlamm- und der Sandfazies liegen. Der graue Schlamm repräsentiert die lagunäre Hintergrundsedimentation. Gröbere Sedimente kommen vor allem in den Randbereichen der Lagunen vor, an Barrieren, Sandbänken, Nehrungen und in „Washover"-Ablagerungen, wie auch entlang der Küste und dem Strand. Mithilfe der Röntgendiffrakometrie wurde Quartz als häufigstes Mineral identifiziert. Weitere Minerale sind Mikroklin, Albit, Andalusit, Muskovit, Kaolinit, Pyrit, Aragonit, Niedrig-Mg-Kalzit und Hoch-Mg-Kalzit. Ankerit wurde nur in Konkretionen in Kern SL6 gefunden. Es ist kein räumliches Verteilungsmuster in der Mineralzusammensetzung der untersuchten Lokalitäten zu erkennen.

Die Maya Mountains dienen als wichtigster Lieferant für die Küstensedimente. Die Sedimente werden durch mehrere Prozesse wie Flusstransport, Küstenerosion, küstenparallele Ströme, Gezeiten, „Overwash" und Wind bewegt. Allerdings gibt es aufgrund von Unterschieden in der Geomorphologie, der Konnektivität zwischen Lagune und Meer, und der antezedenten Topographie und somit verschiedenartiger hydrologischer Regime, Unterschiede zwischen den Lokalitäten.

Die Kerntransekte enthüllen die Sedimentarchitektur und Faziesabfolgen für jede Lokalität:

In Manatee Lagoon ist der mit bis zu vier Meter Mächtigkeit erbohrte pleistozäne Boden von holozänem Schlamm, Schalenlagen und torfigen Sedimenten überlagert. Die Basis der holozänen Sedimente, welche den Beginn der Lagunenentstehung kennzeichnet, weist ein Alter von 5300 Jahren auf. Landwärts die pleistozänen Oberfläche später überflutet.

In Mullins River Beach wurde die Basis der holozänen Sedimente im landwärtigen Kern auf 7000 Jahren vor heute datiert und älter, auf mehr als 8000 Jahre, in den seewärtigeren Kernen. Es wurden keine Anzeichen wie z.B. Schalen gefunden, welche auf die Existenz einer Lagune während früherer Stadien der Küstenentwicklung hindeuten. Die überwiegend feinkörnigen Sedimente wurden vermutlich in einem Sumpfgebiet abgelagert. Sandlagen, die von glimmerhaltigen Laminierungen überlagert sind, und von denen eine über zwei Kerne verfolgbar ist und die mithilfe der Alter korreliert werden können, wurden Sturmereignissen zugeschrieben.

Die Sedimente in Colson Point Lagoon ähneln denen in Manatee Lagoon und bestehen vorwiegend aus Schlamm mit Schalenlagen und torfigen Sedimenten. Die Überflutung des Pleistozän begann vor ca. 6000 Jahren im östlichen Gebiet und später, vor ca. 3600 Jahren bis heute im westlichen Gebiet der Lagune.Die Artzusammensetzung der Schalenlagen in Kern CP6 zeigt eine Retrogradation infolge des Meeresspiegelanstiegs. Das unregelmäßige Relief der Grenze zwischen dem Pleistozän und dem Holozän kann einer Rücken- und Mulden-Morphologie als Ergebnis einer pleistozänen Barrierenbildung zugeschrieben werden.

Die Besiedlung durch Mangroven in Commerce Bight Lagoon begann vor ca. 5500 Jahren im barriererückseitigem Gebiet und vermutlich später im Zentrum und dem westlichen Gebiet der Lagune. Kerne aus der Lagune enthalten feinkörnige Sedimente. Im Vergleich zu Manatee und Colson Point Lagoon sind Schalenlagen selten und kommen nur in einem Kern vor. Grobkörnige Ablagerungen im seewärtigsten Kern zeigen eine Verzahnung von Lagunen- und Barrierensedimenten an und sind ein Hinweis für „Overwash“. Das Auftreten von mariner Fauna im barriererückseitigem Kern und Kernen aus dem „tidal channel“ deuten auch auf „Overwash“ von marinen Sedimenten in die Lagune hin.

Das Pleistozän in Sapodilla Lagoon wurde vor ca. 6000 bis 7000 Jahren überflutet. Torf und torfige Sedimente, die den pleistozänen Boden überlagern, zeigen eine Besiedlung durch Mangroven während der frühen Enstehungsphase der Lagune an. Die lagunären Kerne bestehen aus einer räumlich einheitlichen Schichtenfolge aus Torf und Schlamm. Die vergleichsweise mächtigen schlammigen Sedimente deuten auf beständige Umweltbedingungen seit der Überflutung hin. Gröberkörnige Ablagerungen kommen nur nahe Flussmündungen und „tidal inlets“ vor, wo die Wasserenergie höher ist. Aufgrund des breiten „tidal inlets“ ist Sapodilla Lagoon weniger vom Meer abgeschnitten als die anderen Lagunen und weist daher höhere Salinitäten auf. Die Mangroven nahe des „tidal inlets“ wachsen dort seit ca. 680 Jahren, was durch das Vorkommen von Austern seit dieser Zeit angezeigt wird. Sapodilla Lagoon wurde vermutlich durch die Progradation der Nehrung geformt. Das Einsetzen sandiger Ablagerungen, welche auf 1600 Jahre vor heute datiert wurden, kennzeichnet den Beginn der Entstehung der schmalen südlichen Nehrung.

Aufgrund der Heterogenität und Komplexität der Küstenregionen gestaltet sich die Korrelation der Faziesabfolgen der fünf Lokalitäten schwierig.

2. Die Artzusammensetzung und die Verteilungsmuster innerhalb der Mollusken-Schalenlagen deuten auf Umweltveränderungen im Laufe der holozänen Lagunenentwicklung hin. Für die 16 lagunären Schalenlagen, einer Schalenlage vom „tidal inlet“ und für die drei randmarinen (flaches Subtidal) Schalenlagen wurde eine taxonomische Auswertung der Molluskenfauna durchgeführt. Die vorherrschenden Arten in den Lagunen sind die Bivalve *A. cuneimeris* und cerithide Gastropoden, welche zusammen 78% der gesamten Fauna ausmachen. Cerithide Gastropoden enthalten größtenteils *C. pliculosa* und *C. eburneum*.

Mithilfe der Clusteranalyse wurden zehn Faunen-Vergesellschaftungen, davon sieben lagunäre Vergesellschaftungen, eine „tidal inlet“ Vergesellschaftung und zwei randmarine Vergesellschaftungen, definiert. Die zwei unteren Schalenlagen in Kern CP6 können einer lagunären Umgebung zugeordnet werden, während die zwei darüberliegenden Lagen einen randmarinen Ursprung haben. Die Anteile der jeweils dominierenden Arten in den sieben lagunären Vergesellschaftungen (V1-V7) sind wie folgt:

V1: *A. cuneimeris* (43%) und *C. eburneum* (30%)

V2: *A. cuneimeris* (67%)

V3: *A. cuneimeris* (25%)

V4: *C. pliculosa* (59%) und *A. cuneimeris* (33%)

V5: *C. pliculosa* (97%)

V6: *A. cuneimeris* (98%)

V7: *A. cuneimeris* (66%) und *C. pliculosa* (21%); einziges gemeinsames Auftreten der zwei cerithiden Arten *C. pliculosa* und *C. eburneum*

Artenzahl und Diversität weisen allgemein niedrigere Werte für die lagunären Proben und höhere Werte für die randmarinen und „tidal inlet“-Proben auf. Für eine statistisch robuste Definition von Vergesellschaftungen für die randmarine und „tidal inlet“ Umgebung wurden zu wenig Kerne in diesen Gebieten gebohrt. Die Vergesellschaftung V8 zeigt höhere Diversitäten und größere Schalengrößen. Unterschiede in der Artzusammensetzung der Vergesellschaftungen V9 und V10 sind unterschiedlichen Substraten zuzuordnen.

Das Diagramm der nichtmetrischen multidimensionalen Skalierung (NMDS) bestätigt die Gruppierung der Clusteranalyse. Die Verteilung entlang der Achse NMDS1 zeigt einen lagunären/auflandigen Gradienten, der die lagunäre Vergesellschaftung von den randmarinen und „tidal inlet“ Vergesellschaftung trennt. Die Verteilung der Vergesellschaftungen entlang der Achse NMDS2 basiert auf Umweltveränderungen, welche während der holozänen Evolution der Küstenlagunen stattfanden. Änderungen der Umweltbedingungen werden mit Sturmereignissen und mit Änderungen der Geomorphologie in Zusammenhang gebracht. Sturmereignisse könnten einen Salinitätsanstieg in den Lagunen aufgrund von mariner Überflutung oder eine Salinitätsabnahme aufgrund erhöhter Niederschläge verursacht haben. Änderungen in der Geomorphologie sind wohl auf die Entstehung von Barrieren und Nehrungen zurückzuführen, welche die Lagunen vom offenen Meer trennen. Die beherrschenden Faktoren der Artverteilung sind aufgrund der Heterogenität der Barrieren-Lagunen Systeme und dem Zusammenspiel von paläoökologischen Faktoren und Paläoumweltfaktoren schwer zu bestimmen.

Insgesamt 1827 Klappen von *A. cuneimeris* wurden für die taphonomische Auswertung herangezogen. Neben der Artzusammensetzung (dem Fehlen exotischer Fauna) deuten die

Längen-Häufigkeits-Verteilung der Schalen und das Verhältnis linker zu rechter Klappe auf eine Parautochthonie der lagunären Schalenlagen hin. Die lagunären Schalenlagen sind das Ergebnis biologischer und sedimentologischer Prozesse. Die Schalen aus dem randmarinen und dem „tidal inlet“ Bereich wurden auch überwiegend in ihren ursprünglichen Habitaten abgelagert. Ein Zusammenhang zwischen der Kerntiefe, dem Schalenalter und dem taphonomischen Zustand wurde nicht beobachtet.

3. In 17 Sedimentkernen wurden fünf verschiedene Sturm-Proxies gefunden. Dazu zählen Sandlagen, marine Fauna, Schalenlagen, Hiatuse und umgekehrte Alter. Die Sandlagen und Korallen stellen aufgrund ihrer marinen Herkunft „Washover“-Ablagerungen dar. Im Gegensatz zu Sandlagen, Korallen, Hiatusen und umgekehrten Altern, welche als direkte Hinweise für Hurrikan-Ereignisse interpretiert wurden, stellen die Schalenlagen indirekte Hinweise dar. Die Schalenanreicherungen spiegeln vermutlich Änderungen der Paläoumweltbedingungen wider. Phasen mit niedriger Salinität könnten das Ergebnis eines mit Hurrikanen verbunden erhöhten Flusseintrags sein. Eine erhöhte Salinität kann durch marine Überflutung nach Sturmereignissen erklärt werden. Die potentiellen Sturmablagerungen häufen sich innerhalb dreier Zeiträume, von 6000 bis 4900, von 4200 bis 3600 und von 2200 bis 1500 Jahren vor heute. Weitere Ereignisse wurden auf ca. 180 Jahre vor heute und nach 1950 datiert.

Berücksichtigt man die Häufigkeit von Hurrikanen an der Küste von Belize, ist die Erfassung von Hurrikan-Ereignissen aus den Sedimentkernen gering. Ebenso ist die Korrelation und Konsistenz der Sturmablagerungen gering. Die Eignung des Untersuchungsgebietes für paläotempestologische Rekonstruktionen hängt von mehreren Faktoren ab. Das Erhaltungspotential der einzelnen Eventlagen kann sowohl durch physikalische als auch durch biologische Prozesse wie Bioturbation, Tidenspülung, Amalgamierung einzelner Eventlagen, und dem Fehlen von Material zur Erosion und Ablagerung nach mehreren Sturmereignissen oder einem starken Ereignis verringert sein. Die Anfälligkeit einer Lokalität für „Overwash“ während eines Sturmereignisses ist abhängig von mehreren Faktoren wie der Geomorphologie, der Richtung und Intensität eines Hurrikans und von dem Vorhandensein einer Mangrovenvegetation. Mangroven, welche Sturmfluten abschwächen können, sind an der Küste von Belize häufig. Die Sensitivität der Lokalitäten änderte sich vermutlich im Laufe der Zeit aufgrund der dynamischen Natur des Küstengebietes.

I. Core photos – **Core ML1**

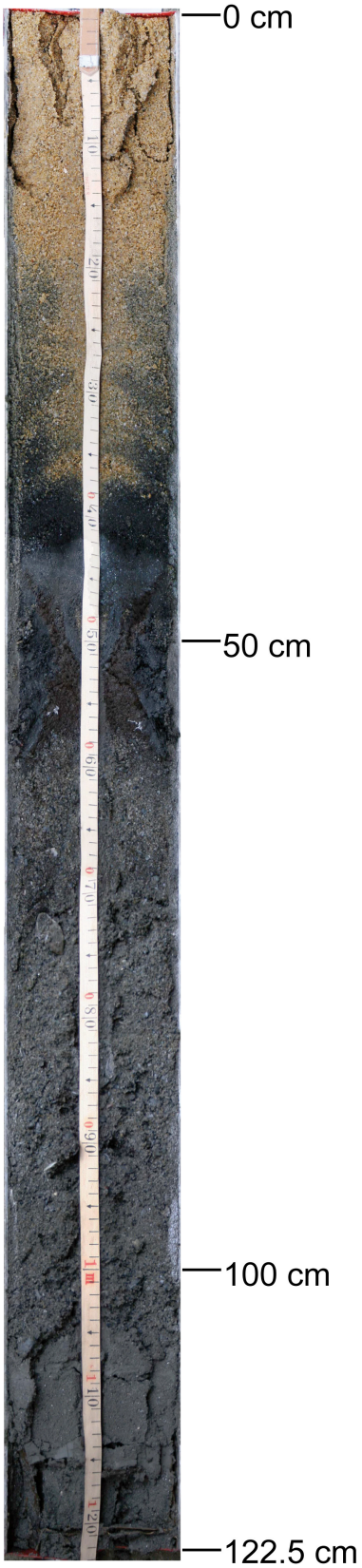

I. Core photos – **Core ML2**

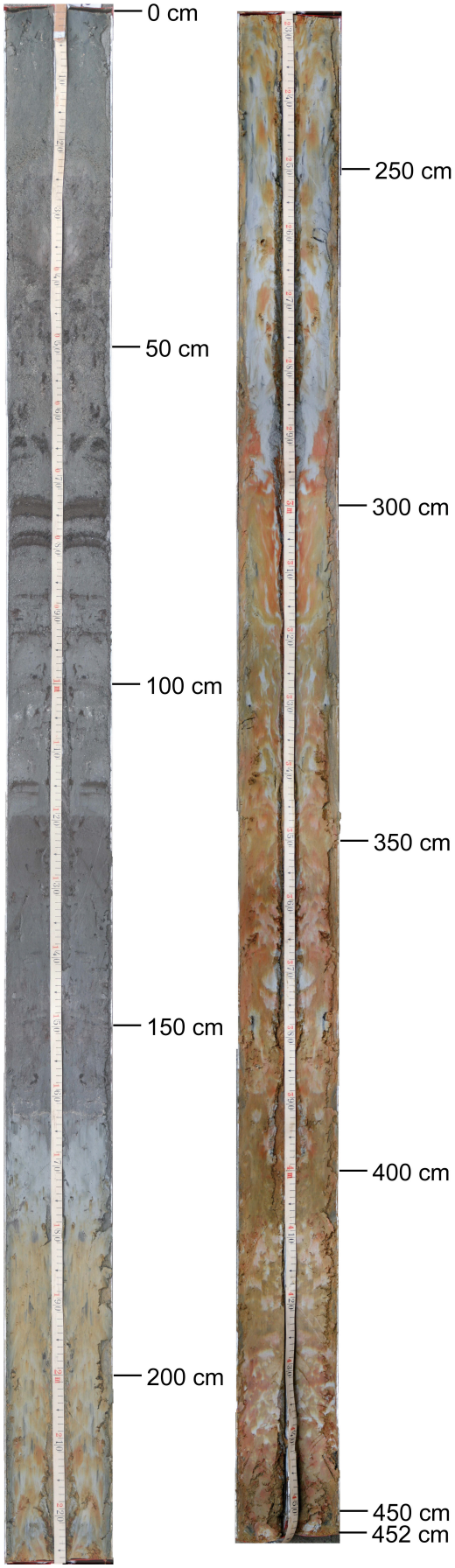

I. Core photos – **Core ML3**

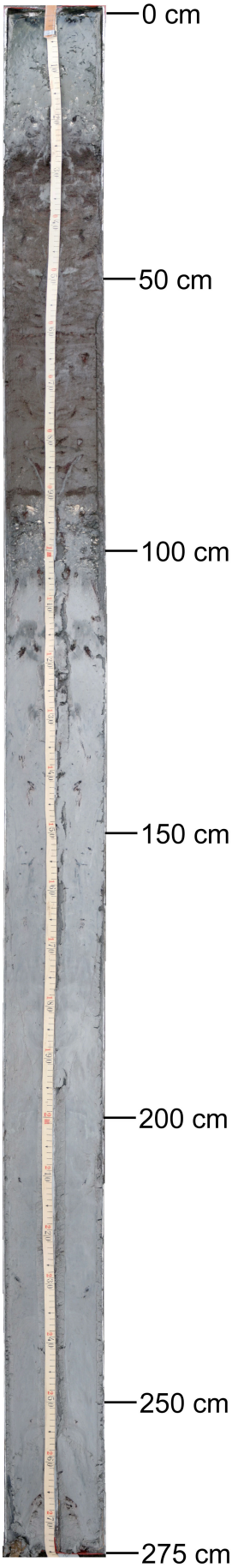

I. Core photos – **Core ML4**

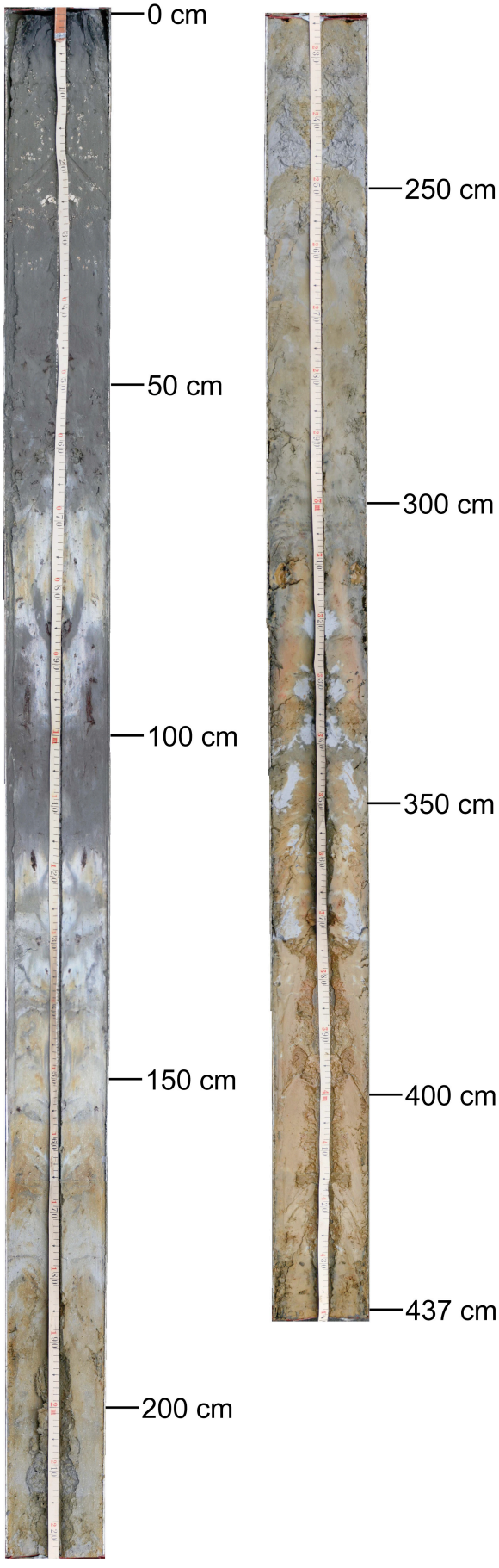

I. Core photos – **Core ML5**

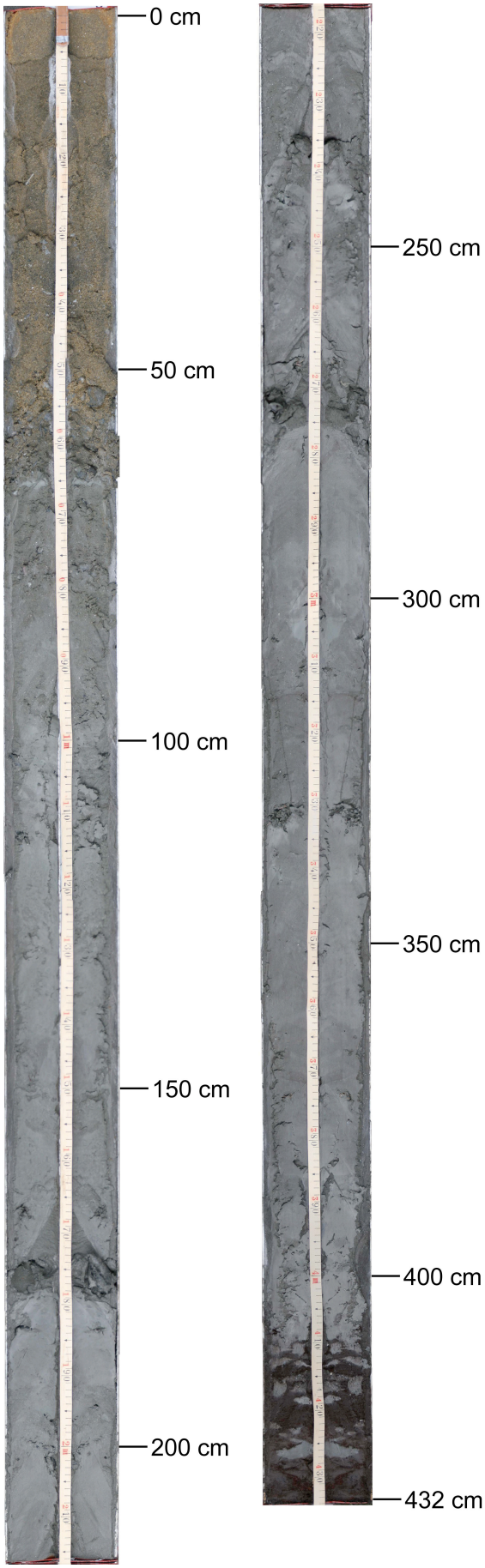

I. Core photos – **Core MRB1**

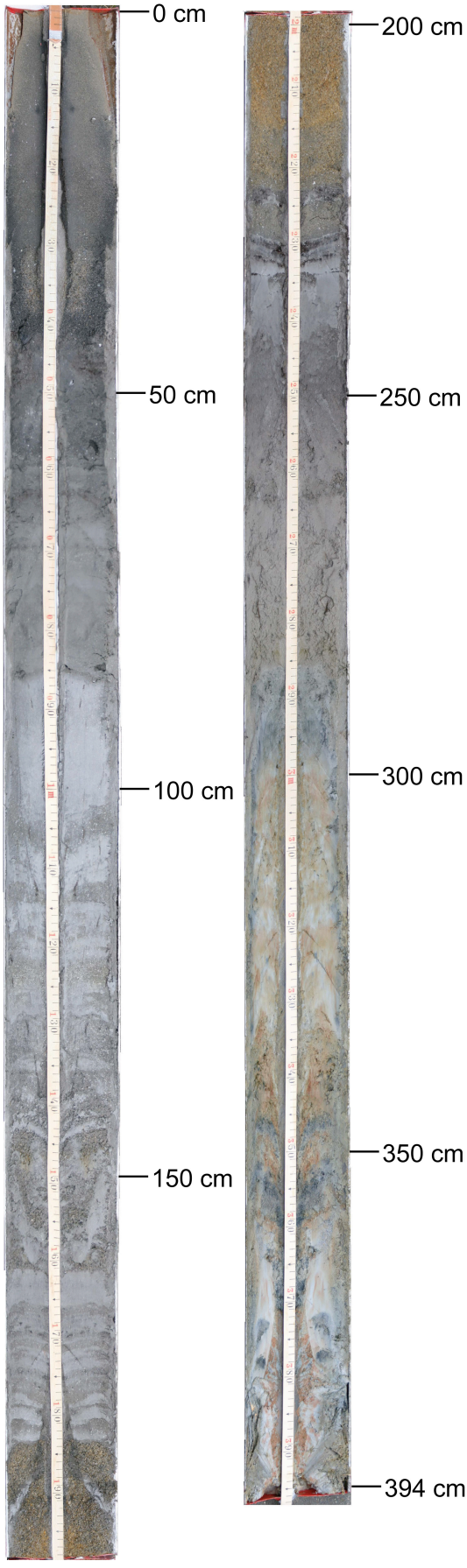

I. Core photos – **Core MRB2**

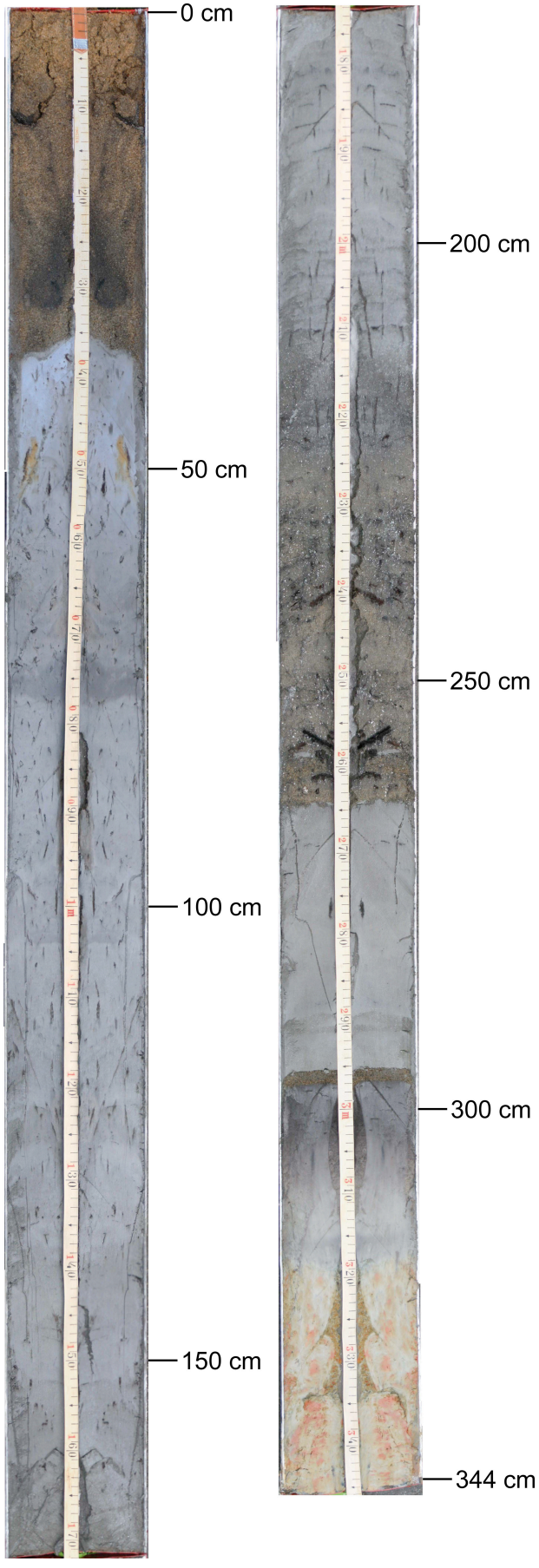

I. Core photos – **Core MRB3**

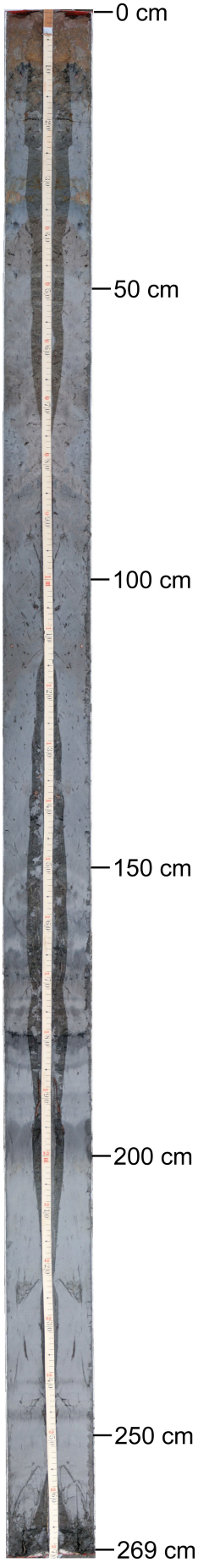

I. Core photos – **Core MRB4**

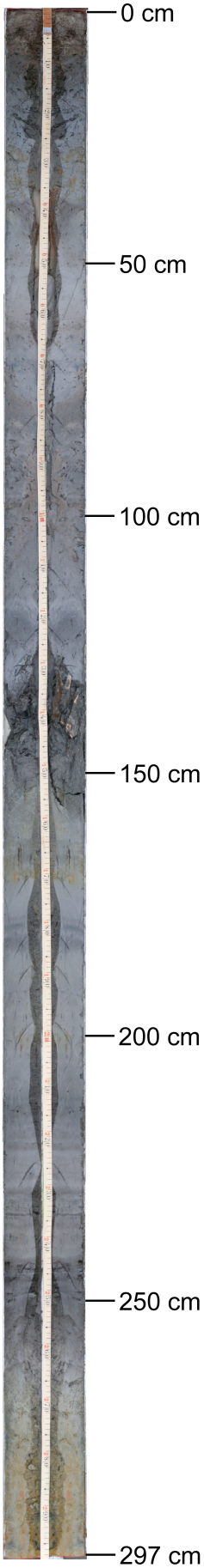

I. Core photos – **Core CP0**

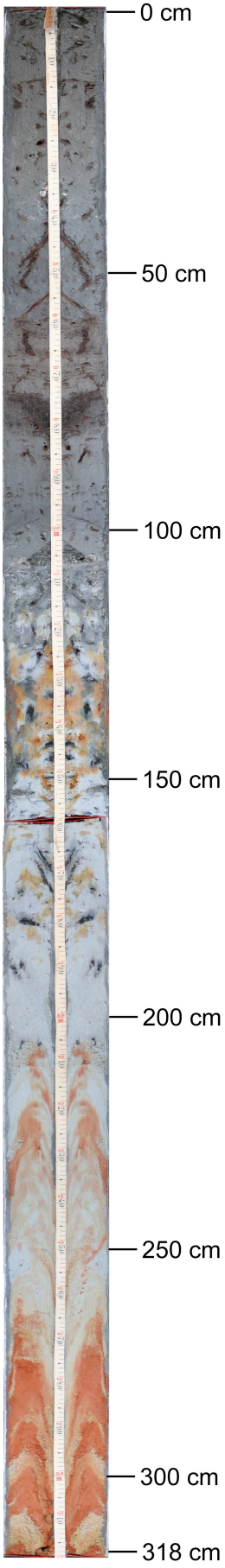

I. Core photos – **Core CP1**

I. Core photos – **Core CP2**

I. Core photos – **Core CP3**

I. Core photos – **Core CP5**

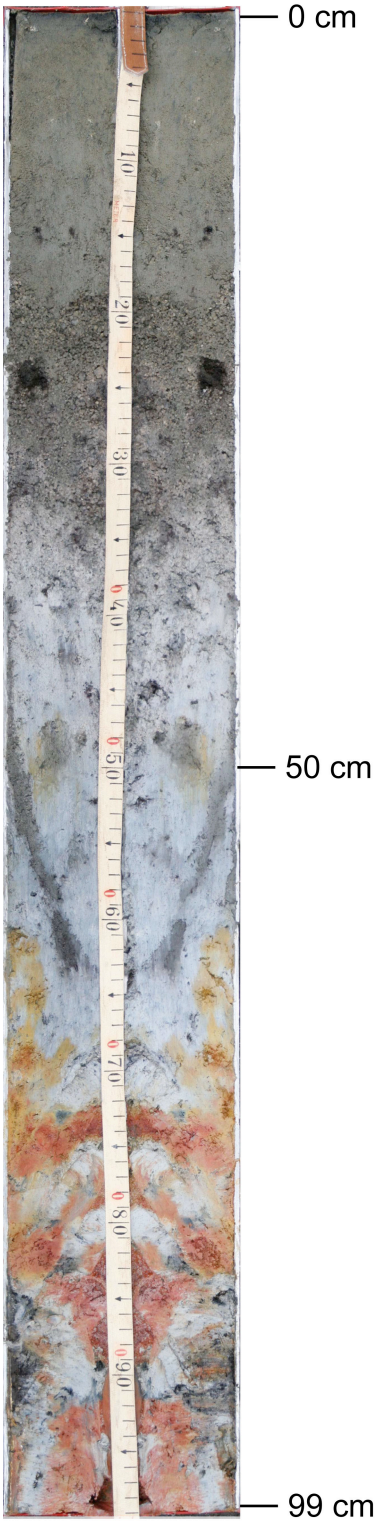

I. Core photos – **Core CP6**

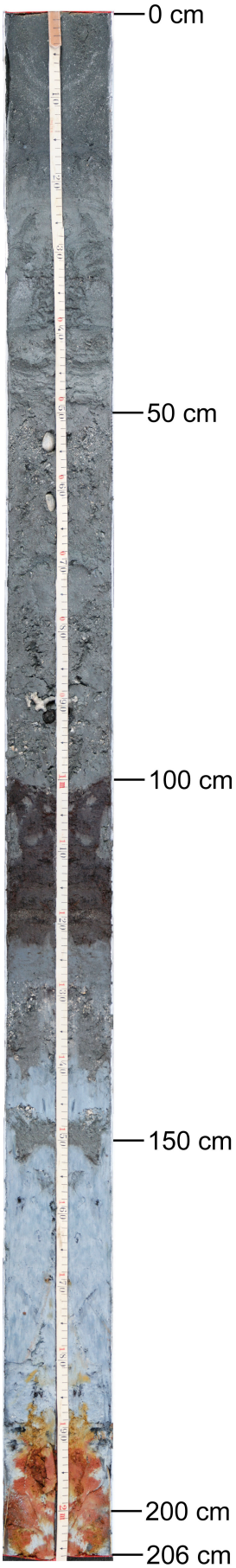

I. Core photos – **Core CBi1**

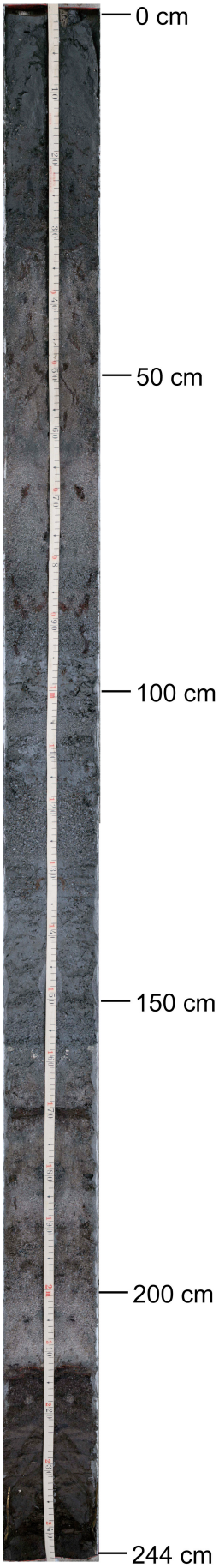

I. Core photos – **Core CBi2**

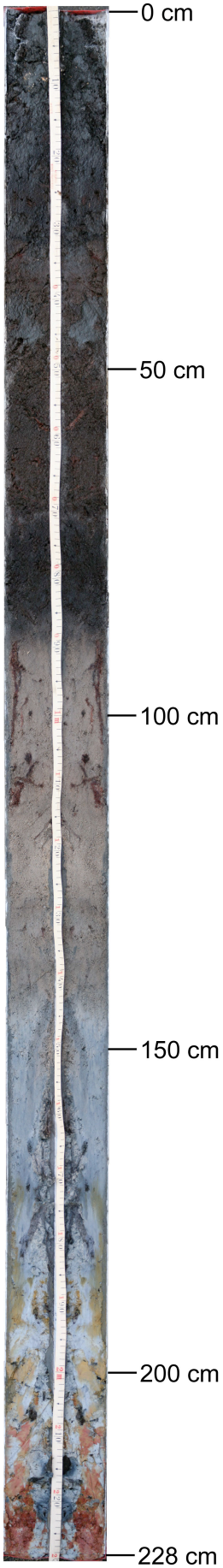

I. Core photos – **Core CBi3**

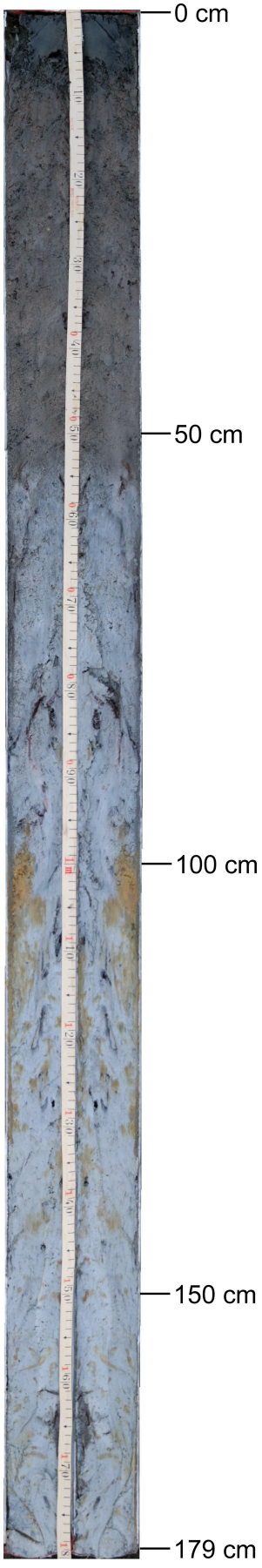

I. Core photos – **Core CBi4**

I. Core photos – **Core CBi5**

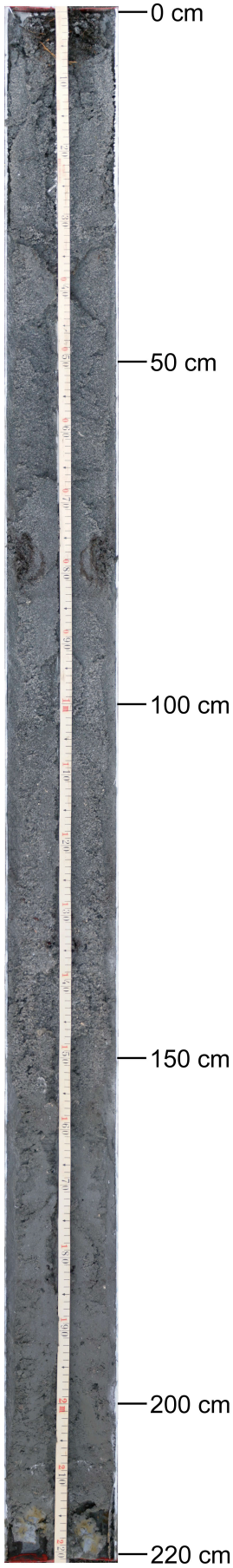

I. Core photos – **Core SL1**

I. Core photos – **Core SL2**

I. Core photos – **Core SL3**

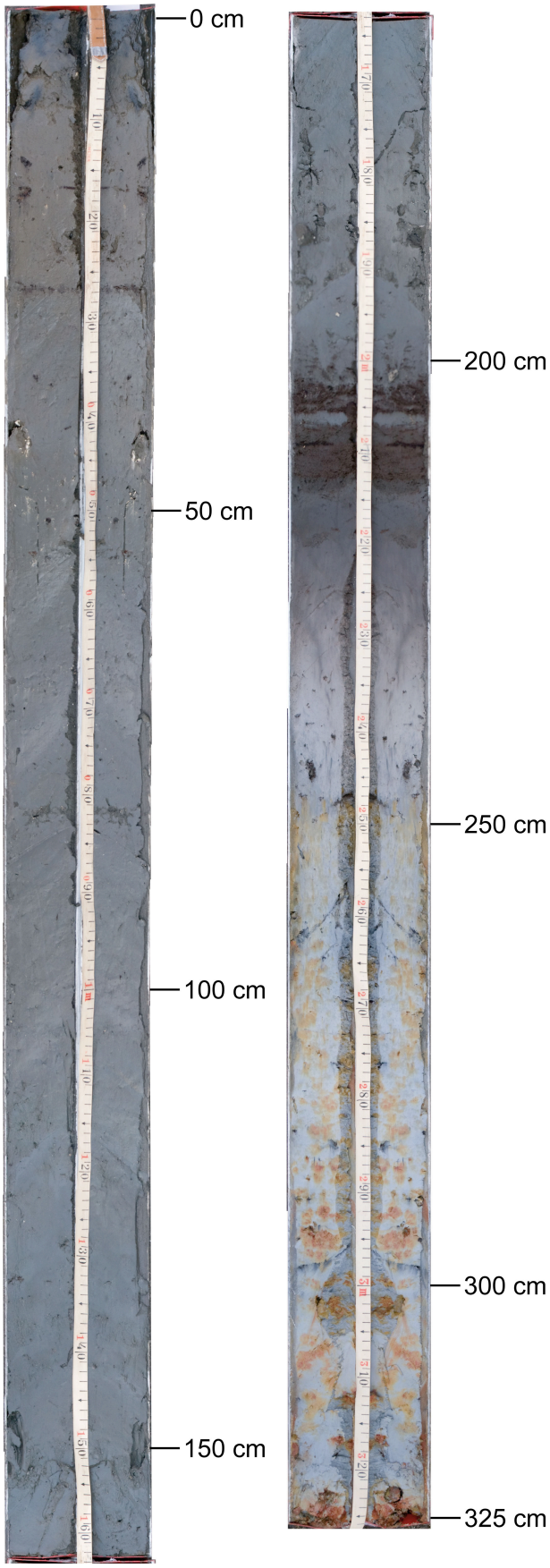

I. Core photos – **Core SL4**

I. Core photos – **Core SL5**

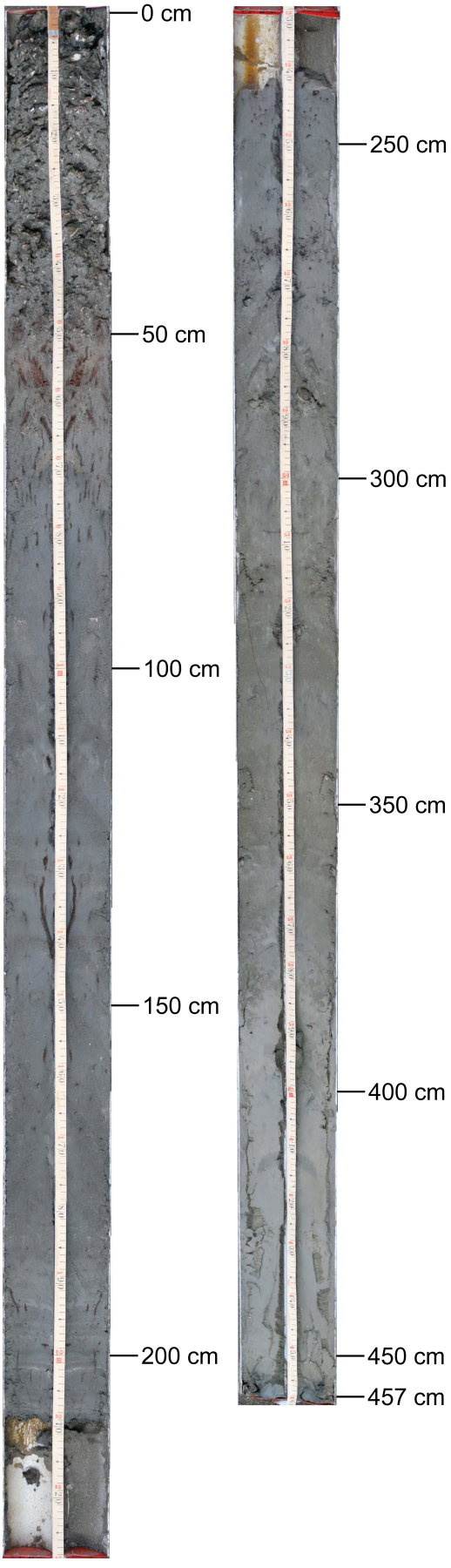

I. Core photos – **Core SL6**

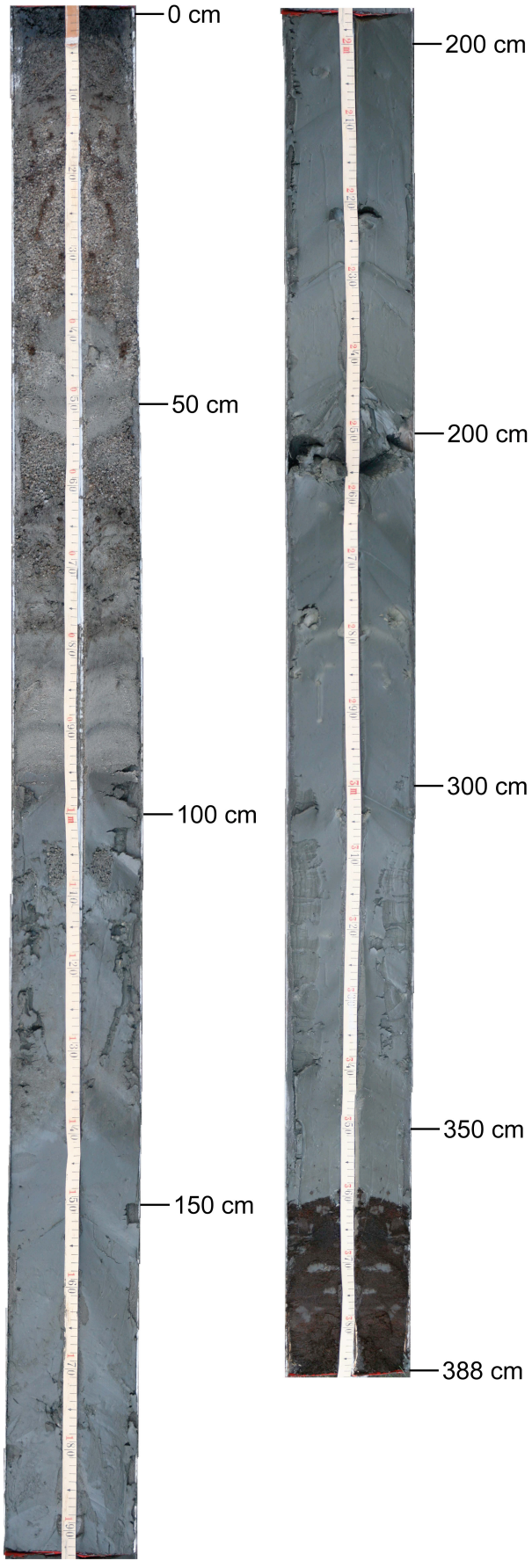

II. Grain size analysis – **Manatee Lagoon**

Core	Sample	<63µm (g)	>63µm (g)	>125µm (g)	>250µm (g)	>500µm (g)	>1 mm (g)	>2mm (g)	Σ (g)	<63µm (%)	>63µm (%)	>125µm (%)	>250µm (%)	>500µm (%)	>1 mm (%)	>2mm (%)
ML 1	0-5	1.25	0.54	0.97	10.98	70.81	7.71	0.61	92.87	1.35	0.58	1.04	11.82	76.25	8.30	0.66
	37-42	3.09	0.79	1.44	19.09	70.87	8.52	1.14	104.94	2.94	0.75	1.37	18.19	67.53	8.12	1.09
	42-47	20.08	21.88	4.98	2.57	4.35	0.99	0.34	55.19	36.38	39.64	9.02	4.66	7.88	1.79	0.62
	58-63	1.91	0.93	1.78	8.92	49.26	23.98	17.07	103.85	1.84	0.90	1.71	8.59	47.43	23.09	16.44
	85-90	2.60	0.92	1.55	12.83	51.78	43.79	59.44	172.91	1.50	0.53	0.90	7.42	29.95	25.33	34.38
	102-107	1.01	0.25	0.56	5.41	30.33	24.20	27.83	89.59	1.13	0.28	0.63	6.04	33.85	27.01	31.06
	114-116	12.04	0.86	1.35	1.49	0.15	0.04	0.00	15.93	75.58	5.40	8.47	9.35	0.94	0.25	0.00
	117-122.5	4.75	4.60	12.51	22.11	8.70	2.44	0.18	55.29	8.59	8.32	22.63	39.99	15.74	4.41	0.33
ML 2	0-5	48.28	13.9	17.79	35.92	7.19	1.72	5.07	129.87	37.18	10.70	13.70	27.66	5.54	1.32	3.90
	12-17	27.61	14.08	22.47	61.69	16.53	2.7	0.1	145.18	19.02	9.70	15.48	42.49	11.39	1.86	0.07
	50-55	13.02	4.56	11.79	37.91	23.49	12.96	3.02	106.75	12.20	4.27	11.04	35.51	22.00	12.14	2.83
	103-105	4.45	17.37	14.07	9.16	2.88	3.6	1.57	53.10	8.38	32.71	26.50	17.25	5.42	6.78	2.96
	120-125	24.22	3.72	4.37	3.8	4.85	2.7	0.54	44.20	54.80	8.42	9.89	8.60	10.97	6.11	1.22
	159-162	28.57	10.14	10.44	1.96	1.13	0.93	1.14	54.31	52.61	18.67	19.22	3.61	2.08	1.71	2.10
ML 3	17-22	102.98	7.61	2.47	1.52	0.97	0.98	9.25	125.78	81.87	6.05	1.96	1.21	0.77	0.78	7.35
	92-99	42.30	7.11	11.83	3.28	5.14	2.87	5.78	78.31	54.02	9.08	15.11	4.19	6.56	3.66	7.38
	99-104	39.03	8.86	10.55	3.68	1.35	1.04	0.62	65.13	59.93	13.60	16.20	5.65	2.07	1.60	0.95
ML 4	10-15	73.25	21.54	6.58	2.19	0.69	0.46	3.71	108.42	67.56	19.87	6.07	2.02	0.64	0.42	3.42
	15-20	76.09	22.45	7.1	2.92	1.09	0.41	1.42	111.48	68.25	20.14	6.37	2.62	0.98	0.37	1.27
	20-25	73.09	26.97	7.79	3.44	1.35	0.71	2.05	115.40	63.34	23.37	6.75	2.98	1.17	0.62	1.78
	55-60	70.6	36.55	18.36	8.5	4.97	1.71	2.77	143.46	49.21	25.48	12.80	5.92	3.46	1.19	1.93
ML 5	0-5	0.57	3.29	34.09	53.77	10.85	0.42	0.71	103.70	0.55	3.17	32.87	51.85	10.46	0.41	0.68
	55-60	3.48	5.71	23.86	42.38	29.69	2.90	71.93	179.95	1.93	3.17	13.26	23.55	16.50	1.61	39.97
	60-65	12.92	14.39	28.94	27.68	11.60	2.41	34.28	132.22	9.77	10.88	21.89	20.93	8.77	1.82	25.93
	75-80	13.25	7.61	2.47	1.52	0.97	0.98	9.25	36.05	36.75	21.11	6.85	4.22	2.69	2.72	25.66
	110-115	86.64	21.90	11.24	2.18	0.22	0.54	3.57	126.29	68.60	17.34	8.90	1.73	0.17	0.43	2.83
	328-333	62.27	14.33	15.87	2.21	0.53	1.09	10.32	106.62	58.40	13.44	14.88	2.07	0.50	1.02	9.68
	403-408	79.13	3.62	3.23	2.75	2.82	2.69	4.67	98.91	80.00	3.66	3.27	2.78	2.85	2.72	4.72

II. Grain size analysis – **Mullins River Beach**

Core	Sample	<63µm (g)	>63µm (g)	>125µm (g)	>250µm (g)	>500µm (g)	>1 mm (g)	>2mm (g)	Σ (g)	<63µm (%)	>63µm (%)	>125µm (%)	>250µm (%)	>500µm (%)	>1 mm (%)	>2mm (%)
MRB 1	5-10	1.56	15.95	85.15	16.46	0.25	0.04	0.02	119.43	1.31	13.36	71.30	13.78	0.21	0.03	0.02
	20-25	3.21	21.23	67.89	40.30	1.54	0.27	0.10	134.54	2.39	15.78	50.46	29.95	1.14	0.20	0.07
	38-43	8.46	10.99	44.85	15.44	27.91	12.08	8.48	128.21	6.60	8.57	34.98	12.04	21.77	9.42	6.61
	53-58	8.62	27.59	56.36	11.87	1.50	0.86	6.39	113.19	7.62	24.37	49.79	10.49	1.33	0.76	5.65
	70-72	18.23	15.98	8.96	0.93	0.24	0.15	0.02	44.51	40.96	35.90	20.13	2.09	0.54	0.34	0.04
	79-84	53.52	43.84	15.30	1.78	0.81	0.28	0.09	115.62	46.29	37.92	13.23	1.54	0.70	0.24	0.08
	90-95	69.49	42.01	26.42	2.43	0.43	0.13	0.02	140.93	49.31	29.81	18.75	1.72	0.31	0.09	0.01
	122-124	9.96	10.77	16.90	3.20	0.45	0.51	0.42	42.21	23.60	25.52	40.04	7.58	1.07	1.21	1.00
	155-160	18.27	15.38	25.06	11.59	11.20	36.18	20.45	138.13	13.23	11.13	18.14	8.39	8.11	26.19	14.80
	187-192	15.49	7.94	10.88	7.41	17.22	50.09	34.25	143.28	10.81	5.54	7.59	5.17	12.02	34.96	23.90
	200-205	4.44	3.25	8.88	5.44	16.58	65.02	26.09	129.70	3.42	2.51	6.85	4.19	12.78	50.13	20.12
	216-221	6.32	4.05	9.97	29.93	66.07	11.16	0.96	128.46	4.92	3.15	7.76	23.30	51.43	8.69	0.75
	224-229	17.59	10.52	39.26	30.23	6.07	1.59	1.10	106.36	16.54	9.89	36.91	28.42	5.71	1.49	1.03
	233-238	59.57	19.04	17.16	10.21	5.67	5.40	1.42	118.47	50.28	16.07	14.48	8.62	4.79	4.56	1.20
	264-269	27.90	1.70	27.38	15.69	6.21	1.61	0.77	81.26	34.33	2.09	33.69	19.31	7.64	1.98	0.95
	310-315	63.82	21.56	17.60	16.85	14.16	9.71	3.67	147.37	43.31	14.63	11.94	11.43	9.61	6.59	2.49
	350-355	36.90	10.49	12.58	25.43	31.13	20.14	15.70	152.37	24.22	6.88	8.26	16.69	20.43	13.22	10.30
MRB 2	5-10	0.53	0.30	2.52	39.58	37.41	2.47	0.30	83.11	0.64	0.36	3.03	47.62	45.01	2.97	0.36
	30-35	4.16	1.72	4.75	32.45	53.18	17.20	3.93	117.39	3.54	1.47	4.05	27.64	45.30	14.65	3.35
	40-45	63.61	6.69	2.23	7.63	15.02	5.45	0.98	101.61	62.60	6.58	2.19	7.51	14.78	5.36	0.96
	100-105	123.25	10.84	2.05	1.49	0.79	0.42	0.19	139.03	88.65	7.80	1.47	1.07	0.57	0.30	0.14
	155-160	109.91	18.17	2.55	0.78	0.54	0.28	0.14	132.37	83.03	13.73	1.93	0.59	0.41	0.21	0.11
	215-220	34.87	38.47	43.23	6.71	0.55	0.41	0.76	125.00	27.90	30.78	34.58	5.37	0.44	0.33	0.61
	225-230	7.65	16.18	63.41	39.13	2.51	0.20	0.50	129.58	5.90	12.49	48.94	30.20	1.94	0.15	0.39
	265-270	113.50	8.72	1.52	0.83	0.20	0.20	0.13	125.10	90.73	6.97	1.22	0.66	0.16	0.16	0.10
	294-296	0.84	1.10	3.41	9.72	5.74	2.00	0.48	23.29	3.61	4.72	14.64	41.73	24.65	8.59	2.06
	300-305	42.96	27.85	26.07	14.82	3.28	0.95	0.41	116.34	36.93	23.94	22.41	12.74	2.82	0.82	0.35
	320-325	95.16	22.09	13.51	7.88	1.86	0.39	1.48	142.37	66.84	15.52	9.49	5.53	1.31	0.27	1.04
MRB 3	5-10	56.24	19.04	22.92	21.10	14.98	6.04	1.07	141.39	39.78	13.47	16.21	14.92	10.59	4.27	0.76
	25-30	120.47	9.58	4.11	4.63	3.88	1.38	0.37	144.42	83.42	6.63	2.85	3.21	2.69	0.96	0.26
	45-50	105.58	6.14	3.89	4.95	4.11	1.63	0.41	126.71	83.32	4.85	3.07	3.91	3.24	1.29	0.32
	100-105	85.37	6.30	2.94	3.08	3.28	1.23	0.12	102.32	83.43	6.16	2.87	3.01	3.21	1.20	0.12
	205-210	116.72	3.78	0.43	0.37	0.18	0.13	0.12	121.73	95.88	3.11	0.35	0.30	0.15	0.11	0.10
	250-255	78.95	1.51	1.39	0.36	0.50	0.54	0.23	83.48	94.57	1.81	1.67	0.43	0.60	0.65	0.28
MRB 4	2-7	42.38	7.08	5.19	4.88	3.02	1.61	1.21	65.37	64.83	10.83	7.94	7.47	4.62	2.46	1.85
	25-30	115.30	11.00	11.35	11.59	6.97	3.97	0.74	160.92	71.65	6.84	7.05	7.20	4.33	2.47	0.46
	45-50	88.77	12.73	13.53	15.17	9.21	3.93	0.62	143.96	61.66	8.84	9.40	10.54	6.40	2.73	0.43
	120-125	97.14	3.26	2.74	2.71	1.94	0.78	0.32	108.89	89.21	2.99	2.52	2.49	1.78	0.72	0.29
	138-152 (cc)	44.94	43.82	74.14	34.64	13.57	6.57	0.60	218.28	20.59	20.08	33.97	15.87	6.22	3.01	0.27
	160-165	54.53	2.04	1.22	38.77	6.02	0.48	0.14	103.20	52.84	1.98	1.18	37.57	5.83	0.47	0.14
	200-205	91.40	0.46	0.34	0.42	0.82	0.39	0.00	93.83	97.41	0.49	0.36	0.45	0.87	0.42	0.00
	235-240	81.65	1.92	1.38	1.10	0.39	1.13	0.76	88.33	92.44	2.17	1.56	1.25	0.44	1.28	0.86
	255-260	63.84	36.88	18.22	14.82	7.85	1.3	0.16	143.07	44.62	25.78	12.74	10.36	5.49	0.91	0.11
	265-270	64.47	25.79	13.07	13.17	30.40	15.42	0.90	163.22	39.50	15.80	8.01	8.07	18.63	9.45	0.55
	292-297	88.83	14.79	6.61	4.56	5.45	1.93	0.16	122.33	72.62	12.09	5.40	3.73	4.46	1.58	0.13

II. Grain size analysis – **Colson Point Lagooon**

Core	Sample	<63µm (g)	>63µm (g)	>125µm (g)	>250µm (g)	>500µm (g)	>1 mm (g)	>2mm (g)	Σ (g)	<63µm (%)	>63µm (%)	>125µm (%)	>250µm (%)	>500µm (%)	>1 mm (%)	>2mm (%)
CP 0	33-38	25.09	4.29	29.38	21.72	6.77	9.99	3.94	101.18	24.80	4.24	29.04	21.47	6.69	9.87	3.89
	105-110	26.53	4.58	31.11	50.27	9.47	12.96	13.18	148.1	17.91	3.09	21.01	33.94	6.39	8.75	8.90
	145-150	70.21	12.18	82.39	26.47	15.61	6.76	2.09	215.71	32.55	5.65	38.19	12.27	7.24	3.13	0.97
	215-220	62.03	20.5	82.53	61.63	30.26	22.38	6.72	286.05	21.69	7.17	28.85	21.55	10.58	7.82	2.35
	270-275	38.07	3.81	41.88	88.33	13.93	34.19	34.45	254.66	14.95	1.50	16.45	34.69	5.47	13.43	13.53
	313-318	31.11	2.43	33.54	86.34	5.97	17.72	30.96	208.07	14.95	1.17	16.12	41.50	2.87	8.52	14.88
CP 1	70-75	30.57	1.45	32.02	8.28	1.26	2	2.98	78.56	38.91	1.85	40.76	10.54	1.60	2.55	3.79
	187-192	30.87	5.57	36.44	21.03	4.71	5.37	5.33	109.32	28.24	5.10	33.33	19.24	4.31	4.91	4.88
	225-230	128.8	13.63	142.43	6.12	4.04	1.25	0.51	296.78	43.40	4.59	47.99	2.06	1.36	0.42	0.17
CP 2	5-10	49.89	15.38	65.27	9.26	5.81	1.27	0.46	147.34	33.86	10.44	44.30	6.28	3.94	0.86	0.31
	20-25	51.76	15.43	67.19	15.71	6.58	2.44	1.59	160.7	32.21	9.60	41.81	9.78	4.09	1.52	0.99
	40-45	42.68	56.98	99.66	24.28	18.33	4.51	1.12	247.56	17.24	23.02	40.26	9.81	7.40	1.82	0.45
	80-85	127.63	6.95	134.58	4.32	2	1.14	0.72	277.34	46.02	2.51	48.53	1.56	0.72	0.41	0.26
	150-155	99.71	10.98	110.69	5.42	3.55	1.17	0.48	232	42.98	4.73	47.71	2.34	1.53	0.50	0.21
CP 3	5-10	43.21	27.55	70.76	27.16	18.16	6	2	194.84	22.18	14.14	36.32	13.94	9.32	3.08	1.03
	40-45	70.54	30.93	101.47	22.85	19.33	1.96	0.61	247.69	28.48	12.49	40.97	9.23	7.80	0.79	0.25
	110-115	106.09	22.7	128.79	3.31	2.71	0.24	0.07	263.91	40.20	8.60	48.80	1.25	1.03	0.09	0.03
	160-165	53.2	32.95	86.15	46.7	41.93	3.5	0.22	264.65	20.10	12.45	32.55	17.65	15.84	1.32	0.08
	185-190	46.49	29.82	76.31	62.03	52.23	8.62	0.6	276.1	16.84	10.80	27.64	22.47	18.92	3.12	0.22
	200-203	12.86	5.53	18.39	76.27	13.36	33.42	20.34	180.17	7.14	3.07	10.21	42.33	7.42	18.55	11.29
	206-210	17.29	9.81	27.1	74.48	25.99	41	5.6	201.27	8.59	4.87	13.46	37.01	12.91	20.37	2.78
	215-216	5.25	3.1	8.35	18.68	6.54	7.33	3.49	52.74	9.95	5.88	15.83	35.42	12.40	13.90	6.62
	220-225	5.32	4.65	9.97	106.2	11.85	18.39	31.03	187.41	2.84	2.48	5.32	56.67	6.32	9.81	16.56
	230-235	13.67	9.75	23.42	84.71	23.82	16.85	30.43	202.65	6.75	4.81	11.56	41.80	11.75	8.31	15.02
	250-255	26.4	12.91	39.31	64.35	24.32	26.12	9.35	202.76	13.02	6.37	19.39	31.74	11.99	12.88	4.61
	260-262	1.02	1.12	2.14	24.49	3.4	6.81	5.1	44.08	2.31	2.54	4.85	55.56	7.71	15.45	11.57
	262-264	3.6	2.82	6.42	9.46	4.3	2.27	1.13	30	12.00	9.40	21.40	31.53	14.33	7.57	3.77
CP 5	5-10	42.04	25.66	67.7	58.61	23.43	20.19	13.4	251.03	16.75	10.22	26.97	23.35	9.33	8.04	5.34
	25-30	13.79	7.42	21.21	84.64	8.63	11.3	28	174.99	7.88	4.24	12.12	48.37	4.93	6.46	16.00
	50-55	76.99	4.48	81.47	50.51	7.76	12.17	15.4	248.78	30.95	1.80	32.75	20.30	3.12	4.89	6.19
	80-85	69.22	8.85	78.07	6.51	6.35	11.41	14.18	194.59	35.57	4.55	40.12	3.35	3.26	5.86	7.29
CP 6	5-10	0.52	33.26	33.78	80.59	67.83	7.98	0.63	224.59	0.23	14.81	15.04	35.88	30.20	3.55	0.28
	25-30	60.75	21.2	81.95	25.46	23.51	1.1	0.09	214.06	28.38	9.90	38.28	11.89	10.98	0.51	0.04
	52-57	20.18	18.67	38.85	57.01	25.56	13.8	8.33	182.4	11.06	10.24	21.30	31.26	14.01	7.57	4.57
	92-97	40.7	10.54	51.24	29.28	8.11	8.98	6.81	155.66	26.15	6.77	32.92	18.81	5.21	5.77	4.37
	124-127	23.54	7.63	31.17	33.65	12.13	11.34	6.12	125.58	18.75	6.08	24.82	26.80	9.66	9.03	4.87
	130-135	21.93	13.13	35.06	86.88	17.36	24.98	24.29	223.63	9.81	5.87	15.68	38.85	7.76	11.17	10.86
	145-152	17.44	6.21	23.65	52.29	28.78	9.93	5.54	143.84	12.12	4.32	16.44	36.35	20.01	6.90	3.85

II. Grain size analysis – **Commerce Bight Lagooon**

Core	Sample	<63µm (g)	>63µm (g)	>125µm (g)	>250µm (g)	>500µm (g)	>1 mm (g)	>2mm (g)	Σ (g)	<63µm (%)	>63µm (%)	>125µm (%)	>250µm (%)	>500µm (%)	>1 mm (%)	>2mm (%)
CBi 1	12-17	24	4.33	2.07	11.68	30	9.52	2.14	83.74	28.66	5.17	2.47	13.95	35.83	11.37	2.56
	55-60	4.46	1.33	1.84	26.43	79.29	14.57	1.08	129	3.46	1.03	1.43	20.49	61.47	11.29	0.84
	120-125	3.68	6.57	1.53	2.48	27.2	61.83	55.71	159	2.31	4.13	0.96	1.56	17.11	38.89	35.04
	145-150	14.83	51.11	8.69	3.07	4.91	8.23	10.43	101.27	14.64	50.47	8.58	3.03	4.85	8.13	10.30
	157-160	3.42	12.85	5.89	13.08	12.32	11.83	20.95	80.34	4.26	15.99	7.33	16.28	15.33	14.72	26.08
	187-192	4.16	4.67	1.36	23.4	61.76	25.06	3.61	124.02	3.35	3.77	1.10	18.87	49.80	20.21	2.91
	207-212	2.96	4.82	3.52	22.25	62.98	16.38	0.99	113.9	2.60	4.23	3.09	19.53	55.29	14.38	0.87
CBi 2	7-12	15.06	0.49	1.09	0.75	0.71	0.93	13.69	32.72	46.03	1.50	3.33	2.29	2.17	2.84	41.84
	42-46	9.41	0.45	0.32	0.42	0.31	0.23	0.15	11.29	83.35	3.99	2.83	3.72	2.75	2.04	1.33
	110-115	8.78	6.85	11.05	26.04	22.53	12.04	3.9	91.19	9.63	7.51	12.12	28.56	24.71	13.20	4.28
	136-141	18.91	7.51	12.95	28.09	33.68	22.27	12.3	135.71	13.93	5.53	9.54	20.70	24.82	16.41	9.06
CBi 3	0-5	17.22	6.8	6.4	13.91	8.29	2.91	3.09	58.62	29.38	11.60	10.92	23.73	14.14	4.96	5.27
	10-15	27.4	9.3	9.55	24.86	29.25	20.86	10.1	131.32	20.87	7.08	7.27	18.93	22.27	15.88	7.69
	50-55	19.94	6.05	6.1	18.64	23.93	20.87	14.86	110.39	18.06	5.48	5.53	16.89	21.68	18.91	13.46
CBi 4	15-20	2.36	1.09	2.03	45	59.4	36.53	11.3	157.71	1.50	0.69	1.29	28.53	37.66	23.16	7.17
	55-60	0.93	1.12	1.67	15.68	56.54	31.27	7.2	114.41	0.81	0.98	1.46	13.71	49.42	27.33	6.29
	95-100	1.4	0.72	0.88	7.04	51.93	48.46	8.36	118.79	1.18	0.61	0.74	5.93	43.72	40.79	7.04
	107-112	1.66	1.55	0.65	4.75	23.55	30.54	29.32	92.02	1.80	1.68	0.71	5.16	25.59	33.19	31.86
	113-116	9.15	9.86	2.56	1.63	3.16	3.48	2.87	32.71	27.97	30.14	7.83	4.98	9.66	10.64	8.77
	120-122	2.25	9.91	8.58	10.52	8.92	0.51	0.06	40.75	5.52	24.32	21.06	25.82	21.89	1.25	0.15
CBi 5	30-35	0.51	3.03	5.91	62.83	27.88	10.91	4.09	115.16	0.44	2.63	5.13	54.56	24.21	9.47	3.55
	125-130	0.94	2.38	2.61	24.97	77.78	28.3	6.84	143.82	0.65	1.65	1.81	17.36	54.08	19.68	4.76
	148-153	5.53	4.78	4.93	19.56	81.92	51.88	13.09	181.69	3.04	2.63	2.71	10.77	45.09	28.55	7.20
	153-158	7.95	17.21	19.29	40.13	28.79	15.62	20.39	149.38	5.32	11.52	12.91	26.86	19.27	10.46	13.65
	195-200	25.39	32.82	13.68	15.98	13.14	13.92	24.88	139.81	18.16	23.47	9.78	11.43	9.40	9.96	17.80
	208-213	37.69	37.41	22.64	32.54	28.02	25.29	28.16	211.75	17.80	17.67	10.69	15.37	13.23	11.94	13.30

II. Grain size analysis – **Sapodilla Lagooon**

Core	Sample	<63µm (g)	>63µm (g)	>125µm (g)	>250µm (g)	>500µm (g)	>1 mm (g)	>2mm (g)	Σ (g)	<63µm (%)	>63µm (%)	>125µm (%)	>250µm (%)	>500µm (%)	>1 mm (%)	>2mm (%)
SL 1	20-25	53.26	1.56	1.82	0.49	0.25	0.15	0.90	58.43	91.15	2.67	3.11	0.84	0.43	0.26	1.54
	40-45	55.71	3.73	5.04	1.30	1.13	1.38	2.67	70.96	78.51	5.26	7.10	1.83	1.59	1.94	3.76
	90-95	70.56	2.96	2.54	1.63	0.52	0.54	1.02	79.77	88.45	3.71	3.18	2.04	0.65	0.68	1.28
	220-225	48.56	2.08	2.66	1.73	2.32	2.85	10.82	71.02	68.38	2.93	3.75	2.44	3.27	4.01	15.24
SL 2	10-15	64.48	2.96	0.35	0.19	0.14	0.3	0.57	68.99	93.46	4.29	0.51	0.28	0.20	0.43	0.83
	40-45	60.91	2.14	0.96	1.13	0.43	0.31	0.57	66.45	91.66	3.22	1.44	1.70	0.65	0.47	0.86
	60-65	48.49	3.15	0.9	0.21	0.33	0.3	1.12	54.50	88.97	5.78	1.65	0.39	0.61	0.55	2.06
	209-214	50.09	2.33	2.05	1.41	1.38	1.37	5.21	63.84	78.46	3.65	3.21	2.21	2.16	2.15	8.16
SL 3	20-25	63.12	9.59	1.83	0.6	0.27	0.14	0.29	75.84	83.23	12.65	2.41	0.79	0.36	0.18	0.38
	47-52	86.23	20.31	2.05	0.57	0.52	0.56	2.3	112.54	76.62	18.05	1.82	0.51	0.46	0.50	2.04
	190-195	55.89	3.77	3.3	2.19	2	2.44	2.8	72.39	77.21	5.21	4.56	3.03	2.76	3.37	3.87
	220-225	97.07	19.66	17.14	4.69	0.61	0	0.09	139.26	69.70	14.12	12.31	3.37	0.44	0.00	0.06
SL 4	20-25	37.46	25.13	17.96	13.76	2.15	0.45	0.18	97.09	38.58	25.88	18.50	14.17	2.21	0.46	0.19
	60-65	47.73	16.58	9.33	2.84	1.07	0.71	0.14	78.40	60.88	21.15	11.90	3.62	1.36	0.91	0.18
	150-155	57.16	0.9	0.73	1.16	2.02	1.61	29.84	93.42	61.19	0.96	0.78	1.24	2.16	1.72	31.94
SL 5	5-10	30.61	2.5	1.68	1.22	1.84	2.26	39.76	79.87	38.32	3.13	2.10	1.53	2.30	2.83	49.78
	25-30	22.84	3.69	8.21	5.65	5.06	5.57	29.04	80.06	28.53	4.61	10.25	7.06	6.32	6.96	36.27
	46-51	17.81	6.56	21.8	14.05	7.55	6.16	27.81	101.74	17.51	6.45	21.43	13.81	7.42	6.05	27.33
	90-95	19.54	13.51	68.18	31.73	11.57	2.88	0.84	148.25	13.18	9.11	45.99	21.40	7.80	1.94	0.57
	150-155	17.4	61.56	46.08	8.92	0.38	0.19	0.16	134.69	12.92	45.70	34.21	6.62	0.28	0.14	0.12
	270-275	50.44	21.68	35.82	5.36	0.86	0.62	6.12	120.90	41.72	17.93	29.63	4.43	0.71	0.51	5.06
	330-335	23.58	41.47	30.5	1.75	0.33	0.26	0.82	98.71	23.89	42.01	30.90	1.77	0.33	0.26	0.83
	452-457	83.39	3.26	1.4	0.64	0.76	0.69	3.34	93.48	89.21	3.49	1.50	0.68	0.81	0.74	3.57
SL 6	30-35	0.94	1.84	12.31	3.39	9.75	40.19	24.77	93.19	1.01	1.97	13.21	3.64	10.46	43.13	26.58
	91-96	4.7	17.47	68.7	3.75	0.15	0.47	0.44	95.68	4.91	18.26	71.80	3.92	0.16	0.49	0.46
	96-101	34.75	10.15	10.4	1.04	0.21	0.24	0.33	57.12	60.84	17.77	18.21	1.82	0.37	0.42	0.58
	354-359	53.65	1.74	1.73	0.74	0.66	0.92	1.58	61.02	87.92	2.85	2.84	1.21	1.08	1.51	2.59

III. Carbonate and organic matter content

Core	Sample	$CaCO_3$ (%)
MRB 1	5-10	1.5
	20-25	1.4
	38-43	2.1
	53-58	4.4
	70-72	6.3
	79-84	3.1
	90-95	0.8
	122-124	0.2
	155-160	0.1
	187-192	0
	200-205	0
	216-221	0
	224-229	1.2
	233-238	0.5
	264-269	0.4
	310-315	0.6
	350-355	0
MRB 2	5-10	3.1
	30-35	2
	40-45	2.6
	100-105	3.8
	155-160	3.4
	215-220	1.7
	225-230	2.5
	265-270	5.7
	294-296	3.4
	300-305	4.9
	320-325	4.4
MRB 3	5-10	0.1
	25-30	0.9
	45-50	0
	100-105	0.1
	205-210	0
	250-255	0.1
MRB 4	2-7	4.6
	25-30	4.2
	45-50	0
	120-125	0
	138-152 (cc)	0.4
	160-165	0
	200-205	0.4
	235-240	0
	255-260	0.2
	265-270	0
	292-297	0.2
CP 0	10-15	
	33-38	7.98
	105-110	18.37
	145-150	3.75
	215-220	3.1
	270-275	3.9
	313-318	3.91
CP 1	20-25	
	70-75	20.55
	187-192	35.37
	225-230	4.02
CP 2	5-10	14.67
	20-25	22.84
	40-45	3.86
	80-85	4.08
	150-155	3.96
CP 4	5-10	6.85
	40-45	3.7
	110-115	3.99
	160-165	2.63
	185-190	2.79
	200-203	2.9
	206-210	4
	215-216	4.49
	220-225	3.59
	230-235	4.88
	250-255	4.35
	260-262	4.06
	262-264	3.13

continued

Core	Sample	$CaCO_3$ (%)
CP 5	5-10	4.16
	25-30	3.5
	50-55	3.72
	80-85	3.97
CP 6	5-10	7.83
	25-30	12.31
	52-57	14.81
	92-97	17.15
	124-127	3.84
	130-135	9.15
	145-152	10.61
CBi 1	12-17	6.79
	55-60	4.6
	120-125	3.89
	145-150	4.08
	157-160	4.94
	187-192	4.25
	207-212	5.33
CBi 2	7-12	11.95
	42-46	4.93
	110-115	4.15
	136-141	2.68
CBi 3	0-5	8.71
	10-15	4.55
	50-55	4.62
CBi 4	15-20	5.09
	55-60	5.29
	95-100	4.17
	107-112	4
	113-116	12.45
	120-122	12.45
CBi 5	30-35	5.73
	125-130	6.13
	148-153	5.78
	153-158	8.79
	195-200	10.05
	208-213	8.37
SL 1	20-25	7.19
	40-45	5.5
	90-95	9.64
	220-225	18.92
SL 2	10-15	6.16
	40-45	2.7
	60-65	9.1
	209-214	11.66
SL 3	20-25	4.97
	47-52	2.9
	190-195	11.36
	220-225	3.7
SL 4	20-25	3.31
	60-65	1.78
	150-155	7.24
SL 5	5-10	51.38
	25-30	50.23
	46-51	26.36
	90-95	3.39
	150-155	4.39
	270-275	6.4
	330-335	5.36
	452-457	11.18
SL 6	30-35	0.58
	91-96	1.03
	96-101	7.13
(concretion)	251-256	52.8
	354-359	6.66

Core	Sample	OM (%)
ML1	55-58	30.3
ML2	74-75	47.4
ML3	27-28	41.1
ML5	425-426	41.6
CP1	86-88	34.9
CP6	119-121	9.6
CBi1	169-170	2.3
CBi1	212-213	18.6
CBi1	215-216	2.0
CBi1	230-231	31.9
CBi1	243-244	71.5
CBi2	84-85	7.9
CBi4	100-101	23.5
CBi4	153-154	19.6
SL1	226-227	56.8
SL1	240-241	73.9
SL2	214-216	76.7
SL3	211-212	43.4
SL4	157-158	33.5
SL4	199-200	72.0
SL6	360-361	43.8

IV. XRD

Probebezeichnung	Quartz	Quartz	Microcline	Albite	Illite/Muscovit	Illite/Muscovit	Kaolinite	Pyrite	Andalusite	Aragonite bioç	Calcite	Mg-Calcite	Ankerite	Zwischensumme															
	01-086-1560	01-086-1560	01-087-1790	01-089-6423	01-089-5401	01-089-5401	01-089-6538	01-079-0617	01-075-1219	self measured	01-072-1652	01-086-2335	01-079-1347		Quartz	Microcline	Albite	Andalusite	Muscovite	Kaolinite	Pyrite	Aragonite	Calcite	Mg-Calcite	Ankerite				
	4.26 Å	3.34 Å	3.22037Å	3.184 Å	10 Å	4.45 Å	7.16854	1.64052	5.4945 Å	3.4625	3.0303	3.02	3.15		rel. %	rel. %	rel. %	rel. %	rel. %	rel. %	rel. %	rel. %	rel. %	rel. %	rel. %				
	Int/100	Int/100	Int/100	Int/100	Int/100	Int/100	Int/100	Int/100	Int/100	Int/100	Int/100	Int/100	Int/100																
	21.2	100		100	100	74.7	100	100	97.4	100	100	100	100																
	Fix	Fix	Fix	Fix	Fix	Fix	Fix	Fix	Fix	Fix	Fix	Fix	Fix																
	1.786	1.400935	1.3513	1.337	4.323	1.8736	3.0584	0.704626	2.3244	1.4531	1.2718	1.255	1.2215																
	RIR	RIR	RIR		RIR	RIR	RIR	RIR	RIR	RIR	RIR	RIR	RIR																
	3.03	3.03	0.55	0.64	0.43	0.43	1	2.59	0.73	0.69	3.2	3.05	3.15																
		zum Vergl.				zum Vergl.																							
SL 5 090-095	5788.73529	6027.25698	449.614364	116.9875	311.65814	256.649544	0	35.3673282	0	0	0	18.104918	0	66.65458942	86.8467624	6.74543745	1.75513046	0	3.8504407	0	0.53060605	0	0	0.27162298	0				
SL 5 150-155	5335.53459	5017.93649	378.364	112.809375	382.032558	513.299088	0	39.7202301	0	0	0	31.2721311	0	64.10999415	83.2246931	5.90179433	1.75962229	0	8.00653774	0	0.61956378	0	0	0.48778871	0				
SL 5 270-275	4404.10984	4642.5044	304.656727	106.542188	542.888372	501.633199	107.044	48.1539776	0	0	0	36.2098361	0	55.08349773	79.953344	5.53081667	1.9341943	0	9.10677826	1.9430434	0.87419971	0	0	0.65736269	0				
SL 5 330-335	4548.68921	4744.22245	378.364	173.392188	643.423256	559.962641	0	38.0878919	124.226041	0	0	36.6213115	0	58.59343282	77.6313827	6.45744722	2.99524269	2.12013592	9.55674748	0	0.65003687	0	0	1.99372857	0				
SL 5 452-457	2246.54088	2219.30297	189.182	213.084375	1015.40233	950.769901	171.2704	31.8305954	0	0	0	77.357377	0	38.80035529	57.900008	4.87578009	5.49181505	0	24.5041545	4.41414515	0.82036866	0	0	0.65077864	0				
SL 6 030-035	6350.37051	6464.18226	520.864727	131.610938	301.604651	128.324772	0	0	0	0	0	0	0	71.31170945	89.0508804	7.30405611	1.84557261	0	1.7994909	0	0	0	0	0	0				
SL 6 091-096	4971.30581	5336.03658	1270.222	217.2625	482.567442	250.8166	0	0	0	30.20525	28.8032787	0	0	67.68615438	73.4464213	18.7663491	3.20985144	0	3.70558207	0	0	0	0	0.96430546	0.42554166				
SL 6 096-101	2015.76997	1826.76376	614.227273	221.440625	693.690698	799.113353	137.628	82.9771931	0	38.154	47.3196721	0	0	39.56630089	50.9466371	15.5240004	5.5966977	0	20.1968174	3.47841463	2.09716833	0	0	0.96430546	1.19595896				
SL 6 354-359	2379.99875	2238.72187	370.993273	225.61875	1105.88372	869.108683	155.9784	116.984239	0	169.562665	32.1924375	0	0	43.20437202	55.0869887	8.58693821	5.22212775	0	20.1162207	3.61024574	2.70769447	3.92466449	0.7451199	0	0				
SL 1 020-025	1684.90566	1756.48583	196.552727	231.885938	1005.34884	985.767566	165.1536	83.7933622	0	110.94841	0	0	0	34.59007264	48.7106714	5.68234503	6.70382916	0	28.4985688	4.77459535	2.42246852	3.20752175	0	0	0				
SL 1 090-095	1773.87758	1824.45198	203.923455	196.371875	1045.56279	968.268734	171.2704	86.7859822	0	150.722369	45.7053125	0	0	35.96925703	49.316492	5.66938189	5.45943651	0	26.9193421	4.76157736	2.41278218	4.19031087	1.27067714	0	0				
SL 1 220-225	1771.0972	1651.53129	388.191636	139.967188	733.904651	717.452134	128.4528	97.6682371	0	477.287501	48.8848125	24.6885246	0	37.93690037	46.6853429	10.2325607	3.68947347	0	18.9117225	3.38595928	2.57449175	12.5810885	1.28858215	0.65077864	0				
SL 2 010-015	3114.01706	3150.94786	226.035636	219.351563	1236.57907	845.776906	143.7448	42.4407938	0	0	0	0	0	45.91366761	67.8233133	4.92305773	4.77747856	0	18.4210269	3.13076274	0.92436078	0	0	0	0				
SL 2 060-065	2227.07827	2209.13117	248.147818	158.76875	663.530233	1009.09934	155.9784	96.0358988	0	169.562665	0	0	0	40.64671149	54.7911059	6.10499126	3.9060663	0	24.8261005	3.83741745	2.36269787	4.17162074	0	0	0				
SL 2 209-214	1568.13002	1648.29481	206.380364	179.659375	603.209302	839.943962	165.1536	119.16069	0	223.990187	32.9873125	0	0	33.35405511	47.0146738	6.18756439	5.38643276	0	25.182664	4.95152987	3.57259979	6.71553087	0.98900456	0	0				
SL 3 020-025	3116.79743	3006.69317	213.751091	225.61875	1105.88372	915.772236	162.0952	78.0801784	0	0	0	0	0	47.1211489	66.144343	4.53620287	4.78805707	0	19.4344208	3.43996706	1.65700922	0	0	0	0				
SL 3 190-195	1798.90093	1792.5495	218.664909	112.809375	562.995349	781.61452	116.2192	152.351568	0	242.830483	33.7821875	0	0	34.5717317	52.0338681	6.32496257	3.26305248	0	22.6084862	3.36168292	4.40682489	7.02396064	0.97716214	0	0				
SL 3 220-225	5588.54848	5756.77943	442.243636	0	0	297.480153	0	0	0	0	0	0	0	63.28272267	88.3108097	6.98837878	0	0	4.70081154	0	0	0	0	0	0				
SL 4 020-025	5763.71194	5770.65008	417.674545	133.7	472.513953	443.303758	0	37.5437792	0	0	0	0	0	67.9593402	84.8111815	6.14594762	1.96735283	0	6.5230733	0	0.55244473	0	0	0	0				
SL 4 060-065	3892.52133	3565.68011	270.26	160.857813	713.797674	629.957971	119.2776	87.330095	0	0	0	0	0	51.60204807	75.4334658	5.23738902	3.11727574	0	12.2080033	2.31148965	1.69237653	0	0	0	0				
SL 4 150-155	1765.53646	1600.20991	159.699091	227.707813	814.332558	1090.76056	180.4456	125.417987	0	157.002467	0	0	0	37.06569979	47.6326218	4.3085411	6.14335663	0	29.4277612	4.86826368	3.38366705	4.23578857	0	0	0				
SL 5 005-010	494.906283	533.557422	0	87.740625	452.406977	524.964976	107.044	57.6759506	0	1182.75192	285.757563	32.9180328	0	27.73759351	17.8424377	0	3.16323855	0	18.9261183	3.8591668	2.07934227	42.6407547	10.3021757	1.186766	0				
SL 5 250-030	875.817299	893.7318	199.009636	91.91875	331.765116	338.310762	103.9856	47.0657521	0	1427.67577	172.487875	24.6885246	0	32.80959969	26.6939343	6.06559173	2.80158097	0	10.3113347	3.16936509	1.43451162	43.5139649	5.25723802	0.75247869	0				
SL 5 046-051	2382.77913	2595.19741	351.338	77.2953125	492.62093	408.306093	73.4016	0	0	715.931251	93.3978125	18.9278689	0	41.21377064	57.8151208	8.52477205	1.87547296	0	9.90703074	1.78099695	0	17.371166	2.26617975	0.45926079	0				
CP0 10-15	8199.31814	6610.28637	651.080909	476.30625	1045.56279	3167.28869	367.008	220.637717	0	0	0	0	0	130.816397	62.6780612	4.97705887	3.64102865	0	24.2117102	2.80551986	1.68662126	0	0	0	0				
CP1 10-15	4573.71256	3899.96262	764.098727	526.44375	1327.06047	3470.60179	535.22	182.821881	307.295997	0	0	0	0	103.601947	44.1469749	7.37533173	5.08140788	2.96612184	33.4993877	5.16611913	1.76465681	0	0	0	0				
Mi1 000-005	27564.6117	30945.4058	1410.26582	0	814.332558	320.81193	0	313.83421	1429.76914	82.2695625	0	0	0	311.215624	88.5707838	4.53147499	0	1.00841406	1.03083491	0	0	4.59414318	0.26434908	0	0				
Mi1 037-042	25281.926	31711.0653	2137.51091	486.751563	713.797674	0	0	1601.86211	1863.09595	140.295438	0	0	0	315.1144199	80.2309397	6.78328497	1.54468197	5.08343006	0	0	0	5.91244268	0.44522062	0	0				
Mi1 042-047	18998.2845	18539.9645	1913.93218	580.759375	1980.53721	1090.76056	293.6064	107.19021	385.75455	1350.22122	441.9505	280.62623	0	254.4308568	74.6697342	7.52240591	2.28258232	1.51614688	4.28706084	1.15397324	0.42129407	5.30682967	1.73701612	1.10295674	0				
Mi1 058-063	29964.0731	28218.4373	1272.67891	0	713.797674	0	0	0	385.75455	2024.28515	137.910813	0	0	337.8470252	88.6912445	3.76702713	0	1.14180242	0	0	0	5.99172109	0.4082049	0	0				
Mi1 085-090	17925.0607	17007.7208	1066.29855	0	743.95814	309.146042	0	34.8232154	173.262637	4881.73005	273.039563	0	0	246.6336077	72.6789057	4.32341138	0	0.70251025	1.25346276	0	0.14119412	19.7934503	1.10706552	0	0				
Mi1 102-107	21837.0446	20635.8188	1201.42855	0	0	0	0	29.382088	0	4123.93147	163.346813	0	0	273.5513357	79.8279584	4.39196739	0	0	0	0	0.10740978	15.0755304	0.59713403	0	0				
Mi1 114-116	12444.9468	11863.0991	970.479091	561.957813	1337.11395	1977.36808	269.1392	131.131171	0	1086.45707	361.668125	299.965574	0	181.0311288	68.744789	5.36084096	3.10420543	0	10.922807	1.48670122	0.72435703	6.00149312	1.99782285	1.65698339	0				
Mi1 117-122	24686.9263	24156.1881	1714.92255	0	1125.9907	734.950967	0	43.5290193	254.990296	1693.53328	260.719	144.427869	0	295.3399931	83.5881591	5.80660454	0	0.86337882	2.48849118	0	0.14738613	5.73418203	0.8827758	0.48902239	0				
Mi2 000-005	22651.6938	23973.558	1449.57636	603.739063	1306.95349	1195.75356	336.424	103.653477	1049.38314	921.081142	0	0	0	283.113045	80.0093608	5.12013272	2.13250175	3.70658703	4.22359046	1.18830272	0.36612046	3.2534041	0	0	0				
Mi2 012-017	28646.1766	29471.8811	1282.50655	476.30625	1045.56279	804.946297	318.0736	66.3817544	248.452083	862.466887	0	0	0	327.0531002	87.5887634	3.92140159	1.45635754	0.75966894	2.4612098	0.97254421	0.20296935	2.63708519	0	0	0				
Mi2 050-055	23469.1232	24643.5101	1184.23018	0	784.172093	583.294418	269.1392	85.4257004	300.757785	736.864913	0	0	0	266.2883543	88.1342457	4.44717226	0	1.129444	2.19046161	1.01070586	0.32080149	2.76716913	0	0	0				
Mi2 103-105	26558.1169	28288.7152	1375.86909	597.471875	884.706977	519.132032	250.7888	70.7346564	993.808332	1362.78142	0	0	0	317.2870315	83.7037581	4.33635464	1.88306428	3.13220596	1.6361159	0.79041617	0.22293586	4.29510595	0	0	0				
Mi2 120-125	9414.34087	9284.08409	928.711636	421.990625	1206.4186	3114.79219	461.8184	352.585056	0	0	0	82.7065574	0	147.7694534	63.7096548	6.28486886	2.85573652	0	21.0787285	3.12526297	2.38604832	0	0.55969996	0	0				
Mi2 159-162	13901.8619	14048.1878	891.858	346.784375	1236.57907	2502.33305	449.5848	313.680995	183.069956	921.081142	0	0	0	195.1025421	71.2541299	4.57122696	1.77744673	0.93832686	12.8257327	2.30435132	1.60777503	4.72101046	0	0	0				
Mi3 017-022	20877.8162	19779.5377	1378.326	789.665625	1085.77674	1493.23371	363.9496	232.880253	0	1473.72983	0	0	0	266.0960119	78.4597109	5.17980706	2.96759662	0	5.61163506	1.3677379	0.87517378	5.53833865	0	0	0				
Mi3 092-097	10037.1443	8825.42815	1162.118	444.970313	864.6	2164.02229	342.5408	332.996998	0	1565.83794	0	93.404918	0	161.4303554	62.1763128	7.19888151	2.7564228	0	13.4052997	2.12191071	2.06279046	9.69977385	0	0.57860814	0				
Mi3 099-104	15247.5621	13688.4758	918.884	355.140625	965.134884	2088.19402	354.7744	216.284815	428.252932	1930.08366	0	63.3672131	0	216.0254378	70.582253	4.25359166	1.64397595	1.982419	9.6664265	1.64228067	1.00120068	8.93452033	0	0.29333218	0				
Mi3 261-262	21419.9888	20652.9259	1378.326	599.560938	2674.22791	3266.44874	541.3368	0	0	0	0	0	0	272.0566127	78.7335716	5.06632052	2.20380946	0	12.0065038	1.98979468	0	0	0	0	0				

IV. XRD

continued

Probebezeichnung	Quartz	Quartz	Microcline	Albite	Illite/Muscovit	Illite/Muscovit	Kaolinite	Pyrite	Andalusite	Aragonite bis; Calcite		Mg-Calcite	Ankerite	Zwischensumme														
	01-086-1560	01-086-1560	01-087-1790	01-089-6423	01-089-5401	01-089-5401	01-089-5401	01-089-6538	01-075-1219	self measured	01-072-1652	01-086-2335	01-079-1347		Quartz	Microcline	Albite	Andalusite	Muscovite	Kaolinite	Pyrite	Aragonite	Calcite	Mg-Calcite	Ankerite	
	4.26 Å	3.34 Å	3.2037Å	3.184 Å	10 Å	4.45 Å	7.16854	1.64052	5.4945 Å	3.4625	3.0303	3.02	3.15		rel. %	rel. %	rel. %	rel. %	rel. %	rel. %	rel. %	rel. %	rel. %	rel. %	rel. %	
	Int/100	Int/100	Int/100	Int/100	Int/100	Int/100	Int/100	Int/100	Int/100	Int/100	Int/100	Int/100	Int/100													
	21.2	100	100	100	100	74.7	100	100	97.4	100	100	100	100													
	Fix	Fix	Fix	Fix	Fix	Fix	Fix	Fix	Fix	Fix	Fix	Fix	Fix													
	1.786	1.400935	1.3513	1.337	4.323	1.8736	3.0584	0.704626	2.3244	1.4531	1.2718	1.255	1.2215													
	RIR	RIR	RIR		RIR	RIR	RIR	RIR	RIR	RIR	RIR	RIR	RIR													
	3.03	3.03	0.55	0.64	0.43	0.43	1	2.59	0.73	0.69	3.2	3.05	3.15													
		zum Vergl.				zum Vergl.																				
ML3 254-265	22818.5161	21630.8063	1378.326	591.204688	2493.26512	2916.47209	547.4536	0	310.565104	0	0	0	0	0	285.6253758	79.88966668	4.82564267	2.06986052	1.08731622	10.2108298	1.91668404	0	0	0	0	0
ML4 010-015	21419.9888	22336.3597	1963.07036	561.957813	1156.15116	1201.5865	302.7816	147.726609	1144.18722	1136.69786	0	0	0	0	278.7799677	76.8347488	7.04164786	2.01577544	4.10426629	4.31016085	1.08609525	0.52990396	4.07740152	0	0	0
ML4 015-020	24534.0059	25257.9796	1422.55036	438.703125	1206.4186	1242.41711	284.4312	135.756129	330.179742	944.10817	0	0	0	0	293.3215169	83.6420257	4.84979888	1.49563908	1.1256581	4.2356835	0.96969088	0.46282363	3.21868024	0	0	0
ML4 020-025	24122.5107	23818.6691	1280.04964	447.059375	1246.63256	927.438125	357.8328	160.785315	362.870805	1038.30965	0	0	0	0	286.9685645	84.0597673	4.46059184	1.55786881	1.26449671	3.23184571	1.24694076	0.56028895	3.61819997	0	0	0
ML4 055-060	25284.7064	24035.9759	1213.71309	442.88125	975.188372	979.934622	302.7816	189.079178	323.641529	0	0	0	0	0	287.3673766	87.9873933	4.22355907	1.54116746	1.12622919	3.4100413	1.05363943	0.65797023	0	0	0	0
ML5 000-005	26955.7102	29009.5263	2783.678	0	1035.5093	402.473148	0	0	836.891227	1138.79123	92.2055	0	0	0	322.097493	83.6880472	8.64234606	0	2.59825439	1.24953828	0	0	3.53554826	0.28626581	0	0
ML5 055-060	8599.69176	8517.0375	830.435273	0	643.423256	0	0	14.1469313	300.757785	2212.68811	44.513	0	0	0	120.0223286	71.6507659	6.91900651	0	2.5058486	0	0	0.11786916	18.4356372	0.37087266	0	0
ML5 060-065	17277.2339	17931.5056	2085.91582	359.31875	1276.79302	647.456804	241.6136	49.7863158	751.894461	2740.2164	111.679938	96.2852459	0	0	243.6140128	70.9205261	8.56238028	1.47495107	3.08641713	2.65771577	0.9917886	0.20436557	11.2481887	0.45842986	0.39523689	0
ML4 075-080	20555.293	21065.3464	2189.106	447.059375	1618.61163	699.953302	266.0808	50.3304286	513.249698	1877.74951	172.487875	130.84918	0	0	269.0215915	76.4075956	8.13728737	1.66179738	1.90783831	2.60184804	0.98906857	0.18708695	6.9799212	0.6411674	0.48638914	0
ML5 110-115	14813.824	14624.2819	1275.13582	576.58125	1367.27442	1265.74889	296.6648	123.241536	251.721189	998.535692	321.1295	213.555738	0	0	201.3613843	73.5683461	6.33257376	2.86341521	1.25009664	6.28595642	1.47329539	0.61204156	4.95892346	1.59479188	1.06055954	0
ML5 328-333	17469.0796	19217.3143	1388.15364	547.334375	1447.70233	1073.26173	266.0808	153.983906	428.252932	906.427578	308.4115	152.245902	0	0	226.93232	76.9792493	6.11703805	2.41188375	1.88713944	4.72943532	1.1725117	0.67854551	3.99426392	1.35904617	0.67088682	0
ML5 403-408	12653.4747	12535.8253	1302.16182	538.978125	1819.6814	2379.84123	370.0664	276.137216	712.665185	1115.7642	211.834188	209.852459	0	0	197.707755	64.0009022	6.58629611	2.72613548	3.60463951	12.037168	1.87178495	1.3966939	5.64350246	1.07145108	1.06142755	0
SL1 40-45	7893.47718	7190.07927	1171.94564	704.014063	2764.7093	3394.77351	339.4824	296.269388	0	820.599563	0	0	0	0	146.2056174	53.9888776	8.01573604	4.81523265	0	23.2191729	2.32195182	2.02638854	5.61264045	0	0	0
SL2 40-45	7326.28121	7156.78972	857.461273	643.43125	2724.49535	3546.43006	339.4824	341.430745	0	0	0	0	0	0	130.5451694	56.1206611	6.568311	4.92880168	0	27.1663063	2.6004976	2.61542228	0	0	0	0
SL3 47-52	11641.4191	12145.5979	1041.72945	777.13125	3237.22326	2659.82255	516.8696	297.085557	0	0	0	0	0	0	169.3405755	68.7455981	6.1516825	4.5891615	0	15.7069417	3.05224899	1.75436723	0	0	0	0
MRB1 005-010	17494.103	20413.8885	2248.07182	958.879688	1890.05581	379.141372	0	0	480.558634	0	0	0	0	0	215.6075451	81.1386401	10.4266844	4.44733827	2.22885815	1.75847915	0	0	0	0	0	0
MRB1 020-025	19629.429	23155.19	3304.54273	570.314063	2091.12558	565.795585	0	0	784.585525	0	96.179875	0	0	0	249.5084676	78.6723961	13.2442107	2.28575033	3.14452464	2.26764082	0	0	3.1260239	0.3854774	0	0
MRB1 038-043	26911.2242	24285.6475	1948.32891	513.909375	1950.37674	454.969646	336.424	0	585.170037	994.34896	64.384875	0	0	0	318.0876004	84.6031854	6.12513316	1.61562216	1.83965058	1.43032814	1.05764575	0	3.1260239	0.2024124	0	0
MRB1 053-058	20224.4287	21596.1297	2513.418	511.820313	2774.76279	530.79792	281.3728	33.1908772	908.811566	1381.62171	80.6798125	0	0	0	264.6614167	76.4162337	9.49672994	1.93386826	3.43386497	2.00557349	1.0631425	0.12540882	5.22033672	0.30484161	0	0
MRB1 070-072	18161.3924	18262.0893	2407.77091	950.523438	7751.23953	624.125027	382.3	53.595105	1036.30671	1212.05905	186.795625	200.388525	0	0	252.1525676	72.0254112	9.54886533	3.76963616	4.10984002	2.47518807	1.51614558	0.2125503	4.80684793	0.74080398	0.79471142	0
MRB1 079-084	19598.8449	19269.098	2284.92545	518.0875	5670.16744	839.943962	367.008	81.3448548	1402.44663	1157.63153	122.013313	140.313115	0	0	265.1255923	73.9228707	8.61827572	1.95412105	5.28974443	3.16809839	1.38427979	0.30681631	4.36635149	0.46020949	0.52923263	0
MRB1 090-095	12389.3393	12705.0472	1653.49982	770.864063	5660.11395	2187.35407	908.3448	108.278436	346.525274	584.049178	0	0	0	0	189.4825495	65.3851204	8.7263963	4.06825887	1.82879782	11.5438286	4.7938177	0.57144278	3.08233756	0	0	0
A.c. chalky	0	0	0	0	0	0	0	0	5913.7596	0	0	0	0	0	59.13759602	0	0	0	0	0	0	0	100	0	0	0
A.c. pristine	0	0	0	0	0	0	0	0	5402.97824	0	0	0	0	0	54.02978242	0	0	0	0	0	0	0	100	0	0	0
MRB1 122-124	17502.4441	19066.1243	4191.48691	917.098438	10586.3233	1481.56782	844.1184	96.0358988	689.781441	0	75.9105625	0	0	0	257.9844358	67.84302234	16.2470534	3.55485956	2.67373277	5.74285738	3.27197413	0.37225462	0	0.29424474	0	0
MRB1 155-160	23079.8711	23688.7474	1960.61345	528.532813	1447.70233	793.280408	315.0152	59.8524015	454.405783	0	0	0	0	0	271.9157116	84.8787698	7.21037208	1.94373767	1.67112735	2.91737614	1.15850312	0.2201138	0	0	0	0
MRB1 187-192	26669.3318	28739.9735	1110.52291	373.942188	1839.78837	379.141372	305.84	0	1219.37667	0	0	0	0	0	300.5815498	88.7257779	3.69458109	1.24406234	4.05672494	1.26135943	1.01749425	0	0	0	0	0
MRB1 200-205	26730.5	27131.4412	2501.13345	749.973438	3257.33023	431.637869	311.9568	0	1909.15811	0	0	0	0	0	326.343597	81.9090685	7.6641107	2.29810986	5.85014729	0.95591519	0	0	0	0	0	0
MRB1 216-221	21233.7038	23329.0354	5358.51873	580.759375	3086.42093	285.814265	0	0	385.75455	0	97.3721875	0	0	0	279.4192295	75.9922783	19.1773442	2.07845171	1.38055835	1.02288688	0	0	0	0.34848062	0	0
MRB1 224-229	21128.0497	21929.9498	3014.62745	689.390625	5680.22093	962.43579	428.176	82.9771931	630.937526	0	67.564375	67.0704918	0	0	270.7122915	78.0461411	11.135909	2.54658044	2.33065711	3.55519797	1.58166442	0.30651432	0	0.24958	0.24775562	0
MRB1 233-238	17608.0983	17734.5425	2550.27164	530.621875	2292.19535	1434.90427	700.3736	96.3079552	640.744845	720.117983	0	0	0	0	242.8144043	72.5166957	10.5029668	2.18529818	2.63882552	5.9094693	2.8843989	0.39663197	2.96571361	0	0	0
MRB1 264-269	24881.5524	25340.7411	1685.43964	467.95	3981.1814	1114.09234	382.3	0	640.744845	0	45.307875	77.357377	0	0	292.9474447	84.9352089	5.75338569	1.5973855	2.1872348	3.80304508	1.30501224	0	0	0.15466213	0.26406572	0
MRB1 310-315	14975.0856	15593.3775	1203.88545	553.601563	2442.99767	2642.32371	623.9136	0	375.947231	0	0	0	0	0	203.7475718	73.4982287	5.90871068	2.71709526	1.84516177	12.9686145	3.06218913	0	0	0	0	0
MRB1 350-355	21450.5729	24495.5565	1800.91436	451.2375	1940.32326	1294.91361	492.4024	0	624.399314	0	0	0	0	0	261.1444007	82.1406579	6.89623962	1.72792332	2.39101169	4.95861142	1.88555603	0	0	0	0	0
MRB2 005-010	25206.856	26487.381	2061.34673	0	924.92093	0	0	0	601.515569	866.65362	0	0	0	0	287.3637188	87.7176008	7.1733019	0	2.0932203	0	0	0	3.01587696	0	0	0
MRB2 030-035	27756.4574	26866.5119	1456.94709	369.764063	1417.54186	0	272.1976	0	787.854631	0	0	0	0	0	306.4322082	90.5794388	4.75454946	1.20667493	2.57105686	0	0.88827999	0	0	0	0	0
MRB2 040-045	20010.34	22410.7988	2719.79836	486.751563	2563.63953	1230.75122	657.556	0	300.757785	0	0	0	0	0	254.0595493	78.7624006	10.7053577	1.91589556	1.18380823	4.84434152	2.58819636	0	0	0	0	0
MRB2 100-105	8249.36484	7783.28046	1203.88545	944.25625	5107.17209	3645.59011	1153.0168	199.689376	258.259402	701.277687	0	0	0	0	163.5533992	50.4383576	7.36080974	5.77338199	1.57905249	22.2899073	7.04978805	1.22094299	4.28775978	0	0	0
MRB2 155-160	12036.232	10948.5613	1434.83491	875.317188	8746.53488	2618.99194	1205.0096	167.858781	290.950466	0	0	0	0	0	186.291949	64.6095126	7.70207686	4.69863133	1.56179839	14.0585353	6.46839333	0.90105225	0	0.15466213	0.26406572	0
MRB2 215-220	20129.896	21619.7098	2547.81473	986.0375	7680.86512	1032.43112	590.2712	97.1241243	784.585525	0	73.1285	0	0	0	262.412887	76.7107753	9.70918294	3.75758032	2.98988946	3.93437659	2.24939867	0.37011949	0	0.27867724	0	0
MRB2 225-230	22351.4135	26001.9084	5965.37527	1245.08125	6333.69767	641.62386	327.2488	48.9701467	853.236758	0	63.1925625	0	0	0	314.9614219	70.9655595	18.9400189	3.95312303	2.7090199	2.03715063	1.03901233	0.15547982	0	0.20063588	0	0
MRB2 265-270	8396.72458	9127.80817	1370.95527	954.701563	6072.30698	3056.46275	1269.236	139.020805	215.761019	0	0	0	0	0	154.0286199	54.5140545	8.90065284	6.1982089	1.40078525	19.8434729	8.24026081	0.90256477	0	0	0	0
MRB2 294-296	17730.4346	22371.961	2830.35927	0	1869.94884	600.793251	351.716	40.5363992	11546.4836	0	120.15082	0	0	0	332.2047403	53.3720098	8.5199244	0	34.7571309	1.80850294	1.05873263	0.12202234	0	0.36167702	0	0
MRB2 300-305	25807.4164	26175.2915	1078.58309	551.5125	2181.60698	1417.40544	379.2416	87.0580386	549.209868	0	0	0	0	0	298.7042693	86.3978826	3.6108727	1.84634957	1.83864084	4.7451797	1.2696223	0.29145227	0	0	0	0

IV. XRD

continued

Probebezeichnung	Quartz	Quartz	Microcline	Albite	Illite/Muscovit	Illite/Muscovit	Kaolinite	Pyrite	Andalusite	Aragonite bio	Calcite	Mg-Calcite	Ankerite	Zwischensumme
	01-086-1560	01-086-1560	01-087-1790	01-089-6423	01-089-5401	01-089-5401	01-089-6538	01-079-0617	01-075-1219	self measured	01-072-1652	01-086-2335	01-079-1347	
	4.26 Å	3,34 Å	3,22037Å	3,184 Å	10 Å	4,45 Å	7.15854	1.64052	5,4945 Å	3.4625	3.0303	3.02	3.15	
	Int/100	Int/100	Int/100	Int/100	Int/100	Int/100	Int/100	Int/100	Int/100	Int/100	Int/100	Int/100	Int/100	
	21.2	100	100	100	100	74.7	100	100	97.4	100	100	100	100	
	Fix	Fix	Fix		Fix	Fix	Fix	Fix	Fix	Fix	Fix	Fix	Fix	
	1.786	1.400935	1.3513	1.337	4.323	1.8736	3.0584	0.704626	2.3244	1.4531	1.2718	1.255	1.2215	
	RIR	RIR	RIR		RIR	RIR	RIR	RIR	RIR	RIR	RIR	RIR	RIR	
	3.03	3.03	0.55	0.64	0.43	0.43	1	2.59	0.73	0.69	3.2	3.05	3.15	
		zum Vergl.				zum Vergl.								
MRB2 320-325	13951.9086	13799.9033	805.866182	549.423438	2664.17442	3406.4394	908.3448	69.6464309	843.429439	0	0	0	0	205.3505828
MRB3 005-010	19901.9055	23387.7545	2808.24709	693.56875	5046.85116	1160.75589	522.9864	0	1212.83846	0	73.1285	0	0	263.7343056
MRB3 025-030	13570.9976	13754.1302	1343.92927	866.960938	2955.72558	3383.10762	1055.148	0	307.295997	0	0	0	0	205.274394
MRB3 045-050	10723.8963	10036.7977	1510.99909	902.475	2855.1907	3628.09128	871.644	133.851734	215.761019	0	0	0	0	179.8671838
MRB 3 100-105	8088.10324	8565.58476	1019.61727	885.7625	4584.3907	4526.36468	1495.5576	141.197256	192.877275	0	0	0	0	163.4947983
MRB 3 205-210	8388.38346	7868.81609	1120.35055	1015.28438	5268.02791	4147.22331	1171.3672	143.91782	310.565104	0	0	0	0	162.9709182
MRB 3 250-255	3308.64313	2982.65072	818.150727	950.523438	3629.3093	4753.84951	1198.8928	192.61591	0	0	0	0	0	112.2267551
MRB 4 002-007	12667.3765	11671.2218	1282.50655	898.296875	3448.34651	3056.46275	914.4616	0	333.448848	0	0	0	0	191.5255317
MRB 4 025-030	16128.9402	15051.4977	1181.77327	816.823438	2292.19535	4345.54341	932.812	0	0	0	0	0	0	234.0589228
MRB 4 045-050	17260.5517	17025.7526	1319.36018	775.042188	2060.96512	3493.93356	755.4248	0	313.83421	0	0	0	0	239.1814666
MRB 4 120-125	8705.34591	8058.38156	1292.33418	933.810938	3910.80698	3622.25834	1330.404	203.770222	0	0	0	0	0	160.8792359
MRB 4 138-152	21311.5543	23775.6701	3407.73291	620.451563	4956.36977	921.60518	406.7672	41.8966811	1075.53599	0	69.154125	0	0	278.5469792
MRB 4 160-165	16523.753	16725.6844	1719.83636	915.009375	8666.10698	1872.37508	1030.6808	72.9111073	712.665185	0	58.025875	0	0	229.0525682
MRB 4 200-205	5165.93188	4677.64336	862.375091	992.304688	5700.32791	5144.65677	1284.528	218.189209	0	0	0	0	0	136.6798563
MRB 4 235-240	4059.34367	3664.62403	840.262909	885.7625	3820.32558	5068.82849	1226.4184	232.064084	0	0	0	0	0	123.1268006
MRB 4 255-260	24678.5852	23297.5953	1083.49691	453.326563	1568.34419	1644.89026	422.0592	0	647.283058	0	0	0	0	289.2964121
MRB 4 265-270	24233.7256	23566.2234	830.435273	482.573438	1638.7186	1493.23371	480.1688	72.3669946	487.096847	0	0	0	0	280.796007
MRB 4 292-297	11794.3396	11495.0647	663.365455	528.532813	1839.78837	3394.77351	929.7536	62.5729653	225.568338	0	0	0	0	175.9890631
SL 6 251-256	3111.23669	3265.61185	1063.84164	311.270313	1377.32791	1329.91127	247.7304	189.351234	0	318.191667	0	756.703279	645.262222	79.73498714
CPO 033-038	6709.03855	6797.63253	463.446762	216.646227	729.390635	1343.81701	212.216259	142.829595	140.375427	574.486681	0	0	0	98.02856508
CPO 105-110	6156.13369	5616.26981	947.416085	154.703434	509.179026	643.951205	203.557929	160.785315	142.74226	1310.90361	0	0	0	97.20193537
CPO 145-150	3585.98527	3505.37055	0	353.745131	1638.16566	2605.5645	749.598548	74.2713892	138.770296	502.937517	0	0	0	80.10872653
CPO 215-220	10547.148	8423.54937	385.100845	356.947664	2859.52375	2116.00549	664.064275	0	192.668052	781.143796	0	0	0	150.4307811
CPO 270-275	8117.99225	9057.66895	442.4795	254.602403	1186.76403	1781.69613	556.521756	0	147.42362	851.522768	0	0	0	121.5223843
CPO 313-318	8067.44508	7610.2673	320.914095	149.693863	737.785298	1220.5494	376.73677	0	133.67049	1094.26324	0	0	0	113.6327293
CP1 070-075	3011.39352	3029.88489	868.166026	211.151992	474.705614	1163.1824	158.535222	170.035232	115.16081	1262.5322	32.1924375	30.0377049	0	70.22387539
CP1 187-192	3564.02033	3218.72445	1398.71589	155.651869	623.085049	980.430422	195.352242	98.2123498	315.576644	2077.08822	46.10275	34.9754098	0	88.66126121
CP1 225-230	5641.48677	5272.13915	325.085926	446.008577	2388.37707	2815.45133	618.298378	120.520972	141.702684	605.732266	0	0	0	107.142869
CP2 005-009	6553.4211	6499.92228	673.706585	202.06457	478.415351	723.016763	141.723198	117.528352	114.150656	974.577116	0	35.3868852	0	95.35575228
CP2 020-025	4737.00383	5307.09317	1254.43145	149.330366	724.585067	1074.125	179.665708	110.998999	167.904571	1823.83068	0	36.6213115	0	95.33911911
CP2 040-045	12021.0234	11646.902	370.779522	207.773978	614.187712	705.786246	197.679684	0	412.724677	1168.44795	0	0	0	150.8421544
CP2 080-085	5387.19391	5458.60683	318.432617	555.531856	2554.41043	3054.83536	610.988802	74.8155019	110.139462	575.857836	0	0	0	106.8779534
CP2 150-155	6821.94947	7132.83975	326.395459	321.803366	1081.50401	1909.04097	407.828465	0	157.956681	635.661123	0	0	0	105.8063553
CP3 005-010	9777.90236	10965.8072	562.710803	202.904373	527.456267	586.537535	159.241713	0	260.923724	1031.16708	0	0	0	125.8138759
CP3 040-045	7820.79824	7022.29072	649.385642	329.242517	2112.85117	1644.68027	472.642078	0	246.660613	793.584671	0	0	0	119.5699404
CP3 110-115	7489.76711	6999.17298	504.899732	428.468808	2455.47405	1880.56454	410.519857	0	0	763.341809	0	0	0	114.7756185
CP3 160-165	10053.2426	9579.02021	1007.20988	330.408214	1376.06117	1034.44932	275.133664	0	272.970381	947.256593	34.9745	0	0	139.5564519
CP3 185-190	10539.0571	10364.8384	858.171319	262.260906	1017.36276	1051.74983	186.871298	0	244.3657	1274.23202	34.179625	38.6786885	0	144.895665
CP3 200-203	11151.7956	11284.3696	904.420176	180.691372	426.398602	445.508611	134.39833	0	615.298122	1520.45167	0	0	0	149.5256384
CP3 206-210	10813.9525	10751.7831	1034.55282	222.771358	703.774347	593.216256	133.774416	0	429.61615	1460.13341	40.1411875	0	0	147.2815812
CP3 215-216	9667.54938	10037.2138	840.090925	196.202661	704.538412	744.948633	123.140359	0	352.239671	1444.04589	31.000125	33.7409836	0	134.3295863
CP3 220-225	11677.3416	12101.258	702.897122	207.040717	420.517312	326.644874	125.519794	0	689.735673	1686.75077	0	0	0	154.1593051
CP3 230-235	11618.5923	11385.9489	761.278196	220.256127	517.855186	454.934648	104.722674	0	363.089835	1664.57575	31.000125	0	0	152.1844964

Probebezeichnung	Quartz rel. %	Microcline rel. %	Albite rel. %	Andalusite rel. %	Muscovite rel. %	Kaolinite rel. %	Pyrite rel. %	Aragonite rel. %	Calcite rel. %	Mg-Calcite rel. %	Ankerite rel. %
MRB2 320-325	67.9418992	3.92434329	2.67553873	4.10726587	16.5884087	4.42338555	0.33915867	0	0	0	0
MRB3 005-010	75.4619519	10.6480159	2.62980104	4.59871329	4.4012321	1.98300482	0	0	0.27728095	0	0
MRB3 025-030	66.1114974	6.54698936	4.22342466	1.49700112	16.4809042	5.14018324	0	0	0	0	0
MRB3 045-050	59.621194	8.40063795	5.01745222	1.19955744	20.1709462	4.8460424	0.74416985	0	0	0	0
MRB 3 100-105	49.4700952	6.23638968	5.41768001	1.17971505	27.6850685	9.14743231	0.86361926	0	0	0	0
MRB 3 205-210	51.4716586	6.87454276	6.22985	1.90564738	25.4476281	7.18758422	0.88308897	0	0	0	0
MRB 3 250-255	29.4817677	7.29015756	8.46966872	0	42.3593242	10.6827717	1.71631007	0	0	0	0
MRB 4 002-007	66.1393624	6.69626934	4.69021998	1.74101513	15.9585133	4.77461982	0	0	0	0	0
MRB 4 025-030	68.9097427	5.04904175	3.48981969	0	18.5660233	3.98537252	0	0	0	0	0
MRB 4 045-050	72.1650885	5.51614722	3.24039399	1.31211759	14.6078775	3.15837515	0	0	0	0	0
MRB 4 120-125	54.1110595	8.0329458	5.80442176	0	22.5153875	8.26958179	1.26660361	0	0	0	0
MRB 4 138-152	76.5097304	12.2339611	2.22745752	3.86123732	3.30861668	1.46031812	0.15041154	0	0.24826737	0	0
MRB 4 160-165	72.1395668	7.50847885	3.99475711	3.11136081	8.17443391	4.49975658	0.31831604	0	0.25332995	0	0
MRB 4 200-205	37.7958539	6.30945272	7.26006534	0	37.6401974	9.39807836	1.59635235	0	0	0	0
MRB 4 235-240	32.9688066	6.82437053	7.19390495	0	41.1675482	9.96061292	1.88475688	0	0	0	0
MRB 4 255-260	85.305535	3.74528291	1.56699684	2.23743894	5.68583014	1.45891612	0	0	0	0	0
MRB 4 265-270	86.303669	2.95743263	1.71859081	1.73470005	5.31785949	1.71002717	0.25772088	0	0	0	0
MRB 4 292-297	67.0174579	3.76935614	3.00321397	1.28171793	19.2896846	5.2830192	0.35555031	0	0	0	0
SL 6 251-256	39.0197177	13.3422187	3.90381091	0	16.6791433	3.10692218	2.37475719	3.99061539	0	9.49022889	8.09258577
CPO 033-038	68.4396282	4.72767057	2.2100316	1.43198492	13.7084228	2.16484102	1.45702015	5.8604008	0	0	0
CPO 105-110	63.3334477	9.74688499	1.59156743	1.46851253	6.62488048	2.09417568	1.65413697	13.4863942	0	0	0
CPO 145-150	44.763978	0	4.41581269	1.73227439	32.5253516	9.35726456	0.92713232	6.2781864	0	0	0
CPO 215-220	70.1129643	2.559987	2.37283661	1.28077545	14.0663066	4.41441752	0	5.19271249	0	0	0
CPO 270-275	66.8024438	3.64113577	2.09510704	1.21313963	14.6614646	4.57958227	0	7.00712691	0	0	0
CPO 313-318	70.9957873	2.82413435	1.31734812	1.17633793	10.7411783	3.31538961	0	9.62982446	0	0	0
CP1 070-075	42.8827589	12.3628327	3.00684049	1.63990963	16.5639163	2.25756869	2.42133079	17.9786745	0.45842582	0.42774206	0
CP1 187-192	40.1981687	15.775953	1.75557923	3.55935207	11.0581601	2.20335509	1.10772561	23.4272351	0.51998753	0.39448356	0
CP1 225-230	52.6538707	3.03413498	4.16274625	1.32255824	26.2775428	5.77078422	1.12486228	5.65350052	0	0	0
CP2 005-009	68.7260175	7.06519081	2.1190601	1.19710298	7.58230883	1.48625745	1.23252504	10.2204334	0	0.37110383	0
CP2 020-025	49.6858359	13.1575733	1.56630738	1.76112988	11.2663618	1.88449096	1.16425451	19.12993	0	0.38411632	0
CP2 040-045	79.692732	2.45806302	1.37742648	2.73613619	4.67897219	1.3105069	0	7.74616322	0	0	0
CP2 080-085	50.4050998	2.97940414	5.19781525	1.0305162	28.582465	5.71669631	0.70000874	5.3879946	0	0	0
CP2 150-155	64.4758006	3.08483794	3.04143702	1.49288462	18.0427817	3.85447985	0	6.00777828	0	0	0
CP3 005-010	77.7172016	4.47256552	1.61273446	2.0738867	4.66194631	1.26569277	0	8.19597264	0	0	0
CP3 040-045	65.4077289	5.43101084	2.75355592	2.06289818	13.7549644	3.95285032	0	6.63699144	0	0	0
CP3 110-115	65.2557329	4.39901556	3.73309953	0	16.384704	3.57671657	0	6.6507314	0	0	0
CP3 160-165	72.037104	7.21722191	2.36755958	1.95598539	7.4124077	1.97148652	0	6.78762307	0.25061185	0	0
CP3 185-190	72.7354894	5.92268457	1.80999829	1.68649421	7.2586701	1.28969558	0	8.7941349	0.23589129	0.26694165	0
CP3 200-203	74.58116	6.04859598	1.2084307	4.1150008	2.97947974	0.89883134	0	10.1685014	0	0	0
CP3 206-210	73.4236585	7.02431909	1.51255409	2.91697133	4.02776947	0.90829019	0	9.91389012	0.27254723	0	0
CP3 215-216	71.9688763	6.25395305	1.46060646	2.62220469	5.54567801	0.91670318	0	10.7500211	0.2307766	0.25118058	0
CP3 220-225	75.7485352	4.5595504	1.34303095	4.47417477	2.11887874	0.81422133	0	10.9416086	0	0	0
CP3 230-235	76.3454397	5.00233739	1.44729675	2.38585299	2.98936264	0.68812972	0	10.9378799	0.20370094	0	0

IV. XRD

continued

Probebezeichnung	Quartz	Quartz	Microcline	Albite	Illite/Muscovit	Illite/Muscovit	Kaolinite	Pyrite	Andalusite	Aragonite bioz	Calcite	Mg-Calcite	Ankerite	Zwischensumme	Quartz	Microcline	Albite	Andalusite	Muscovite	Kaolinite	Pyrite	Aragonite	Calcite	Mg-Calcite	Ankerite
	01-086-1560	01-086-1560	01-087-1790	01-089-6423	01-089-5401	01-089-5401	01-089-6538	01-079-0617	01-075-1219	self measured	01-072-1652	01-086-2335	01-079-1347		rel. %	rel. %	rel. %	rel. %	rel. %	rel. %	rel. %	rel. %	rel. %	rel. %	rel. %
	4.26 Å	3.34 Å	3.22037Å	3.184 Å	10 Å	4.45 Å	7.1585Å	1.64052	5.4945 Å	3.4625	3.0303	3.02	3.15												
	Int/100	Int/100	Int/100	Int/100	Int/100	Int/100	Int/100	Int/100	Int/100	Int/100	Int/100	Int/100	Int/100												
	21.2	100	100	100	100	74.7	100	100	97.4	100	100	100	100												
	Fix	Fix	Fix		Fix	Fix	Fix	Fix	Fix	Fix	Fix	Fix	Fix												
	1.786	1.400935	1.3513	1.337	4.323	1.8736	3.0584	0.704626	2.3244	1.4531	1.2718	1.255	1.2215												
	RIR	RIR	RIR		RIR	RIR	RIR	RIR	RIR	RIR	RIR	RIR	RIR												
	3.03	3.03	0.55	0.64	0.43	0.43	1	2.59	0.73	0.69	3.2	3.05	3.15												
CP3 250-255	11494.5599	11688.144	909.641108	0	678.198272	779.007194	175.478758	0	473.14757	1300.59379	34.9745	0	0	151.6740279	75.7846286	5.99734259	0	3.1195029	5.13606189	1.15694665	0	8.57492745	0.23058991	0	0
CP3 260-262	12208.3927	12337.2902	674.424002	168.409773	387.019088	349.976651	113.84894	0	303.902665	1701.87325	0	0	0	155.2082796	78.6581277	4.34528367	1.08505663	1.95803127	2.2548839	0.73352363	0	10.9650932	0	0	0
CP3 262-264	9836.48481	10104.995	801.881075	219.004778	765.945119	774.352505	151.054376	0	210.736403	1325.73511	29.8078125	34.152459	0	133.8320933	73.4986995	5.99169493	1.6364145	1.57463279	5.7860001	1.12868575	0	9.90595814	0.22272544	0.25518886	0
CP5 005-010	12657.395	12643.1378	398.586819	180.413527	589.838163	419.971981	149.580227	0	286.419484	1403.35295	0	0	0	154.9572	81.6831681	2.57223813	1.16427973	1.84837803	2.71024503	0.96530027	0	9.05639072	0	0	0
CP5 025-030	14527.7515	14662.6111	0	156.886505	376.865065	314.61151	164.107627	0	167.03172	1303.12257	0	0	0	166.3351144	87.3402562	0	0.94319534	1.00418796	1.89143171	0.98660844	0	7.83432035	0	0	0
CP5 050-055	4848.88601	5558.98406	265.343725	237.119039	526.832951	2645.53183	680.680562	108.550492	112.149963	592.504285	0	37.4442623	0	95.28210175	50.8897886	2.78482233	2.48860001	1.17703074	27.7652548	7.14384496	1.13925375	6.21842165	0	0.39298317	0
CP5 080-085	4722.6015	6021.70873	0	232.543992	1238.85116	2677.76468	729.177611	74.5434456	114.114696	518.600083	0	0	0	90.69346011	52.0721284	0	2.56406572	1.25824613	29.5254441	8.04002417	0.82192746	5.71816405	0	0	0
CP6 005-010	10095.5321	9933.04527	1501.41223	472.278538	544.828695	396.640204	147.512749	0	115.716558	556.737029	68.7566875	49.7885246	0	134.0437462	75.3152041	11.2009122	3.52331646	0.86327457	2.9590355	1.10048214	0	4.15339801	0.51294215	0.37143489	0
CP6 025-030	6904.19288	6806.23233	1576.63296	659.059527	663.81173	627.729787	0	0	106.615366	505.210913	81.4746875	97.1081967	0	105.5802432	65.3928488	14.9330302	6.24226187	1.00980413	5.94552321	0	0	4.7850895	0.77168498	0.91975727	0
CP6 052-057	8695.78143	8603.08173	981.677683	409.351797	415.701691	378.756397	0	0	114.016622	912.573701	64.3848475	61.3098361	0	116.1785234	74.8484416	8.44973454	3.52347219	0.98139156	3.26012404	0	0	7.85492597	0.55418913	0.52772091	0
CP6 092-097	7118.44838	6902.30965	828.088925	323.700234	365.383981	793.467063	122.81311	59.0362324	0	1097.25466	73.1285	88.4672131	0	105.0440431	67.7663213	7.88325449	3.08156679	0	7.55366072	1.16915826	0.56201409	10.4456628	0.69616989	0.84219162	0
CP6 124-127	12304.1209	10526.3389	405.655346	194.142845	734.809465	1095.25193	228.477772	91.1388842	161.967874	909.76859	15.5000625	35.3868852	0	154.4141109	79.6826199	2.62706137	1.25728694	1.04891887	7.09295234	1.47964309	0.59022381	5.89174516	0.10037983	0.22916873	0
CP6 130-135	11471.316	11665.6274	568.209365	217.891308	449.179807	525.775755	105.205902	0	168.208598	819.402157	0	0	0	138.7600905	82.670139	4.09490484	1.57027361	1.21222606	3.78909926	0.75818559	0	5.90517168	0	0	0
CP6 145-152	8873.03017	8803.14264	914.69497	268.897858	405.165635	712.51163	176.747994	100.388801	99.9235048	808.688309	36.9616875	32.095082	0	120.2394001	73.7946976	7.60728155	2.23635395	0.83103795	5.925775	1.46996737	0.8349077	6.72565156	0.3074008	0.2669265	0
CBi 1 12-17	3698.00648	3858.1565	695.327385	272.30303	311.748621	385.685935	98.48048	68.5582054	77.5007043	528.618934	24.641125	21.3967213	0	58.70518996	62.9928372	11.8443937	4.63848307	1.32016785	6.56987798	1.67754299	1.16783892	9.00463714	0.41974355	0.36447751	
CBi 1 55-60	6344.50392	6102.89823	1274.8287	201.377269	343.035077	213.660745	79.5153416	0	0	733.680903	29.410375	0	0	88.76977261	71.471445	14.3610676	2.26853424	0	2.40690878	0.89574795	0	8.26498572	0.33131069	0	
CBi 1 120-1	6557.42484	6815.7106	957.155273	233.431844	287.389019	0	77.8454552	0	55.3753925	291.932481	25.436	0	0	81.98601285	79.9822386	11.6746167	2.84721547	0.67542488	0	0.94949678	0	3.56075958	0.31024804	0	
CBi 1 145-1	4513.01703	4558.71647	756.742741	307.675036	504.584581	385.919253	77.866864	0	47.643956	630.965702	25.0385625	22.6311475	0	67.67500294	66.6866174	11.1820127	4.54636162	0.70401114	5.70253766	1.15060008	0	9.32346788	0.36998244	0.33440926	
CBi 1 157-1	5961.36861	5550.47673	1166.78121	293.809928	368.480456	241.058084	75.5027208	0	69.6385036	645.790922	26.6283125	24.2770492	0	85.04855343	70.0937096	13.7190013	3.45461406	0.8188088	2.84335843	0.8877602	0	7.59320289	0.31309542	0.28544929	
CBi 1 187-1	5658.75288	5704.85699	916.589247	229.60677	297.442507	0	98.6119912	0	68.1804821	692.475082	34.5770625	0	0	76.98793515	73.5018139	11.9056219	2.98237341	0.88559957	0	1.28087591	0	8.99459222	0.44912313	0	
CBi 1 207-2	5883.10113	5722.88883	883.95658	220.870311	253.810367	0	78.9464792	0	44.2506236	816.984319	25.436	0	0	79.5354544	73.9682846	11.1139942	2.77700445	0.5563635	0	0.99259481	0	10.2719514	0.31980706	0	
CBi 2 7-12	894.1816568	783.478678	295.689009	130.182019	360.357237	512.120833	124.6298	134.395847	64.1137138	338.817605	0	0	0	24.94130485	35.8514386	11.8553945	5.21953521	2.57058379	20.5330409	4.99692381	5.388485	13.5845982	0	0	
CBi 2 110-1	1340.32855	1206.44546	385.710158	163.607019	329.141156	649.136692	153.8314043	137.660524	66.8564941	0	0	0	0	28.97130841	46.2639979	13.3135222	5.64720849	2.30767948	22.4061918	5.30978446	4.75161569	0	0	0	
CBi 2 136-1	6804.12728	6906.88696	204.115093	104.150211	254.996679	0	107.285614	0	78.3572102	903.524079	0	0	0	82.01559488	82.9613842	2.48873515	1.26988302	0.95539404	0	1.30811236	0	11.0164912	0	0	
CBi 2 136-1	6463.67068	6650.55747	185.919225	98.4658719	290.606135	463.882385	152.702854	0	0	570.634888	0	0	0	79.35275906	81.4548953	2.34294594	1.24086261	0	5.84582553	1.92435468	0	7.1911159	0	0	
CBi 3 0-5	5111.15854	5053.44533	249.545799	157.569628	309.707763	348.220935	96.981864	0	63.2604771	313.104787	0	0	0	63.39842031	80.6196513	3.93615169	2.48538729	0.99782418	5.49258062	1.52972051	0	4.93868437	0	0	
CBi 3 10-15	7232.74949	7082.44307	215.795239	127.792131	261.179574	328.033115	83.5738384	0	106.974967	587.817238	0	0	0	86.82736015	83.30035	2.48533687	1.47179565	1.23204215	3.77799249	0.96252884	0	6.76995404	0	0	
CBi 3 50-55	6904.10947	7114.57673	0	135.674164	356.275521	326.843194	90.3114936	0	84.928114	559.594474	0	0	0	81.01460911	85.2205491	0	1.67468763	1.04830616	4.03437353	1.11475565	0	6.90732795	0	0	
CBi 4 15-20	6667.05492	6691.66081	1126.38717	231.135964	261.9738	145.193647	75.756568	0	53.0739417	783.574194	32.9873125	0	0	91.1516372	73.1424594	12.3572895	2.53573025	0.58225988	1.59288029	0.83110485	0	8.59638091	0.3618949	0	
CBi 4 55-60	6264.34579	6739.19088	935.780164	175.514675	214.209677	0	116.6015	0	45.9603662	750.377592	26.230875	0	0	83.1481096	75.3396056	11.2543769	2.11086789	0.55275299	0	1.40233495	0	9.02458993	0.31547169	0	
CBi 4 95-10	6350.23149	6738.40488	909.152183	177.401098	247.426402	261.695041	75.3345088	0	202.942853	783.423472	25.436	0	0	87.85616646	72.7798609	10.3481886	2.01922193	2.30994433	2.97867584	0.85747548	0	8.91711422	0.28951866	0	
CBi 4 107-1	6789.75276	7218.7915	871.411603	193.031464	280.220881	196.109416	86.3325152	0	68.0268341	736.44624	22.2565	0	0	89.63367328	75.7500224	9.72192225	2.15355967	0.75894284	2.18788891	0.96317056	0	8.21617829	0.24830512	0	
CBi 4 113-1	3231.5434	3139.89758	746.445835	362.080491	689.840212	502.321487	76.3346056	0	63.2604771	313.104787	0	0	0	53.39114919	60.5258259	13.9807037	6.78165756	0.77908249	9.40832881	1.42972397	0	5.19374195	0.72950059	1.17143503	
CBi 4 120-1	4117.53686	4010.17875	1149.89733	342.930055	501.186502	246.056917	77.1603736	0	0	411.612322	46.5001875	40.3245902	0	64.32018643	64.0162458	17.8777052	5.33160853	0	3.82550069	1.1996292	0	6.39942675	0.72294858	0.62693522	
CBi 5 30-35	6074.00149	6361.44702	957.484499	208.208503	346.031016	210.102649	78.0350776	0	57.5591556	652.560868	25.0385625	0	0	82.62990808	73.5085108	11.5876263	2.51977169	0.69658985	2.54269494	0.94439263	0	7.89739313	0.30302058	0	
CBi 5 125-1	5798.91145	5624.26855	970.813231	176.845408	216.883905	143.589587	83.402568	0	77.9354955	717.453128	23.84625	0	0	79.92797118	72.5517158	12.1461012	2.2125597	0.97507161	1.79648732	1.0434716	0	8.97624596	0.29834674	0	
CBi 5 148-1	6566.79469	6517.35306	861.362844	175.740294	256.876681	0	78.539712	0	864.535133	25.0385625	0	0	0	85.7201124	76.6073972	10.0485501	2.05016406	0	0	0.91623436	0	10.0855576	0.29209671	0	
CBi 5 153-1	5160.56576	5761.54169	978.591805	252.279366	297.402293	0	0	0	100.171957	685.12946	27.820625	27.5688525	0	72.32127822	71.3561193	13.5311741	3.48831453	1.3850966	0	0	0	9.4734147	0.38468105	0.38119974	
CBi 5 195-2	4949.06283	5131.49082	910.977667	374.853019	619.415526	370.403621	101.609223	0	81.9630345	335.681742	26.230875	39.5016393	0	71.90283651	68.8298692	12.6695651	5.21332728	1.13991378	5.15144658	1.41314624	0	4.66854659	0.36481002	0.54937526	
CBi 5 208-2	4764.72414	4753.09967	713.55765	267.97867	416.70704	358.866058	108.964675	0	166.639427	537.559701	31.3975625	0	0	69.49687887	68.5602608	10.2674776	3.85598137	2.39779728	5.1637723	1.56790747	0	7.73501933	0.45178378	0	

V. Taxonomic analysis showing abundance data of the shell concentration

Class/Family	Species	Author	ML2 0-5	ML3 17-22	ML3 92-99	ML4 10-25	ML5 55-65	CP0 33-38	CP0 105-110	CP1 70-75	CP1 187-192	CP2 5-25	CP3 5-10	CP6 52-57	CP6 92-97	CP6 130-135	CP6 145-152	CBI3 0-19	SL1 220-225	SL5 5-51	Total number of individuals (gastropods, scaphopods) and of valves (bivalves)
Gastropods																					
Potamididae	*Cerithidea pliculosa*	Menke, 1829	59	116	0	50	0	0	0	0	8	64	47	0	0	0	0	92	0	0	436
Cerithiidae	*Cerithium eburneum*	Bruguière, 1792	0	0	0	0	0	5	1	9	34	1	0	0	0	0	0	0	8	84	142
Cerithiidae	*Cerithium atratum*	Born, 1778	0	0	0	0	0	0	0	0	0	0	0	0	0	0	0	0	0	7	7
Cerithiidae	*Bittium reticulatum*	da Costa, 1778	0	0	0	0	0	0	0	0	0	0	0	0	0	0	0	0	0	2	2
Fissurellidae	*Diodora* sp.	Gray, 1821	0	0	0	0	1	0	0	0	1	0	0	1	0	0	1	0	0	0	3
Calyptraeidae	*Crepidula incurva*	Broderip, 1834	0	0	0	0	2	0	0	0	1	0	0	0	0	0	0	0	0	7	10
Olivellidae	*Olivella* sp.	Swainson, 1831	0	0	0	0	11	0	0	0	0	0	0	2	1	0	1	0	2	1	18
Calliostomidae	*Calliostoma* sp.	Swainson, 1840	0	0	0	0	1	0	0	0	0	0	0	1	0	0	0	0	0	1	3
Modulidae	*Modulus modulus*	Linnaeus, 1758	0	0	0	0	0	0	0	0	0	0	0	0	0	0	0	0	0	5	5
Naticidae	*Eusipira* sp.	Agassiz, 1839	0	0	0	0	1	0	0	1	0	0	0	0	0	0	0	0	0	1	1
Marginellidae	*Prunum apicinum*	Menke, 1828	0	0	0	0	0	1	0	1	1	0	0	0	0	0	0	0	0	0	4
Neritidae	*Neritina virginea*	Linnaeus, 1758	0	0	0	0	0	1	0	1	6	7	0	0	0	0	0	16	7	53	91
Bullidae	*Bulla striata*	Bruguière, 1792	0	0	0	0	0	0	2	19	1	1	0	0	0	0	0	0	6	14	43
Epitoniidae	*Epitonium* sp.	Röding, 1798	0	0	0	0	0	0	0	1	0	0	0	0	0	0	0	0	0	0	1
Buccinidae	*Cantharus* sp.	Röding, 1798	0	0	0	0	0	0	0	1	0	0	0	0	0	0	0	0	0	0	1
Melongenidae	*Melongena melongena*	Linnaeus, 1758	0	0	0	0	0	0	0	1	0	0	0	0	0	0	0	0	0	0	1
Littorinidae	*Littorina* sp.	Ferussac, 1822	0	0	0	0	0	0	0	0	0	0	0	1	0	0	1	0	0	0	2
Conidae	*Conus* sp.	Linnaeus, 1758	0	0	0	0	0	0	0	0	0	0	0	1	1	0	2	0	0	0	4
Truncatellidae	*Truncatella pulchella*	Pfeiffer, 1839	0	0	0	0	0	0	0	0	0	0	0	0	1	0	0	0	0	0	1
Nassariidae	*Nassarius vibex*	Say, 1822	0	0	0	0	0	0	0	0	0	0	0	0	0	0	0	0	4	0	4
Columbellidae	*Anachis obesa*	Adams, 1845	0	0	0	0	0	0	0	0	0	0	0	0	0	0	0	0	0	3	3
Vitrinellidae	*Anticlimax* sp.	Pilsbry & McGinty, 194	0	0	0	0	0	0	0	0	0	0	0	0	0	0	0	0	0	1	1
Rissoinidae	*Zebinella* sp.	Mörch, 1876	0	0	0	0	0	0	0	0	0	0	0	0	0	0	0	0	0	1	1
Mangeliidae	*Mangelia* sp.	Risso, 1826	0	0	0	0	0	0	0	0	0	0	0	0	0	0	0	0	0	2	2
Turbonillidae	*Turbonilla incisa*	Bush, 1899	0	0	0	0	0	0	0	0	0	0	0	0	0	0	0	0	0	1	1
Bivalves																					
Veneridae	*Anomalocardia cuneimeris*	Conrad, 1846	66	6	103	35	0	21	218	19	412	347	73	5	4	171	38	279	30	0	1827
Veneridae	*Chione cancellata*	Linnaeus, 1767	0	0	0	0	29	0	0	0	0	0	5	5	0	2	0	0	0	6	47
unidentified 1			7	0	0	2	0	11	0	0	0	1	3	0	0	0	0	0	0	0	24
Corbulidae	*Corbula* sp.	Bruguière, 1797	0	0	0	0	15	0	0	0	0	0	0	2	1	1	0	0	0	53	72
Mytilidae	*Brachidontes exustus*	Linnaeus, 1758	2	0	0	0	1	0	0	0	0	0	0	1	0	0	0	0	0	11	15
Lucinidae	*Lucina pectinata*	Gmelin, 1791	3	0	0	0	0	0	0	1	0	9	0	0	0	0	0	12	1	0	35
Lucinidae	*Lucina muricata*	Sprengler, 1798	0	0	0	0	6	0	0	0	0	0	0	2	0	0	0	0	16	8	32
Lucinidae	*Lucina nassula*	Conrad, 1846	0	0	0	1	0	0	0	0	0	0	0	0	0	1	0	0	0	0	2
Lucinidae	*Lucinoma filosa*	Stimpson, 1851	0	0	0	0	0	0	0	1	0	0	0	0	0	0	0	0	0	0	1
Nuculanidae	*Nuculana acuta*	Conrad, 1832	0	0	0	0	0	0	0	0	0	0	0	3	0	0	2	0	0	0	5
Nuculanidae	*Nuculana concentrica*	Say, 1824	0	0	0	0	0	0	0	0	0	0	0	0	0	0	0	0	12	9	21
Nuculidae	*Nucula* sp.	Lamarck, 1799	0	0	0	0	0	0	0	0	0	0	0	0	0	0	0	0	1	3	4
Arcidae	*Anadara chemnitzii*	Philippi, 1851	0	0	0	0	8	0	0	0	0	0	0	0	0	0	0	0	0	0	8
Arcidae	*Lunarca ovalis*	Bruguière, 1789	0	0	0	0	9	0	0	0	0	0	0	4	1	0	0	0	0	0	14
Arcidae	*Arcopsis adamsi*	Dall, 1886	0	0	0	0	4	0	0	0	0	0	0	0	0	0	0	0	0	3	7
Tellinidae	*Tellina* spp.	Linnaeus, 1758	0	0	1	0	6	0	0	0	0	1	0	2	5	1	1	0	0	14	31
Tellinidae	*Strigilla mirabilis*	Philippi, 1841	0	0	0	0	3	0	0	0	0	0	0	1	0	0	0	0	0	0	4
Cardiidae	*Trigoniocardia* sp.	Dall, 1900	0	0	0	0	2	0	0	0	0	0	0	0	0	0	0	0	0	0	2
Cardiidae	*Laevicardium* sp.	Conrad, 1830	0	0	0	0	0	0	3	0	20	0	0	0	0	0	2	0	1	0	26
Cardiidae	*Dallocardia muricata*	Linnaeus, 1758	0	0	0	0	0	0	0	0	0	0	0	0	0	0	0	0	0	2	2
Donacidae	*Donax* sp.	Linnaeus, 1758	0	0	0	0	3	0	0	0	0	0	0	0	0	0	0	0	0	0	2
Plicatulidae	*Plicatula gibbosa*	Lamarck, 1801	0	0	0	0	1	0	0	0	0	0	0	0	0	0	0	0	0	0	1
Ungulinidae	*Diplodonta* sp.	Bronn, 1831	0	0	0	0	0	0	0	0	0	0	0	6	10	0	2	0	0	7	25
Crassatellidae	*Crassinella lunulata*	Conrad, 1834	0	0	0	0	0	0	0	0	0	0	0	1	1	1	2	0	0	1	6
Thraciidae	*Thracia corbuloides*	Blainville, 1824	0	0	0	0	0	0	0	0	0	0	0	0	1	0	0	0	0	0	1
Sanguinolaridae	*Tagelus divisus*	Sprengler, 1794	0	0	0	0	0	0	0	0	0	0	0	0	0	0	0	0	1	0	1
Ostreidae	*Crassostrea rhizophorae*	Guilding, 1828	0	0	0	0	0	0	0	0	0	0	0	0	0	0	0	0	0	13	13
Pectinidae	*Aequipecten exasperatus*	Sowerby, 1842	0	0	0	0	0	0	0	0	0	0	0	0	0	0	0	0	0	1	1
Hiatellidae	*Hiatella* sp.	Bosc, 1801	0	0	0	0	0	0	0	0	0	0	0	0	0	0	0	0	0	1	1
unidentified 2			0	0	0	0	0	0	0	4	0	0	0	0	0	0	0	0	0	0	4
unidentified 3			0	0	0	0	0	0	0	0	0	4	0	0	0	0	0	0	0	0	4
unidentified 4			0	1	0	0	0	0	0	0	0	0	0	0	0	0	0	0	0	0	1
unidentified 5			0	1	0	0	0	0	0	0	0	0	0	0	0	0	0	0	0	0	1
unidentified 6			0	0	0	0	3	0	0	0	0	0	0	0	0	0	0	0	0	2	5
Scaphopods																					
Dentaliidae	*Dentalium* sp.	Linnaeus, 1758	0	0	0	0	9	0	0	0	0	0	0	0	0	0	0	0	0	2	11

VI. Taphonomic analysis of *Anomalocardia cuneimeris* valves from lagoonal shell concentrations

Sample	Length	Height	Valve	External			Internal			
				C,L	O	P	L,C	PL	MS	O
ML2 0-5	11.1	8.42	L	-	-	-	-	-	-	-
N = 66	11.05	8.38	R	-	-	-	-	-	-	-
	10.43	7.62	L	x	-	-	-	-	-	-
	12.28	8.8	L	x	x	x	x	x	x	x
	10.55	7.74	R	x	-	-	-	-	-	-
	11.51	8.55	L	x	x	x	x	x	-	x
	8.85	6.71	L	x	x	x	x	-	-	x
	10.06	7.99	L	-	-	-	-	-	-	-
	10.04	7.99	R	-	-	-	-	-	-	-
	9.06	6.42	R	x	x	x	-	-	-	-
	8.85	6.25	L	-	-	-	-	-	-	-
	8.71	6.67	R	x	-	x	x	x	-	x
	7.22	5.9	R	-	x	-	-	-	-	-
	7.75	5.65	R	-	-	-	-	-	-	-
	6.86	5.82	L	x	x	-	x	x	x	x
	7.26	5.64	L	-	-	-	-	-	-	-
	6.84	4.96	R	x	-	-	-	-	-	-
	5.53	4.48	R	x	x	-	x	-	-	-
	5.51	4.87	R	x	-	x	-	-	-	-
	6.88	4.83	L	x	-	-	-	-	-	-
	4.2	3.49	R	x	-	-	-	-	-	-
	4.53	3.47	R	x	-	-	-	-	-	x
	6.61	5.06	L	-	-	-	-	-	-	-
	5.79	4.5	L	-	-	-	-	-	-	-
	4.48	3.38	L	x	-	-	-	-	-	x
	5.25	4.52	L	x	-	x	x	-	-	x
	6.25	5.23	R	-	-	-	-	-	-	-
	5.55	4.74	R	x	x	-	-	-	-	-
	6.52	4.93	L	x	-	-	x	-	-	-
	7.94	5.63	L	-	-	-	x	-	-	-
	7.05	5.46	R	-	-	-	-	-	-	-
	6.87	5.2	L	x	-	x	x	x	-	-
	7.25	5.45	L	-	-	-	-	-	-	-
	6.65	5.67	R	x	x	x	x	x	-	x
	5.68	4.57	R	x	-	-	x	-	-	-
	6.56	5.1	R	x	-	-	x	-	-	-
	5.33	3.87	L	-	-	-	-	-	-	-
	5.9	4.56	L	-	-	-	-	-	-	-
	5.75	4.55	R	-	-	-	x	-	-	-
	5.31	4.03	R	-	-	-	x	-	-	-
	4.65	3.9	R	x	-	x	-	-	-	-
	4.38	3.77	L	-	-	-	-	-	-	-
	3.46	2.99	R	-	-	-	-	-	-	x
	4.51	3.61	L	-	-	-	x	-	-	-
	4.47	3.62	L	-	-	-	x	-	-	-
	4.36	3.53	R	x	x	x	x	-	-	x
	4.69	3.63	L	x	-	-	x	-	-	x
	4.31	3.6	L	x	-	-	-	-	-	-
	4.4	3.55	L	x	x	-	x	-	-	x
	3.87	3.06	L	-	-	-	x	-	-	-
	3.95	3.4	R	x	-	-	x	-	-	x
	3.94	3.28	R	x	x	-	x	-	-	-
	4.4	3.55	L	x	-	-	x	-	-	x
	3.86	3.22	L	x	-	-	-	-	-	-
	3.49	2.95	L	-	-	-	-	-	-	-
	3.68	3.02	R	-	-	-	x	-	-	x
	3.5	2.98	L	-	-	-	x	-	-	x
	3.6	3	L	x	-	-	x	-	-	x
	3.51	3.01	R	x	-	-	x	x	-	x
	3.88	3.24	R	-	-	-	-	-	-	-
	3.46	3.01	L	-	-	-	x	-	-	-
	3.38	2.7	R	x	x	x	x	-	-	x
	3.47	3.97	R	-	-	-	-	-	-	-
	3.54	2.9	L	-	-	-	x	-	-	-
	8.98	6.55	R	-	-	-	-	-	-	-
	8.97	6.5	L	-	-	-	-	-	-	-
ML3 17-22	11.1	7.94	L	x	-	x	x	-	-	x
N = 6	9.72	7.94	R	x	-	x	x	-	-	x
	7.94	6.48	R	x	-	x	x	-	-	x
	6.33	4.87	L	x	-	x	x	-	-	x
	4.91	4.44	L	x	x	-	x	-	-	x
	3.46	3.02	L	x	x	-	x	-	-	x
ML3 92-99	10.48	7.75	R	x	x	x	x	-	-	x
N = 103	11.28	7.96	L	x	x	-	x	-	-	x
	9.93	7.03	L	x	x	x	x	-	-	-
	9.26	7.04	R	x	-	-	x	-	-	x
	12	7.89	L	x	-	-	x	-	-	-
	9.41	6.96	R	x	x	-	x	-	-	x
	8.58	6.41	R	x	x	-	x	-	-	x
	11.5	8.12	R	x	-	-	x	x	-	x
	9.24	6.23	L	x	-	x	x	x	x	x
	9.47	7.13	L	x	-	x	x	x	x	x
	9.08	7.06	L	x	x	x	x	-	-	x
	9.99	7.05	R	x	x	x	x	-	-	x
	11.63	7.95	R	x	x	x	x	-	-	x
	10.18	7.91	R	x	x	x	x	-	-	x
	7.17	5.91	R	x	x	x	x	x	-	x
	8.3	6.99	R	x	-	-	x	-	-	x
	10.88	7.56	L	x	x	-	x	-	-	x
	10.47	7.65	R	x	-	-	x	-	-	x
	7.51	5.92	L	x	x	-	x	x	-	x
	9.95	7.62	L	x	x	-	x	-	-	x
	10.41	7.64	R	-	-	x	x	-	-	-
	9.84	6.68	R	x	-	x	x	x	-	x
	8.09	6.05	L	x	-	x	x	x	-	-
	8.74	6.14	L	x	x	x	x	x	-	x
	7.9	6.44	R	x	-	-	-	-	-	-
	7.5	5.7	R	-	-	-	x	-	-	-
	6.81	5.64	R	x	x	-	x	x	-	x
	6.97	5.74	R	x	x	-	x	-	-	x
	10.17	7.24	L	x	-	x	x	-	-	-
	7.22	5.89	L	x	-	-	x	-	-	-
	7.2	5.59	L	x	-	-	x	-	-	-
	6.38	5.1	R	x	-	-	x	-	-	-
	5.29	4.77	L	x	-	x	x	-	-	x
	6.48	5	L	x	x	-	x	-	-	x
	6.86	5.26	R	x	x	-	-	-	-	-
	6.76	5.38	L	x	x	-	x	-	-	x
	8.9	6.13	R	x	x	-	x	-	-	x
	5	4.34	L	x	x	-	x	x	-	-

continued

Sample	Length	Height	Valve	External			Internal			
				C,L	O	P	L,C	PL	MS	O
	5.3	4.01	L	x	x	-	x	x	x	x
	5.43	4.19	R	x	x	-	x	-	-	x
	6.53	5.65	R	x	x	-	x	x	-	x
	4.71	3.9	R	x	x	-	x	-	-	-
	6.88	4.98	L	x	x	-	x	-	-	x
	5.87	4.45	L	x	-	-	x	-	-	-
	7.17	5.18	R	x	x	x	x	x	-	x
	6.11	4.64	R	x	x	-	x	-	-	-
	5.05	4.05	L	x	-	-	x	-	-	x
	6.37	4.7	L	x	-	-	-	-	-	x
	4.9	3.91	L	x	-	-	x	-	-	-
	4.63	4.01	R	x	-	-	x	-	-	-
	5.37	4.32	L	x	-	-	x	-	-	-
	7.16	5.3	R	x	x	-	x	-	-	x
	6.01	4.32	L	x	-	-	x	-	-	-
	3.9	3.23	L	x	x	x	-	-	-	-
	5.32	4.15	L	-	-	-	x	-	-	-
	4.35	3.56	L	x	-	x	x	-	-	-
	5.43	4.38	R	x	-	x	x	-	-	-
	5.01	3.68	L	x	x	-	x	-	-	-
	5.18	4.02	R	x	-	-	x	x	-	x
	5.03	4.28	R	x	-	-	x	x	-	x
	4.02	3.52	R	x	x	-	x	-	-	x
	3.93	3.4	R	x	x	x	x	x	-	x
	5.54	4.23	R	x	x	x	x	-	-	x
	5.38	4.53	R	x	x	-	x	-	-	x
	4.1	3.15	L	x	-	-	x	-	-	x
	6.08	4.78	L	x	x	x	x	-	-	x
	4.24	3.96	R	x	-	-	x	-	-	x
	4.12	3.37	L	x	x	x	x	-	-	-
	3.54	3.93	L	x	x	x	x	-	-	x
	5.32	4.4	R	x	x	x	x	-	-	x
	3.95	3.2	R	x	-	-	x	-	-	-
	3.34	2.85	R	x	-	-	-	-	-	-
	3.12	2.88	R	x	-	-	x	-	-	-
	3.75	2.95	L	-	-	-	x	-	-	x
	3.97	3.45	L	x	-	x	x	-	-	-
	3.66	3.2	R	-	-	-	x	-	-	-
	4.12	3.64	L	x	-	-	x	-	-	-
	6.19	5.3	L	-	-	-	x	-	-	-
	5.81	4.82	R	x	x	-	x	x	x	x
	3.37	2.87	R	x	x	-	x	-	-	x
	3.93	3.5	L	x	x	x	x	x	-	x
	3.81	3.22	L	x	-	-	x	x	-	x
	3.79	3.25	R	x	x	x	x	-	-	x
	4.63	3.78	R	x	x	-	x	-	-	x
	4.52	3.7	L	x	x	-	x	x	-	x
	3.59	2.96	R	x	x	x	x	-	-	x
	3.34	2.75	R	x	-	-	x	x	-	x
	3.5	3.18	L	x	x	-	x	-	-	x
	3.92	3.61	L	x	-	-	x	-	-	-
	3.53	2.92	L	x	-	-	x	-	-	x
	3.29	2.96	R	x	-	x	x	-	-	x
	3.23	2.86	L	x	-	-	x	-	-	-
	3.3	2.97	L	x	x	x	x	x	-	x
	3.44	3.06	L	x	x	-	x	x	-	x
	4.04	3.45	R	x	x	-	x	x	-	x
	3.99	3.53	R	x	x	-	x	-	-	x
	4.49	3.8	L	x	x	-	x	x	-	x
	3.83	3.14	L	x	x	-	x	x	-	x
	2.23	1.92	L	x	x	-	x	x	-	x
	3.19	2.83	L	x	x	-	x	-	-	x
	2.77	2.59	R	x	-	-	x	-	-	x
	3.81	3.9	R	x	x	x	x	x	x	x
	4.02	3.61	R	x	-	-	x	-	-	x
ML4 10-25	16.21	10.6	L	x	x	x	-	-	-	-
N = 35	16.02	10.84	R	x	-	x	-	-	-	-
	9.05	7.02	L	x	-	x	-	-	-	-
	8.3	6.28	R	x	-	x	-	-	-	-
	9.1	6.58	R	x	x	x	x	-	-	x
	8.76	6.37	L	x	x	x	x	-	-	-
	8.75	6.74	R	x	-	x	x	-	-	-
	8.77	6.5	L	x	-	-	x	-	-	x
	8.71	6.7	R	x	-	x	x	-	-	x
	9.22	7.11	R	x	x	x	x	-	-	-
	9.51	7.47	R	x	x	x	-	-	-	-
	8.34	6.24	L	x	-	x	-	-	-	-
	5.44	4.04	L	x	-	x	x	-	-	x
	5.88	4.8	L	x	x	x	x	-	-	-
	7.49	5.39	R	x	x	x	-	-	-	x
	6.33	5.07	R	x	x	-	x	-	-	-
	6.24	5.09	R	x	x	-	x	x	-	x
	6.69	5.48	L	x	-	x	x	-	-	-
	6.18	4.78	L	x	x	x	x	-	-	x
	4.11	3.34	R	x	-	-	x	-	-	x
	4.1	3.37	L	-	-	-	-	-	-	-
	4.34	3.65	R	x	-	x	x	-	-	x
	4.52	3.46	R	x	-	-	x	x	-	x
	4.28	3.52	R	x	-	-	-	-	-	-
	4.41	3.34	L	x	-	x	x	-	-	x
	3.93	3.18	R	x	x	-	x	-	-	x
	3.32	2.61	R	x	-	-	x	-	-	x
	3.19	2.82	L	x	-	-	x	-	-	x
	3.81	3.26	L	x	x	x	x	x	-	x
	2.83	2.38	R	x	x	-	-	-	-	x
	2.58	2.77	R	x	-	-	x	-	-	x
	5.71	4.84	L	x	-	x	x	-	-	x
	5.23	3.9	L	x	x	-	x	-	-	x
	11.58	9.38	R	x	x	x	x	-	-	x
	11.56	9.2	L	x	x	x	x	-	-	x

continued

Sample	Length	Height	Valve	External				Internal			
				C,L	O	P		L,C	PL	MS	O
CP0 33-38	10.87	7.57	R	x	-	x		x	-	-	-
N = 21	6.86	5.34	L	-	-	x		x	-	-	-
	7.41	5.56	L	-	-	-		x	-	-	x
	5.83	4.36	L	-	-	-		x	-	-	-
	7.87	5.77	R	x	-	x		x	-	-	-
	7.74	5.49	R	-	-	x		x	-	-	-
	7.98	5.56	L	-	-	x		x	-	-	-
	8.2	6.1	R	-	-	x		x	-	-	-
	7.96	5.63	L	-	-	-		x	-	-	x
	7.67	5.8	R	-	-	-		x	-	-	x
	7.84	4.23	L	-	-	x		x	-	-	x
	5.94	4.26	L	-	-	x		x	-	-	x
	4.88	3.87	R	-	x	-		x	x	x	x
	4.25	3.69	L	-	-	-		x	-	-	x
	5.35	4.03	R	-	-	-		x	-	-	-
	4.7	3.8	L	x	x	x		x	-	-	x
	5.12	4.07	R	-	-	-		x	-	-	x
	4.01	3.29	L	-	-	-		x	-	-	-
	4.75	3.76	R	-	-	x		x	-	-	-
	3.9	3.09	R	-	-	-		x	-	-	x
	3.63	2.83	L	-	-	-		x	-	-	x
CP0 105-110	11.67	8.22	R	x	-	-		x	-	-	x
N = 218	11.49	8.27	R	x	x	-		x	-	-	x
	10.82	8.02	L	x	x	-		x	-	-	-
	13.82	9.42	L	x	-	-		x	-	-	-
	11.46	8.15	L	x	x	-		x	-	-	x
	10.18	8	L	x	x	-		x	x	-	x
	9.46	6.66	L	-	-	-		x	-	-	-
	11.34	8.4	L	-	-	-		x	-	-	-
	10.69	8.06	L	-	-	-		x	-	-	-
	10.47	7.5	L	x	x	-		x	-	-	x
	10.84	8.13	R	x	-	-		x	-	-	x
	12.1	7.78	L	x	x	-		x	-	-	x
	10.22	7.08	L	x	x	-		x	-	-	-
	8.83	6.38	L	x	x	-		x	-	-	x
	9.98	6.9	L	x	x	-		-	-	-	-
	10.1	7.38	R	-	x	-		x	-	-	-
	9.14	6.94	L	-	x	-		x	-	-	-
	9.75	7.48	L	-	x	-		x	-	-	-
	9.8	7.11	L	-	-	-		x	-	-	x
	8.37	6.65	R	-	x	-		x	-	-	-
	9.47	7.45	R	-	x	-		x	-	-	-
	8.56	6.47	R	-	-	-		x	-	-	-
	7.87	6.23	R	x	x	-		x	-	-	-
	7.19	5.55	R	-	x	-		x	-	-	-
	8.53	6.1	L	-	x	-		x	-	-	-
	7.82	6.3	L	-	-	-		x	-	-	x
	7.75	6.11	L	x	-	-		x	-	-	x
	8.41	6.34	R	x	-	-		x	-	-	-
	8.75	6.81	R	-	x	x		x	-	-	x
	8.53	6.63	L	-	-	-		x	-	-	x
	7.55	5.82	R	-	x	-		x	-	-	x
	7.99	6.33	L	-	x	-		x	-	-	-
	7.92	5.99	L	-	x	-		-	-	-	-
	7.47	5.53	R	-	-	-		x	-	-	-
	7.3	5.67	L	x	x	-		x	-	-	x
	7.52	5.88	R	-	-	-		x	-	-	x
	8.08	6.04	L	-	x	-		-	-	-	-
	6.21	5.29	R	x	x	-		x	-	-	x
	6.69	5.54	L	x	-	-		x	-	-	x
	7.71	5.78	L	x	-	-		x	-	-	x
	7.87	5.97	R	x	-	x		x	-	-	x
	7.64	5.73	R	-	-	-		x	-	-	x
	5.48	4.68	L	-	x	-		x	-	-	x
	7.43	5.23	R	x	x	-		-	-	-	x
	7.55	5.88	L	x	-	-		x	-	-	-
	6.42	5.25	R	-	x	-		x	-	-	-
	7.53	5.88	R	-	x	-		x	-	-	-
	7.26	5.55	L	-	x	-		x	-	-	-
	7.47	6.22	R	x	x	-		x	x	-	x
	7.29	5.54	L	x	x	-		x	-	-	-
	7.59	5.3	L	-	-	-		x	-	-	x
	7.02	5.54	R	-	x	-		-	-	-	-
	7.13	5.56	L	-	x	-		-	-	-	-
	5.78	4.72	L	x	x	-		x	-	-	-
	7.17	5.45	R	x	x	-		x	-	-	-
	6.72	5.09	L	x	x	-		x	-	-	x
	6.9	5.52	R	x	x	-		x	-	-	x
	6.8	5.18	R	x	x	-		x	-	-	x
	6.55	5.66	R	-	x	-		x	-	-	x
	6.86	5.35	L	x	-	-		x	-	-	x
	5.21	3.94	L	x	x	-		x	-	-	x
	6.17	4.94	L	x	x	-		x	-	-	x
	6.35	4.87	L	-	x	-		x	-	-	x
	6.31	4.89	R	x	x	-		x	-	-	x
	5.5	4.24	L	x	x	-		x	x	-	x
	5.78	4.64	L	-	x	-		x	-	-	x
	5.41	4.5	R	x	-	-		x	-	-	x
	6.87	5.3	L	-	-	-		x	-	-	-
	6.5	5.17	R	x	x	-		x	-	-	x
	5.55	4.53	R	x	x	-		x	-	-	-
	5.94	4.82	L	x	x	-		x	-	-	x
	5.57	4.34	R	x	x	-		x	-	-	x
	4.39	3.84	R	x	x	-		x	x	-	x
	5.94	4.71	R	-	x	-		x	-	-	-
	5.35	4.35	L	-	x	-		x	-	-	x
	5.49	4.38	R	-	x	-		x	-	-	x
	6	4.58	L	x	x	-		x	x	-	x
	5.71	4.64	R	-	x	-		x	-	-	x
	6.09	5.09	L	x	x	-		x	-	-	-
	5.43	4.25	L	-	x	-		x	-	-	-
	5.91	4.77	L	x	x	-		x	-	-	-
	6.1	4.83	L	x	x	-		x	-	-	x
	6.05	4.66	R	x	x	-		x	-	-	x
	5.09	4.03	R	x	x	-		x	-	-	x
	5.75	4.29	L	x	x	-		x	-	-	x
	5.73	4.76	R	-	x	-		x	-	-	x
	5.69	4.31	R	x	x	-		x	-	-	x
	5.55	4.87	L	x	x	-		x	-	-	x
	5.31	4.55	L	x	x	-		x	x	-	x
	5.64	4.45	R	x	x	-		x	-	-	x
	6.16	5.06	R	-	x	-		x	-	-	x

continued

Sample	Length	Height	Valve	External			Internal			
				C,L	O	P	L,C	PL	MS	O
	6.18	4.48	L	x	x	-	x	-	-	x
	5.05	4.13	R	x	x	-	x	-	-	x
	4.96	3.99	L	-	-	-	x	-	-	-
	6.23	4.81	R	-	x	-	-	-	-	-
	4.61	3.89	R	x	x	-	x	-	-	x
	4.84	3.88	L	x	x	-	x	-	-	x
	6.48	5.32	L	x	x	-	x	-	-	x
	5.1	4.46	L	x	x	-	x	x	-	x
	5.11	4.13	R	x	x	-	x	-	-	x
	5.82	4.51	L	-	x	-	x	-	-	x
	5.81	4.56	L	x	x	-	x	-	-	x
	6.44	5.05	L	x	x	-	x	-	-	x
	6.41	4.86	L	-	-	-	x	-	-	-
	4.77	4.54	L	-	x	-	x	-	-	-
	6.44	3.73	R	x	-	-	x	-	-	-
	6.5	4.81	L	-	-	-	x	-	-	x
	5.22	4.16	R	x	x	-	x	-	-	-
	6.74	5.12	L	-	-	-	x	-	-	x
	6.38	5.11	R	x	x	-	x	-	-	x
	5.82	4.55	L	-	x	-	x	-	-	x
	4.29	3.71	L	x	-	-	x	-	-	-
	3.67	2.96	L	x	-	-	x	-	-	x
	5.76	4.49	L	x	x	-	x	x	-	x
	4.86	3.92	L	-	x	-	x	-	-	-
	5.52	4.2	L	x	x	-	x	x	-	x
	4.95	3.9	R	x	x	-	x	x	-	x
	4.93	4.14	R	x	x	-	x	x	x	x
	5.23	3.92	R	x	x	-	x	-	-	x
	5.96	4.75	R	x	x	-	x	-	-	x
	4.65	3.35	L	x	x	-	x	-	-	x
	3.88	3	L	x	x	-	x	x	-	x
	6.45	4.75	L	-	x	-	x	-	-	x
	4.12	3.59	L	x	x	-	x	-	-	x
	4.41	3.36	L	x	x	-	x	-	-	-
	5.03	4.02	L	-	x	-	x	x	-	x
	5.89	3.18	R	-	x	-	x	-	-	x
	4.54	3.43	L	-	x	-	x	-	-	x
	5.11	4.04	R	x	x	-	x	x	-	x
	4.09	3.36	L	-	x	-	x	x	-	x
	5	3.76	L	-	-	-	-	-	-	-
	3.87	2.99	L	-	x	-	x	-	-	x
	3.6	2.91	L	-	x	-	x	-	-	x
	3.92	3.3	L	x	x	-	x	x	-	x
	3.2	2.82	R	x	x	-	x	-	-	x
	4.19	3.28	L	-	x	-	x	-	-	-
	5.7	4.41	L	x	x	-	x	-	-	x
	3.9	3.17	L	x	x	-	x	-	-	x
	5.15	4.06	R	x	x	-	x	x	-	x
	5.2	4.25	R	-	x	-	x	-	-	x
	3.28	2.55	R	x	x	-	x	-	-	x
	3.55	2.79	L	x	x	-	x	-	-	x
	5.24	3.74	R	x	x	-	x	-	-	x
	5.31	4.12	R	x	x	-	x	-	-	x
	4.65	3.92	R	x	-	-	x	-	-	x
	4.86	4.27	R	-	-	-	x	-	-	x
	4.37	4.26	L	-	x	-	x	-	-	x
	3.54	2.75	R	x	x	-	x	-	-	x
	3.61	3.04	L	x	x	-	x	-	-	x
	3.47	3.01	L	-	x	-	x	-	-	x
	4.34	3.93	L	-	x	-	x	x	-	x
	5	3.64	R	x	x	-	x	-	-	x
	3.37	3.03	R	x	x	-	x	-	-	x
	4.53	3.88	R	x	x	-	x	x	-	x
	3.55	3.96	L	-	-	-	x	-	-	x
	4.48	3.56	R	x	x	-	x	-	-	x
	4.07	3.48	R	x	x	-	x	x	-	x
	3.52	3.06	L	x	x	-	x	x	-	x
	4.5	3.57	R	x	x	-	x	-	-	x
	4.46	3.48	L	-	x	-	x	-	-	x
	3.51	2.88	L	x	x	-	x	x	-	x
	3.39	2.86	R	x	-	-	x	-	-	x
	4.56	3.45	R	x	x	-	x	x	-	x
	4.12	3.7	L	x	x	-	x	x	-	x
	4.27	3.5	L	-	x	-	x	-	-	-
	5.31	4.01	L	x	x	-	x	x	-	x
	4.03	3.5	L	x	x	-	x	x	-	x
	4.08	3.23	L	x	x	-	x	x	-	x
	4.33	3.8	R	-	x	-	x	x	-	x
	4.69	3.73	L	-	-	-	x	-	-	x
	3.42	3.3	L	x	x	-	x	-	-	x
	4.26	3.49	L	x	x	-	x	-	-	x
	3.68	2.92	R	x	x	-	x	-	-	x
	3.75	3.19	L	x	x	-	x	x	-	x
	5.64	4.78	L	-	x	-	x	-	-	x
	4.13	3.34	R	x	x	-	x	-	-	x
	5.04	3.96	L	-	x	-	x	-	-	x
	3.34	2.91	R	x	x	-	x	-	-	-
	4.52	3.48	R	x	x	-	x	x	-	x
	4.57	3.89	L	x	-	-	x	-	-	-
	5.08	4.43	R	x	x	-	x	-	-	x
	6.77	5.51	R	x	x	-	x	-	-	-
	4.85	3.84	L	x	x	-	x	x	-	x
	4.99	4.13	R	-	x	-	x	-	-	x
	4.82	3.68	L	x	-	-	x	x	-	x
	3.63	3.05	L	x	x	-	x	x	-	x
	5.71	4.37	R	x	x	-	x	-	-	x
	5.09	4.43	L	x	x	-	x	x	-	x
	3.8	2.79	L	x	x	-	x	-	-	x
	4.34	3.52	R	x	x	-	x	x	-	x
	4.41	3.69	R	-	x	-	x	-	-	x
	5.28	4.11	L	-	x	-	x	-	-	x
	3.46	3	L	-	x	-	x	-	-	x
	4.18	3.33	L	x	x	-	x	-	-	x
	3.77	3.12	L	-	x	-	x	-	-	x
	4.61	4.06	R	x	-	-	x	-	-	-
	3.47	2.81	R	-	x	-	x	x	-	x
	6.88	5.8	R	x	x	-	x	-	-	x
	5.01	4.35	R	x	x	-	x	x	-	x
	5.32	4.38	L	x	x	-	x	x	-	x
	5.75	4.63	L	x	x	-	x	x	-	x
	3.59	2.88	L	-	x	-	x	-	-	x
	3.9	3.21	L	x	-	-	x	-	-	x
	4.34	3.6	R	-	-	-	x	-	-	x
	4.44	3.75	R	x	x	-	x	-	-	x
	3.38	2.82	L	x	x	-	x	-	-	-
	3.35	2.88	L	x	-	-	x	-	-	x
	3.66	3.31	R	x	x	-	x	-	-	x
	4.49	3.79	R	x	x	-	x	x	-	x
	3.48	3.53	R	x	x	-	x	-	-	x
	4.66	2.97	L	x	x	-	x	-	-	x
	3.8	2.69	L	x	x	-	x	-	-	x
	5.28	4.53	L	x	x	-	x	x	-	x
	4.25	3.37	R	x	x	-	x	-	-	x
	3.4	2.83	R	x	x	-	x	x	-	x
	4.31	3.33	R	x	x	-	x	-	-	x
	5.05	3.74	L	x	x	-	x	-	-	x
	3.67	3.11	L	x	x	-	x	-	-	x

continued

Sample	Length	Height	Valve	External			Internal			
				C,L	O	P	L,C	PL	MS	O
CP1 70-75	10.83	8.14	R	-	-	-	x	-	-	-
N = 19	5.54	4.23	R	-	-	-	-	-	-	-
	10.63	8.08	R	x	-	x	x	-	-	-
	7.82	5.8	L	-	-	-	x	-	-	-
	6.25	4.97	R	-	-	-	-	-	-	-
	5.31	4.22	R	x	-	x	x	-	-	-
	4.83	3.84	R	x	-	x	-	-	-	-
	4.88	3.74	L	-	-	-	x	-	-	-
	5.15	4.04	L	x	-	x	-	-	-	-
	6.65	5.05	L	x	x	-	x	-	-	x
	4.56	3.7	L	x	x	-	x	-	-	x
	4.13	3.26	L	x	-	-	-	-	-	x
	3.41	2.68	L	x	x	-	-	-	-	-
	4.16	3.45	R	-	-	-	-	-	-	-
	3.82	3.05	L	x	x	-	x	-	-	x
	3.73	2.87	L	-	-	-	-	-	-	-
	3.62	2.96	L	x	x	-	-	-	-	x
	4.19	3.29	L	-	-	-	x	-	-	x
	3.88	2.97	R	-	-	-	-	-	-	-
CP1 187-192	8.61	6.35	R	-	-	-	-	-	-	x
N = 412	7.82	6.32	L	-	-	-	x	-	-	x
	8.27	6.65	R	-	x	-	x	-	-	-
	7.73	5.64	R	x	x	-	x	-	-	x
	9.55	7.31	L	-	x	-	x	-	-	-
	7.90	6.01	L	x	x	-	x	x	-	x
	7.93	6.43	R	x	x	-	x	-	-	x
	8.05	5.90	L	-	-	-	x	-	-	-
	8.60	6.25	L	-	-	-	x	-	-	-
	9.11	6.48	R	-	-	-	-	-	-	-
	8.24	6.47	R	-	-	-	-	-	-	-
	8.15	6.41	L	-	-	-	-	-	-	-
	9.23	7.08	R	-	x	-	x	-	-	x
	8.43	6.55	L	-	-	-	x	-	-	-
	8.56	7.05	L	-	-	-	x	-	-	-
	8.69	6.49	L	-	-	-	-	-	-	-
	7.75	5.74	L	-	-	-	x	-	-	x
	9.95	6.74	L	-	-	-	x	-	-	x
	7.79	5.96	R	x	x	-	x	-	-	x
	7.25	5.72	L	x	-	-	x	-	-	x
	7.07	5.65	L	-	-	-	x	-	-	x
	7.21	5.55	L	-	-	-	x	x	-	x
	8.21	6.23	R	-	x	-	x	-	-	-
	7.02	5.50	L	x	-	-	x	-	-	x
	8.91	6.55	L	x	x	-	-	-	-	-
	7.29	5.62	L	-	-	-	-	-	-	-
	7.47	5.61	R	-	-	-	-	-	-	-
	7.62	5.39	R	x	x	-	-	-	-	-
	7.13	5.60	R	-	-	-	-	-	-	-
	7.87	6.03	R	x	x	-	x	-	-	x
	7.12	5.48	R	-	-	-	x	-	-	-
	7.10	5.17	L	x	x	-	-	-	-	-
	6.86	5.47	R	-	-	-	-	-	-	-
	7.42	5.85	L	-	-	-	x	-	-	x
	8.29	6.14	R	-	-	-	-	-	-	-
	7.40	5.74	R	x	x	-	x	-	-	x
	6.98	5.59	L	-	-	-	-	-	-	-
	7.45	5.63	R	-	-	-	x	-	-	-
	7.44	5.80	R	x	x	-	x	-	-	x
	7.54	5.79	L	-	-	-	x	-	-	x
	7.58	5.64	L	x	x	-	x	-	-	x
	7.28	5.52	R	-	-	-	x	-	-	-
	7.03	5.49	L	-	-	-	-	-	-	-
	7.69	5.67	L	x	x	-	x	-	-	-
	6.97	5.68	R	-	x	-	x	-	-	-
	7.48	5.97	R	x	x	-	x	-	-	-
	7.29	5.46	R	-	x	-	-	-	-	-
	7.05	5.22	L	x	-	-	x	-	-	x
	6.71	4.85	R	-	-	-	-	-	-	-
	6.69	5.32	L	-	x	-	x	-	-	-
	6.60	5.23	R	-	-	-	-	-	-	-
	7.20	5.35	R	-	-	-	-	-	-	-
	6.59	5.05	R	x	x	-	x	-	-	x
	7.52	5.51	L	-	-	-	-	-	-	-
	6.94	5.43	L	-	x	-	-	-	-	-
	7.76	5.57	L	x	x	-	x	-	-	-
	6.76	5.20	L	x	x	-	x	-	-	x
	8.53	6.47	L	x	x	-	x	-	-	x
	6.46	5.03	L	x	x	-	x	-	-	x
	6.55	5.03	L	-	-	-	x	-	-	x
	7.67	5.83	R	-	-	-	x	-	-	-
	7.39	5.97	L	x	x	-	-	-	-	x
	6.45	4.66	L	x	x	-	-	-	-	-
	6.79	4.83	R	-	-	-	-	-	-	-
	6.67	5.06	L	x	x	-	x	-	-	-
	6.47	4.75	R	-	-	-	-	-	-	-
	6.78	5.35	R	x	x	-	x	-	-	x
	6.52	4.95	R	-	x	-	x	-	-	x
	6.30	4.75	R	-	x	-	x	-	-	x
	6.30	5.12	R	x	x	-	x	-	-	-
	6.24	4.84	R	-	-	x	-	-	-	-
	5.92	4.69	R	x	x	-	-	-	-	x
	6.80	5.12	R	x	-	-	-	-	-	-
	6.44	5.12	R	-	-	-	x	-	-	x
	6.82	5.17	R	x	-	-	x	-	-	-
	7.09	5.52	R	-	x	-	x	-	-	-
	7.08	5.36	R	-	-	-	x	-	-	x
	6.41	4.96	L	x	x	-	x	-	-	x
	6.24	5.00	L	-	-	-	x	-	-	x
	6.62	5.04	R	-	x	-	-	-	-	x
	6.74	5.06	L	x	x	-	x	-	-	-
	6.47	4.80	R	x	x	-	x	-	-	x
	6.88	4.17	L	x	x	-	x	-	-	-
	8.00	5.65	L	-	-	-	-	-	-	-
	6.51	5.20	L	-	-	-	x	-	-	-
	6.66	5.51	L	-	x	-	-	-	-	-
	7.13	5.05	L	-	x	-	x	-	-	-
	6.23	5.18	R	x	x	-	x	-	-	x
	7.35	4.92	R	-	x	-	x	-	-	x
	6.66	5.01	L	x	x	x	x	-	-	x
	6.31	4.90	R	-	-	-	x	-	-	-
	6.50	4.96	R	-	-	-	-	-	-	x
	6.38	5.02	R	x	x	-	x	-	-	x

continued

Sample	Length	Height	Valve	External			Internal			
				C,L	O	P	L,C	PL	MS	O
	6.15	4.80	L	x	x	-	x	x	-	-
	6.66	5.75	R	-	-	-	-	-	-	-
	6.26	4.65	L	-	x	-	x	-	-	-
	6.47	4.68	L	-	x	-	x	-	-	-
	6.15	4.75	R	x	x	-	x	-	-	-
	6.09	4.60	L	-	x	-	x	-	-	-
	6.38	4.87	R	-	x	-	-	-	-	-
	6.10	4.81	R	x	x	-	x	-	-	x
	6.31	4.63	L	-	-	-	-	-	-	-
	6.18	4.85	R	x	x	-	-	-	-	-
	6.03	4.64	L	x	x	-	x	-	-	x
	6.01	4.91	L	-	-	-	-	-	-	-
	6.34	5.30	L	x	x	-	x	-	-	x
	6.07	4.84	L	-	-	-	-	-	-	-
	7.00	5.17	L	-	-	-	x	-	-	-
	6.25	4.45	L	-	-	-	-	-	-	-
	6.05	4.80	R	x	x	x	x	-	-	x
	5.99	4.80	L	x	x	-	-	-	-	-
	5.66	4.31	L	-	-	-	-	-	-	-
	6.34	4.96	R	x	-	-	-	-	-	-
	5.83	4.74	R	-	-	-	-	-	-	-
	5.90	4.73	L	-	-	-	x	-	-	x
	6.27	4.99	L	-	-	-	-	-	-	-
	5.88	4.48	L	x	x	-	x	-	-	-
	6.22	4.80	R	x	x	x	x	-	-	x
	5.33	4.19	L	x	x	-	x	-	-	-
	6.33	4.86	L	x	x	-	x	-	-	x
	6.09	4.68	R	-	x	-	x	-	-	x
	5.60	4.77	R	-	-	-	-	-	-	-
	5.10	4.38	R	x	x	x	x	x	-	x
	5.42	4.61	L	x	x	-	x	-	-	x
	5.82	4.28	R	x	x	-	x	-	-	x
	5.18	4.20	L	-	-	-	-	-	-	-
	5.37	4.23	L	x	x	-	x	-	-	x
	5.59	4.45	R	x	x	-	x	-	-	x
	5.78	4.36	R	-	x	-	-	-	-	-
	5.18	3.92	L	x	x	-	x	-	-	x
	5.89	4.68	R	-	x	-	-	-	-	-
	5.14	4.06	R	x	x	-	x	-	-	x
	5.77	4.63	R	x	x	-	x	-	-	x
	5.87	4.75	L	-	-	-	-	-	-	-
	5.66	4.54	L	-	x	-	x	-	-	x
	6.09	4.49	L	x	x	-	x	-	-	x
	5.73	4.88	L	x	x	-	x	-	-	x
	5.61	4.15	L	x	x	-	x	-	-	-
	5.68	4.65	R	-	-	-	-	-	-	-
	6.02	4.66	R	-	-	-	x	-	-	x
	5.51	4.35	L	-	x	-	-	-	-	-
	5.98	4.77	R	-	x	-	-	-	-	-
	5.51	4.21	L	x	x	-	x	-	-	x
	5.45	4.38	L	-	-	-	x	-	-	-
	5.62	4.30	R	-	x	-	x	-	-	-
	5.06	4.49	R	x	x	-	x	-	-	x
	5.18	3.81	L	x	x	-	x	x	-	x
	5.70	4.24	L	x	-	-	x	-	-	x
	6.07	4.88	R	-	-	-	-	-	-	-
	5.86	4.70	L	-	x	-	-	-	-	-
	5.70	4.40	L	x	x	-	-	-	-	-
	5.34	4.55	R	-	-	-	x	-	-	-
	5.80	4.17	R	x	-	-	x	-	-	x
	5.46	4.53	R	-	-	-	x	-	-	-
	5.75	4.46	L	-	-	-	x	-	-	-
	5.50	4.70	R	x	x	-	-	-	-	-
	5.36	4.41	L	-	-	-	x	-	-	-
	5.57	4.72	R	x	x	-	x	-	-	x
	5.98	4.37	R	-	-	-	x	-	-	-
	5.46	4.21	L	-	x	-	x	-	-	-
	5.87	4.52	R	x	x	-	x	-	-	x
	5.44	4.46	R	-	-	-	x	-	-	x
	5.83	4.50	L	-	-	-	x	-	-	x
	5.64	4.61	L	x	x	-	x	-	-	x
	5.30	4.42	R	-	-	-	-	-	-	-
	5.30	3.94	R	-	x	-	x	-	-	x
	5.54	4.38	R	-	-	-	x	-	-	-
	4.89	3.95	L	x	x	x	x	-	-	-
	6.65	4.26	R	-	x	-	x	-	-	-
	6.03	4.59	R	x	x	-	x	x	-	x
	5.26	4.10	L	x	x	-	x	x	-	x
	5.34	5.23	R	-	x	-	x	-	-	-
	5.66	4.52	R	-	x	-	x	-	-	x
	5.68	4.34	L	-	-	-	x	-	-	-
	5.36	4.25	L	x	x	-	x	-	-	-
	5.59	4.21	L	-	-	-	x	-	-	-
	5.13	4.05	R	x	x	-	-	-	-	-
	5.49	4.19	R	x	-	-	x	-	-	x
	5.34	4.16	R	-	-	-	x	-	-	-
	5.54	4.11	R	-	x	-	x	-	-	x
	5.68	4.33	R	-	-	-	-	-	-	-
	5.45	4.37	R	-	-	-	x	-	-	-
	5.14	4.20	R	-	x	-	x	-	-	-
	5.20	4.18	L	-	-	-	-	-	-	-
	5.39	4.25	L	-	x	-	-	-	-	-
	4.66	3.97	R	x	-	-	x	-	-	-
	5.88	4.51	R	-	-	-	x	-	-	-
	5.00	4.09	L	-	x	-	-	-	-	-
	5.06	3.93	R	-	x	-	x	-	-	x
	5.16	3.92	L	-	x	-	x	-	-	-
	5.05	3.70	R	x	x	-	x	-	-	x
	5.17	4.12	R	-	-	-	x	-	-	x
	5.52	4.24	R	x	x	-	x	-	-	x
	5.38	4.06	L	-	x	-	x	-	-	x
	4.86	3.80	R	-	-	-	-	-	-	-
	5.16	4.04	L	x	x	-	x	x	-	x
	4.97	3.95	R	-	x	-	x	-	-	-
	5.89	4.33	R	x	x	-	x	-	-	-
	4.82	3.73	L	x	x	-	x	-	-	x
	4.96	3.91	R	x	x	-	x	-	-	x
	4.73	4.09	R	x	-	-	x	-	-	x
	4.83	3.91	R	-	-	-	x	-	-	x
	5.22	3.75	L	x	x	x	x	-	-	x
	5.04	4.02	R	x	x	x	x	-	-	-
	5.25	3.95	R	-	x	-	x	-	-	x

continued

Sample	Length	Height	Valve	External			Internal			
				C,L	O	P	L,C	PL	MS	O
5.10	4.00	R	x	x	-		x	x	-	x
5.07	4.02	L	-	-	-		x	-	-	-
5.37	4.18	R	-	-	-		x	-	-	-
5.13	3.99	R	-	x	x		x	-	-	x
5.14	3.97	L	-	x	-		x	-	-	-
4.92	3.99	R	-	-	-		-	-	-	-
5.19	4.33	L	-	x	-		x	-	-	x
5.37	4.43	L	x	x	-		x	-	-	x
5.45	4.16	R	x	x	-		x	x	-	x
4.95	4.24	R	-	-	-		-	-	-	-
5.74	3.97	L	-	x	-		x	-	-	x
5.36	4.28	R	-	-	-		x	-	-	-
5.62	4.38	R	-	-	-		-	-	-	-
4.66	3.59	R	-	-	-		-	-	-	-
5.03	3.77	L	-	-	-		-	-	-	-
4.51	3.71	R	x	x	-		x	-	-	x
4.85	3.96	R	-	x	-		x	-	-	x
4.68	3.77	R	-	-	-		x	-	-	x
5.04	3.88	L	-	-	-		-	-	-	-
4.83	4.01	L	-	-	-		-	-	-	x
4.83	3.99	R	x	x	-		x	-	-	x
3.25	4.10	R	-	-	-		-	-	-	-
3.96	3.78	R	-	-	-		x	-	-	-
4.70	3.87	L	-	-	-		-	-	-	-
4.97	3.84	L	-	-	-		-	-	-	-
4.38	3.55	R	x	x	-		x	-	-	x
5.74	4.63	R	x	x	-		x	-	-	x
4.54	3.66	R	x	x	-		x	-	-	x
4.67	3.95	L	-	-	-		x	-	-	x
4.47	3.39	L	-	-	-		x	-	-	x
4.66	3.97	R	x	x	-		x	-	-	x
5.06	3.90	L	-	-	-		-	-	-	-
5.05	3.91	R	-	x	-		x	-	-	-
5.09	3.75	L	-	x	-		x	-	-	-
5.28	4.10	R	-	-	-		-	-	-	-
5.12	3.93	R	-	-	-		-	-	-	-
4.97	3.90	R	-	-	-		x	-	-	x
5.04	3.89	L	-	x	-		-	-	-	-
4.82	3.77	R	-	-	-		x	-	-	-
4.96	3.94	R	-	x	-		x	-	-	x
5.26	4.37	L	-	-	-		x	-	-	-
4.97	3.70	L	x	x	x		x	-	-	x
4.19	3.91	L	x	x	-		x	-	-	x
5.15	3.98	L	-	-	-		x	-	-	x
4.21	3.44	L	x	x	-		-	-	-	-
3.97	3.88	L	x	x	-		x	-	-	x
5.10	3.83	L	-	x	-		x	-	-	x
5.20	4.04	L	x	x	-		x	-	-	x
5.89	4.05	R	-	-	-		-	-	-	-
4.75	3.80	R	-	x	-		x	-	-	-
5.01	3.81	L	-	x	-		x	-	-	-
4.88	3.91	L	x	x	-		x	-	-	-
4.78	3.95	R	x	x	-		x	-	-	x
4.66	3.73	R	-	-	-		-	-	-	-
4.62	3.97	R	-	-	-		-	-	-	-
3.93	3.30	R	x	x	-		x	-	-	x
4.08	3.64	R	x	x	-		x	x	-	x
4.46	3.69	R	x	x	-		x	-	-	x
4.60	3.44	L	x	x	x		x	-	-	x
4.57	3.75	R	-	-	-		-	-	-	-
3.17	3.35	L	x	x	-		x	-	-	x
3.44	2.94	R	x	x	-		x	x	-	x
3.69	3.88	L	-	-	-		x	-	-	-
3.91	3.33	R	-	-	-		-	-	-	-
4.86	3.69	L	x	x	-		x	-	-	x
4.28	3.47	R	x	-	-		x	-	-	x
3.69	3.04	R	-	-	-		-	-	-	-
4.40	3.60	L	x	-	-		x	-	-	x
3.34	2.90	R	-	-	-		x	-	-	-
4.59	3.62	R	-	-	-		x	x	-	x
4.75	3.61	R	-	x	-		x	-	-	x
4.18	3.27	L	x	x	-		x	x	-	x
4.34	3.24	R	-	-	-		-	-	-	-
4.54	3.50	R	-	-	-		x	-	-	-
4.07	3.36	L	x	-	-		x	-	-	x
4.41	3.62	R	-	x	-		-	-	-	x
4.05	3.02	L	-	-	-		x	-	-	x
4.95	3.47	L	-	x	-		x	-	-	x
3.72	3.02	L	x	x	-		x	x	-	x
4.49	3.55	L	-	-	-		-	-	-	x
3.46	2.80	R	x	x	-		x	x	-	x
4.12	3.51	R	x	x	-		x	-	-	x
4.37	3.63	L	-	x	-		x	-	-	x
3.36	3.86	R	x	x	-		x	-	-	x
4.74	3.65	R	-	x	-		x	-	-	-
4.66	3.63	L	-	-	-		-	-	-	-
4.24	3.54	R	x	x	-		x	-	-	x
4.44	3.68	L	-	-	-		x	-	-	x
4.78	3.50	L	x	x	-		x	-	-	x
4.89	3.96	R	x	x	-		x	x	-	x
4.21	3.11	L	x	x	x		x	-	-	x
3.67	3.18	R	-	x	-		-	-	-	-
4.78	3.99	R	-	x	-		x	-	-	-
4.12	3.12	L	x	x	-		x	-	-	x
4.59	3.77	R	-	-	-		-	-	-	x
4.42	3.43	R	-	-	-		-	-	-	-
4.43	3.26	L	-	-	-		-	-	-	-
4.23	3.31	L	-	x	-		x	-	-	-
4.32	3.33	L	x	-	-		x	-	-	x
4.60	3.40	L	x	x	-		x	-	-	x
4.31	3.53	L	-	x	-		-	-	-	-
4.17	3.49	L	x	x	-		x	-	-	x
3.62	2.95	R	-	-	-		-	-	-	x

continued

Sample	Length	Height	Valve	External			Internal			
				C,L	O	P	L,C	PL	MS	O
	4.47	3.60	R	-	-	-	x	-	-	x
	3.80	3.19	R	x	x	-	x	x	-	x
	4.45	3.55	L	x	x	-	x	-	-	-
	4.10	3.59	R	-	-	-	x	-	-	x
	4.38	3.51	R	x	x	-	-	-	-	-
	4.11	3.20	L	x	-	-	x	-	-	x
	4.41	3.77	R	x	x	-	x	x	-	x
	4.83	3.48	L	-	-	-	-	-	-	-
	4.89	3.80	L	-	x	-	-	-	-	-
	4.26	3.36	L	-	x	-	x	-	-	x
	4.48	3.53	L	-	-	-	-	-	-	-
	4.18	3.30	L	x	x	-	x	-	-	x
	4.10	3.24	L	x	x	-	x	-	-	x
	4.58	3.71	R	-	-	-	-	-	-	-
	4.56	3.60	L	-	-	-	x	-	-	-
	4.14	3.33	L	-	-	-	-	-	-	-
	4.61	3.83	L	-	-	-	-	-	-	x
	4.94	3.70	L	-	-	-	x	-	-	-
	4.36	3.47	R	-	-	-	x	-	-	x
	4.61	3.81	L	x	x	-	x	-	-	x
	4.82	3.60	L	x	x	-	x	-	-	-
	4.19	3.33	R	x	x	-	x	-	-	x
	4.97	3.50	L	-	-	-	-	-	-	-
	4.29	3.25	L	-	-	-	x	-	-	-
	3.90	3.07	R	x	x	-	x	-	-	x
	3.97	2.93	R	-	-	-	-	-	-	x
	3.85	3.03	L	x	x	-	x	-	-	x
	4.02	3.32	L	x	x	-	x	-	-	x
	3.85	3.23	R	x	x	-	x	-	-	x
	4.23	3.56	L	x	-	-	x	-	-	-
	3.68	3.01	L	-	x	-	x	-	-	x
	4.61	3.81	L	x	x	-	x	-	-	-
	3.46	3.11	L	x	x	-	-	-	-	-
	4.11	3.20	L	-	x	-	-	-	-	-
	4.57	3.44	R	-	x	-	x	-	-	x
	4.43	3.61	R	-	x	-	-	-	-	-
	3.54	3.03	R	x	x	-	x	x	-	x
	3.98	3.66	L	x	x	-	x	x	-	x
	3.82	3.03	L	x	x	-	x	-	-	x
	3.76	3.02	R	x	-	-	x	-	-	x
	3.40	2.77	R	-	-	-	x	-	-	-
	3.64	3.07	L	x	x	-	x	-	-	x
	4.13	3.25	R	-	x	-	x	x	-	x
	3.62	3.00	L	x	x	-	x	-	-	x
	4.99	3.93	L	x	x	-	x	-	-	x
	3.79	3.38	R	-	-	-	-	-	-	-
	3.01	2.91	R	-	-	-	x	-	-	x
	3.64	3.00	R	-	x	-	x	-	-	x
	3.95	3.15	R	-	x	-	-	-	-	x
	4.20	3.47	L	-	x	-	x	-	-	x
	4.40	3.30	L	x	x	-	x	-	-	x
	4.05	3.30	L	-	-	-	-	-	-	-
	3.57	2.92	L	-	x	-	x	-	-	x
	3.63	3.08	R	-	-	-	-	-	-	-
	4.61	3.58	R	x	x	-	x	x	-	x
	4.84	3.80	R	-	-	-	x	-	-	-
	4.15	3.44	R	x	x	x	x	-	-	x
	4.12	3.48	R	-	x	-	x	-	-	-
	3.80	3.14	R	x	-	-	x	-	-	x
	4.50	3.53	R	x	-	-	x	-	-	-
	3.87	3.15	L	x	x	-	x	-	-	x
	4.08	3.51	R	-	x	-	-	-	-	x
	3.55	2.89	R	-	-	-	x	-	-	x
	4.03	2.95	L	-	x	-	x	-	-	-
	3.59	3.14	R	x	x	-	x	-	-	-
	3.20	3.19	R	-	x	-	x	-	-	-
	3.48	2.91	L	x	-	-	-	-	-	-
	2.49	2.14	L	x	x	-	x	-	-	x
	3.86	3.01	R	-	-	-	-	-	-	-
	3.74	2.95	R	x	x	-	x	-	-	x
	3.59	3.11	R	-	x	-	x	-	-	x
	4.07	3.24	L	-	-	-	x	-	-	-
	3.64	2.91	L	-	-	-	-	-	-	-
	2.59	2.03	L	x	x	-	x	-	-	x
	3.98	3.12	R	x	x	-	x	-	-	x
	3.31	3.16	R	x	x	-	x	-	-	x
	3.86	3.28	R	-	x	-	-	-	-	x
	3.76	3.04	R	x	x	-	x	-	-	x
	3.50	2.93	L	-	-	-	-	-	-	-
	4.01	2.97	L	-	-	-	-	-	-	x
	4.19	3.39	R	-	x	-	x	-	-	x
	3.54	2.71	L	x	x	-	x	-	-	x
	3.41	2.86	L	x	x	x	x	x	-	x
	3.51	2.92	R	-	x	-	-	-	-	x
	3.92	3.28	L	x	-	-	x	x	-	x
	3.92	3.25	L	-	x	-	-	-	-	x
	3.61	3.07	R	-	x	-	x	-	-	x
	3.38	2.93	L	-	-	-	-	-	-	-
	3.44	3.11	L	-	x	-	x	-	-	x
	3.81	2.99	L	-	-	-	-	-	-	-
	3.99	3.08	R	x	x	-	x	-	-	x
	3.66	2.51	L	x	x	-	x	-	-	x
	3.46	3.20	L	x	-	-	x	x	-	x
	3.58	2.90	L	x	x	-	x	-	-	x
	3.89	2.99	L	x	x	-	x	x	-	x
	3.44	2..77	R	-	-	-	-	-	-	-
	3.63	2.79	L	-	-	-	-	-	-	x
	3.75	3.25	L	-	x	-	x	-	-	x
	3.93	3.04	R	-	x	-	x	-	-	x
	3.53	3.28	R	x	x	-	x	-	-	x
	2.73	2.37	R	x	-	-	-	-	-	x
	2.70	2.21	L	x	x	-	x	-	-	x
	3.04	2.51	R	x	x	-	-	-	-	-
	2.98	2.45	L	x	x	-	x	-	-	x

continued

Sample	Length	Height	Valve	External			Internal			
				C,L	O	P	L,C	PL	MS	O
CP2 5-25	9.38	7.09	R	x	x	x	x	x	x	x
N = 347	11.12	7.99	R	-	-	-	x	-	-	-
	10.77	7.59	L	x	x	-	x	-	-	-
	10.73	7.12	L	x	x	-	x	-	-	-
	10.53	7.30	R	-	-	-	-	-	-	-
	9.49	7.18	L	x	x	-	x	-	-	-
	8.43	6.93	L	x	x	x	x	-	-	-
	11.25	8.00	L	x	x	x	x	-	-	-
	10.51	7.46	R	x	x	-	x	-	-	-
	12.21	8.72	R	-	-	-	x	-	-	-
	9.31	6.77	L	x	x	-	x	-	-	-
	8.85	6.58	R	x	x	-	x	-	-	x
	7.91	6.00	L	-	-	-	x	-	-	-
	9.74	7.64	L	x	x	-	x	-	-	x
	8.29	6.35	L	x	x	-	x	-	-	-
	7.28	5.60	L	x	-	-	x	-	-	-
	9.39	6.72	R	x	x	x	x	-	-	x
	9.54	6.81	L	x	x	x	x	x	-	x
	9.03	7.02	R	x	x	-	x	-	-	x
	8.48	6.03	R	-	-	-	-	-	-	-
	7.86	5.86	L	x	x	-	x	-	-	-
	9.43	6.68	L	x	x	x	x	x	-	x
	8.59	6.19	R	x	-	-	-	-	-	-
	5.32	5.27	R	-	-	-	x	-	-	-
	8.15	5.83	R	x	x	-	x	x	-	x
	7.05	5.86	L	x	x	x	x	x	-	x
	9.78	7.2	L	x	x	x	x	x	-	x
	6.92	5.19	L	x	x	-	x	-	-	x
	7.93	6.24	R	x	x	-	x	x	x	x
	8.12	6.31	R	x	x	-	x	-	-	x
	6.98	5.53	R	x	x	x	x	x	-	x
	7.89	5.97	L	x	x	x	x	-	-	x
	6.89	5.41	L	x	x	-	x	x	-	x
	6.4	6.01	L	x	x	x	x	x	-	x
	5.48	4.11	L	x	x	-	x	-	-	x
	8.3	6.24	L	x	x	-	x	x	-	x
	7.92	5.74	L	x	x	x	x	-	-	x
	7.86	5.99	L	x	x	x	x	x	-	x
	6.39	5.19	L	x	x	-	x	-	-	x
	7.49	5.7	R	x	-	-	x	x	-	x
	6.54	5.29	L	x	x	x	x	x	-	x
	7.23	5.46	L	x	x	x	x	-	-	x
	4.83	4.03	R	-	-	-	-	-	-	-
	5.81	4.38	L	x	x	-	x	-	-	-
	4.8	3.79	L	x	x	-	x	-	-	x
	8.18	6.13	R	x	x	x	x	x	x	x
	6.16	4.93	L	x	-	-	x	-	-	-
	6.98	5.18	L	x	x	-	x	-	-	x
	4.89	4.06	L	x	x	x	x	-	-	x
	5.53	4.07	R	x	-	-	x	-	-	x
	6.24	5.06	R	x	x	-	x	x	x	x
	5.26	5.35	R	x	x	-	x	-	-	x
	5.84	4.81	L	x	x	-	x	x	-	x
	5.12	3.63	L	x	x	x	x	-	-	x
	6.22	5.15	L	x	x	-	x	-	-	x
	5.83	4.33	R	x	x	-	x	-	-	x
	7.26	6.53	L	x	x	x	x	-	-	x
	6.74	5.41	R	-	-	-	-	-	-	-
	4.9	3.78	L	x	-	-	-	-	-	-
	4.48	3.43	R	x	x	x	x	-	-	x
	4.81	3.5	R	x	-	-	x	-	-	x
	4.35	3.52	L	x	-	-	x	-	-	x
	5.1	4.11	R	x	-	-	x	-	-	x
	5.3	4	R	x	-	-	x	-	-	x
	4.8	3.8	L	x	x	-	x	x	-	x
	6.54	2.64	L	x	x	-	x	x	-	x
	6.66	4.24	R	x	x	-	x	-	-	x
	3.37	3.49	R	x	x	-	x	-	-	x
	4.7	4.79	L	x	x	-	x	x	-	x
	4.16	3.37	R	x	x	x	x	x	x	x
	3.3	2.85	R	x	x	-	-	-	-	-
	3.04	2.76	L	x	x	-	-	-	-	-
	3.61	2.92	L	x	-	-	x	-	-	-
	3.83	3.14	R	-	-	-	-	-	-	-
	6.82	3.57	L	x	x	-	-	-	-	-
	4.18	3.33	R	x	x	x	x	-	-	-
	4.1	2.85	L	x	x	-	x	-	-	x
	4.02	3.32	R	x	x	-	x	-	-	x
	3.78	3.42	R	x	x	x	x	-	-	x
	4.37	3.45	R	x	x	x	x	-	-	x
	3.98	2.95	L	-	-	-	-	-	-	-
	3.67	2.95	L	x	x	-	x	-	-	x
	4.05	3.34	L	x	x	-	x	-	-	x
	4.89	3.87	R	x	-	-	x	-	-	-
	3.95	3.12	L	x	-	-	-	-	-	-
	4.36	3.32	L	x	x	-	x	-	-	x
	3.89	3.01	R	x	x	-	x	x	-	x
	11.87	7.98	L	x	-	-	x	x	-	x
	11.74	8.39	R	x	x	-	x	x	-	x
	11.8	8.13	L	x	x	-	x	-	-	-
	10.63	7.66	L	x	x	x	x	x	-	x
	10.16	7.54	L	x	x	x	x	-	-	x
	11.26	7.88	R	x	x	x	x	-	-	x
	12.17	8.66	L	x	-	-	-	-	-	-
	8.7	6.15	L	x	x	x	x	-	-	x
	11.19	7.69	R	x	x	-	x	x	-	x
	10.18	7.91	R	-	-	-	x	-	-	x
	10.13	7.79	R	x	x	-	x	x	-	x
	10.28	7.46	L	x	x	-	x	-	-	x
	10.56	7.71	L	x	-	-	x	-	-	-
	10.16	6.93	L	x	-	-	-	-	-	-
	10.13	7.2	R	x	x	-	x	-	-	-
	10.52	7.42	R	x	x	-	x	-	-	x
	9.91	7.49	L	x	x	-	x	-	-	x
	11.25	8.12	R	x	x	-	-	-	-	-
	9.96	6.73	L	x	x	-	x	-	-	-
	10.46	7.32	L	x	x	-	x	-	-	x
	10.77	7.36	R	x	-	-	x	-	-	-
	9.29	6.53	L	x	-	-	x	-	-	-
	10.95	7.55	R	x	x	-	x	x	-	x
	11.38	7.06	L	x	-	-	x	-	-	x
	11.77	7.78	R	-	-	-	x	-	-	x

continued

Sample	Length	Height	Valve	External			Internal			
				C,L	O	P	L,C	PL	MS	O
	10.21	7.04	L	-	x	-	x	-	-	x
	10.93	7.63	R	x	x	-	x	x	-	x
	9.57	7.05	R	x	x	-	x	-	-	x
	11.52	8.02	R	x	x	-	x	x	-	x
	10.79	7.68	R	x	-	-	x	-	-	x
	10.96	7.46	R	x	x	-	x	-	-	x
	10.29	7.35	L	x	x	x	x	-	-	x
	12.02	8.11	L	x	x	-	x	-	-	x
	10.4	7.58	L	x	x	-	x	-	-	x
	10.56	7.39	L	x	x	-	x	-	-	x
	10.17	7.37	R	x	x	-	x	-	-	x
	10.9	7.71	L	x	x	-	x	-	-	x
	10.44	6.77	L	x	x	-	x	-	-	x
	10.79	7.49	L	x	-	-	x	-	-	x
	11.99	7.81	R	x	x	x	x	-	-	-
	9.96	7.19	R	x	-	-	-	-	-	-
	10.02	7.2	R	-	-	-	x	-	-	-
	10.69	7.82	R	x	-	-	x	-	-	-
	10.12	7	L	-	x	-	x	-	-	-
	9.75	6.67	L	x	x	-	x	-	-	-
	9.1	6.99	R	-	-	-	x	-	-	-
	10.06	7.49	L	x	x	-	x	-	-	x
	8.74	6.4	R	x	-	-	x	x	-	x
	9.04	6.55	R	x	x	x	x	x	-	x
	9.82	7.37	L	x	x	-	x	-	-	-
	9.21	6.5	L	x	x	-	x	-	-	x
	8.07	5.65	R	x	x	-	x	-	-	-
	8.08	6.09	R	x	-	-	x	-	-	x
	8.57	6.7	R	x	x	-	x	x	-	x
	8.87	6.86	R	x	-	-	x	x	-	x
	10.03	7.29	R	x	-	-	x	-	-	x
	12.3	8.36	L	x	x	-	x	x	-	x
	9.75	6.19	L	x	-	-	x	-	-	-
	7.79	5.68	R	-	-	-	x	x	-	x
	9.58	6.89	R	x	x	-	x	x	-	x
	9.1	6.29	L	x	x	-	x	-	-	x
	9.42	6.72	L	x	x	-	x	-	-	x
	8.82	6.94	R	x	x	-	x	-	-	x
	8.95	6.99	R	x	x	-	x	x	-	x
	9.38	6.45	L	x	x	-	x	x	-	x
	9.29	6.94	R	x	x	-	x	-	-	-
	8.88	6.21	L	x	-	-	x	-	-	-
	8.15	6.34	R	x	x	-	x	-	-	x
	9.02	6.62	R	x	x	-	x	-	-	x
	9.09	6.23	L	x	-	-	x	-	-	-
	8.25	6.28	R	x	-	-	x	-	-	-
	8.82	7.38	L	x	x	-	x	x	-	x
	8.51	6.72	L	x	-	-	-	-	-	-
	8.5	6.36	L	x	-	-	x	-	-	x
	8.14	6.06	L	-	-	-	x	-	-	x
	8.78	6.25	L	x	x	-	x	x	-	x
	9.44	6.97	L	x	x	x	x	x	-	x
	3.16	6.62	L	x	x	-	x	x	-	x
	8.72	6.86	L	x	x	x	x	x	-	x
	8.73	6.44	R	x	x	-	x	-	-	x
	9.16	6.83	L	x	x	-	x	-	-	x
	7.52	6.05	R	x	x	-	x	-	-	-
	8.75	6.55	R	-	-	-	x	-	-	-
	8.91	6.25	R	x	x	-	x	-	-	x
	8.05	5.71	R	-	-	-	x	-	-	-
	8.39	6.32	R	-	-	-	x	-	-	-
	7.95	6.03	L	x	x	-	x	x	x	x
	9.06	7.71	L	x	x	-	x	x	x	x
	8.1	6.28	L	x	x	-	x	-	-	x
	8.11	6.06	L	x	x	-	x	-	-	x
	7.4	5.1	R	x	x	-	x	-	-	x
	8.23	6.29	R	x	x	-	x	-	-	x
	7.2	6.13	L	x	x	-	x	-	-	-
	6.06	7.74	L	x	x	-	-	-	-	-
	8.18	6.87	L	x	-	-	x	-	-	x
	8.31	6.17	L	x	x	-	x	-	-	x
	8.58	6.01	L	x	x	-	x	-	-	x
	8.61	6	L	x	x	-	x	-	-	x
	9.1	4.65	R	x	x	-	x	-	-	x
	8.13	6.38	R	x	-	-	x	-	-	-
	7.47	5.54	L	x	x	-	x	-	-	x
	7.14	5.86	L	x	x	-	x	x	-	x
	7.18	5.38	L	-	-	-	x	-	-	-
	8.94	7.2	R	x	x	-	x	-	-	x
	8.03	6.53	R	x	x	-	x	-	-	x
	8.16	5.37	L	x	x	-	x	-	-	x
	7.5	5.84	L	-	-	-	x	-	-	x
	8.31	6.09	L	x	x	-	x	-	-	-
	7.17	5.61	L	x	x	-	x	x	-	x
	7.11	5.44	R	x	-	-	x	-	-	x
	6.9	5.57	R	x	-	-	x	-	-	x
	7.7	5.85	R	x	-	-	x	-	-	x
	6.88	5.69	L	x	x	-	x	x	x	x
	8.25	6.02	L	x	x	-	x	x	x	x
	7.05	5.2	R	-	-	x	x	-	-	-
	9.2	6.69	L	x	x	-	x	x	x	x
	7.84	6.04	L	x	x	-	x	x	-	x
	6.61	5.14	R	x	-	-	x	-	-	-
	7.16	5.23	L	x	x	-	x	-	-	x
	8.71	6.33	R	x	x	-	x	-	-	x
	8.1	6.22	L	-	-	-	x	-	-	x
	7.34	5.84	R	x	x	-	x	-	-	x
	7.75	6.04	L	x	x	-	x	-	-	x
	7.44	6.05	R	-	-	-	x	-	-	-
	6.63	5.33	R	x	x	x	x	x	x	x
	6.54	5.17	R	x	-	-	x	-	-	-
	6.92	5.36	R	-	x	-	x	-	-	x
	7.73	5.74	L	x	x	-	x	-	-	x
	6.5	5.41	R	x	-	-	-	-	-	-
	6.18	4.7	L	-	x	-	x	-	-	x
	6.09	5.02	R	x	x	-	x	-	-	x
	5.66	4.72	L	x	x	-	x	x	-	x
	6.87	5.62	R	-	-	-	x	-	-	-
	7.62	6.49	R	x	x	-	x	x	-	x
	7.41	5.76	R	-	x	-	-	-	-	-
	6.62	5.09	R	-	-	-	-	-	-	-
	7.56	5.54	L	x	x	-	-	-	-	-

continued

Sample	Length	Height	Valve	External			Internal			
				C,L	O	P	L,C	PL	MS	O
	7.87	5.59	L	-	-	-	x	-	-	-
	6.61	5.22	R	x	x	-	x	-	-	x
	6.63	5.16	L	x	x	-	x	-	-	-
	7.13	5.2	L	x	-	-	-	-	-	-
	6.58	4.98	R	x	x	-	x	-	-	x
	6.63	5.35	R	x	x	-	x	-	-	-
	6.21	5.24	R	x	x	-	x	-	-	x
	7.11	5.53	R	x	x	-	x	-	-	-
	7.2	4.88	L	x	x	-	x	-	-	x
	6.85	4.79	L	x	x	x	x	-	-	x
	7.67	5.63	L	x	x	x	x	-	-	x
	6.31	5.04	R	x	x	-	x	-	-	-
	7.04	5.25	L	x	x	x	x	x	-	x
	6.26	5.16	L	x	x	-	-	-	-	x
	4.85	4.47	R	x	x	-	x	-	-	x
	6.4	5.28	R	x	-	-	x	-	-	-
	5.17	3.96	R	x	-	-	x	-	-	x
	6.39	5.07	L	x	x	-	x	x	-	x
	6.17	4.6	R	x	-	-	-	-	-	-
	5.27	4.05	R	x	x	-	x	-	-	x
	5.54	4.19	L	-	-	-	-	-	-	-
	6.79	5.14	R	x	-	-	x	-	-	x
	6.34	5.76	R	x	x	x	x	-	-	x
	7.26	5.44	R	x	-	-	-	-	-	x
	6.02	4.71	L	x	-	-	x	-	-	-
	6.1	4.62	R	-	-	-	x	-	-	-
	5.42	4.42	R	x	x	-	x	x	x	x
	7.57	5.77	R	x	x	-	x	-	-	-
	6.26	5.01	L	x	x	-	x	x	-	x
	6	4.72	R	x	x	-	x	-	-	x
	7.15	5.38	R	x	x	-	x	x	-	x
	6.44	5.02	L	x	-	-	x	-	-	x
	6.27	4.83	R	x	x	-	x	-	-	x
	6.88	4.83	L	x	x	x	x	x	x	x
	5.3	4.16	L	-	-	-	-	-	-	-
	5.76	4.51	R	x	x	-	-	-	-	-
	5.66	4.62	R	x	x	-	x	-	-	x
	6.53	4.86	R	x	x	-	x	-	-	x
	6.61	4.9	L	-	x	-	-	-	-	x
	5.51	5.03	L	x	x	x	x	x	-	x
	6.42	4.6	L	x	-	-	x	-	-	-
	7.38	5.35	L	x	x	-	x	-	-	x
	6.82	5.21	R	-	-	-	-	-	-	-
	5.63	4.26	L	-	-	-	-	-	-	-
	6.79	5.45	R	x	x	-	x	x	-	x
	5.7	4.41	R	x	x	x	x	-	-	x
	5.74	4.49	R	x	-	-	x	-	-	-
	6.91	4.75	R	x	x	-	x	-	-	x
	5.35	4.12	L	x	x	-	x	-	-	x
	5.38	4.36	R	x	-	-	x	-	-	-
	5.52	4.16	L	x	x	-	x	-	-	x
	5.25	3.92	R	x	-	-	x	-	-	x
	4.71	3.81	L	-	-	-	-	-	-	-
	5.07	3.93	L	x	x	-	x	-	-	-
	5.39	4.5	R	x	x	-	x	-	-	x
	5.68	4.59	L	x	x	-	x	-	-	x
	5.82	4.29	R	x	x	-	x	-	-	x
	6.98	5.09	L	x	x	-	x	-	-	x
	5.28	4.43	L	x	x	-	x	-	-	x
	5.16	3.93	L	x	-	-	x	-	-	-
	5.32	4.44	L	x	x	x	x	x	-	x
	5.08	4.21	R	x	x	-	x	-	-	-
	5.13	4.24	L	x	-	-	-	-	-	-
	4.84	3.83	R	x	x	x	x	x	-	x
	5.24	4.23	L	x	x	-	x	x	-	x
	4.49	3.7	R	x	x	-	x	-	-	x
	4.91	3.71	R	x	x	-	x	-	-	x
	4.98	3.93	L	x	-	-	x	-	-	x
	4.72	4.18	L	x	x	-	x	x	-	x
	5.35	4.01	R	x	x	-	x	x	-	x
	4.61	3.79	R	x	x	x	x	x	x	x
	5.65	4.63	R	x	x	-	x	x	x	x
	4.34	3.58	R	x	x	-	x	-	-	x
	4.93	3.65	L	x	-	-	-	-	-	-
	4.37	3.96	R	x	-	-	x	x	-	x
	4.5	3.83	R	x	x	x	x	-	-	x
	4.5	3.48	L	x	-	-	-	-	-	-
	4.85	3.8	R	-	-	-	-	-	-	-
	3.76	3.22	R	x	x	-	x	-	-	x
	4.53	3.82	L	x	x	-	x	x	-	x
	4.34	3.61	L	x	x	-	x	-	-	x
	4.1	3.66	R	x	x	-	x	-	-	x
	4.02	2.87	L	x	x	-	x	-	-	x
	4.06	3.09	L	x	x	-	x	x	-	x
	4.82	4.33	R	x	x	-	x	x	x	x
	3.7	3.99	R	x	x	-	x	-	-	x
	3.79	2.94	L	x	-	-	x	-	-	x
	3.69	3.03	L	x	-	-	x	-	-	x
	4.19	3.7	L	x	x	-	x	-	-	x
	3.72	2.86	L	x	x	-	x	-	-	x
	4.54	3.66	L	-	-	-	-	-	-	-
	3.79	3.04	R	-	-	-	-	-	-	x
	4	3.4	R	x	x	-	-	-	-	x
	4.49	3.6	R	x	x	-	x	-	-	x
	4.51	3.77	R	x	x	x	x	x	-	x
	3.81	3.12	R	x	x	-	x	-	-	x
	4.26	3.19	R	x	x	-	x	-	-	x
	3.77	3.31	R	x	x	-	x	-	-	x
	3.36	2.84	R	x	x	-	x	x	-	x
	3.34	2.91	R	x	-	-	x	-	-	x
	4.58	3.52	R	x	x	-	x	x	-	x
	4.03	3.39	L	x	x	-	x	-	-	x
	3.77	3.31	R	x	x	-	x	-	-	x
	4.48	3.88	R	x	x	-	x	-	-	x
	3.66	3.92	R	x	-	-	x	-	-	x
	3.92	3.01	R	x	-	-	x	-	-	x
	3.72	3.29	R	x	x	-	x	-	-	x
	3.68	2.94	R	x	x	-	x	-	-	x
	4.4	3.5	R	-	-	-	x	-	-	x
	4.58	3.77	L	x	x	-	x	-	-	x
	3.72	2.66	L	x	x	-	x	x	-	x
	4.77	4.05	L	x	x	x	x	-	-	x

continued

Sample	Length	Height	Valve	External			Internal			
				C,L	O	P	L,C	PL	MS	O
	3.75	2.77	L	x	x	-	x	x	-	x
	3.97	3.32	L	x	x	-	x	x	-	x
	4.17	3.42	L	x	x	-	x	-	-	x
	5.24	3.91	R	x	x	x	x	x	-	x
	3.72	3.22	L	x	x	-	x	-	-	x
	4.75	3.13	L	x	x	-	x	x	-	x
	4.88	3.81	L	x	x	x	x	-	-	x
	4.12	3.24	R	x	x	-	x	-	-	x
	3.67	2.87	L	x	x	-	x	-	-	x
	3.82	3.28	R	x	x	-	x	-	-	x
	3.72	3.04	L	-	-	-	-	-	-	x
CP3 5-10	13.7	9.28	L	x	x	x	x	-	-	x
N = 73	10.13	7.36	L	x	x	x	x	-	-	x
	9.87	7.93	R	x	x	x	x	-	-	x
	7	5.6	R	x	-	x	x	x	-	x
	10.71	7.85	L	x	x	-	x	-	-	x
	5.86	4.7	L	x	x	x	x	-	-	x
	7.9	6.1	R	x	x	x	x	x	-	x
	8.58	6.46	L	x	x	x	x	x	-	x
	7.43	5.51	R	x	x	x	x	-	-	x
	9	6.9	L	x	x	-	x	-	-	x
	10.04	7.57	R	x	x	-	x	-	-	x
	7.91	6.05	R	-	-	x	x	-	-	x
	10.77	7.53	L	x	x	-	x	x	-	x
	8.91	6.11	L	x	-	-	x	-	-	x
	7.76	5.31	R	x	-	-	x	-	-	x
	8.45	6.28	L	x	-	x	x	-	-	x
	7.63	6.06	R	x	x	x	x	-	-	x
	8.76	7.26	R	x	x	x	x	x	-	x
	7.7	6.1	R	x	x	x	x	-	-	x
	7.47	5.63	R	-	-	x	x	-	-	x
	7.12	5.01	L	-	-	-	x	-	-	-
	7.73	5.94	L	-	x	-	x	-	-	-
	5.5	4.65	L	-	-	-	-	-	-	-
	6.5	5.07	L	x	x	x	x	-	-	x
	6.7	5.15	L	x	x	-	x	-	-	x
	6.76	5.33	R	x	x	-	x	-	-	x
	4.75	3.68	R	x	x	-	x	-	-	x
	6	4.65	R	x	x	x	x	-	-	x
	7.54	5.53	R	x	x	x	x	x	-	x
	6.46	5	R	x	-	-	x	-	-	x
	7.73	5.61	L	x	x	-	x	-	-	x
	6.01	4.39	L	x	x	x	-	-	-	-
	5.06	4.31	R	x	x	x	x	x	-	x
	6.22	4.65	R	-	-	-	x	-	-	x
	6.02	4.58	R	x	x	-	-	-	-	-
	6.89	5.15	R	x	-	-	x	-	-	-
	6.7	5.19	R	-	-	-	x	-	-	-
	6.4	5.04	R	-	-	-	x	-	-	-
	5.54	4.43	R	-	-	x	x	-	-	x
	3.6	2.93	R	x	-	-	x	-	-	x
	4.59	4.01	R	x	x	-	x	x	-	x
	4.03	3.13	L	x	x	-	x	-	-	x
	4.96	3.94	L	-	-	-	x	-	-	x
	4.34	3.49	L	x	x	-	x	-	-	x
	3.89	3.1	L	x	-	-	x	-	-	x
	4.99	4.45	R	x	x	x	x	x	x	x
	5.15	4	R	x	x	-	x	x	-	x
	4.26	3.32	R	x	-	-	x	-	-	x
	4.11	3.43	L	x	x	-	x	x	-	x
	4.21	3.54	R	x	-	-	x	-	-	x
	4.5	3.41	R	x	x	-	x	-	-	x
	6.58	5.25	L	x	-	-	x	-	-	x
	5.92	4.72	R	x	-	-	-	-	-	x
	5.45	4.3	L	x	x	-	x	-	-	x
	4.21	3.45	L	x	-	-	x	-	-	x
	4.07	2.95	L	x	-	-	x	-	-	x
	4.03	3.41	L	x	x	-	x	-	-	x
	4.88	4.55	R	x	x	-	x	x	x	x
	4.64	3.84	R	x	-	-	x	-	-	x
	4.06	3.01	L	x	-	-	x	x	-	x
	4.87	4.06	R	x	x	x	x	x	-	x
	2.82	2.48	R	-	-	-	-	-	-	-
	5.74	4.51	L	x	x	x	x	x	x	x
	6.1	4.64	L	-	-	-	-	-	-	-
	4.4	3.59	R	x	x	x	x	-	-	x
	3.59	2.81	L	-	-	-	-	-	-	x
	4.25	3.42	L	x	x	-	x	-	-	x
	4.13	3.25	R	x	-	-	x	-	-	x
	3.48	3.18	L	x	x	-	x	x	-	x
	3.82	2.86	R	x	x	-	x	-	-	x
	4.08	3.09	R	x	-	-	x	x	x	x
	4.27	3.56	R	x	x	x	x	x	-	x
	3.61	3.01	L	x	x	x	x	x	-	x
CP6 52-57	7.45	5.63	R	x	x	x	x	-	-	x
N = 5	8.8	6.82	L	x	x	x	x	x	x	x
	4.68	4	R	x	x	x	x	x	x	-
	7.79	5.69	R	x	x	x	x	x	-	x
	3.97	3.29	L	x	-	x	x	-	-	x
CP6 92-97	7.69	6.03	R	x	x	-	x	x	-	x
N = 4	7.71	5.81	L	x	x	-	x	x	x	x
	7.73	6.31	R	x	x	x	x	x	-	x
	3.98	3.95	R	x	x	x	x	x	x	x

continued

Sample	Length	Height	Valve	External			Internal			
				C,L	O	P	L,C	PL	MS	O
CP6 130-135	8.96	6.42	R	x	x	-	x	x	-	x
N = 171	8.87	6.54	R	x	x	-	x	x	-	x
	7.64	5.79	L	x	x	-	x	-	-	x
	9.08	6.63	R	x	x	-	x	x	-	x
	10.93	6.98	L	x	x	-	x	x	-	x
	9.08	6.72	R	x	x	-	x	x	-	x
	10.04	7.14	L	x	x	-	x	-	-	x
	10.02	7.69	L	x	x	-	x	x	-	x
	8.84	6.5	R	x	x	-	x	-	-	x
	8.05	6.17	L	x	x	-	x	x	-	x
	9.79	7.28	L	x	x	-	x	-	-	x
	9.97	7.05	R	x	x	-	x	x	-	x
	8.15	6.08	L	x	x	-	x	-	-	x
	10.5	8.31	R	x	x	-	x	x	-	x
	9.11	6.58	R	x	x	-	x	x	-	x
	8.31	6.48	L	x	-	-	x	x	-	x
	9.54	6.88	L	x	x	-	x	-	-	x
	9.18	6.75	R	x	x	-	x	-	-	x
	8.75	6.74	L	x	x	-	x	x	-	x
	8.91	7.11	L	x	x	-	x	x	-	x
	9.12	6.99	R	x	x	-	x	-	-	x
	8.52	6.44	R	x	x	-	x	x	-	x
	8.02	6.04	R	x	x	-	x	x	-	x
	9.23	6.66	R	x	x	-	x	-	-	x
	8.7	6.39	L	x	x	-	x	-	-	x
	9.66	7.17	R	x	x	-	x	-	-	x
	8.86	6.04	R	x	x	-	x	-	-	-
	8.89	6.55	L	x	x	-	x	-	-	x
	9.32	6.65	L	x	x	-	x	x	-	x
	7.65	5.47	L	x	-	-	x	-	-	-
	8.98	6.86	R	x	x	-	x	x	-	x
	8.85	6.92	L	x	-	-	x	x	-	x
	7.11	5.57	R	x	x	-	x	x	x	x
	7.27	5.64	L	x	x	-	x	x	-	x
	9.15	6.94	L	x	x	-	x	x	-	x
	6.83	5.63	L	x	x	-	x	x	-	x
	9.13	6.95	R	x	-	-	x	-	-	x
	8.48	6.3	R	x	x	-	x	-	-	x
	8.62	6.49	L	x	x	-	x	x	x	x
	8.16	6.36	L	x	x	-	x	x	-	x
	7.19	5.27	L	x	x	-	x	-	-	x
	6.96	5.33	R	x	x	-	x	-	-	x
	6.99	5.41	L	x	x	-	x	-	-	x
	7.6	5.87	L	x	x	-	x	-	-	x
	8.9	6.69	L	x	x	-	x	x	-	x
	8.15	6.23	L	x	x	-	x	x	-	x
	7.27	5.62	L	x	x	-	x	x	-	x
	7.94	6.86	R	x	x	-	x	x	-	x
	7.52	6.11	R	x	x	-	x	x	x	x
	6.38	5.07	L	x	x	-	x	x	x	x
	7.51	5.74	R	x	x	-	x	-	-	x
	7.35	5.81	L	x	x	-	x	x	-	x
	7.95	6	R	x	x	-	x	x	-	x
	7.98	5.55	L	x	x	-	x	x	-	x
	6.23	4.4	L	x	x	-	x	x	-	x
	7.13	5.27	R	x	x	-	x	-	-	x
	7.19	5.03	R	x	x	-	x	-	-	x
	7.55	5.67	L	x	x	-	x	x	-	x
	7.56	5.65	L	x	x	-	x	x	-	x
	7.53	5.67	R	x	x	-	x	x	-	x
	6.28	5.32	L	x	x	-	x	x	-	x
	7.68	6.08	R	x	x	-	x	-	-	x
	7.34	5.33	L	x	x	-	x	x	-	x
	7.29	5.97	R	x	x	-	x	x	-	x
	7.18	5.87	L	x	x	-	x	x	-	x
	6.82	5.09	L	x	x	-	x	x	-	x
	8.5	6.29	L	x	x	-	x	x	-	x
	7.43	5.53	L	x	-	-	x	-	-	x
	7.45	5.47	R	x	x	-	x	-	-	x
	8.1	6.17	L	x	x	-	x	x	-	x
	7.19	6.12	R	x	x	-	x	x	-	x
	6.86	5.52	R	x	x	-	x	x	-	x
	6.97	5.24	R	x	x	-	x	x	-	x
	6.24	4.87	L	x	x	-	x	x	-	x
	7.06	5.84	R	x	x	-	x	-	-	x
	6.34	4.9	L	x	x	-	x	-	-	x
	6.32	5.82	R	x	x	-	x	-	-	x
	5.68	4.38	L	x	x	-	x	-	-	x
	6.14	5.28	L	x	x	-	x	-	-	x
	6,83	5.77	R	x	x	-	x	-	-	x
	6.96	4.97	R	x	x	-	x	-	-	x
	6.76	5.15	L	x	x	-	x	-	-	x
	6.75	5.57	R	x	x	-	x	x	-	x
	6.72	5.02	L	x	x	-	x	-	-	x
	5.38	4.52	R	x	x	-	x	x	-	x
	5.85	4.58	L	x	x	-	x	x	-	x
	6.93	4.89	R	x	x	-	x	x	x	x
	6	4.83	R	x	x	-	x	x	-	x
	5.37	3.92	L	x	x	-	x	x	-	x
	5.97	4.32	R	x	x	-	x	x	-	x
	5.7	4.51	L	x	x	-	x	x	-	x
	6.26	5.21	R	x	x	-	x	x	-	x
	6.96	5.13	L	x	x	-	x	x	-	x
	5.73	5.77	R	x	x	-	x	x	-	x
	5.13	4.03	L	x	x	-	x	x	x	x
	6.24	5.11	R	x	x	-	x	x	-	x
	4.54	3.8	R	x	x	-	x	x	x	x
	6.48	4.72	L	x	x	-	x	x	-	x
	6.95	5.24	R	x	x	-	x	-	-	x
	6.95	5.2	L	x	x	-	x	x	-	x
	7.6	5.3	L	x	x	-	x	-	-	x
	7.17	5.49	R	x	-	-	x	x	-	x
	6.28	5.09	R	x	x	-	x	x	x	x
	5.12	4	L	x	x	-	x	x	-	x
	5.72	4.67	R	x	x	-	x	x	-	x
	6.36	4.73	L	x	x	-	x	x	-	x
	5.36	4.21	L	x	x	-	x	x	-	x
	3.98	3.25	L	x	x	-	x	x	x	x
	4.06	3.29	L	x	x	-	x	x	-	x
	5.63	4.35	L	x	x	-	x	x	-	x
	3.96	3.43	R	x	x	-	x	-	-	x
	6.75	4.77	L	x	x	-	x	x	x	x

continued

Sample	Length	Height	Valve	External			Internal			
				C,L	O	P	L,C	PL	MS	O
	5.98	4.61	R	x	x	-	x	x	-	x
	5.89	4.81	L	x	x	-	x	x	-	x
	5.82	4.53	L	x	x	-	x	x	-	x
	4.85	4.05	L	x	x	-	x	x	-	x
	4.08	4.31	R	x	x	-	x	-	-	x
	6.85	4.85	R	x	x	-	x	x	-	x
	4.49	3.51	R	x	-	-	x	x	-	x
	4.77	3.95	R	x	x	-	x	-	-	x
	5.43	3.99	R	x	x	-	x	x	-	x
	4.88	3.9	L	x	x	-	x	x	x	x
	5.96	4.52	L	x	x	-	x	x	-	x
	6.05	5.29	R	x	-	-	x	x	x	x
	4.93	3.83	R	x	x	-	x	x	-	x
	4.28	3.42	L	x	x	-	x	x	-	x
	3.66	2.99	L	x	-	-	x	x	-	x
	4.12	3.63	R	x	x	-	x	x	x	x
	5.54	4.18	L	x	x	-	x	x	-	x
	5.26	4.09	L	x	-	-	x	-	-	-
	4.35	3.41	R	x	x	-	x	x	-	x
	3.85	3.2	L	x	x	-	x	x	x	x
	4.82	4.01	R	x	x	-	x	x	-	x
	4.05	3.18	R	x	x	-	x	x	x	x
	5.69	3.87	L	x	x	-	x	x	-	x
	4.22	3.59	L	x	x	-	x	x	-	x
	5.83	4.24	L	x	x	-	x	x	-	x
	6.38	5.1	L	x	x	-	x	x	x	x
	4.38	3.83	R	x	x	-	x	-	-	x
	3.23	2.84	R	x	x	-	x	x	-	x
	4.45	3.51	L	x	-	-	x	-	-	x
	4.31	3.58	R	x	x	-	x	x	x	x
	3.59	3.09	L	x	x	-	x	x	x	x
	5.45	4.52	L	x	x	-	x	x	x	x
	5.44	4.26	R	x	x	-	x	x	-	x
	5.74	4.78	R	x	x	-	x	x	-	x
	4.4	3.57	L	x	x	-	x	x	-	x
	4.36	3.7	R	x	x	-	x	x	x	x
	4.55	3.82	R	x	x	-	x	x	-	x
	4.17	3.71	R	x	x	-	x	x	x	x
	5.02	3.98	L	x	x	-	x	x	-	x
	3.73	2.94	L	x	x	-	x	-	-	x
	4.95	4.04	L	x	x	-	x	x	-	x
	3.45	2.91	R	x	x	-	x	x	-	x
	3.89	3.05	R	x	x	-	x	x	-	x
	3.61	2.92	R	x	-	-	x	-	-	x
	4.43	3.79	L	x	x	-	x	x	x	x
	4.15	3.6	L	x	x	-	x	-	-	x
	3.69	3.87	R	x	-	-	x	-	-	x
	3.44	2.74	L	x	x	-	x	x	-	x
	3.88	3.59	L	x	x	-	x	x	-	x
	3.77	3.11	R	x	x	-	x	x	-	x
	3.52	2.74	R	x	x	-	x	x	-	x
	4.73	3.79	R	x	x	-	x	-	-	x
	4.52	3.76	L	x	x	-	x	x	-	x
	3.88	2.93	L	x	x	-	x	x	x	x
	5.48	4.15	R	x	x	-	x	x	-	x
	4.16	3.33	L	x	x	-	x	x	-	x
	3.3	2.78	R	x	x	-	x	x	-	x
	3.7	2.98	R	x	x	-	x	x	x	x
	5.26	3.9	L	x	x	-	x	x	x	x
CP6 145-152	8.22	6.46	R	x	x	x	x	x	-	x
N = 38	7.84	6.12	L	x	-	-	x	-	-	x
	7.99	6.8	R	x	x	x	x	-	-	x
	8.86	6.92	L	x	x	x	x	-	-	x
	9.13	6.72	R	x	-	-	x	x	-	x
	9.81	7.74	L	-	x	-	x	-	-	x
	8.67	6.76	L	-	x	-	x	-	-	x
	9.41	6.72	L	x	-	-	x	-	-	x
	8.94	7.05	R	-	x	-	x	-	-	x
	6.46	4.93	R	x	-	-	x	-	-	x
	8.27	6.38	L	x	-	-	x	-	-	x
	7	5.43	R	-	-	-	x	-	-	x
	8.65	6.42	R	x	x	-	x	-	-	x
	8.89	6.51	R	x	x	-	x	-	-	x
	9.13	6.74	R	-	x	-	x	x	-	x
	9.9	7.49	R	-	x	-	x	x	-	x
	6.57	5.24	R	x	x	-	x	-	-	x
	12.07	8.55	R	x	x	-	x	-	-	x
	8.21	6.88	L	x	x	-	x	x	-	x
	8.68	7.26	L	-	-	x	x	-	-	x
	8.41	6.95	L	x	x	-	x	x	-	x
	7.25	5.77	R	x	x	-	x	-	-	x
	7.09	5.6	R	x	x	-	x	-	-	x
	4.73	3.58	L	x	-	-	x	-	-	x
	6.83	5.49	L	x	x	x	x	x	-	x
	7.65	5.87	R	x	x	-	x	-	-	x
	5.76	4.56	L	x	-	-	x	-	-	x
	5.8	4.54	L	x	x	-	x	-	-	x
	4.5	3.7	R	-	-	-	x	-	-	x
	4.49	3.62	L	x	-	-	x	-	-	x
	9.01	6.49	L	-	-	-	x	-	-	x
	5.93	4.8	R	x	-	-	x	-	-	x
	6.95	5.76	R	x	x	x	x	x	-	x
	6.34	5.76	L	x	x	x	x	-	-	x
	5.17	4.42	R	x	x	-	x	-	-	x
	3.95	3.42	R	-	x	-	x	-	-	x
	4.05	2.93	L	x	x	-	x	-	-	x
	3.33	3.85	R	-	x	-	x	x	-	x

continued

Sample	Length	Height	Valve	External			Internal			
				C,L	O	P	L,C	PL	MS	O
CBi3 0-19	11.31	8.34	R	x	x	-	x	-	-	-
N = 279	11.64	8.15	R	x	-	x	-	-	-	-
	12	9.67	R	x	x	x	x	-	-	x
	13.26	9.45	L	x	-	x	x	x	-	x
	12.45	9.49	R	x	-	x	x	x	-	-
	13.05	9.44	L	x	-	-	x	-	-	x
	8.81	7.22	R	x	x	x	x	x	-	x
	11.61	7.94	L	x	-	x	x	x	x	-
	11.31	8.24	L	x	x	-	x	-	-	-
	10.91	8.35	L	x	x	x	x	-	-	x
	9.31	7.21	R	x	-	x	x	x	-	x
	7.14	5.7	R	x	x	x	x	x	-	x
	9.72	7.03	L	x	x	x	x	x	x	x
	9.45	7.7	R	x	-	x	x	-	-	x
	7.6	5.69	L	x	x	x	x	x	-	x
	11.62	8.56	R	x	-	x	x	x	-	x
	6.22	4.95	R	x	-	x	x	-	-	x
	9.23	6.96	R	x	-	x	x	-	-	x
	9.65	7.42	L	x	x	-	x	x	x	x
	7.81	5.76	L	-	-	-	x	-	-	-
	10.75	8.6	R	x	x	x	x	x	x	x
	11.01	7.52	L	x	-	-	-	-	-	-
	11.24	8.85	R	x	-	-	x	x	-	x
	7.77	5.74	R	x	-	x	x	-	-	-
	11.28	8.5	L	x	-	x	x	x	-	-
	12.28	9.38	R	x	x	-	x	-	-	-
	13.08	10.26	R	x	-	x	x	x	-	x
	11.12	8.48	L	x	x	x	x	-	-	x
	6.78	5.05	R	x	-	-	-	-	-	-
	8.85	6.73	L	x	x	-	x	-	-	-
	11.17	8.16	L	x	-	-	x	-	-	x
	6.33	4.65	L	x	-	x	-	-	-	-
	12.21	9.01	L	x	-	x	x	-	-	-
	9.75	8.04	R	x	x	x	x	-	-	x
	9.42	6.94	R	x	x	-	x	-	-	x
	12.94	9.2	L	x	-	-	x	-	-	-
	10.33	7.54	R	x	-	x	x	-	-	x
	11.63	8.85	R	x	-	-	x	-	-	x
	9.89	7.89	R	x	-	-	x	-	-	-
	11.89	8.68	L	x	-	x	x	-	-	-
	11.52	9.45	R	x	-	x	x	x	-	x
	8.32	6.41	L	x	-	x	x	x	x	x
	11.1	7.72	R	x	-	x	-	-	-	-
	11.89	9.56	L	x	-	-	x	x	x	x
	11.64	8.68	R	x	-	-	x	x	-	x
	9.4	6.78	R	x	-	-	-	-	-	-
	6.18	4.61	R	x	-	-	-	-	-	-
	9.13	7.37	L	x	-	-	x	x	-	x
	12.68	8.81	R	x	-	x	x	-	-	x
	12.06	8.64	R	x	-	x	-	-	-	-
	9.87	7.64	R	x	x	x	x	-	-	x
	12.07	9.46	L	x	-	-	x	-	-	-
	11.09	8.07	L	x	-	x	x	x	-	x
	8.45	6.2	L	x	-	x	x	x	-	x
	11.46	7.64	L	x	-	-	-	-	-	-
	10.61	7.74	L	x	-	x	-	-	-	x
	9.86	7.54	L	x	-	x	x	x	-	-
	8.76	6.83	R	x	x	-	x	-	-	x
	9.55	7.27	L	x	-	x	x	-	-	-
	8.4	6.87	R	x	-	x	x	-	-	-
	8.39	6.23	R	x	-	x	x	-	-	x
	7.25	5.87	L	x	-	x	x	-	-	-
	8.07	6.1	R	x	-	x	x	-	-	x
	10.85	8.44	R	x	x	-	x	-	-	x
	11.43	8.37	L	x	x	-	x	-	-	x
	10.34	8.51	L	x	-	x	x	-	-	-
	7.97	6.45	L	x	x	-	x	-	-	-
	9.8	7.13	R	x	-	x	x	-	-	x
	9.94	6.99	R	x	x	-	x	x	-	x
	11.99	8.72	R	x	x	-	x	x	-	x
	8.85	6.46	R	x	-	x	x	-	x	x
	10.64	7.11	R	x	-	-	x	-	-	x
	11.39	8.75	L	x	x	-	x	-	-	x
	9.68	7.69	R	x	x	-	x	x	x	x
	9.78	7.53	L	x	-	x	x	-	-	x
	9.45	6.6	L	x	x	-	x	-	-	-
	9.24	7.34	L	x	-	-	x	x	-	x
	9.67	7.44	L	x	-	-	x	-	-	x
	9.71	7.55	R	x	x	-	x	x	-	x
	8.61	6.21	R	x	-	x	x	-	-	-
	6.23	4.8	L	x	x	x	x	x	x	x
	7.58	5.63	R	x	-	-	x	-	-	-
	6.59	5.82	R	x	-	-	x	-	-	-
	8	6.28	R	x	-	x	x	-	-	x
	10.16	8.85	L	x	-	x	x	-	-	-
	5.52	4.25	L	-	-	x	x	-	-	x
	7.09	5.83	R	x	x	x	x	-	-	x
	9.31	7.34	R	x	x	x	x	-	-	x
	7.9	6.1	L	x	x	x	x	x	-	x
	10.57	7.72	R	x	-	-	x	x	-	-
	7.03	5.54	L	x	-	x	-	-	-	-
	11.21	8.4	L	x	x	x	x	-	-	x
	8.64	6.52	R	x	x	x	x	x	-	x
	5.12	4.37	L	-	-	x	x	-	-	x
	8.29	6.86	L	x	x	-	-	-	-	-
	12.72	8.98	L	x	x	x	x	x	-	x
	9.85	7.48	R	x	x	x	x	x	-	x
	9.4	7.57	L	x	x	x	x	-	-	x
	9.8	7.04	L	x	-	x	x	-	-	-
	8.53	6.25	R	x	-	x	x	x	-	-
	6.7	5,72	R	x	-	x	x	x	-	x
	9.03	6.37	R	x	-	x	x	-	-	x
	10.61	8.23	R	x	x	x	x	x	-	x
	11.9	9.55	L	x	x	x	x	x	x	x
	6.82	5.31	R	x	-	x	-	-	-	-
	10.53	7.72	L	x	-	x	x	-	-	x
	8.34	6.45	L	x	-	x	x	-	-	x
	4.03	3.57	R	x	-	x	x	-	-	x
	7.57	5.7	L	-	-	-	x	-	-	-
	11.89	8.96	L	x	-	x	x	-	-	-
	9.27	7.34	L	x	x	x	x	-	-	x
	7.7	6.55	L	x	x	-	x	x	x	x

continued

Sample	Length	Height	Valve	External			Internal			
				C,L	O	P	L,C	PL	MS	O
	6.39	5.05	R	x	-	-	-	-	-	-
	9.2	6.88	R	x	-	x	x	-	-	x
	11.41	8.25	R	x	x	x	x	x	-	x
	5.43	4.17	R	x	-	-	x	-	-	x
	9.06	7.03	L	x	x	-	x	-	-	x
	4.92	4.28	R	-	-	-	x	-	-	-
	7.91	6.13	R	x	x	-	x	-	-	x
	8.38	6.58	R	x	-	x	x	-	-	x
	9.72	7.6	R	x	x	-	x	-	-	x
	6.56	5.02	L	x	-	-	-	-	-	-
	8.68	6.96	L	x	x	-	x	x	x	x
	7.86	6.14	L	-	-	x	x	-	-	-
	8.68	6.37	R	x	-	-	x	-	-	x
	8.89	6.64	R	x	-	x	x	-	-	x
	7.3	5.99	R	x	x	x	x	x	x	x
	9.04	7.23	L	x	-	x	x	-	-	-
	7.77	6.07	R	x	x	x	x	x	-	x
	8.93	7.38	R	x	x	x	x	-	-	x
	7.52	5.68	R	x	x	x	x	-	-	x
	9.14	6.83	L	x	x	-	x	-	-	x
	8.5	7.08	L	x	x	-	x	x	-	x
	8.28	6.57	L	x	x	x	x	-	-	x
	8.09	6.76	R	x	x	x	x	-	-	x
	9.31	7.25	L	x	-	-	x	x	-	x
	7.6	6.3	L	x	x	-	x	x	x	x
	5.9	4.4	R	x	-	-	-	-	-	x
	5.91	4.46	R	x	x	x	x	x	-	x
	8.01	6.66	R	x	x	x	x	x	x	x
	8.32	7.02	R	x	x	x	x	-	-	x
	8.2	6.63	R	x	-	-	x	-	-	x
	9.38	6.98	R	x	x	x	x	-	-	x
	9.17	7.4	L	x	x	x	x	-	-	x
	7.09	5.82	L	-	-	x	x	-	-	x
	4.71	3.67	L	x	x	-	x	x	-	x
	7.18	5.64	L	x	x	-	x	x	x	x
	7.01	5.74	L	x	-	x	x	-	-	x
	5.12	4.12	R	x	-	x	-	-	-	-
	6.15	4.51	L	x	x	x	x	x	-	x
	6.92	5.53	L	x	-	-	x	x	-	x
	7.62	5.64	R	x	x	-	x	-	-	x
	7.74	5.81	R	x	x	-	x	-	-	x
	8.6	6.76	R	x	x	-	x	-	-	x
	7.48	6.24	R	x	x	x	x	x	-	x
	6.45	5.63	L	x	-	x	x	-	-	-
	4.9	3.98	L	x	-	x	x	-	-	-
	7.62	5.97	L	x	-	-	x	x	-	x
	6.78	5.39	L	x	-	-	x	-	-	x
	8.91	6.94	L	-	-	-	-	-	-	x
	4.18	3.56	R	x	x	x	x	-	-	x
	7.97	6.62	L	x	-	x	x	-	-	x
	6.97	6.1	L	x	x	-	x	-	-	x
	6.2	5.2	L	x	x	x	x	x	-	x
	6.54	5.28	L	x	x	x	x	x	-	x
	8.76	7.05	L	-	-	-	-	-	-	x
	5.51	3.95	R	x	x	-	x	x	x	x
	6.88	6.09	L	x	x	-	x	x	-	x
	7.72	6.43	L	-	-	-	-	-	-	x
	5.56	3.98	L	x	-	-	x	x	x	x
	6.74	5.21	R	x	x	-	x	x	-	x
	8.65	7.07	L	x	x	x	x	x	-	x
	8.1	6.04	R	x	x	x	x	-	-	x
	7.39	5.46	R	x	x	x	x	-	-	x
	7.33	6.08	R	x	x	-	x	-	-	x
	6.94	5.64	R	x	x	x	x	-	-	x
	5.52	4.65	L	x	x	-	x	-	-	x
	6.2	5.52	R	x	x	-	x	x	-	x
	8.5	6.93	R	x	x	-	x	x	x	x
	8.6	7.32	L	x	x	-	x	-	-	x
	8.44	6.04	L	x	x	-	x	-	-	x
	7.09	5.39	R	x	x	-	x	x	x	x
	6.87	5.97	R	x	-	x	x	-	-	x
	7.16	5.59	L	x	-	-	x	-	-	x
	4.32	3.72	L	x	x	x	x	-	-	x
	7.74	6.2	L	x	-	-	-	-	-	-
	4.3	3.15	R	x	x	-	x	x	-	x
	7.38	6.27	L	x	-	-	x	-	-	x
	6.88	5.53	L	x	x	-	x	x	-	x
	7.48	6.02	L	x	-	x	x	-	-	x
	6.03	4.69	L	x	-	-	x	-	-	x
	7.74	5.85	R	x	x	-	x	-	-	x
	4.22	3.32	R	x	x	x	x	-	-	x
	5.29	4.5	L	x	x	-	x	-	-	x
	4.72	4.39	L	x	-	x	x	-	-	x
	4.82	3.69	R	x	-	-	x	-	-	x
	4.16	3.59	L	x	x	x	x	-	-	x
	4.27	3.86	L	x	x	-	x	-	-	x
	8.31	6.25	R	x	x	x	x	-	-	x
	7.52	6.06	R	x	-	x	x	-	-	x
	7.98	5.89	R	x	x	-	x	-	-	x
	5.43	4.2	L	x	x	-	x	x	-	x
	7.43	6.33	L	x	-	x	x	x	x	x
	7.77	5.74	L	x	x	x	x	-	-	x
	6.57	5.17	R	x	x	-	x	-	-	x
	6.15	5.25	L	x	-	x	x	-	-	x
	5.9	4.93	L	x	x	x	x	-	-	x
	5.84	4.58	L	x	x	x	x	-	-	x
	7.06	5.1	R	x	-	-	x	-	-	x
	7.85	5.93	L	x	-	-	x	-	-	x
	7.4	6.43	L	x	x	-	x	x	-	x
	4.81	4.22	R	x	x	-	x	x	x	-
	5.35	4.39	R	x	-	-	x	-	-	x
	7.42	5.57	L	x	x	x	x	x	-	x
	5.04	4.31	R	x	-	x	x	x	-	x
	5.77	5.15	R	x	x	-	x	-	-	x
	5.31	4.55	R	x	x	-	x	x	-	x
	4.08	3.5	L	x	-	-	x	x	-	x
	5.33	4.08	L	x	x	-	x	-	-	x
	5.77	4.99	L	x	-	x	x	-	-	x
	6.54	5.2	R	x	x	-	x	-	-	x
	4.93	4.17	R	x	-	-	x	-	-	-
	6.82	5.33	L	x	-	-	x	-	-	x
	4.98	4.34	R	x	x	-	x	x	-	x

continued

Sample	Length	Height	Valve	External			Internal			
				C,L	O	P	L,C	PL	MS	O
	4.55	3.42	L	x	x	-	x	-	-	x
	5.42	4.32	R	x	x	-	x	x	-	x
	5.67	4.49	R	x	x	-	x	-	-	x
	3.42	2.94	L	-	-	-	-	-	-	-
	4.99	3.8	L	x	-	x	x	-	-	x
	6.29	5.76	R	x	x	-	x	-	-	x
	5.94	4.86	L	x	x	x	x	x	-	x
	4.75	3.78	R	x	-	x	x	-	-	x
	5.17	4.73	R	x	x	-	x	x	-	x
	4.03	3.36	L	x	-	-	x	-	-	x
	4.57	3.63	R	x	-	-	x	-	-	x
	3.85	2.98	R	x	x	x	x	x	-	x
	4.73	3.73	R	x	-	-	x	-	-	x
	4.03	3.46	L	x	x	x	x	-	-	x
	4.43	3.39	R	x	x	x	x	-	-	x
	3.82	3.02	R	x	-	-	x	-	-	x
	5.54	4.57	L	x	-	-	x	-	-	x
	4.89	3.92	R	x	-	-	x	-	-	x
	4.15	3.63	R	x	-	x	x	-	-	x
	5.4	4.43	R	x	-	-	x	-	-	x
	4.27	3.77	L	x	-	-	x	-	-	x
	3.33	3.06	L	x	x	-	x	-	-	x
	5.06	4.24	R	x	-	-	x	x	-	x
	3.91	3.06	L	x	-	x	x	-	-	-
	3.57	2.93	L	x	-	-	x	-	-	x
	4.34	3.48	R	x	x	-	x	x	-	x
	5.1	4.51	L	x	x	-	x	x	-	x
	4.92	4.11	L	x	-	-	x	-	-	x
	4.93	3.77	L	x	x	x	x	x	-	x
	3.84	3.5	R	x	x	x	x	-	-	x
	3.7	3.04	L	x	-	-	x	-	-	x
	5.56	4.33	R	x	x	x	x	-	-	x
	4.62	3.78	L	x	x	x	x	-	-	x
	5.42	4.17	R	x	x	-	x	-	-	x
	3.4	3.04	R	x	x	x	x	x	-	x
	4.87	4.75	R	x	x	-	x	x	x	x
	4.45	3.8	R	x	x	x	x	x	-	x
	4.44	3.89	L	x	x	-	x	x	-	x
	5.84	4.31	R	x	x	-	x	x	-	x
	3.74	3.13	L	x	-	x	x	-	-	x
	4.3o	3.38	L	x	-	x	x	x	-	x
	3.82	3.17	R	x	x	x	x	-	-	x
	4.62	3.4	L	x	x	-	x	x	x	x
	4.74	4.12	R	x	x	-	x	x	x	x
	3.95	3.62	L	x	x	x	x	-	-	x
	3.97	3.59	R	x	x	x	x	-	-	x
	3.95	2.93	R	x	x	-	x	-	-	x
	4.17	2.78	L	x	x	-	x	x	-	x
	3.55	3.7	L	x	x	x	x	x	-	x
	4.33	3.23	R	x	x	-	x	-	-	-
	4.07	3.6	L	x	x	-	x	-	-	x
	5.52	3.23	L	x	-	x	x	x	-	x
	5.51	4.36	L	x	-	x	x	-	-	x
	5.29	4.61	R	x	x	x	x	-	-	x
	3.9	3.58	R	x	x	x	x	-	-	x
SL1 220-225	9.34	7.16	R	x	-	-	x	-	-	-
N = 30	9.44	7.02	L	x	-	-	x	-	-	-
	8.33	6.39	R	-	-	x	x	-	-	-
	10.69	7.28	L	-	-	-	x	-	-	-
	8.2	5.68	L	x	-	x	x	-	-	-
	8.43	6.2	L	x	-	-	x	-	-	x
	7.03	5.57	R	x	x	-	x	-	-	x
	6.29	4.62	L	x	-	-	x	-	-	-
	8.04	6.28	R	x	-	x	x	-	-	-
	7.8	5.93	R	x	x	-	x	-	-	x
	6.29	4.78	L	x	-	-	-	-	-	-
	5.32	3.81	R	x	-	-	x	-	-	x
	4.23	3.61	R	-	-	-	-	-	-	-
	5.4	4.16	L	x	x	x	x	-	-	x
	4.26	3.54	L	x	-	-	x	-	-	x
	4.86	3.67	L	x	-	-	-	-	-	-
	6.18	4.77	L	x	-	x	x	-	-	x
	4.79	3.76	L	x	-	x	x	-	-	x
	5.46	3.88	R	x	-	-	-	-	-	-
	3.89	3.2	L	x	-	-	x	-	-	x
	5.64	4.34	R	x	x	x	x	-	-	x
	4.05	3.37	R	x	x	x	x	-	-	x
	3.97	3.3	L	x	-	-	x	-	-	x
	4.06	3.43	R	x	x	-	x	x	-	x
	4.24	3.26	L	x	x	-	x	-	-	x
	3.7	3.02	R	-	-	-	-	-	-	-
	3.62	2.92	L	x	x	-	x	x	-	x
	3.71	3.11	R	x	x	-	x	-	-	x
	3.4	2.75	R	x	-	x	x	-	-	x
	3.29	2.68	L	-	-	-	-	-	-	-